CRITICAL PROPERTIES OF THE EMERGENT RANDOM SOLID AT THE VULCANIZATION/GELATION TRANSITION

BY

SWAGATAM MUKHOPADHYAY

B.Sc., North Bengal University, 1997
M.Sc., Indian Institute of Technology, Kanpur, 2000

DISSERTATION

Submitted in partial fulfillment of the requirements
for the degree of Doctor of Philosophy in Physics
in the Graduate College of the
University of Illinois at Urbana-Champaign, 2005

Urbana, Illinois

CRITICAL PROPERTIES OF THE EMERGENT RANDOM SOLID AT THE VULCANIZATION/GELATION TRANSITION

Swagatam Mukhopadhyay, Ph.D.
Department of Physics
University of Illinois at Urbana-Champaign, 2005
Prof. Paul M. Goldbart, Advisor

The vulcanization/gelation transition is a continuous equilibrium phase transition from a liquid state to a random solid state, controlled by the density of permanent crosslinks between the constituent particles. The emergent random solid state is characterized by nonzero shear rigidity and particle localization (in high enough dimensions) about random positions; the particle localization lengths are statistically distributed. Founded upon previous work that had constructed a replicated Landau-Wilson free energy for the transition, and had analyzed the critical region within the liquid state, this Thesis focuses on the nature of fluctuations in the random solid state and the critical behavior of physical quantities detecting it. The first part of this Thesis investigates the Goldstone-type low energy, long wave-length fluctuations associated with the spontaneous breakdown of a (global, continuous) translational symmetry at the transition. These fluctuations are identified with the shear deformations of the emergent random solid, whose shear modulus and elastic free energy are derived utilizing this identification. The impact of such fluctuations on the statistical distribution of localization lengths is ascertained. In the second part of this Thesis, a thorough analysis of the the critical region within the random solid state is presented on implementing a Renormalization Group approach. The critical-fluctuation-correction to the mean-field distribution of localization lengths is determined from a perturbative calculation of the Equation of State for the vulcanization/gelation field theory (to lowest order in an expansion in epsilon, i.e., the upper critical dimension minus the spatial dimension). Such a calculation is challenging owing to the nature of translational symmetry breaking in the replicated field theory. The third part of this Thesis deduces the scaling of entropic shear rigidity near the vulcanization/gelation transition. The shear modulus exponent is analyzed within a Renormalization Group approach, and it is shown that the critical exponent can assume two distinct fixed-point values depending on the strength of the excluded-volume interaction between the constituent particles, thereby resolving an old controversy over its value.

To my parents who made this flute, and to Adhyatma who filled it with wine!

Acknowledgments

Overwhelmed by the excitement of writing this section, which, in spite of its location, is attended to at the end of the writing process, I browsed through the acknowledgements of other dissertations. A vast majority of them impressed upon me the time-honored tradition of beginning this section with the line, *This Thesis would not have been possible without...*; I was amused. It reminded me of a hackneyed line that the hero in mainstream Hindi movies almost unerringly blurts out to the heroine in the very precious moments between clobbering an entire army of hoodlums, *It is not possible for me to live without you!* However, even in the movies, the heroes seem to live on. Our *will to explore*, arguably, rivals our *will to exist*. It is quite possible that my Thesis wouldn't come into existence under certain contingencies, but what could be a very probable one? I hope there weren't any!

However, *this* Thesis would not have been possible without the invaluable mentorship of Prof. Paul. M. Goldbart. Over the past four years of my interaction with him, I have developed a deep respect for his inhuman ability to tolerate harangues on unbaked ideas, maintain an encouraging smile through out, and calmly respond; *That's very interesting, but may be you should try this out!* His favorite line with his students is, *Call me anytime!*—and he means it. He has a sense of urgency and precision in formulating ideas, which, when coupled to his mathematical prowess, makes him a formidable thinker to challenge, and an enviable mentor to emulate. He is caring of his students' as a gardener is of his seasonal flowering plants, and his affection is untainted by superficiality.

I have gained enormously through my interaction with Prof. Y. Oono. It's a trifle embarrassing to knock on his office door because he is always so welcoming of students; one can be assured to be offered his help, and conversations with him always cross the allotted time. His deep insight and unassuming knowledge is an example that I have sought, for gentle inspiration, during those hard times of theoretical research.

Numerous informal discussions on my research with many other physicists at the Physics department, UIUC, has been instrumental in my progress. The first person who comes to my mind is Dr. D. Toublan. During the early years of my Ph.D. career, I have learnt many aspects of field theory from him. He is a patient teacher, an inspiring listener and a charming friend. The second person to thank is my collaborator Dr. Xiangjun Xing. His willingness to think deeply on core issues and his uncompromising attitude in evaluating the soundness of ideas has constantly challenged me to refine my own thoughts. I have learned enormously from him. The third person is my collaborator Xiaoming Mao. I thank her for our rich exchange of ideas on research, and for her perceptive comments. Prof. Eduardo Fradkin, Prof. Michael Stone and Michael Lawler has educated me on various topics, some of which are closely related to the work presented in this Thesis. Outside the Physics department at UIUC, I have had educative discussions on some aspects of my research with Dr. Olaf Stenull, Prof. Deepak Dhar and Prof. Tom Lubensky; their helpful input is acknowledged with gratitude.

Life at Urbana-Champaign would be lacking in luster and love without my 'family' of dear ones here; Smitha Vishveshwara, Kalin Vetsigian, Abhishek Singh, Sunayana Saha and Namita Vishveshwara. Their unstinting care has catalyzed my thrill in doing research and has nurtured my joyous life in countless ways. Smitha is an exemplary teacher and an extraordinarily affectionate friend. We have shared our creative vitality, and my mind has always been galvanized in her presence. On many occasions Tzu-Chieh, Kalin, Rahul, Smitha and Abhishek bore the brunt of my frustration with research and tolerated my complaining tirades. Thank you all! Tzu-Chieh Wei is the best officemate one can imagine! I thank Michelle Nahas for her precious friendship, and for setting an unambiguous example on how chocolate can be the elixir of human life and a practical solution to all its petty problems. On a similar note, I thank my colleague and friend David Pekker, not only for the research we did together (not presented in this Thesis), but for his ability to focus on the priorities of life— good brainteasers, good bicycle, good car and good cheesecake. I thank my friends at UIUC— Rahul Biswas, Hector G. Martin, John Veysey, Jean-Jacques (Farah) Toublan, Jeff Warner, Nick Peters, Parag Ghosh, Satwik Rajaram, Eun-ah Kim and many others.

I thank my collaborators Prof. A. Zippelius, Prof. N. Trivedi and Kenneth P. Esler.

By dabbling in art I try to maintain a crucial balance of nonacademic activities necessary

to refresh my brain. I thank all the artists at High Cross Art Studio (Urbana) and Studio Be (Champaign) for their warmth and stimulation. I particularly thank Jenny Southlyn and William C. Baker.

I thank my parents. Above all, I thank Adhyatma Chaitanya. My own words will always be inadequate in expressing the depth of my gratitude and love for them; in the words of the poet, Rabindranath Tagore,

> *Thy infinite gifts come to me only on these very small hands of mine.*
> *Ages pass, and still thou pourest, and still there is room to fill.*

The work presented in this Thesis was supported by the National Science Foundation through grants DMR99-75187, EIA01-21568 and DMR02-05858.

Table of Contents

List of Figures

List of Abbreviations

V/G Vulcanization/Gelation

OP Order Parameter

SSB Spontaneous Symmetry Breaking

RG Renormalization Group

HRS Higher Replica Sector

LRS Lower Replica Sector

0RS Zero Replica Sector

1RS One Replica Sector

MF Mean-Field

EOS Equation of State

Chapter 1

Prologue

> I shall entertain you with a hasty and unpremeditated, but so much the more natural, discourse. My venting is *ex tempore*, I would not have you think proceeds from any principles of vain glory by which ordinary orators square their attempts... because it was always my humour constantly to speak that which lies uppermost... let no one be so fond as to imagine, that I should so far stint my invention to the method of other pleaders, as first to define, and then divide my subject...
> — Desiderius Erasmus, *The Praise of Folly* (1509)

The word 'critical' is derived from the Greek word '$\kappa\rho\iota\tau\iota\kappa\acute{o}s$' and the Latin word 'critic-us' which means 'to judge'. By the seventeenth century, this English word began to mean the act of 'passing severe and unfavorable judgement', in addition to the older meaning of 'passing erudite and accurate judgement'. The word was used in scientific parlance in the middle of nineteenth century to mean 'constituting or relating to a point at which some action, property or condition passes over into another; constituting an extreme or limiting case'. The jargon 'critical temperature' arguably appeared first in the *Philosophical Transactions* in the year 1869, and since then, the physicist's mind has been captivated by what we know to be the 'theory of critical phenomena' today.

Though an etymological investigation on all the words in the title of this Thesis doesn't clarify its meaning, it may add humor to a formal enterprize. The word 'property', is derived from a word that meant 'to own' 'emergent' from 'out + to dip', 'random' from 'to run fast, gallop', 'vulcanization' from 'the god of fire', 'gelation' from 'an excellent white broth made of the fish Maigre' and 'transition' from 'to cross'. A few centuries back, the title of my Thesis might have created very confusing images in the mind of an unsuspecting plebian, about my dealing with fish broth and the God Vulcan, crossing something somewhere in a fast gallop. Fortunately, in science

the words we use are usually divested of frills and veils. They are like rafts that carry specific meaning across the waters of scientific knowledge — burnished and lean. Let me use these 'rafts' now, *vulcanization/gelation transition*, *emergent random solid* and *critical properties*, to introduce some the central ideas of this Thesis. This chapter is to be regarded as an informal invitation to the problems at hand, some of whose solution are presented in this Thesis, and others that merit further enquiry. My purpose here is primarily an advertisement— I wish to convey the thrill of research in soft-condensed matter physics in general, and random systems in particular. In order to put the work presented in this Thesis in proper context, I also outline the development of the theory of V/G transition along the way.

1.1 Vulcanization/Gelation— a primer

Imagine the process of making Jello^{TM}, mixing Epoxy^{TM}glue, vulcanization of natural rubber or of synthetic elastomers[1]. What is the physical principle underlying all of these processes? How can we understand (or better still, predict) some of the physical properties of the *gel* produced in these processes? It turns out that all of these phenomena involve the formation of *crosslinks* between *polymer* chains. Polymers chains are covalently-bonded macromolecules made up of small chemical units called *monomers*. The typical number of these repeating units in a single polymer may range from hundreds to thousands (can be as large as a billion for some biological macromolecules). Over the last several decades, polymers have gained enviable notoriety in captivating the minds of talented physicists. Polymers display a very large number of possible conformations in a solution at non-zero temperature, defy the canonical point-particle description of statistical physics of fluids, and get entangled with each other causing considerable vexation to scientists grappling to process or model them. However, polymer science has also rewarded the persevering theoreticians with rich ideas, for example, a polymers are a playground for concepts in knot theory and the path-integral formalism of statistical field theory [1].

Coming back to gels, depending on the nature of crosslinks, they can be broadly classified into *physical gels* and *chemical gels*. Chemical gels are formed through a chemical reaction that introduces chemical crosslinks, i.e., essentially permanent covalent bonds. For example, in the

[1] I am counting on you to have performed the 'experiment' of making Jello^{TM}.

case of natural rubber, the process of *vulcanization* discovered by Goodyear in 1839 involves the addition of sulphur to a melt of polymers (natural *cis*-polyisoprene, to be specific). Sulphur reacts with double-bonds along the polymer chains, resulting in the joining of two chains by a link made up of two to four sulphur atoms. The time-scale for the breaking and reforming of these chemical bonds is very large compared to the observational time-scale; therefore in this specific example the crosslinks are *effectively permanent*. In physical gels the crosslinks originate from a physical (rather than chemical) process, for example, in the case of Jello$^{\mathrm{TM}}$, it's the micro-crystallization of atoms on cooling. Physical gels can either be *strong* or *weak* depending on the time-scale over which the crosslinks break and reform. Strong physical gels are analogous to chemical gels and can melt or flow only when external conditions are changed, for example the heating up of a thermo-reversible gel. On the other hand, weak physical gels are formed by very weak bonds that constantly break and recover at the observational time-scale. Typically examples of weak crosslinks are hydrogen bonds and ionic associations. Weak gels are not truly solid, although they appear to be so at short enough time scales. In this Thesis we shall concern ourselves with strong physical gels and chemical gels alone. To emphasize the point, in such gels there is a distinct separation of time-scales, making them amenable to an *equilibrium* statistical-mechanics description; the lifetime of crosslinks will always be assumed to be very large compared to the observational time-scale.

Let us take a moment to investigate the physical process of vulcanization/gelation. Imagine a melt of polymers at non-zero temperature. The polymers in the solvent are undergoing thermal motion and exploring the entire volume of the system, within a time-scale much shorter than the observational time scale. Now we link the polymers together. Specifically, we add crosslinks at a certain instant of time with a fixed probability, between randomly chosen pair of monomers that happen to find themselves close to each other at that instant of time. The restriction on the physical proximity of monomers originates from the nature of chemical bonding. The process of crosslinking will create even larger macromolecules (branched polymers) from the original constituent polymers. If this linking process continues with high enough probability, one will eventually end up with a gigantic 'molecule' that spans the entire volume of the system, however large a system size one begins with. This 'infinite network' is what we call the *gel*. Such a mammoth molecule will not dissolve in the solvent. Its constituents are unable to explore the entire volume of the system in a

finite time and is *localized* is space. The transition from a system with only finite-sized polymer networks (finite clusters) to that with a single infinite network (infinite cluster)[2] is called the *vulcanization/gelation(V/G) transition*. The fraction of finite clusters is called the *sol* fraction.

The qualitative description of V/G transition presented in the previous paragraph is strongly reminiscent of percolation problems. An example of a percolation problem is that of *bond percolation*, where bonds are introduced with a fixed probability between randomly chosen neighboring points on a regular finite-dimensional lattice. Like the V/G transition, percolation is also a connectivity transition: beyond a certain probability a typical configuration contains an infinite cluster that spans the lattice. Percolation has been studied extensively over the last several decades, owing to the broad spectrum of physical phenomena it is relevant to, for example, forest fire, spreading of contagious diseases, soaking of porous rocks etc. The first attempt to understand V/G transition in the light of purely percolative model, was the mean-field model of Flory and Stockmayer [2]. Critical percolation theory was applied with varying success to the V/G problem in the seventies by de Gennes and by Stauffer[3]. I mention, in passing, that over the past several decades the percolation transition has received a great deal of attention from physicists in its own right. A sophisticated field-theoretical description of the percolation transition has emerged through the cumulative work of Harris, Lubensky, Jannsen, Stenull and collaborators [4], based on the Random Resistor Network model (RRN).

A pertinent question to ask at this point is whether a purely percolative model suffices to describe the V/G transition. To answer this question, we need to decide what aspects of V/G transition we want to analyze. To this purpose, we need to identify the *universal*[3] aspects of the underlying physical phenomena in the V/G transition. In other words, we reduce the details of the transition in specific systems into simple *elements*, for example, physical interactions, symmetries etc. that are common to all of them and are indispensable in a minimal model of the phenomena. What are the necessary ingredients in a model of V/G transition? It is easy to identify one such ingredient based on the discussion above: it is the aspect of the random connectivity of the

[2]There exists a proof that there is one, and only one, incipient infinite cluster at the *percolation* transition. Read on for a sketch of connection between vulcanization/gelation and percolation transition.

[3]In the unlikely event that the reader is uninitiated to the philosophy of the Renormalization Group, the word 'universal' is explained in the next section. It is a 'raft' that carries a lot of ideas across, and is known to command both love and awe.

constituent particles (or other entities) that form clusters. A percolation model would capture this aspect. However, the particles also execute thermal motion; the particles in the gel vibrate thermally in a localized region of space whereas the sol fraction explores the entire remaining volume of the system. Is thermal motion of particles a necessary ingredient in the analysis of the V/G transition? That the answer to this question is an overwhelming 'Yes' is one of the central themes of the theoretical work presented in this Thesis, as an extension of earlier work in the same spirit pioneered by Edwards, and by Goldbart and collaborators [5, 7]. The other important ingredient in modeling the V/G transition is the excluded-volume (or repulsive) interaction between the constituent particles, and we will come back to a detailed discussion of this aspect in the next chapter.

Significant progress in the theory of polymer networks was made by Edwards and collaborators [5], who included the effects of thermal fluctuations in their model of gels in the well-crosslinked limit, i.e., deep inside the solid phase away from the critical point. This line of research was continued by Panyokov and collaborators [6]. However, these theories were inadequate in capturing the critical properties of the V/G transition because they were restricted to the well-crosslinked limit, i.e., deep inside the solid state.

Goldbart and Goldenfeld [7] made key progress in the understanding of V/G transition by identifying an *order parameter* for the V/G transition. Goldbart and collaborators eventually formulated a microscopic theory of the vulcanization transition and derived the Landau-Wilson *effective theory*. Later work proved that the universality class of the transition is the same as the percolation universality class. Chapter 2 provides an introduction to this line of research on which the work presented in this Thesis is founded. In the next section, I present a stormy introduction to critical phenomena, and prepare the reader for the presentation that follows.

1.2 Critical phenomena for pedestrian

In this section, I reiterate the key concepts of the renormalization group theory of continuous phase transitions that form the core of the discussion in this Thesis. Given the excellent references that exist on the subject [16], I hope that my cavalier introduction will be excusable. In the previous section, I have alluded to the Landau-Wilson effective theory. The concept of an *effective theory* is

so deeply ingrained in our mathematical modeling and current physical understanding of natural phenomena, that this introduction is probably superfluous to anyone who would care to read this Thesis in the first place. The philosophical impact of the theory of continuous phase transitions developed over the past several decades, starting from Landau's theory of phase transitions and culminating in the Renormalization Group(RG) theory due, inter alia, to Kadanoff and Wilson, has galvanized almost all branches of physics — in the very pith of the questions we pose and the manner in which we hope to answer them.

Central to the description of a continuous transition is the concept of *critical degrees of freedom* in the system. What are the critical degrees of freedom? Consider a specific example, a ferromagnet, where all the spins are more or less aligned along a particular direction induced by the interaction among the spins that make this aligned state energetically favorable. Now, imagine increasing the temperature. The entropy of the system increases, manifesting itself in the thermal fluctuation of the individual spins about their average direction. Eventually, the entropy of the system wins over the energy and the ferromagnetic state makes a transition to the paramagnetic state in which all the spins are randomly oriented in space. In the ferromagnetic state there exit long-range correlations in the spin degrees of freedom, whereas, in the paramagnetic state these correlations are short-ranged. In this particular example, it is the fluctuations of the local magnetization of the system that are the critical degrees of freedom; the ferromagnet has non-zero magnetization whereas the paramagnet does not. One can choose to study a wide variety of ferromagnets in nature that undergo the same transition; each of them differ in details such as chemical composition, lattice structure etc., but it is the behavior of the local magnetization that is sufficient to detect and characterize the continuous ferromagnetic-paramagentic transition. Note, however, that the critical degrees of freedom in a phase transition are not necessarily the degrees of freedom that are common to all the specific systems undergoing the same phase transition. For example, the lattice vibrations (i.e., phonons) are common to the various ferromagnets, however they are not *critical*; their fluctuation do not drive the system through the magnetic transition. Identifying the critical degrees of freedom for a phase transition is often not obvious; input from experimental observations and theoretical insight is required. Once the critical degrees of freedom are identified, the *order parameter* can be conjured. I say 'conjured', because in interesting scenarios the identification of the correct order parameter

is a major step in achieving a thorough understanding of the phase transition.

An *order parameter* is a mathematical function that detects the continuous phase transition; it takes a non-zero value in the *ordered* state and a zero value in the *disordered* state. The qualifications *ordered* and *disordered* are with reference to a *symmetry* that is *spontaneously broken* in a continuous phase transition. The concept of *spontaneous symmetry breaking* (SSB) is pivotal in the understanding of continuous phase transitions, so I shall discuss it briefly here, particularly because a major portion of this Thesis in devoted to the implications of SSB for the random solid state.

Symmetries are invariances of a system under the operation of a physical transformation, for example rotation, translation etc. In a continuous phase transition, a symmetry of the system is usually *broken*, i.e. when compared with the disordered state, the ordered state has reduced symmetry[4]. For example, in the magnetic transition, the paramagnet (i.e., the disordered state) is symmetric under the operation of global spin rotation of all the spins along any axis in spin space, whereas in the ferromagnetic (i.e., the ordered state) the orientation of spins are biased towards a preferred axis, and therefore the latter has reduced global spin rotation symmetry. However, the preferred axis is chosen by the system *spontaneously*, i.e., without any tangible external influence. Symmetries of a physical system can be either discrete or continuous, depending on the corresponding group of symmetry transformations being discrete or continuous. For example, reflection symmetry is a discrete symmetry whereas rotation symmetry is a continuous one. In the V/G transition, a continuous symmetry, namely translational symmetry in replicated space, is spontaneously broken and we shall discuss the consequences elaborately in Chapters 3 and 5.

Once the symmetries and the order parameter of a continuous phase transition are understood, an *effective theory* of the transition can be formulated. The concept of an *effective theory* goes well beyond the realm of the theory of phase transitions however. An effective theory is a theoretical description of a physical system at a particular length/energy scale. It includes all the *relevant* interactions in the system at that length/energy scale, where relevance of interactions is determined by their behavior under renormalization group transformations. An important example of an effective theory is the hydrodynamic theory of fluids. In order to understand the properties of

[4]A symmetry needn't always be broken in a continuous phase transition, the Kosterlitz-Thouless transition being a well-known exception.

fluids at the length/energy scale of macroscopic fluid behavior, (such a fluid flow, fluid pressure, sound waves, etc.), one can *renormalize*, i.e., integrate out, the microscopic degrees of freedom, such as the details of Coulomb interaction between innumerable constituent molecules of the fluid. The price paid in doing so is that there are phenomenological parameters in the effective theory that are not determined from first principles; however, considering the enormous simplification achieved in formulating an effective theory, this is a minor price to pay. The hidden power of effective theories became manifest in physics much before they were recognized by that name; consider for example, the thermodynamic theory of gases. The phenomenal success of this effective theory preceded the microscopic knowledge of molecular interactions. This revolutionary wisdom—that answers to a lot of questions about a system at a particular length/energy scale are independent of the details of the system at a very different length/energy scale— is the basis of the enormous simplification we fondly call *universality* (in physics jargon). Without the principle of universality, essentially all interacting systems would be too hopelessly difficult to be amenable to any sensible mathematical modeling and we would be deprived of almost any predictive power concerning natural phenomena. However, a distinct separation of length/energy scales is not present in all physical phenomena of interest: consider the defiant, and thereby interesting examples of chaotic systems, like turbulent fluid flow.

In a continuous phase transition, the correlation length scale of critical fluctuations diverge. The effective theory for the transition is a description of the system at very large length-scales. This theory is determined by the symmetries of the system, the dimensionality of space, and the order parameter. The effective theory determines the *universality class* of the transition, unifying the behavior of apparently disparate physical systems. The claim made in the previous section that Jello$^{\mathrm{TM}}$, Epoxy$^{\mathrm{TM}}$glue and vulcanized rubber, though completely different in their microscopic details, can nevertheless be understood using the same theory of V/G transition, would be heresy if it weren't for their belonging to the same universality class. Physical systems in the same universality class share common critical properties, for example, the elastic shear modulus near the transition of all of the systems mentioned above scales with the density of crosslinks in exactly the same fashion, varying only with the dimensionality of the system. The universal scaling of physical quantities as a function of the control parameters near the transition is one of the striking

unification predicted by the Renormalization Group theory.

In this Thesis, I present some of our current understanding of the critical properties of the random solid state emerging from the V/G transition. Some of the key questions addressed herein are: What is the universal behavior of the distribution of localization lengths for the localized fraction of particles, i.e., the gel fraction? (see Chapter 4). How does the shear modulus of the random solid scale with the density of crosslinks? How important is the excluded-volume interaction in determining the universal behavior of elasticity in these solids? (see Chapter 6). Along the way, we shall present a thorough RG treatment of the the critical region in the random solid, and calculate the exponents that characterize it (see Chapter 4).

1.3 Emergent random solid for the skeptic

One may ask: Why study the random solid state emerging from the V/G transition? To begin with, it is a quite unique and unconventional solid. For example, the shear modulus (a measure of material's resistance to volume preserving deformation) is of the order of 10^4 to 10^6 Pa, whereas the bulk modulus (a measure of its resistance to volume-changing deformations) is equal to that of a typical liquid, i.e., about 10^9 to 10^{10} Pa. As we all know very well, random solids, such as rubber, are highly flexible. In contrast, in crystalline solids the bulk and shear moduli are of the same order of magnitude magnitude. Another very interesting feature of the random solid is that locally it is indistinguishable from a fluid in the sense that the constituent polymer chains continue to enjoy great mobility and explore a very large number of configuration, as they do in the liquid state. This freedom becomes apparent in *liquid crystal elastomers*. Liquid crystal elastomers are gels made from liquid-crystalline-polymer units. These polymers typically have rigid rod-like 'pendents' attached to them (main-chain ones as well as side-chain ones). These pendent moieties can exhibit ordering in liquid crystalline phases. It turns out that the liquid crystal degree of freedom is essentially unhindered by the presence of the crosslinked network, giving rise to fascinating properties, such as soft elasticity etc. [12, 13]. Our understanding of gels and rubber has been extended to the theory of elasticity for liquid crystal elastomers; I do not present this direction of research here; see however Ref. [15].

Another interesting aspect of shear rigidity in rubber is that it is almost entirely *entropic*

in origin. For crystalline solids, in contrast, the shear rigidity is energetic in origin. Though the presence of a crosslinked infinite cluster is crucial in making a random solid shear-rigid, the mechanism responsible for this rigidity is not the 'pushing and pulling' of particles chemically bonded to each other in the cluster, as one would naïvely imagine. The elastic response arises from the change of the local environment of the particles constituting the random solid, and therefore number of accessible statistical configurations of these particles, i.e., the entropy. A different way of stating this idea is that the polymers act as *entropic springs*. Their free energy is almost entirely contributed by the entropy arising from the large number of possible configurations accessible to them for fixed end points. If these end points are stretched, the number of possible configurations decreases, thereby increasing the free energy of the system. The free energy is therefore a linear function of temperature.

The random solid state is an *intrinsically random* system, as opposed to a *perturbatively random* system, for example, crystalline solids with defects. The local environment of the particles in the random solid varies widely in a sample. For example, a fraction of particles in the gel may be be very strongly constrained by other particles in the network and execute rather limited thermal motion—they are *strongly localized*. Other particles may be very loosely bound to the network, making it possible for them to execute very floppy thermal motion—they are *weakly localized*. The wide spectrum of local environments of particles in the random solid necessitates the concept of a *distribution of localization lengths* of particles, as mentioned earlier.

There exists a fascinating variety of *random solids* that are not the subject matter of this Thesis, however, ideas presented here may be useful in understanding and modeling some aspects of their physical properties. The most noteworthy (and notorious) of them is structural glass. Granular media, colloids, foams, pastes, amorphous solids (e.g., amorphous silicon), etc. are other examples that are at the focus of active research in condensed matter physics. Glasses exhibit very interesting non-equilibrium phenomena and slow relaxation dynamics [17]; these are topics outside the scope of the equilibrium statistical mechanics treatment of static properties of the class of random solids presented in this Thesis. I would also like to draw the attention of the reader to the topic of the dynamics of V/G transition explored by various authors, for a review see Ref. [18].

Chapter 2

Introduction to the theory of vulcanization/gelation transition

With skill divine had Vulcan formed the bower,
Safe from access of each intruding power.
— Homer

In this chapter I summarize the main theoretical developments in the understanding of vulcanization and gelation, and the framework within which the research presented in this Thesis is built upon. This chapter serves to familiarize the reader with the central concepts that are invoked repeatedly in the chapters that follow, for example, the order parameter, the Landau-Wilson free energy etc., besides introducing some of the notation used throughout this Thesis.

2.1 Microscopic model

A microscopic theory of the vulcanization transition was first developed by Goldbart and collaborators [7], for a pedagogical review see Ref.[19]. In this Thesis, my attention is focussed on the critical properties of the vulcanization/gelation universality class and not any particular microscopic model. Having the assurance that a microscopic model exists from which the Landau-Wilson effective theory for the V/G transition can be derived, I choose to discuss that microscopic model cursorily in this presentation.[1] Nevertheless, it is instructive to summarize the essential ingredients of a microscopic model that belongs to the universality class defined by the V/G effective theory. Recall that the V/G transition is an equilibrium continuous phase transition from a liquid

[1] Historically, however, as is often the case, the effective theory was derived using a small wave-vector expansion (long wave-length description) of a specific microscopic model such as that summarized in the next subsection.

state to a random solid state tuned by the density of permanent random crosslinks— the *quenched* randomness—introduced between the constituent particles whose locations are thermally fluctuating variables—the *annealed* randomness. Therefore, any microscopic model should feature the crosslinking of pairs of particles chosen at random with a certain probability. The probability distribution of crosslinks should depends on the physical proximity of randomly chosen particle pair. We require the latter condition, envisaging the physical scenario where it is more likely for two particles that are close to each other to form a crosslink, for example, through a chemical reaction. Another indispensable ingredient of the model is some sort of repulsive interaction between particles, for example, the excluded-volume interaction. Such an interaction maintains density homogeneity in the random solid, and prevents the infinite cluster from collapsing, i.e., it keeps it *swollen*. The excluded volume interaction also ensures that the bulk moduli of the sol and the gel are of the same order of magnitude, and therefore the bulk modes are noncritical in the theory—an aspect we know to be true from experimental observation. Lastly, the microscopic model should include thermal fluctuations of the particles if it is to be considered a *statistical mechanical model* for equilibrium gels. Without the inclusion of thermal motion, the model can at best be a *statistical* model, determined by the statistics of the random crosslinking of the constituent particles. We wish to capture the elastic properties of the random solid in our model as well; as elasticity in such solids in entropic in origin, a purely statistical model (for example, any purely percolative model) will fail to capture any elastic behavior. To summarize, the ingredients of a microscopic model are

- Permanent random constraints between classical particles, i.e., quenched randomness
- A probability distribution of the random constraints
- An excluded volume interaction between particles
- Thermal fluctuation of particle positions, i.e., annealed randomness

2.1.1 Vulcanization model

In this and the next subsections I document without derivation the essentials of a particular microscopic model that has all the necessary ingredients listed above; for a review see Ref. [19]. Imagine

a melt of N polymers of the same fixed length. The effective Hamiltonian of the system is given by

$$\mathcal{H}^{\mathrm{E}} = \frac{1}{2}\sum_{i=1}^{N}\int_0^1 ds\Big|\frac{d}{ds}\mathbf{c}_i(s)\Big| + \frac{\lambda^2}{2}\sum_{i,i'=1}^{N}\int_0^1 ds\int_0^1 ds'\delta^D\left(\mathbf{c}_i(s)-\mathbf{c}_{i'}(s')\right), \tag{2.1}$$

where the D-dimensional vector $\mathbf{c}_i(s)$ is the (rescaled) position of the s-th monomer (as $0 \leq s \leq 1$ the monomer index s is a fraction of the polymer length, which is rescaled to unity) on the i-th polymer, λ^2 is the strength of excluded volume interaction between the monomers, and $\delta^D(\cdots)$ is the D-dimensional delta function. The first term in the effective Hamiltonian is the Wiener measure for polymer configurations, and the second term is the excluded volume interaction between monomers constituting the polymers. This effective Hamiltonian determines the weight of configurations in the Gibbs measure for canonical ensembles, $e^{-\beta\mathcal{H}^{\mathrm{E}}}$, where $\beta = 1/k_{\mathrm{B}}T$, i.e., the inverse temperature. The M permanent random crosslinks between the N polymers is specified by the set of M constraint equations,

$$\mathbf{c}_{i_e}(s_e) = \mathbf{c}_{i'_e}(s'_e), \text{ where } e = 1,\ldots,M. \tag{2.2}$$

This implies that the monomer s_e on the i_e-th polymer is crosslinked to the s'_e-th monomer of the i'_e-th polymer. What is the partition function $Z(\chi)$ of the system with a particular realization of crosslinking, which we denote by the shorthand χ [and define by Eq. 2.2]? This partition function is given by

$$Z^{\chi} \propto \left\langle \prod_{e=1}^{M}\delta^D\left(\mathbf{c}_{i_e}(s_e)-\mathbf{c}_{i'_e}(s'_e)\right)\right\rangle^{\mathrm{E}}, \tag{2.3}$$

where the angular brackets denote a thermal average using the effective Hamiltonian given by Eq. (2.1). Any configuration not obeying the configuration is explicitly excluded by the product of δ-functions.

A distribution determining the probability of a particular realization χ of crosslinks is to be specified. The intuitive assertion, that two particles physically close to each other at the instant prior to the introduction of crosslinks are more likely to get crosslinked, in comparison to particle pairs that are separated by a large distance, should be captured by a meaningful probability distribution of crosslinks. Deam and Edwards [5] proposed a distribution of crosslinks that is indeed

capable of capturing such liquid-like correlations of the system at the instance of crosslinking. The Deam-Edwards distribution is given by

$$P_M(\chi) \propto \frac{\left(\mu^2\right)^M}{M!} Z(\chi), \tag{2.4}$$

where χ is a particular realization of M crosslinks and μ^2 is a parameter that controls the average crosslink density. One allows the number of crosslinks to vary in a Poisson-like distribution; in the thermodynamic limit this is equivalent to having a fixed number of crosslinks. To understand the Deam-Edwards distribution, note that the constrained partition function $Z(\chi)$ is used to assign a statistical weight for a particular realization of crosslinking. This is a clever gadget; a realization of the constraints that demands a rare liquid-state configuration of polymers, or is energetically unfavorable, would be penalized. For example, imagine a crosslinking configuration where the crosslinks glue the polymers together into compact entity in the solution. This is an staggeringly rare event entropically. Moreover, the excluded-volume interaction between the polymers in the liquid also makes it highly unfavorable energetically. The Deam-Edwards probability has such information encoded into it, because $Z(\chi)$ for such a configuration would be very small in comparison to its value for a typical configuration.

2.1.2 Replica formalism

In order to obtain meaningful quantities, we need to average the free energy over the quenched disorder. The free-energy, for a particular realization of disorder, is proportional to the logarithm of the partition function, which itself is an average over the annealed (thermally fluctuating) degrees of freedom. We disorder-average over the free energy because we expect that in the thermodynamic limit physical quantities are *self-averaging*, i.e., do not depend on a particular realization of disorder. The notion of *self-averaging* is roughly as follows. Imagine dividing up equally a D-dimensional system of macroscopic volume $L_{\rm sys}^D$ into a very large number $N_{\rm sub}$ of subsystems that are also of macroscopic volume themselves[2]. Each of these macroscopic volumes can be regarded as a particular realization of the disorder, and since they are macroscopic systems, interactions at the boundary

[2]What can be considered a macroscopic volume for a particular physical system is determined by the typical lower length-cutoff ξ_0 in the problem, for example, the typical size of constituent objects, and the typical correlation length $\xi_{\rm cor}$; hence, *macroscopic* roughly implies $L_{\rm sys} > \xi_{\rm cor} \gg \xi_0$.

can be ignored. If $N_{\rm sub}$ is large enough, or more precisely, $L_{\rm sys}^D/N_{\rm sys}$ approaches a macroscopic volume $L_{\rm sub}^D$ when both $L_{\rm sys}$ and $N_{\rm sub}$ go to infinity, one can regard the free energy of the system of volume $L_{\rm sys}^D$ to be a disorder average over the free energies of all the subsystems.

It is not obvious how to compute the disorder average of the free energy because the free energy is the *logarithm* of the partition function. One typically has to resort to tricks to do this averaging, and a common one is the replica method. Other tricks used in the literature include the supersymmetry method and the dynamical method, for a parallel discussion of these methods see Ref. [22]. In the replica method, the averaged free energy $\mathcal{F}$ is computed using the mathematical identity

$$-\frac{\mathcal{F}}{T} = \ln\left[Z(\chi)\right] = \lim_{n\to 0}\frac{[Z(\chi)^n]-1}{n}, \tag{2.5}$$

where square brackets denote disorder averaging. The quantity $Z(\chi)^n$ is disorder averaged for integral number n of *replica* of the system, and the $n\to 0$ limit is taken at the end of all calculations.[3] Note that in our problem, the replicated partition function to be disorder averaged is $Z(\chi)^n$, i.e., the replicated partition function of the system after the specific realization χ of crosslinks has been imposed. The Deam-Edwards distribution asserts that the probability distribution of crosslinks is also equal to $Z(\chi)$, hence we end up with $n+1$ replicas, instead of the usual n, replicas of the system, where the zeroth replica encodes information about the crosslink distribution. After exponentiating the sum over all crosslink configurations and all possible numbers of crosslinks, the quantity $[Z(\chi)^n]$ is given by

$$\begin{aligned}
[Z(\chi)^n] &\propto \int \mathcal{D}\mathbf{c}\exp\left\{-\frac{1}{2}\sum_{i=1}^{N}\int_0^1 ds\sum_{\alpha=0}^{n}\left|\frac{d}{ds}\mathbf{c}_i^\alpha(s)\right| - \mathcal{H}_{n+1}^I\right\},\\
\mathcal{H}_{n+1}^I &\equiv \frac{\lambda^2}{2}\sum_{i,i'=1}^{N}\int_0^1 ds\int_0^1 ds'\sum_{\alpha=0}^{n}\delta^D\left(\mathbf{c}_i^\alpha(s)-\mathbf{c}_{i'}^\alpha(s')\right)\\
&\qquad -\frac{\mu^2 V}{2N}\sum_{i,i'=1}^{N}\int_0^1 ds\int_0^1 ds'\prod_{\alpha=0}^{n}\delta^D\left(\mathbf{c}_i^\alpha(s)-\mathbf{c}_{i'}^\alpha(s')\right),
\end{aligned} \tag{2.6}$$

and the path integral over the replicated monomer locations is denoted by the shorthand $\int\mathcal{D}\mathbf{c}$. The

[3] If taking the integral number of replicas to zero makes you queasy, I completely empathize! On numerous occasions, whenever I have worried a bit too much about replicated quantities, I have had nightmares which inevitably ended with the ominous vision of my grave with the epitaph: 'Herein vanished the residue, in the $n\to 0$ limit, of a misguided soul.'

main reasons for presenting the replicated interaction Hamiltonian $\mathcal{H}^I_{n+1}$ is two-fold. Firstly, I want to draw your attention to the $n+1$ fold permutation symmetry of the replicas. This is an artifact of the Deam-Edwards distribution, not an intrinsic symmetry in the problem. The *preparational ensemble* (i.e. the zeroth replica which determines the crosslink distribution) is identical to the *measurement ensembles* (i.e. the replicas 1 to n which are used to do the disorder averaging) in the Deam-Edwards prescription. One can envisage using other forms of crosslink distribution that do not have this feature, and the resulting theory would have permutation symmetry of the n measurement ensembles alone. However, it is technically easier to work with more symmetric theory, and we will relax the $n+1$ permutation symmetry to n permutation symmetry only when it becomes necessary to do so in the work presented in Chapter 5 of this Thesis. Secondly, the competition between the excluded volume interaction of strength λ^2, and the 'crosslink interaction' (which is proportional to the crosslink density control parameter μ^2), has very interesting implications for the critical degrees of freedom of the theory, and I will discuss it in Section 2.3. Also note that the excluded volume interaction is a *sum* over delta functions; it is a two-body interaction energy. In contrast, the terms arising from crosslinking are *products* over delta functions. In the next, section the order parameter for the V/G transition is discussed.

2.2 Order parameter

The order parameter[4] of the for the V/G transition must be able to distinguish between the liquid and the random solid. In the liquid, all particles are delocalized, owing to their thermal motion, and are therefore randomly distributed over the entire system volume. On the other hand, in the random solid, a fraction of particles are localized about their mean positions, meaning that their thermal motion is limited to a region of space much smaller than the system volume. However, these mean positions are, in turn, randomly distributed in space owing to the random nature of the crosslinking. In contrast, in a crystalline solid, the mean positions of particles form a regular lattice. Imagine introducing a lot of tracer particles and taking a snapshot of the liquid and the random solid and imaging them at an instant of time. If one compares a single such image, one cannot

[4]It seems that the word 'order' first bore this contextual meaning associated with phase transitions as late as 1933, when the equivalent German word 'ordnung' was introduced in the scientific literature by P. Ehrenfest.

distinguish the liquid and the random solid, because the all the particles will appear to be randomly distributed in space with, at most, short-ranged correlations. On the other hand, a crystalline solid can indeed be distinguished from a liquid using a single such image because the particles, to a good approximation, will appear in the image to occupy the site of a regular lattice. The situation here is similar to the distinction between a spin glass (analogous to random solid), a ferromagnet (analogous to a crystalline solid) and a paramagnet (analogous to the liquid). The construction of the order parameter for the V/G transition was indeed inspired by this analogy [7]. To carry on further with our *Gedanken* experiment of imaging the particles, imagine taking successive images of the solid during a long period of time and comparing these images with each other. In these images there will be some particles that always appear to be close to certain positions in space; they are the localized fraction of particles. Hence, a particle-specific density auto-correlation function will be able to distinguish the liquid and the random solid because there are static density fluctuations in the random solid; such a function is of the form $\langle \exp i\mathbf{k} \cdot (\mathbf{R}_j(t) - \mathbf{R}_j(0)) \rangle_\chi$, where $\mathbf{k}$ is the probe wave vector, $\mathbf{R}_j(t)$ is the position vector of the j-th particle at time t, and angular brackets imply a thermal average for a specific realization of disorder (denoted by χ). If the particle j is localized then its position remains correlated to itself, even in the infinite-time limit. In this limit the auto-correlation function becomes $\langle \exp i\mathbf{k} \cdot \mathbf{R}_j \rangle_\chi \langle \exp -i\mathbf{k} \cdot \mathbf{R}_j \rangle_\chi$ because the variables $\mathbf{R}_j(t)$ and $\mathbf{R}_j(0)$ becomes independent of each other.

The appropriate order parameter for the V/G transition is a generalization of the above suggestion. The order parameter depends on an arbitrary number ν (≥ 2) of tunable (but nonzero) wave vectors $\left(\mathbf{k}^1, \mathbf{k}^2, \ldots, \mathbf{k}^\nu\right)$:

$$\Omega(\mathbf{k}^1, \ldots \mathbf{k}^\nu) = \Big[\frac{1}{J} \sum_{j=1}^{J} \langle \mathrm{e}^{i\mathbf{k}^1 \cdot \mathbf{R}_j} \rangle \langle \mathrm{e}^{i\mathbf{k}^2 \cdot \mathbf{R}_j} \rangle \cdots \langle \mathrm{e}^{i\mathbf{k}^\nu \cdot \mathbf{R}_j} \rangle \Big]. \tag{2.7}$$

where J is rthe number of particles. Recall that angular brackets $\langle \cdots \rangle$ denote an equilibrium thermal expectation value, taken in the presence of a given realization of the quenched random constraints and that square brackets $[\cdots]$ denote an average over the various realizations of the quenched random constraints. Additional discussion of this circle of ideas is given in Refs. [19, 21].

To acquire some feeling for how this order parameter works, consider the illustrative example in which a fraction $1 - Q$ of the particles are delocalized whilst the remaining fraction Q are localized,

harmonically and isotropically but randomly, having random mean positions $\langle \mathbf{R}_j \rangle$ and random mean-square displacements from those positions

$$\left\langle \left(\mathbf{R}_j - \langle \mathbf{R}_j \rangle\right)_d \left(\mathbf{R}_j - \langle \mathbf{R}_j \rangle\right)_{d'} \right\rangle = \delta_{dd'} \, \xi_j^2, \tag{2.8}$$

where d and d' are cartesian indices running from 1 to D. It is straightforward to see that for this example the order parameter becomes

$$\Omega(\mathbf{k}^1, \ldots \mathbf{k}^\nu) = Q \; \delta_{\mathbf{0}, \sum_{a=1}^{\nu} \mathbf{k}^a} \int_0^\infty d\xi^2 \mathcal{N}(\xi^2) \, \exp\Big(- \frac{\xi^2}{2} \sum_{a=1}^{\nu} |\mathbf{k}^a|^2 \Big), \tag{2.9}$$

where

$$\mathcal{N}(\xi^2) \equiv \left[(QJ)^{-1} \sum_{j \, \text{loc.}} \delta(\xi^2 - \xi_j^2) \right] \tag{2.10}$$

is the disorder-averaged distribution of squared localization lengths ξ^2 of the localized fraction of particles [20, 19, 21]. Note that for a crystalline solid, the order parameter is nonzero not only when $\sum_{a=1}^{\nu} \mathbf{k}^a = \mathbf{0}$, but also when $\sum_{a=1}^{\nu} \mathbf{k}^a = \mathbf{G}$, where $\mathbf{G}$ is any reciprocal lattice vector of the appropriate Bravais lattice. However, in conventional crystalline solids the particles are strictly localized; they can diffuse via vacancy defects. The collective density pattern of the particles are however frozen. This is a fundamentally different from the localization of particles in random solids discussed here.

We now mention the important issue of spontaneous symmetry breaking in the V/G transition; a more detailed discussion will be given in the next chapter. The above illustrative example correctly captures the pattern in which symmetry is spontaneously broken when there are enough random constraints to produce the amorphous solid state: microscopically, random localization fully eliminates translational symmetry; but macroscopically this elimination is not evident. Owing to the absence of any residual symmetry, such as the discrete translational symmetry of crystallinity, all macroscopic observables are those of a translationally invariant system. This shows up as the vanishing of the order parameter, even in the amorphous solid state, unless the wave vectors sum to zero, i.e., $\sum_{a=1}^{\nu} \mathbf{k}^a = \mathbf{0}$.

The case $\nu = 1$ is excluded from the list of order parameter components shown in Eq. (2.7). This

case corresponds to *macroscopic* density fluctuations, and these are assumed to remain small and stable (i.e. non-critical) near the amorphous solidification transition, being suppressed by forces, such as the excluded-volume interaction, that tend to maintain homogeneity. This stabilization, of what we call, the *Lower Replica Sector* for the order parameter, is derivable from the microscopic model, and we discuss this *Replica Sector Constraint* in the next section. Additional insight into the nature of the constraint-induced instability of the liquid state and its resolution (in terms of the formation of the amorphous solid state—a mechanism for evading macroscopic density fluctuations) can be found in Ref. [21], especially Sec. 4.2.

2.3 Landau-Wilson effective theory and summary of mean-field results

In this section we introduce the Landau-Wilson effective energy for the V/G transition. The details of its derivation from the microscopic model is presented elsewhere and we do not reproduce it here; see Ref. [19]. One of the important feature of this effective theory is that the critical degrees of freedom are restricted to what we call the *Higher Replica Sector*. To understand this constraint, consider the space of replicated wave-vectors $\hat{k} = \left(\mathbf{k}^0, \mathbf{k}^1, \ldots, \mathbf{k}^n\right)$, where $\mathbf{k}^\alpha$ is the D-dimensional wave-vector for the α-th replica. We decompose this space into three disjoint sets:

1. The *Higher Replica Sector* (HRS), which consists of all $\hat{k}$ containing at least two nonzero component-vectors $\mathbf{k}^\alpha$. For example, if $\hat{k} = \left(\mathbf{0}, \ldots, \mathbf{0}, \mathbf{k}^\alpha \neq \mathbf{0}, \ldots, \mathbf{k}^\beta \neq \mathbf{0}, \mathbf{0}, \ldots, \mathbf{0}\right)$ then $\hat{k}$ lies in HRS. For this particular example, $\hat{k}$ lies in the Two-Replica Sector of the HRS.

2. The *One-Replica Sector* (1RS), which consists of those $\hat{k}$ containing exactly one nonzero component vector $\mathbf{k}^\alpha$, e.g., $\hat{k} = (\mathbf{0}, \ldots, \mathbf{0}, \mathbf{k}^\alpha \neq \mathbf{0}, \mathbf{0}, \ldots, \mathbf{0})$.

3. The *Zero-Replica Sector* (0RS) which consists of the vector $\hat{k} = 0$.

For wave-vectors $\hat{k}$ lying in the 0RS or the 1RS we say that the corresponding order parameter $\Omega(\hat{k})$ is in the *Lower Replica Sector* (LRS). Similarly, for $\hat{k}$ lying in the HRS, we say that the corresponding order parameter $\Omega(\hat{k})$ to be in the HRS. The important point is the LRS order parameter fields are stabilized by a strong excluded volume interaction, and they are non-critical,

i.e., neither do they exhibit critical fluctuations at the vulcanization transition nor do they acquire non-zero expectation value in the amorphous solid state. If one reminds oneself of the simpler incarnation of the order parameter in the language of auto-correlation functions discussed in the first paragraph of the previous section., it is easy to see that a LRS order parameter would measure the local monomer density and not auto-correlations; the disorder-averaged local density is identical in both the liquid and the amorphous solid state and hence fails to distinguish them.

We finally present the effective replica free energy governing the vulcanization/gelation transition (V/G);

$$\mathcal{H}_{\rm VG} = \sum_{\hat{k}\in{\rm HRS}} \frac{1}{2}(\hat{k}^2+\tau_0)|\Omega(\hat{k})|^2 - \frac{g_0}{3!}\sum_{\hat{k}_1,\hat{k}_2,\hat{k}_3\in{\rm HRS}} \Omega(\hat{k}_1)\Omega(\hat{k}_2)\Omega(\hat{k}_3)\delta(\hat{k}_1+\hat{k}_2+\hat{k}_3) \quad (2.11a)$$

$$= \int_{\rm HRS} d^{(n+1)D}\hat{x}\left\{\frac{1}{2}|\widehat{\nabla}\Omega(\hat{x})|^2 + \frac{1}{2}\tau_0\Omega(\hat{x})^2 - \frac{g_0}{3!}\Omega(\hat{x})^3\right\}. \quad (2.11b)$$

Here, $\Omega(\hat{k})$ is the order parameter as a function of the $(n+1)$-fold replicated momentum $\hat{k} \equiv (\mathbf{k}_0,\ldots,\mathbf{k}_n)$ and $\Omega(\hat{x})$ is its Fourier transform [23], which is a function of the $(n+1)$-fold replicated position $\hat{x} \equiv (\mathbf{x}_0,\ldots,\mathbf{x}_n)$ conjugate to $\hat{k}$. In Eq. (2.11) the control parameter τ_0 measures the the deviation of the crosslink density from its critical value, and the parameter g_0 is the bare coupling constant of the cubic interaction. In the $n \to 0$ limit, power counting indicates that the upper critical dimension of this theory is six. The restriction on momentum summations, $\hat{k} \in$ HRS, indicates the inclusion only of Higher Replica Sector (HRS) vectors, as discussed above. In real space, the HRS subscript on the integral is just a reminder that the space of fields is restricted accordingly, for example, by imposing the condition,

$$\Omega_\alpha(\mathbf{x}^\alpha) \equiv \int \prod_{\beta(\neq\alpha)} d\mathbf{x}^\beta\, \Omega(\hat{x}) \to \infty, \quad (2.12)$$

which ensures that order parameter fluctuations in the LRS are disallowed, or equivalently, LRS fields have infinite mass; see Eq. (5.26) and the discussion following it. The subscript zero is used to distinguish bare parameters from their corresponding renormalized parameters; wherever this distinction is unnecessary I will drop the subscripts without warning. I hope this will create no confusion. It is only in Chapter 4 that this distinction is crucial.

We now summarize the results of the mean-field treatment of the Landau-Wilson theory, Eq. (2.11), see refs. [20, 34, 21, 19] for details. The saddle-point value $M_0(\hat{k})$ of the expectation value of the order parameter $\langle\Omega(\hat{k})\rangle_0$, is obtained by solving the stationarity condition

$$\tau_0 M_0(\hat{k}) + \hat{k}^2 M_0(\hat{k}) - \frac{g_0}{2} \sum_{\hat{l}\in \mathrm{HRS}} M_0(\hat{k}) M_0(\hat{k}-\hat{l}) = 0, \tag{2.13}$$

subject to the constraint that the solution is a field that obeys the HRS constraint. The nature of spontaneous symmetry breaking in this problem will be analyzed in the next chapter. To streamline the presentation, we adopt the notation in which the D-component vector $k_\parallel$ is proportional to the 'center of mass' coordinate in momentum space, and corresponds to the conserved translational symmetry, and $k_\perp$ denotes the nD-dimensional subspace of $\hat{k}$ transverse to $k_\parallel$, i.e.,

$$\hat{k} = (k_\parallel, k_\perp) \quad \text{and} \quad k_\parallel = \frac{1}{\sqrt{1+n}} \sum_{\alpha=0}^{n} \mathbf{k}^\alpha . \tag{2.14}$$

A detailed discussion of the geometry of decomposing the space of replicated $(n+1)D$-dimensional vectors $\hat{k}$ into a D-dimensional *longitudinal* space $k_\parallel$ and nD-dimensional *transverse* space $k_\perp$ will be given in section 3.3.1. In terms of these coordinates, it has been shown [19] that the solution of the saddle-point equation has a form

$$M_0(\hat{k}) = -Q\,\delta_{\hat{k},\hat{0}} + Q\,\delta_{k_\parallel,\mathbf{0}} \int_0^\infty d\zeta \;\; \mathcal{P}_0(\zeta)\, e^{-\hat{k}^2/2|\tau_0|\zeta} =: Q\, m_0(|\tau_0|^{-1/2}\hat{k}), \tag{2.15}$$

where Q is the gel fraction (fraction of localized particles) and $\mathcal{P}_0(\zeta)$ is the scaled distribution of (inverse squared) localization lengths. Compare this equation with Eq. (2.9); it turns out that the Ansatz form in which a fraction of particles are localized harmonically solves the saddle-point equation, and therefore, Eq. (2.15) and Eq. (2.9) have the same content. The fraction of localized particles Q are those that form the infinite cluster in the random solid state. It is useful, for later discussion, to reveal the connection between the distribution of squared localization lengths $\mathcal{N}(\xi^2_{\mathrm{loc}})$ appearing in Eq. (2.9), and the scaled distribution of localization lengths $\mathcal{P}(\zeta)$ appearing in Eq. (2.15) in terms of the distribution of (squared) localization length $\mathcal{N}(\xi^2_{\mathrm{loc}})$. The saddle point

solution is given by

$$M_0(\hat{k}) = -Q\,\delta_{\hat{k},\hat{0}} + Q\,\delta_{k_\parallel,\mathbf{0}} \int_0^\infty d\xi_{\rm loc}^2\, \mathcal{N}(\xi_{\rm loc}^2)\, e^{-\xi_{\rm loc}^2 \hat{k}^2/2}, \tag{2.16a}$$

$$\mathcal{N}(\xi_{\rm loc}^2) = \left(\xi_0^2/|\tau_0|\xi_{\rm loc}^4\right) \mathcal{P}_0\left(\xi_0^2/|\tau_0|\xi_{\rm loc}^2\right). \tag{2.16b}$$

where ξ_0 is the linear size of objects being crosslinked and serves as the short-distance cutoff[5]. Fourier transform shows that in real space, the saddle-point solution takes the form

$$M_0(\hat{x}) = Q \int d\mathbf{z} \int d\zeta\, \mathcal{P}_0(\zeta)\, \left(\frac{\zeta}{2\pi}\right)^{(n+1)D/2} \exp\left[-\frac{\zeta}{2}\sum_{\alpha=0}^{n} (\mathbf{x}^\alpha - \mathbf{z})^2\right] - \frac{Q}{V^{1+n}}. \tag{2.17}$$

By introducing the mean-field scaling variables $\theta_0 = \tau_0(g_0 Q)^{-1}$ and $\hat{q} \equiv \hat{k}\,|\tau_0|^{-1/2}$ along with the mean-field scaling function $m_0(\hat{q})$, the saddle-point equation can be recast in the form

$$\theta_0 m_0(\hat{q}) + |\theta_0|\,\hat{q}^2\, m_0(\hat{q}) - \frac{1}{2}\sum_{\hat{p}\in HRS} m_0(\hat{p})\, m_0(\hat{q}-\hat{p}) = 0. \tag{2.18}$$

By making the Ansatz (2.15) for the solution of this form of the saddle-point equation we obtain the following condition on θ_0 and $\mathcal{P}_0$:

$$\delta_{q_\parallel,\mathbf{0}} \left[(\theta_0 + 1 + |\theta_0|\, q^2) \int_0^\infty d\zeta\ \ \mathcal{P}_0(\zeta)\, e^{-\hat{q}^2/2\zeta} - \frac{1}{2}\int_0^\infty d\zeta_1\ \ \mathcal{P}_0(\zeta_1) \int_0^\infty d\zeta_2\ \ \mathcal{P}_0(\zeta_2) e^{-\hat{q}^2/2(\zeta_1+\zeta_2)}\right] = 0. \tag{2.19}$$

By taking the $\hat{q} \to 0$ limit of this equation through a sequence for which $q_\parallel = 0$, one finds that $\theta_0 = -1/2$. Therefore, when $\tau_0 < 0$ there is a solution with non-zero gel fraction: $Q = 2|\tau_0|/g$. Then, by using $\theta_0 = -1/2$, Eq. (2.19) reduces to a integro-differential equation [19] for $\mathcal{P}_0(\zeta)$, i.e.,

$$2\zeta^2 \frac{d}{d\zeta}\mathcal{P}_0(\zeta) = (1-4\zeta)\mathcal{P}_0(\zeta) - \int_0^\zeta d\zeta'\, \mathcal{P}_0(\zeta')\, \mathcal{P}_0(\zeta-\zeta'). \tag{2.20}$$

Note that the above equation does not involve replicated quantities. The resulting mean-field distribution of localization lengths can be found by solving the integro-differential equation numerically; the solution is shown in Fig. 2.1. The asymptotic form of the solution is as follows:

[5] It is customary to absorb the short-distance cutoff ξ_0 in the Hamiltonian for a field theory by rescaling the order parameter; this is implicit in the expression for the effective Hamiltonian given by Eq. (2.11). If this rescaling were not performed then the gradient term in the Hamiltonian, for example, would be $\xi_0^2 \hat{k}^2 |\Omega(\hat{k})|^2$.

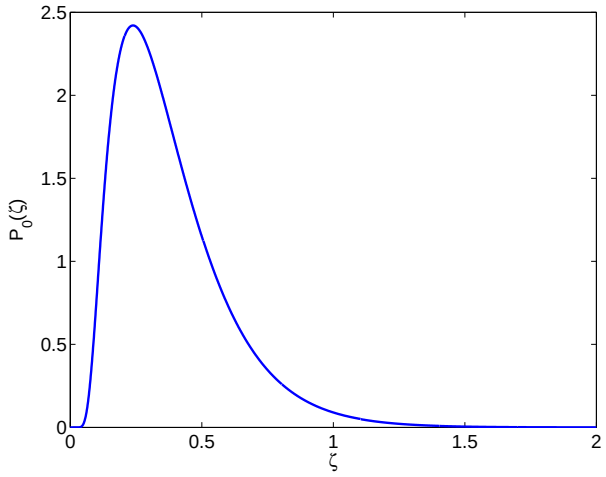

Figure 2.1: The distribution function $\mathcal{P}_0(\zeta)$

$$\mathcal{P}_0(\zeta) \approx \begin{cases} \frac{a}{4\zeta^2} e^{-\frac{1}{2\zeta}}, a = 4.554 & \text{for } \zeta \ll 1 \ ; \\ 12(4b\zeta - 3/5)e^{-4b\zeta}, \ b = 1.678 & \text{for } \zeta \gg 1. \end{cases} \tag{2.21}$$

Recalling the relationship between $\mathcal{P}_0(\zeta)$ and the distribution $\mathcal{N}(\xi^2_{loc})$ given by Eq. (2.16b), it is clear that the distribution of (squared) localization lengths is peaked around a typical localization length, away from which it decays rather rapidly. This implies that, at the mean-field level, a large fraction of the localized fraction of particles are localized with a localization length close to the typical localization length, where as only a small fraction of localized particles have localization lengths that deviate drastically from the typical value. Data from numerical simulations agree well with the universal distribution function $\mathcal{P}(\zeta)$, see Ref. [24].

Chapter 3

Goldstone fluctuations and their implications for the random solid—Part 1

> The gigantic flames trembled and hid
> Coldness, darkness, obstruction, a Solid
> Without fluctuation, hard as adamant
> Black as marble of Egypt; impenetrable
> Bound in the fierce raging Immortal.
>
> — William Blake, *The Book of Los*

3.1 Introduction

When a continuous symmetry is spontaneously broken in a quantum field theory massless excitations of the ordered state arise; a result known as the *Goldstone theorem* [25]. In a condensed matter system, these Goldstone excitations correspond to long-wavelength, low-energy fluctuations of the ordered state because the 'mass' of a field corresponds to the inverse correlation length for the fluctuations associated with that field; therefore massless excitations give rise to diverging correlation lengths. Goldstone fluctuations are fundamentally different from other fluctuations considered in a critical theory. All other critical fluctuations are long-ranged in the critical region alone, and are massless (i.e. infinite-ranged) strictly at the critical point. In contrast, the Goldstone excitations are infinite-ranged throughout the entire ordered state of an (infinite) system. Consider the example of the $O(N)$ model for the ferromagnetic-paramagnetic transition, where the Goldstone fluctuations are the spin-waves associated with the spin direction transverse to the direction of magnetization. These fluctuations are infinite-ranged on the coexistence curve, which is defined

to be a line of critical points given by the zero of the function f in the magnetic scaling relation $h/M^{\delta} = f(\tau/M^{1/\beta})$, where, h is the external magnetic field, M is the magnetization, β and δ are the critical exponents. In the h vs. T parameter space, this curve terminates on an ordinary critical point (also known as the critical isotherm) where *both* the correlation lengths for the longitudinal and transverse fluctuations diverge, see Ref. [49]. The $O(N)$ model is an example of an *internal symmetry breaking* system; the broken symmetry is associated with an internal degree of freedom of the order parameter, viz., the spin. In contrast, our discussion in this chapter will reveal that the symmetry breaking is *external* in the V/G problem, i.e., the broken symmetry group is associated with the *argument* of the order parameter; viz., the spatial coordinates.

The aim of this chapter is to identify the long wave-length, low energy fluctuations of the random solid state, and to investigate their physical consequences. In particular, by constructing an effective free energy that governs these *Goldstone-type* fluctuations, we shall determine the elastic properties of the amorphous solid, including its static shear modulus. We shall also analyze the effect of these fluctuations on the random solid order parameter, and hence determine their impact on physical quantities such as the distribution of localization lengths and the order parameter correlations. Along the way we shall reveal the physical information encoded in these correlations. As the Goldstone fluctuations are dominant deep inside the amorphous solid state, the effective theory that excludes all other fluctuations is valid deep inside the random solid state, ie., far from the critical point associated with the V/G phase transition.

We shall pay particular attention to systems of spatial dimension two, for which we shall see that the effect of fluctuations is strong: particle localization is destroyed, the order parameter is driven to zero, and order-parameter correlations decay as a power law in the separation between points in the sample. Thus we shall see that the amorphous solid state is, in many respects, similar to other states of matter exhibiting (or nearly exhibiting) spontaneously broken continuous symmetry.

This chapter is organized as follows. IIn Section 3.3 we describe the structure of the low energy, long wave-length Goldstone-type excitations of the amorphous solid state in terms of distortions of the value of the order parameter. Here, we also make the identification of these order-parameter distortions as local displacements of the amorphous solid. In Sections. 3.4 and 3.5 we determine the energetics of these Goldstone-type excitations by beginning with a Landau-type free energy ex-

pressed in terms of the amorphous solid order parameter and ending with elasticity theory. Along the way, we derive a formula for the elastic shear modulus, which shows how this modulus vanishes, as the liquid state is approached, at the classical (i.e. mean-field theory) level. In Section 3.6 we discuss the impact of Goldstone-type fluctuations on the structure of the amorphous solid state by examining how they diminish the order parameter and modify the distribution of localization lengths. We analyze the impact of such fluctuations on the order-parameter correlations, and also catalog the various length-scales that feature in the chapter. In Section 3.7 we take a closer look at the effects of Goldstone-type fluctuations on structure and correlations in two-dimensional amorphous solids. In particular, we show that Goldstone-type fluctuations destroy particle localization, the order parameter is driven to zero, and power-law order-parameter correlations hold, and we illustrate these features for certain special cases. In Section 3.8 we discuss the physical content of order-parameter correlations in terms of spatial correlations in the statistics of the localization lengths. We also introduce distributions of correlators, and relate their moments to order-parameter correlators. Some concluding remarks are given in Section 3.9. Technical details are relegated to four appendices; A, B, C and D.

The work presented in this Chapter was done in collaboration with A. Zippelius and P. M. Goldbart.

3.2 Amorphous solid state; symmetries and symmetry breaking

We have introduced the order parameter for the V/G transition in the previous chapter; see Section 2.2. We have also alluded to the nature of spontaneous symmetry breaking in the V/G transition. In this section we present an elaborate discussion of it. How does the order parameter (2.7) transform under translations of the particles? If, in the element $\langle \exp i\mathbf{k}^a \cdot \mathbf{R}_j \rangle$, one makes the translation $\mathbf{R}_j \to \mathbf{R}_j + \mathbf{r}^a$ then the element is multiplied by a factor $\exp i\mathbf{k}^a \cdot \mathbf{r}^a$ and so the order parameter acquires a factor $\exp i \sum_{a=1}^{\nu} \mathbf{k}^a \cdot \mathbf{r}^a$. Now, in the fluid state no particles are localized and the order parameter has the value zero, so it is invariant under the aforementioned translations. By contrast, in the amorphous solid state the order parameter is nonzero, provided the wave vectors sum to zero. Thus, the order parameter varies under the translations unless the translation is common to each element, i.e., $\mathbf{r}^a = \mathbf{r}$. To summarize, the liquid-state symmetry

of the independent translations of the elements is broken down, at the amorphous solidification transition, to the residual symmetry of the common translation of the elements.

When replicas are employed to perform the average over the quenched disorder (i.e. the number and location of the constraints), what emerges is a theory of a field $\widehat{\Omega}(\hat{x})$ defined over $(1+n)$-fold replicated space $\hat{x}$, so that the argument $\hat{x}$ means the collection of $(1+n)$ position D-vectors $(\mathbf{x}^0, \mathbf{x}^1, \ldots, \mathbf{x}^n)$ conjugate to the wave vectors $(\mathbf{k}^0, \mathbf{k}^1, \ldots, \mathbf{k}^n)$, as we have mentioned in Chapter 2. According to the replica methodology, it is understood that the limit $n \to 0$ is to be taken at the end of any calculation. In terms of replicas, the expectation value of this field $\langle \Omega(\hat{x}) \rangle$ is proportional to

$$\left\langle J^{-1} \sum_{j=1}^{J} \prod_{\alpha=0}^{n} \delta\big(\mathbf{x}^\alpha - \mathbf{R}_j^\alpha\big) \right\rangle \tag{3.1}$$

and its Fourier transform $\Omega(\hat{k}) = \int dx \, \exp(i\hat{k} \cdot \hat{x}) \, \widehat{\Omega}(x)$, has the form

$$\Omega(\hat{k}) = \left\langle J^{-1} \sum_{j=1}^{J} \exp i \sum_{\alpha=0}^{n} \mathbf{k}^\alpha \cdot \mathbf{R}_j^\alpha \right\rangle . \tag{3.2}$$

The field $\widehat{\Omega}(\hat{x})$ fluctuates subject to the demand, mentioned above, that the critical freedoms are only the corresponding Fourier amplitudes $\Omega(\hat{k})$ for which at least two of the D-component entries in the argument $\hat{k} \equiv (\mathbf{k}^0, \mathbf{k}^1, \ldots, \mathbf{k}^n)$ are nonzero. Both a semi-microscopic approach and arguments based on symmetries and length-scales yield a Landau-Wilson effective Hamiltonian governing the fluctuations of this field, which is invariant under independent translations of the replicas but whose precise structure we shall discuss later. For now, let us just mention that the corresponding expectation value of this field is the order parameter (2.7) with $\nu = 1+n$: it becomes nonzero in the amorphous solid state and, in doing so, realizes the pattern of spontaneous symmetry breaking described above. Invariance under independent translations of the replicas breaks down to invariance under the subgroup of common translations of the replicas.

3.3 Goldstone fluctuations: Structure and identification

3.3.1 Formal construction of Goldstone fluctuations

In the amorphous solid state, one of the symmetry-related family of classical values of the order parameter has the form

$$\Omega(\hat{k}) = \delta_{\mathbf{k}_{\rm tot},\mathbf{0}}\, \mathcal{W}(k_\perp) = \int_{\mathcal{V}} \frac{d\mathbf{x}_{\rm cm}}{V}\, e^{i\mathbf{k}_{\rm tot}\cdot\mathbf{x}_{\rm cm}}\, \mathcal{W}(k_\perp), \tag{3.3}$$

in which $\mathcal{W}$ is real and depends only on the magnitude of $k_\perp$, and $\mathbf{k}_{\rm tot}$ and $\mathbf{x}_{\rm cm}$ are defined in Eq. (3.8). We remind the reader of the results introduced in Section 2.3. Making $\mathcal{H}_{\rm VG}$ given by Eq. 2.11, stationary with respect to Ω results in the classical state (3.3), with the following relationships

$$\mathcal{W}(k_\perp) \equiv Q \int_0^\infty d\xi^2\, \mathcal{N}(\xi^2)\, e^{-\xi^2 k_\perp^2/2}, \tag{3.4a}$$

$$Q = 2|\tau|/g, \tag{3.4b}$$

$$\mathcal{N}(\xi^2) = \big(\xi_0^2/|\tau|\xi^4\big)\, \mathcal{P}\big(\xi_0^2/|\tau|\xi^2\big), \tag{3.4c}$$

where $\mathcal{P}(\zeta)$ is the universal classical scaling function discussed in Section 2.3. Note that Eq. (3.4c) is identical to Eq. (2.16b), and is reproduced here for convenience. Eq. (3.4a) that defines $\mathcal{W}(k_\perp)$ is obtained from comparing the Eq. (2.16a) with Eq. (3.3) and ignoring the LRS-subtraction $(-Q\delta_{\hat{k},\hat{0}})$ for the moment[1]. Some geometry is needed to define the variables in this formula. We introduce a complete orthonormal basis set in replica space $\{\epsilon^\alpha\}_{\alpha=0}^n$, in terms of which vectors k are expressed as

$$k = \sum_{\alpha=0}^{n} \mathbf{k}^\alpha\, \epsilon^\alpha. \tag{3.5}$$

[1]The *very* cautious reader may disagree with me here. The saddle-point solution, given by Eq. (2.16a), strictly speaking, is $\Omega(\hat{k}) = \delta_{k_\parallel,\mathbf{0}}\, \mathcal{W}(\hat{k})$ and not $\Omega(\hat{k}) = \delta_{k_\parallel,\mathbf{0}}\, \mathcal{W}(k_\perp)$. The latter expression of the saddle-point is a rather innocuous simplification of the former. However, once the Goldstone-fluctuations are incorporated to 'deform' the saddle-point, the two seemingly equivalent forms of the saddle-point solution mentioned here become inequivalent in the results they produce; read Chapter 5 right after reading this chapter to see why. At this point I am not expecting the reader to be *that* cautious!

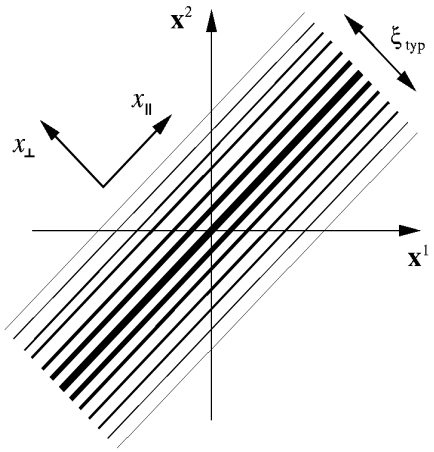

Figure 3.1: Schematic representation of a classical state in replicated real space using two replicas: a hill in $\hat{x}$ space with its ridge aligned in the $x_\parallel$ direction and passing through the origin. The thickness of the lines is intended to suggest the amplitude of the order parameter, the thicker the line the larger the amplitude. Symmetry-related classical states follow from rigid displacements of the hill perpendicular to the ridge, i.e., in the $x_\perp$ direction.

We also introduce the *replica body-diagonal* unit vector

$$\epsilon \equiv \frac{1}{\sqrt{1+n}} \sum_{\alpha=0}^{n} \epsilon^\alpha, \tag{3.6}$$

relative to which we may decompose vectors k into longitudinal ($\parallel$) and transverse ($\perp$) components:

$$k = k_\parallel + k_\perp, \quad k_\parallel \equiv (k \cdot \epsilon)\, \epsilon, \quad k_\perp \equiv k - (k \cdot \epsilon)\, \epsilon. \tag{3.7}$$

We find it convenient to parametrize the longitudinal components of position and wave vectors in the following distinct ways:

$$x_\parallel = (1+n)^{1/2}\, \mathbf{x}_{\rm cm}\, \epsilon, \quad \mathbf{x}_{\rm cm} \equiv \frac{1}{1+n} \sum_{\alpha=0}^{n} \mathbf{x}^\alpha, \tag{3.8a}$$

$$k_\parallel = (1+n)^{-1/2}\, \mathbf{k}_{\rm tot}\, \epsilon, \quad \mathbf{k}_{\rm tot} \equiv \sum_{\alpha=0}^{n} \mathbf{k}^\alpha. \tag{3.8b}$$

Then $\mathbf{x}_{\rm cm}$ and $\mathbf{k}_{\rm tot}$ are, respectively, the analogs of the following conjugate pair of vectors: the center-of-mass position and the total momentum. With them one then has, e.g., $k_\parallel \cdot x_\parallel = \mathbf{k}_{\rm tot} \cdot \mathbf{x}_{\rm cm}$.

The variables just introduced exhibit the structure of a classical state (3.3) as a rectilinear *hill* in x-space, with contours of constant height oriented along $x_\parallel$, as shown in Fig. 3.1. The peak

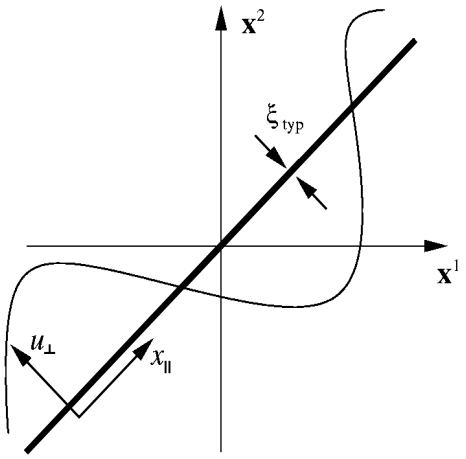

Figure 3.2: Schematic represeantation of Goldstone-distorted state in replicated real space using two replicas: the hill is displaced perpendicular to the ridge to an extent $u_\perp$ that varies with position $x_\parallel$ along the ridge. Note that the scale of this figure is much larger than that used for Fig. 3.1: the thick line lies along the ridge of the classical state, but now it is the *width* of the line that indicates the width of the hill $\xi_{\rm typ}$. The Goldstone-type fluctuations occur on wave-lengths longer than $\xi_{\rm typ}$.

height of the ridge determines the fraction of localized particles; the decay of the height in the direction $x_\perp$ determines the distribution of localization lengths. The width of the hill corresponds to the typical value of the localization length. Translational symmetry induced symmetry-related classical states are generated from Eq. (3.3) by translating the hill rigidly, perpendicular to the ridge-line (i.e. parallel to $x_\perp$). Such a transformation corresponds to relative (but not common) translations of the replicas.

This pattern of symmetry breaking suggests that the Goldstone excitations of a classical state are constructed from it via $x_\parallel$ (or equivalently $\mathbf{x}_{\rm cm}$) -dependent translations of the hill in the $x_\perp$ direction, i.e., ripples of the hill and its ridge. In two equivalent realizations, this gives

$$V\Omega(\hat{k}) = \int_{\mathcal{V}} d\mathbf{x}_{\rm cm}\, e^{i\mathbf{k}_{\rm tot}\cdot\mathbf{x}_{\rm cm} + ik_\perp\cdot u_\perp(\mathbf{x}_{\rm cm})}\, \mathcal{W}(k_\perp), \tag{3.9a}$$

$$V\widehat{\Omega}(x) = \widehat{\mathcal{W}}\left(x_\perp - u_\perp(\mathbf{x}_{\rm cm})\right). \tag{3.9b}$$

Note that we are choosing to define Fourier transforms as follows:

$$\widehat{A}(x) = \int đk_\perp \, đ\mathbf{k}_{\rm tot} \, e^{-ik_\perp \cdot x_\perp} \, e^{-i\mathbf{k}_{\rm tot}\cdot \mathbf{x}_{\rm cm}} \, A(\hat{k}), \tag{3.10a}$$

$$A(\hat{k}) = \int dx_\perp \, d\mathbf{x}_{\rm cm} \, e^{ik_\perp \cdot x_\perp} \, e^{i\mathbf{k}_{\rm tot}\cdot \mathbf{x}_{\rm cm}} \, \widehat{A}(x); \tag{3.10b}$$

also note that

$$\widehat{\mathcal{W}}(x_\perp) \equiv \int đk_\perp \, e^{-ik_\perp \cdot x_\perp} \, \mathcal{W}(k_\perp). \tag{3.10c}$$

Here and elsewhere, bars indicate division by factors of 2π; on integration measures there is one such division for each variable of integration. The details of the excitation are encoded in the replica-transverse field $u_\perp(\mathbf{x}_{\rm cm})$, an nD-component field that depends on the replica-longitudinal position $\mathbf{x}_{\rm cm}$; these are the *Goldstone bosons*, or phonon excitations, of the amorphous solid state. For consistency, we require that the Fourier content of the Goldstone field $u_\perp(\mathbf{x}_{\rm cm})$ occurs at wavelengths long compared with the hill width (i.e. the typical localization length). Otherwise, the energy of the field $u_\perp(\mathbf{x}_{\rm cm})$ would be comparable to other excitations which have been neglected.

The Goldstone excitations that we have just constructed are analogs of the capillary excitations of the interface between coexisting liquid and gas states; see Ref. [26] for a review. In the liquid-gas context they similarly accompany a spontaneous breaking of translational symmetry associated with the choice of interface location. Recently, Low and Manohar [27] have given a general discussion of the structure of Goldstone excitations in the setting of space-time symmetry breaking. The structure discussed here is in accord with the Low-Manohar picture.

Do the Goldstone excitations exhaust the spectrum of low energy excitations of the broken-symmetry state? The complete spectrum of excitations is accounted for by decorating the Goldstone-type parameterizations (3.9a) with additional freedoms $w(k_\perp)$, so that the field $\Omega(\hat{k})$ is expressed as

$$V\Omega(\hat{k}) = \int_{\mathcal{V}} d\mathbf{x}_{\rm cm} \, e^{i\mathbf{k}_{\rm tot}\cdot \mathbf{x}_{\rm cm} + ik_\perp \cdot u_\perp(\mathbf{x}_{\rm cm})} \Big(\mathcal{W}(k_\perp) + w(\hat{k}) \Big), \tag{3.11}$$

where w is a real-valued field that depends on $k_\perp$, suitably constrained to be independent of the Goldstone excitations.

To see that the Goldstone modes (3.9a) do indeed exhaust the spectrum of low energy excita-

tions, we make contact with the linear stability analysis of the classical broken-symmetry state, due to Castillo et al. [28], which identified a family of linearly additive Goldstone-type normal modes of excitation indexed by $\mathbf{k}_{\rm tot}$:

$$V\Omega(\hat{k}) = \int_{\mathcal{V}} d\mathbf{x}_{\rm cm}\, e^{i\mathbf{k}_{\rm tot}\cdot\mathbf{x}_{\rm cm}}\, \mathcal{W}(k_\perp) + ik_\perp \cdot v_\perp(\mathbf{k}_{\rm tot})\, \mathcal{W}(k_\perp), \tag{3.12}$$

with arbitrary replica-transverse amplitude $v_\perp(\mathbf{k}_{\rm tot})$. That this linear glimpse of the Goldstone-type excitations is in accordance with the nonlinear view focused on in the present chapter follows by expanding Eq. (3.11) to linear order in the Goldstone fields $u_\perp$ and omitting the non-Goldstone fields w, thus arriving at

$$V\Omega(\hat{k}) \approx \int_{\mathcal{V}} d\mathbf{x}_{\rm cm}\, e^{i\mathbf{k}_{\rm tot}\cdot\mathbf{x}_{\rm cm}}\, \mathcal{W}(k_\perp) + ik_\perp \cdot \int_{\mathcal{V}} d\mathbf{x}_{\rm cm}\, e^{i\mathbf{k}_{\rm tot}\cdot\mathbf{x}_{\rm cm}}\, u_\perp(\mathbf{x}_{\rm cm})\, \mathcal{W}(k_\perp), \tag{3.13}$$

which shows that $v_\perp(\mathbf{k}_{\rm tot})$ is the Fourier transform of $u_\perp(\mathbf{x}_{\rm cm})$. The reality of $\Omega(x)$ ensures that $\Omega(-k) = \Omega(\hat{k})^*$ and, via Eq. (3.12), that $v_\perp(-\mathbf{k}_{\rm tot}) = v_\perp(\mathbf{k}_{\rm tot})^*$. Via Eq. (3.13), this in turn ensures the reality of $u_\perp(\mathbf{x}_{\rm cm})$. In Ref. [28] it was shown that no other branches of low energy excitations exist; hence the Goldstone excitations of Eq. (3.9a) exhaust the spectrum of low energy excitations.

Some insight into the structure of the Goldstone excitations, which induce deformations of the classical state, is obtained from its replicated real-space version. Consider the interpretation of $\widehat{\Omega}(x)$ as a quantity proportional to the probability density for the positions of the $1+n$ replicas of a particle to have the values $\{\mathbf{x}^\alpha\}_{\alpha=0}^n$; see Eq. (3.1). Then classical states, Eq. (3.9b) at constant $u_\perp$, are ones that describe a translationally invariant *bound states*: $\widehat{\Omega}(x)$ does not depend on the *mean* location of the replicas $\mathbf{x}_{\rm cm}$, but does depend on their *relative* locations, through $x_\perp$, and decays the more the replicas are separated. This point is exemplified by the particular form given in Eq. (3.4a). Now, the Goldstone-distorted state, Eq. (3.9b) with $u_\perp$ varying with $\mathbf{x}_{\rm cm}$, also describes bound states of the replicas, but ones in which the dependence of the probability density on relative locations varies with $\mathbf{x}_{\rm cm}$. The particular form (3.4a), which gives

$$V\widehat{\Omega}(x) = Q \int_0^\infty d\xi^2\, \mathcal{N}(\xi^2)\, \left(2\pi\xi^2\right)^{-nD/2} \exp\left(-|x_\perp - u_\perp(\mathbf{x}_{\rm cm})|^2/2\xi^2\right), \tag{3.14}$$

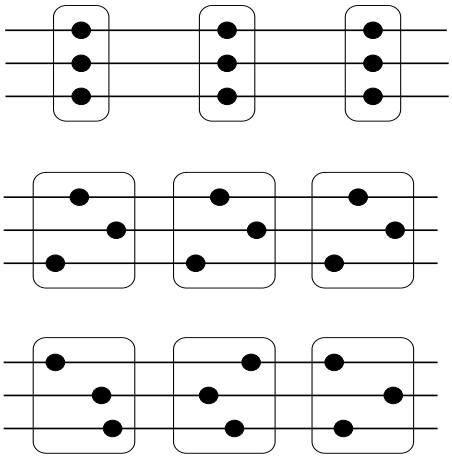

Figure 3.3: *Molecular bound state* view of the classical and Goldstone-distorted states in replicated real space. The full circles within a border represent the replicas of a given monomer location. Repetitions of them along a row indicate that the center of mass of the bound states is distributed homogeneously. Upper bars: one classical state; the probability density is peaked at the shown configurations, in a manner independent of the location of the center of mass of the bound state of the replicated particles. Middle bars: another classical state, obtained by the former one via a relative translation of the replicas that does not vary with the location of the center of mass. Lower bars: a Goldstone-distorted state; the the probability density is peaked in a manner that varies with the location of the center of mass.

exemplifies this point; in particular, one sees that the most probable value $u_\perp$ of the *relative* locations $x_\perp$ now depends on the *center-of-mass* location $\mathbf{x}_{\rm cm}$. These remarks are amplified in Fig. 3.3.

Returning to the issue of the structure and properties of the Goldstone-type excitations of the amorphous solid state, recall that the critical Fourier amplitudes of the field are those that reside in the higher-replica sector [i.e. HRS, for which at least two D-vector elements of the argument of $\Omega(\hat{k})$ are nonzero]. Do the proposed Goldstone distortions of the classical state excite the lower-replica sectors? If so, they would be suppressed by interactions, such as particle repulsion, that tend to preserve homogeneity. To see that they do not, let us examine the Goldstone-distorted state in the zero- (i.e. $k = 0$) and one- (i.e. $k = \mathbf{q}\,\epsilon^\alpha$ with $\mathbf{q} \neq \mathbf{0}$) replica sectors. In the former, one readily sees from Eq. (3.9a) that it has its undistorted value. A straightforward calculation shows that in the latter sector the distorted order parameter contains the factor:

$$\int_{\mathcal{V}} \frac{d\mathbf{x}_{\rm cm}}{V}\, \exp\big(i\mathbf{q}\cdot\mathbf{x}_{\rm cm} + i\mathbf{q}\cdot\mathbf{u}^\alpha(\mathbf{x}_{\rm cm})\big), \tag{3.15}$$

where $\mathbf{u}^\alpha = u_\perp \cdot \epsilon^\alpha$. By introducing the transformation $\mathbf{x}_{\rm cm} \to \mathbf{x}'_{\rm cm} \equiv \mathbf{x}_{\rm cm} + \mathbf{u}^\alpha(\mathbf{x}_{\rm cm})$ we see that the Goldstone-distorted state remains zero in the one-replica sector, provided all D-vector elements $\mathbf{u}^\alpha$ of the Goldstone field $u_\perp(\mathbf{x}_{\rm cm})$ obey the condition

$$\left| \det \left(\delta_{dd'} + \partial_d \, u^\alpha_{d'} \right) \right| = 1, \tag{3.16}$$

which, for small amplitude distortions, reduces to $\partial_d \, u^\alpha_d = 0$. That this condition corresponds to incompressibility (i.e. *pure shear*) will be established in Section 3.3.2. (Here and elsewhere, summations from 1 to D are implied over repeated Cartesian indices, such as d and d'.) This is as it should be: to make density fluctuations there must be some compression amongst the elements $\mathbf{u}^\alpha$ of $u_\perp$.

3.3.2 Identifying the Goldstone fluctuations as local displacements

In this subsection our aim is to establish the connection between the Goldstone fields and the displacement fields of conventional elasticity theory [29, 30]. *Inter alia*, this identifies the stiffness associated with the Goldstone fluctuations as the elastic modulus governing shear deformations of the amorphous solid. As we shall see, the discussion is general enough to apply to *any* amorphous solid that breaks translational symmetry microscopically but preserves it macroscopically, in regimes where the constituent particles are strongly localized in position.

Recall the amorphous solid order parameter, Eq. (2.7),

$$\Big[J^{-1} \sum_{j=1}^{J} \langle \mathrm{e}^{i\mathbf{k}^1 \cdot \mathbf{R}_j} \rangle \langle \mathrm{e}^{i\mathbf{k}^2 \cdot \mathbf{R}_j} \rangle \cdots \langle \mathrm{e}^{i\mathbf{k}^\nu \cdot \mathbf{R}_j} \rangle \Big],$$

and focus on a single element $\langle \mathrm{e}^{i\mathbf{k}\cdot\mathbf{R}_j} \rangle$. It is convenient to consider the element in the form

$$\mathrm{e}^{i\mathbf{k}\cdot\mathbf{r}_j} \, \wp_j(\mathbf{k}), \tag{3.17}$$

where $\mathbf{r}_j$ is the mean of the position of particle j, and $\wp$ describes fluctuations about the mean. Now consider the impact of a long wave-length shear displacement, encoded in the field $\mathbf{v}(\mathbf{x})$, which deforms the probability density associated with the position $\mathbf{R}_j$ of particle j. By assuming that

the typical localization length is much smaller than the length-scale associated with variations of the deformation we are able to retain only the *rigid* displacement of the probability density for $\mathbf{R}_j$ and neglect any deformation of its *shape*. Thus, under the displacement the element is deformed as

$$\langle \mathrm{e}^{i\mathbf{k}\cdot\mathbf{R}_j}\rangle = \mathrm{e}^{i\mathbf{k}\cdot\mathbf{r}_j}\,\wp_j(\mathbf{k}) \longrightarrow \mathrm{e}^{i\mathbf{k}\cdot(\mathbf{r}_j+\mathbf{v}(\mathbf{r}_j))}\,\wp_j(\mathbf{k}), \tag{3.18}$$

Inserting such deformations into the order parameter, with an independent displacement field for each element, gives the distorted form

$$\Big[\frac{1}{J}\sum_{j=1}^{J}\mathrm{e}^{i\sum_{a=1}^{\nu}\mathbf{k}^a\cdot\mathbf{r}_j}\,\mathrm{e}^{i\sum_{a=1}^{\nu}\mathbf{k}^a\cdot\mathbf{v}^a(\mathbf{r}_j)}\,\wp_j(\mathbf{k}^1)\cdots\wp_j(\mathbf{k}^\nu)\Big] = \int\frac{d\mathbf{r}}{V}\,\mathrm{e}^{i\sum_{a=1}^{\nu}\mathbf{k}^a\cdot(\mathbf{r}+\mathbf{v}^a(\mathbf{r}))}\Big[\wp_j(\mathbf{k}^1)\cdots\wp_j(\mathbf{k}^\nu)\Big], \tag{3.19}$$

where we have arrived at the second form by noting that, in the amorphous solid state, the mean position of any particle is distributed homogeneously. Next, we decompose the collection of displacement fields $\{\mathbf{v}^a\}$ into longitudinal and transverse parts, according to the geometrical prescription given in Section 3.3.1, but keeping in mind the fact that there are now ν copies (rather than $1+n$). The essential point is that the longitudinal part of $\{\mathbf{v}^a\}$, which corresponds to *common* deformations of the elements, does not generate a new value of the order parameter, in contrast with the transverse part (which generates *relative* deformations). Therefore, the *physical* displacements are the transverse part of $\{\mathbf{v}^a\}$. To see this point, consider the special situation in which the transverse part of $\{\mathbf{v}^a\}$ *is* position dependent but the longitudinal part *is not*. In this case, (V times) the order parameter becomes

$$\int d\mathbf{r}\,\mathrm{e}^{i\sum_{a=1}^{\nu}\mathbf{k}^a\cdot\mathbf{r}}\,\mathrm{e}^{ik_\perp\cdot v_\perp(\mathbf{r})+i\mathbf{k}_{\mathrm{tot}}\cdot\mathbf{v}_{\mathrm{cm}}}\Big[\wp_j(\mathbf{k}^1)\cdots\wp_j(\mathbf{k}^\nu)\Big]. \tag{3.20}$$

As things stand, in the presence of $v_\perp(\mathbf{r})$, a longitudinal part $\mathbf{v}_{\mathrm{cm}}$ would have the effect of producing a new value of the order parameter. As, on physical grounds, we expect that it should not, we see that *physical* displacements are purely transverse. This is a consequence of the fact that, for the long wave-length displacements under consideration, the deformed amorphous solid state continues to preserve translational invariance macroscopically. This argument for the absence of

the longitudinal part of the displacement field continues to hold when it has position-dependence: if, when constant, it does not generate a new state degenerate with the old one then, when varying, it should not generate a low-energy deformation.

Thus we have realized the goal of this section: by comparing Eqs. (3.9a) and (3.20) we see that the formally-constructed Goldstone fields $u_\perp$ are in fact the physical displacement fields $v_\perp$. Actually, there is one further point to address, concerning the argument of the final factor in Eq. (3.20), viz., $\big[\, \wp_j(\mathbf{k}^1) \cdots \wp_j(\mathbf{k}^\nu) \,\big]$. Apparently, there is dependence on the full set of wave vectors $\{\mathbf{k}^1, \ldots, \mathbf{k}^\nu\}$, whereas Eq. (3.9a) indicates dependence only on the transverse part of this collection. The resolution of this apparent discrepancy lies in the observation that, for position-independent $v_\perp$, Eq. (3.20) must revert to a classical state, for which the final factor does not depend on $\mathbf{k}_{\rm tot}$. As the final factor consists of probability clouds, which we are assuming to be undeformed by the displacements, this factor continues to be independent of $\mathbf{k}_{\rm tot}$ in Eq. (3.20).

3.4 Energetics of Goldstone fluctuations; elastic free energy

In this section we determine the effective theory of Goldstone fluctuations; that is all non-Goldstone fluctuations are neglected in the Landau-Wilson effective Hamiltonian. In Section 2.3 we introduced the field-theoretic effective Hamiltonian for the V/G transition. In field theory, it is customary to rescale the order parameter field and control parameters in the effective Hamiltonian in a such a manner that the 'gradient term' has no constant multiplying it, and the Hamiltonian has engineering dimension zero, which in turn determines the engineering dimension of the order parameter field.[2] In this section, we revert to the 'unrescaled' form of the Hamiltonian because we are after the expression for the shear modulus and we want its dependence on the parameters of the microscopic theory to be explicit. The effective Hamiltonian in its 'primitive' form is,

$$\mathcal{H}_\Omega = V \sum_{k \in \mathrm{HRS}} \big(a\tau + \tfrac{1}{2}\xi_0^2\, k \cdot k \big)\, \Omega(\hat{k})\, \Omega(-k) - V\, \frac{g}{3!} \sum_{k_1,k_2,k_3 \in \mathrm{HRS}} \delta_{k_1+k_2+k_3,0}\; \Omega(k_1)\, \Omega(k_2)\, \Omega(k_3), \quad (3.21)$$

[2]The engineering dimension of the Hamiltonian is zero only when the the factor $1/k_{\rm B}T$, which has dimensions of energy inverse, is absorbed in the Hamiltonian. This is the usual practice in the field theory literature, but in order to make the temperature dependence of quantities such as the shear modulus explicit, we do not perform this rescaling in this chapter.

where c is the number of entities being constrained per unit volume, and $(a\tau, \xi_0, g)$ are, respectively, the control parameter for the density of constraints, the linear size of the underlying objects being linked, and the nonlinear coupling constant controlling the strength with which the Ω fluctuations interact. HRS indicates that only wave vectors in the higher-replica sector are to be included in the summations. The microscopic model of vulcanized macromolecular matter briefly discussed in Section 2.1.1 yields $a = 1/2$, $\tau = (m_c^2 - m^2)/m_c^2$, $\xi_0^2 = L\ell_p/2D$ and $g = 1$, where m controls the mean number of constraints (and has critical value $m_c = 1$), ℓ_p is the persistence length of the macromolecules, and L/ℓ_p is the number of segments per macromolecule.

Distorting the classical state given by Eqs. (3.3,3.4a), via Eq. (3.9a) or (3.9b), inserting the resulting state into $\mathcal{H}_\Omega$ and computing the *increase*, $\mathcal{H}_u$, in $\mathcal{H}_\Omega$ due to the distortion $u_\perp$ (i.e. the elastic free energy) gives the following contribution, which arises solely from the quadratic 'gradient'term in $\mathcal{H}_\Omega$:

$$\mathcal{H}_u = \frac{\mu_n}{2T} \int_{\mathcal{V}} d\mathbf{x} \, (\partial_{\mathbf{x}} u_\perp \cdot \partial_{\mathbf{x}} u_\perp) \,, \tag{3.22a}$$

$$\mu_n \equiv \frac{T\,c}{(1+n)^{1+\frac{D}{2}}} \int V^n đk_\perp \, \frac{\xi_0^2\, k_\perp^2}{nD} \, \mathcal{W}(k_\perp)^2, \tag{3.22b}$$

in the former of which there are scalar products over both the nD independent components of $u_\perp$ and the D components of $\mathbf{x}$. The derivation of this elastic free energy is given in Appendix A. As we have discussed in Section 3.3.2, and shall revisit in Section 3.5, μ_0 is the elastic shear modulus. By using the specific classical form for $\mathcal{W}$, Eq. (3.4a), and passing to the replica limit, $n \to 0$, we obtain

$$\mu_0 = Tc\,Q^2 \int d\xi^2 \, \mathcal{N}(\xi^2) \, d\xi'^2 \, \mathcal{N}(\xi'^2) \, \frac{\xi_0^2}{\xi^2 + \xi'^2} \tag{3.23a}$$

$$= Tc\,|\tau|^3 \, \frac{4a^2}{9g^2} \int d\zeta \, d\zeta' \, \frac{\mathcal{P}(\zeta)\,\mathcal{P}(\zeta')}{\zeta^{-1} + \zeta'^{-1}} \tag{3.23b}$$

which, for the case of the semi-microscopic parameters stated shortly after Eq. (3.21), becomes

$$\mu_0 = 2\,T\,c\,|\tau|^3 \int d\zeta \, d\zeta' \, \frac{\mathcal{P}(\zeta)\,\mathcal{P}(\zeta')}{\zeta^{-1} + \zeta'^{-1}} \,. \tag{3.23c}$$

The main technical steps of this derivation are given in Appendix B. Thus, we have arrived at the

effective free energy controlling elastic deformations, in the harmonic approximation. It is consistent with the result obtained in Refs. [31], in which the free energy cost of imposing a macroscopic shear deformation of the sample was determined.

3.5 Identification of the shear modulus: Macroscopic view

In Section 3.3.2, we have explained why the Goldstone-type fluctuations are identified with local displacements of the amorphous solid by considering the impact of these fluctuations at a semi-microscopic level. In the present section we again address this identification, but now from a more macroscopic perspective, by coupling the Goldstone fields to a force-density field.

Accounting solely for the Goldstone-type fluctuations [i.e. ignoring the field w in the parameterization of the field Ω in Eq. (3.11)], we approximate the replica partition function for the V/G transition as

$$\mathcal{Z}_{1+n}[f_\perp] \sim e^{-\mathcal{H}_{\Omega,\mathrm{cl}}} \int \mathcal{D}u_\perp \exp\Big(-\frac{\mu_0}{2T} \int_{\mathcal{V}} d\mathbf{x}\, \partial_{\mathbf{x}} u_\perp \cdot \partial_{\mathbf{x}} u_\perp + \frac{1}{T} \int_{\mathcal{V}} d\mathbf{x}\, f_\perp(\mathbf{x}) \cdot u_\perp(\mathbf{x}) \Big), \qquad (3.24)$$

in which $\mathcal{H}_{\Omega,\mathrm{cl}}$ is the effective free energy (3.21) evaluated in the classical state (3.3), and $\mathcal{D}u_\perp$ indicates functional integration over replicated displacement fields $\{\mathbf{u}^\alpha(\mathbf{x})\}$ subject to the following conditions: u is replica-transverse [cf. Eq. (3.7)]; the D-vector elements it contains are pure shear [cf. Eq. (3.16)]; and the Fourier content is restricted to wave-lengths longer than a short-distance cut-off $\ell_<$ (which is we take to be on the order of the typical localization length) but shorter than a long-distance cut-off $\ell_>$ (which is commonly on the order of the linear size of the sample). The reason for the restriction to wave-lengths longer than the typical localization length is that by restricting our attention to the Goldstone sector of fluctuations we are omitting the effects of massive fluctuations. To be consistent, we should also omit the effects of Goldstone-type fluctuations with wave-lengths sufficiently short that their energy scale is comparable to or larger than the scale for the (omitted) least massive fluctuations. The appropriate criterion is that the short-distance cut-off be taken to be on the order of the typical localization length. This can be appreciated pictorially from Figs. 3.1 and 3.2: Goldstone-type fluctuations having wave-lengths smaller that the hill width are omitted. Note that we have ignored the Jacobian factor connected with the change of functional

integration variable from Ω to u.

In order to re-confirm the identification of the shear modulus, we have, in Eq. (3.24), coupled the displacement field u linearly to a replicated *force density field* f though a term $-\frac{1}{T}\int d\mathbf{x}\, f(\mathbf{x})\cdot u(\mathbf{x})$; because $u_\parallel$ is zero, only the transverse term, $-\frac{1}{T}\int d\mathbf{x}\, f_\perp(\mathbf{x})\cdot u_\perp(\mathbf{x})$, remains. As for f itself, it is taken to have D-vector elements that vanish in the zeroth replica and are identically equal to $\mathbf{f}$ in the remaining replicas. This reflects the fact that the force density is envisaged as being applied *subsequent* to the cross-linking process, and therefore does not feature in the replica that generates the cross-link distribution, but is repeated in the *thermodynamic* replicas (by which we mean the replicas that generate the logarithm of the partition function, not the disorder distribution). Thus, one has

$$f_\perp\cdot f_\perp = f\cdot f - f_\parallel\cdot f_\parallel = n\,\mathbf{f}\cdot\mathbf{f} - (f\cdot\epsilon)^2 = \frac{n}{1+n}\,\mathbf{f}\cdot\mathbf{f} \stackrel{n\to 0}{\longrightarrow} n\,\mathbf{f}\cdot\mathbf{f}. \tag{3.25}$$

The integration over u in Eq. (3.24) is Gaussian, and thus straightforward, requiring only the elastic correlator $\langle u_d(\mathbf{y})\, u_{d'}(\mathbf{y}')\rangle$, which is given in terms of the elastic Green function $\mathcal{G}_{dd'}(\mathbf{y}-\mathbf{y}')$:

$$\langle u_d(\mathbf{y})\, u_{d'}(\mathbf{y}')\rangle \equiv \frac{\int\mathcal{D}\mathbf{u}\,\exp\left(-\frac{\mu_0}{2T}\int_{\mathcal{V}} d\mathbf{x}\,\partial_{\mathbf{x}}\mathbf{u}\cdot\partial_{\mathbf{x}}\mathbf{u}\right)\,u_d(\mathbf{y})\,u_{d'}(\mathbf{y}')}{\int\mathcal{D}\mathbf{u}\,\exp\left(-\frac{\mu_0}{2T}\int_{\mathcal{V}} d\mathbf{x}\,\partial_{\mathbf{x}}\mathbf{u}\cdot\partial_{\mathbf{x}}\mathbf{u}\right)} = \frac{T}{\mu_0}\,\mathcal{G}_{dd'}(\mathbf{y}-\mathbf{y}'), \tag{3.26a}$$

$$\mathcal{G}_{dd'}(\mathbf{y}) = \int_{2\pi/\ell_>}^{2\pi/\ell_<} \text{đ}\mathbf{k}\, e^{-i\mathbf{k}\cdot\mathbf{y}}\,\mathcal{G}_{dd'}(\mathbf{k}),$$

$$\mathcal{G}_{dd'}(\mathbf{k}) = \frac{\left(k^2\,\delta_{dd'} - k_d\,k_{d'}\right)}{k^4}, \tag{3.26b}$$

where $\ell_>$ and $\ell_<$ are, respectively, the long- and short-distance cut-offs on the wave-vector integration, mentioned above. This elastic Green function is derived in Appendix D. In terms of the elastic Green function and the force density, one finds for the increase $F[\mathbf{f}]-F[\mathbf{0}]$ in free energy due to the applied force-density field:

$$F[\mathbf{f}]-F[\mathbf{0}] = -T\lim_{n\to 0}\frac{\mathcal{Z}_{1+n}[\mathbf{f}]-\mathcal{Z}_{1+n}[\mathbf{0}]}{n\,\mathcal{Z}_1[\mathbf{0}]} = -T\lim_{n\to 0}\frac{\partial}{\partial n}\,\ln\frac{\mathcal{Z}_{1+n}[\mathbf{f}]}{\mathcal{Z}_{1+n}[\mathbf{0}]} \tag{3.27a}$$

$$\approx -\frac{1}{2\mu_0}\int_{\mathcal{V}} d\mathbf{x}\,d\mathbf{x}'\sum_{d,d'=1}^{D} f_d(\mathbf{x})\,\mathcal{G}_{dd'}(\mathbf{x}-\mathbf{x}')\,f_{d'}(\mathbf{x}'), \tag{3.27b}$$

which indicates that μ_0 is the shear modulus; see Refs. [29, 30].

3.6 Effect of Goldstone fluctuations on the order parameter and its correlations

In this section we discuss how Goldstone fluctuations affect the expectation value and the correlations[3] of the order parameter. Our discussion is based on harmonic elasticity theory, as described by the free energy (3.22a). We shall make frequent use of the elastic Green function, which is defined in Eqs. (3.26b) and computed in Appendix D. The effects of Goldstone fluctuations are most striking in two dimensions, hence the two-dimensional solid will be discussed separately in Section 3.7.

3.6.1 Order parameter reduction due to Goldstone fluctuations

Classically, the order parameter expectation value is given by Eq. (3.3) or, equivalently,

$$\big\langle V\Omega(\mathbf{x}, k_\perp)\big\rangle \equiv \Big\langle \int đ\mathbf{k}_{\rm tot}\, e^{-i\mathbf{k}_{\rm tot}\cdot\mathbf{x}} V\Omega(\hat{k})\Big\rangle \approx \mathcal{W}(k_\perp). \tag{3.28}$$

The effect of Goldstone fluctuations on the order parameter expectation value is estimated from the Gaussian theory (3.22a), via which we compute the mean value of the distorted classical state:

$$\big\langle V\Omega(\mathbf{x}, k_\perp)\big\rangle = \Big\langle \int đ\mathbf{k}_{\rm tot}\, e^{-i\mathbf{k}_{\rm tot}\cdot\mathbf{x}}\, V\Omega(\hat{k})\Big\rangle \approx \big\langle e^{ik_\perp\cdot u_\perp(\mathbf{x})}\big\rangle\, \mathcal{W}(k_\perp). \tag{3.29a}$$

This is readily evaluated via the Gaussian property of u, and hence we find

$$\big\langle V\Omega(\mathbf{x}, k_\perp)\big\rangle \;\approx\; \widetilde{\mathcal{W}}(k_\perp), \tag{3.30a}$$

$$\widetilde{\mathcal{W}}(k_\perp) \;\equiv\; \exp\big(-T\,\Gamma_D\, k_\perp^2/2\mu_0\big)\; \mathcal{W}(k_\perp), \tag{3.30b}$$

for the fluctuation-renormalized form of $\mathcal{W}(k_\perp)$. Here $D\,\Gamma_D \equiv \mathcal{G}_{dd}(\mathbf{x})|_{\mathbf{x}=\mathbf{0}}$ and summation over repeated cartesian indices is implied. Recalling the classical structure for $\mathcal{W}$, Eq. (3.4a), we see

[3]The word 'correlation' was first used to mean 'statistical interdependence' by F. Galton in 1888. In 1896, K. Pearson used the word in the *Proceedings of the Royal Society* in a 'scientific' article: *We conclude that there is a sensible correlation between fertility and height in the mothers of daughters.* I leave it up to you to interpret that.

that the effect of the fluctuations is to induce, in say Eq. (3.3) or (3.28), the replacement

$$\mathcal{W}(k_\perp) = Q\int_0^\infty d\xi^2\,\mathcal{N}\left(\xi^2\right)\,e^{-\xi^2 k_\perp^2/2} \longrightarrow \widetilde{\mathcal{W}}(k_\perp), \tag{3.31a}$$

$$\begin{aligned}\widetilde{\mathcal{W}}(k_\perp) &\equiv e^{-T\,\Gamma_D k_\perp^2/2\mu_0}\,Q\int_0^\infty d\xi^2\,\mathcal{N}\left(\xi^2\right)\,e^{-\xi^2 k_\perp^2/2}\\ &= Q\int_{T\,\Gamma_D/\mu_0}^\infty d\xi^2\,\mathcal{N}\left(\xi^2-(T\,\Gamma_D/\mu_0)\right)\,e^{-\xi^2 k_\perp^2/2}\\ &= Q\int_0^\infty d\xi^2\,\widetilde{\mathcal{N}}\left(\xi^2\right)\,e^{-\xi^2 k_\perp^2/2},\end{aligned} \tag{3.31b}$$

i.e., a rigid shift of the distribution $\mathcal{N}$ to longer (squared) localization lengths, as encoded in the new distribution $\widetilde{\mathcal{N}}$. This is to be expected: the locally fluctuating localized objects are also subject to collective fluctuations—phonons.

This shift of $\mathcal{N}$ is determined by the value of Γ_D which, as shown in Appendix D, has the following leading-order dependence on D:

$$\Gamma_D \approx \begin{cases} \frac{\Sigma_D}{(2\pi)^2}\frac{D-1}{D(D-2)}\,\frac{1}{\ell_<^{D-2}}, & \text{for} \quad D>2;\\ \\ \frac{1}{4\pi}\ln\left(\ell_>/\ell_<\right), & \text{for} \quad D=2. \end{cases} \tag{3.32}$$

where Σ_D is the area of the $(D-1)$-dimensional surface of a D-dimensional sphere of radius unity, viz,

$$\Sigma_D = 2\pi^{D/2}/\Gamma(D/2), \tag{3.33}$$

in which $\Gamma(D)$, [not to be confused with Γ_D of Eq. (3.32)] is the conventional Gamma function. We see that in dimension D greater than two the shift is *finite*. However, at and below $D=2$ the shift *diverges* with the long-distance cut-off $\ell_>$, viz., the linear size of the system, doing so logarithmically in two dimensions. Not surprisingly, fluctuations destroy particle localization in two-dimensional amorphous solids and thus restore the symmetry broken at the classical level (see below).

We now consider the scaling behavior of the fluctuation-induced shift of the distribution from $\mathcal{N}$ to $\widetilde{\mathcal{N}}$. We see from Eqs. (3.31) that this shift is parametrized by the length $\xi_{\rm fl}$, which is defined

via

$$\xi_{\rm fl}^2 \equiv \Gamma_D \, T/\mu_0 \, . \tag{3.34}$$

How does this length compare with the typical localization length $\xi_{\rm typ}$, as defined, say, via the most probable value of ξ predicted by the classical theory? From Eq. (3.4c) we see that

$$\xi_{\rm typ}^2 \sim \xi_0^2/\tau, \tag{3.35}$$

and thus we have that

$$\xi_{\rm fl}^2/\xi_{\rm typ}^2 \sim \Gamma_D \, T \, \tau/\mu_0 \, \xi_0^2 \, . \tag{3.36}$$

Now, from Eq. (3.23c) we have that

$$\mu_0/T \sim c \, \tau^3, \tag{3.37}$$

and we use this to eliminate μ_0/T in Eq. (3.36). Furthermore, from Eq. (3.32) we have that, for $D > 2$,

$$\Gamma_D \sim \ell_<^{2-D} \sim \xi_{\rm typ}^{2-D}, \tag{3.38}$$

provided we take the short-distance cut-off to be of order $\xi_{\rm typ}$, as discussed in Section 3.5. We use this to eliminate Γ_D in favor of $\xi_{\rm typ}$. Finally, by using Eq. (3.35) to eliminate τ in favor of $\xi_{\rm typ}/\xi_0$ we obtain, for $D > 2$,

$$\xi_{\rm fl}^2 \, / \, \xi_{\rm typ}^2 \sim \left(c \, \xi_0^D \right)^{-1} \left(\xi_{\rm typ}/\xi_0 \right)^{6-D}. \tag{3.39}$$

At $D = 6$ we find *one-parameter scaling* in the sense that $\xi_{\rm fl} \sim \xi_{\rm typ}$, up to the factor $c \, \xi_0^D$, which measures the number of crosslinked entities within a region of order the size of a single one. This is to be expected, because we have used classical exponents for the divergence of $\xi_{\rm typ}$ and vanishing of μ_0 with τ, and six is the upper critical dimension for the transition to the amorphous solid state. In fact, if we were to replace these classical exponent by their anomalous values we would expect to recover one-parameter scaling at arbitrary D.

3.6.2 Two-field order parameter correlations

As with their effect on the order parameter itself, the effect of Goldstone fluctuations on the two-field correlator can be determined from the Gaussian theory (3.22a), which gives

$$\left\langle V\Omega(\mathbf{x}, k_\perp)\, V\Omega(\mathbf{x}', k'_\perp)^* \right\rangle \approx \left\langle e^{ik_\perp \cdot u_\perp(\mathbf{x})}\, e^{-ik'_\perp \cdot u_\perp(\mathbf{x}')} \right\rangle \mathcal{W}(k_\perp)\, \mathcal{W}(k'_\perp). \tag{3.40}$$

The required correlator $\left\langle \exp ik_\perp \cdot u_\perp(\mathbf{x})\, \exp -ik'_\perp \cdot u_\perp(\mathbf{x}') \right\rangle$ is also readily evaluated via the Gaussian property of u, and hence we have

$$\begin{aligned} &\left\langle V\Omega(\mathbf{x}, k_\perp)\, V\Omega(\mathbf{x}', k'_\perp)^* \right\rangle \\ &\approx \exp\left(-\frac{T\,\Gamma_D}{2\mu_0} |k_\perp - k'_\perp|^2 \right) \exp\left(-\frac{T}{\mu_0} \left(\mathcal{G}_{dd'}(\mathbf{0}) - \mathcal{G}_{dd'}(\mathbf{x} - \mathbf{x}') \right) k_{\perp d} \cdot k'_{\perp d'} \right) \mathcal{W}(k_\perp)\, \mathcal{W}(k'_\perp), \end{aligned} \tag{3.41}$$

where the scalar products $k_{\perp d} \cdot k'_{\perp d'}$ and $|k_\perp - k'_\perp|^2$ are respectively taken over n and nD components.

Recall, from Eq. (3.32), that $\Gamma_D|_{D=2}$ diverges with the long-distance cut-off. This, together with the positive-semi-definiteness of the quadratic form $\left(\mathcal{G}_{dd'}(\mathbf{0}) - \mathcal{G}_{dd'}(\mathbf{x} - \mathbf{x}') \right) k_{\perp d} \cdot k'_{\perp d'}$ in Eq. (3.41), makes it evident that the correlator $\left\langle V\Omega(\mathbf{x}, k_\perp)\, V\Omega(\mathbf{x}', k'_\perp)^* \right\rangle$ given in Eq. (3.41) vanishes at $D = 2$ (and below) unless $k = k'$. This vanishing is a second facet of the fluctuation-induced restoration of symmetry discussed for the case of the order parameter, following Eq. (3.32). [The correlator $\left\langle V\Omega(\hat{k})\, V\Omega(k')^* \right\rangle$ vanishes in *any* dimension unless $k_\parallel = k'_\parallel$, owing to the preserved symmetry of common translations of the replicas, which encodes the homogeneity of the randomness in the amorphous solid state, i.e., its macroscopic translational invariance.] If $k = k'$ then, regardless of dimension, the correlator decays with increasing separation $\mathbf{x} - \mathbf{x}'$, as shown by Eq. (3.41).

For $D > 2$ it is convenient to analyze the two-field correlator normalized by its disconnected part, i.e.,

$$\frac{\left\langle \Omega(\mathbf{x}, k_\perp)\, \Omega(\mathbf{x}', k'_\perp)^* \right\rangle}{\left\langle \Omega(\mathbf{x}, k_\perp) \right\rangle \left\langle \Omega(\mathbf{x}', k'_\perp)^* \right\rangle}. \tag{3.42}$$

Equations (3.41) and (3.30) show this quotient to be given by

$$\exp\left(\frac{T}{\mu_0}\, \mathcal{G}_{dd'}(\mathbf{r})\, k_{\perp d} \cdot k'_{\perp d'} \right), \tag{3.43}$$

where the separation $\mathbf{r} \equiv \mathbf{x} - \mathbf{x}'$.

We illustrate this behavior by considering the case of $D = 3$ and the regime $\ell_< \ll |\mathbf{r}| \ll \ell_>$, for which, as shown in Appendix D (see also, e.g., Ref. [30]), we may use

$$\mathcal{G}^{(3)}_{dd'}(\mathbf{r}) \approx \frac{1}{8\pi\,|\mathbf{r}|}\,(\delta_{dd'} + \hat{r}_d\,\hat{r}_{d'})\,, \tag{3.44}$$

where the unit vector $\hat{\mathbf{r}} \equiv \mathbf{r}/|\mathbf{r}|$, and by choosing $k = k' = \{\mathbf{0}, \mathbf{q}, -\mathbf{q}, \mathbf{0}, \ldots, \mathbf{0}\}$. Then in this regime the normalized two-field correlator is given by

$$\exp\left(\frac{T}{4\pi\mu_0}\frac{|\mathbf{q}|^2}{|\mathbf{r}|}\,[1 + \cos^2\varphi]\right), \tag{3.45}$$

which depends strongly on the angle φ between the vectors $\mathbf{q}$ and $\mathbf{r}$.

We may also examine the normalized two-field correlator in the regime $|\mathbf{r}| \ll \ell_<$. Making use of $\mathcal{G}^{(3)}_{dd'}(\mathbf{r})$ in this regime, as given in Eq. (D.10) of Appendix D, we find that the normalized two-field correlator is given by

$$\exp\Big(\frac{4\,T}{3\pi\mu_0}\frac{|\mathbf{q}|^2}{\ell_<}\Big)\,\exp\Big(\frac{2\,T}{45\pi\mu_0}\frac{|\mathbf{q}|^2}{\ell_<}\frac{|\mathbf{r}|^2}{\ell_<^2}\,[-2 + \cos^2\varphi]\Big), \tag{3.46}$$

where $\ell\!\!\!^{-}_< \equiv \ell_</2\pi$ (and $\ell\!\!\!^{-}_> \equiv \ell_>/2\pi$). Of course, in this regime the result for the correlator is incomplete, as there will also be contributions from the non-Goldstone excitations.

3.6.3 Intermezzo on length-scales

We pause to catalog the various length-scales featuring in the present chapter, and to indicate where they first appear.

The shortest length is ℓ_p, the persistence length of a macromolecule, which appears alongside L, the arclength of a macromolecule, shortly after Eq. (3.21). Together, they yield ξ_0, the linear size of the objects being linked, which may be substantially larger than ℓ_p. It is only through ξ_0 that ℓ_p and L feature in the free energy, Eq. (3.21). The density c of entities being constrained also first features in Eq. (3.21), and sets a length-scale, $c^{-1/D}$, in Eq. (3.39). Comparable to or longer than ξ_0 is the length ξ, the (distributed) localization length, first featuring in Eqs. (2.8) and

(2.10). The typical value of ξ is denoted $\xi_{\rm typ}$, first mentioned around Eq. (3.35). The amount by which fluctuations shift the distribution of ξ is encoded in the fluctuation length $\xi_{\rm fl}$, first mentioned around Eq. (3.34). The short- and long-distance cut-offs for the Goldstone-type fluctuations are respectively denoted $\ell_<$ and $\ell_>$, and are first mentioned in Section 3.5. The linear size of the sample is denoted $\mathcal{L}$; see the beginning of Section 3.7.

3.7 Amorphous solids in two dimensions

We now focus on amorphous solids in *two* dimensions. By taking the long-distance cut-off $\ell_>$ to be the linear size of the sample $\mathcal{L}$, so that its area is $\mathcal{L}^2$, we see from Eqs. (3.30) and (3.32) that the expectation value of the order parameter does indeed *vanish algebraically* with the sample size, doing with an exponent that depends, inter alia, on $k_\perp$:

$$\left\langle \mathcal{L}^2\, \Omega(\mathbf{x}, k_\perp) \right\rangle \approx \mathcal{W}(k_\perp)\, \exp\left(-\tfrac{1}{2}\eta(k_\perp^2) \ln\left(\mathcal{L}/\ell_<\right)\right) = \mathcal{W}(k_\perp)\left(\mathcal{L}/\ell_<\right)^{-\eta(k_\perp^2)/2}, \tag{3.47}$$

where the exponent $\eta(\kappa^2)$ varies continuously with wave-number and is defined via

$$\eta(\kappa^2) \equiv \frac{T\kappa^2}{4\pi\mu_0}. \tag{3.48}$$

To arrive at this result we have made use of the two-dimensional real-space elastic Green function evaluated at the origin, computed in Appendix D and stated in Eq. (3.32). It confirms the expectation, mentioned above, that in two-dimensions fluctuations destroy particle localization and restore the broken symmetry. Note, however that, due to the purely entropic nature of the elasticity the exponent does not depend on temperature [cf. Eq. (3.23c)].

Similarly, from Eq. (3.41) we see that the $k_\perp$-diagonal two-field correlator is given by

$$\begin{aligned} &\left\langle \mathcal{L}^2\, \Omega(\mathbf{x}, k_\perp)\, \mathcal{L}^2\, \Omega(\mathbf{x}', k_\perp)^* \right\rangle \approx \\ &\mathcal{W}(k_\perp)^2\, \exp\left(-\frac{T}{\mu_0}\big(\mathcal{G}_{dd'}(\mathbf{0}) - \mathcal{G}_{dd'}(\mathbf{r})\big) k_{\perp d} \cdot k_{\perp d'}\right), \end{aligned} \tag{3.49}$$

where, as before, the separation is denoted by $\mathbf{r} \equiv \mathbf{x} - \mathbf{x}'$ and the unit vector by $\hat{\mathbf{r}} \equiv \mathbf{r}/|\mathbf{r}|$. In the

regime $\ell_< \ll |\mathbf{r}| \ll \mathcal{L}$, the Green function is given by [see Eq. (D.28) in Appendix D]

$$\mathcal{G}_{dd'}(\mathbf{0}) - \mathcal{G}_{dd'}(\mathbf{r}) = \frac{1}{4\pi}\left\{\delta_{dd'} \ln\left(r/\widetilde{\ell}_<\right) - \hat{r}_d\,\hat{r}_{d'}\right\}, \tag{3.50}$$

where, for convenience, we have introduced the numerically rescaled short-distance cut-off $\widetilde{\ell}_<$, defined via

$$\widetilde{\ell}_< \equiv \frac{\ell_<}{\pi e^{\gamma+\frac{1}{2}}} \tag{3.51}$$

In consequence, the correlator decays algebraically with the *magnitude* r of the distance, and with an amplitude that depends on the *orientation* $\hat{\mathbf{r}}$ of the distance (relative to $k_\perp$). Ignoring, for the moment the dependence on $\hat{\mathbf{r}}$, we have the leading-order result:

$$\left\langle \mathcal{L}^2\,\Omega(\mathbf{x},k_\perp)\,\mathcal{L}^2\,\Omega(\mathbf{x}',k_\perp)^*\right\rangle \approx \mathcal{W}(k_\perp)^2\,\left(\widetilde{\ell}_</r\right)^{\eta(k_\perp^2)}. \tag{3.52}$$

As mentioned above, the $k_\perp$-off-diagonal two-field correlator—like the order parameter—vanishes in the thermodynamic limit, reflecting the fluctuation-induced restoration of symmetry.

This scenario is similar to the theory of two-dimensional regular solids, taking into account harmonic phonons only, as discussed in Ref. [32]. The main difference is the absence of Bragg peaks at reciprocal lattice vectors. Instead, there is a divergence in the scattering function [32] at zero wave-number, as can be seen from the Fourier transform of the correlator (3.52) with respect to $\mathbf{r}$ ($\equiv \mathbf{x}-\mathbf{x}'$):

$$\begin{aligned} S(\mathbf{q},k_\perp) &= \int d\mathbf{r}\, e^{i\mathbf{r}\cdot\mathbf{q}}\left\langle \mathcal{L}^2\,\Omega(\mathbf{x},k_\perp)\,\mathcal{L}^2\,\Omega(\mathbf{x}',k_\perp)^*\right\rangle \\ &= \mathcal{W}(k_\perp)^2\,\ell_<^2\left\{\left(\frac{\ell_>}{\ell_<}\right)^{2-\eta}\frac{\mathrm{J}_1(q\ell_>)}{q\ell_>} + B\big(\eta\big)\,\big(q\ell_<\big)^{\eta-2}\right\}, \\ B(x) &\equiv 2^{-x}\,\frac{x\Gamma(1-x/2)}{\Gamma(1+x/2)}. \end{aligned} \tag{3.53}$$

In these formulæ, J_1 denotes a Bessel function and we have abbreviated $\eta(k_\perp^2)$ as η. One needs to keep the two exhibited terms because there is an exchange of dominance as η passes through the value 1/2, i.e., at $k_\perp^2 = 2\pi\mu_0/T$. Specifically, for $(\ell_>/\ell_<) \to \infty$ at fixed $q\ell_<$ the dimensionless

factor $\{\cdots\}$ behaves as:

$$(q\ell_<)^{-3/2}\,(\ell_>/\ell_<)^{\frac{1}{2}-\eta}, \quad \text{for} \quad \eta < 1/2; \tag{3.54a}$$

$$(q\ell_<)^{\eta-2}, \quad \text{for} \quad \eta > 1/2. \tag{3.54b}$$

Restoring the dependence on orientation $\hat{\mathbf{r}}$, we arrive at the full, anisotropic form for the decay of the two-field correlator:

$$\mathcal{W}(k_\perp)^2 \left(\widetilde{\ell}_</r\right)^{\eta(k_\perp^2)} \exp\left(\eta(k_\perp^2)\,\hat{k}_{\perp d_1}\cdot\hat{k}_{\perp d_2}\,\hat{r}_{d_1}\hat{r}_{d_2}\right). \tag{3.55}$$

Here, the symbol $\hat{k}_{\perp d}$ indicates the unit vector $k_{\perp d}/|k_\perp|$. For the illustrative case of $k = (\mathbf{0}, \mathbf{q}, -\mathbf{q}, \mathbf{0}, \ldots)$ this correlator reduces to

$$\mathcal{W}\Big(\sqrt{2}\,|\mathbf{q}|\Big)^2 \left(\widetilde{\ell}_</r\right)^{2\eta(q^2)} \exp\left(2\eta(q^2)\,\cos^2\varphi\right), \tag{3.56}$$

where, once again, φ is the angle between $\mathbf{q}$ and $\mathbf{r}$.

The framework adopted in the present chapter allows the identification of the *quasi-localized fraction* $\widetilde{Q}$, i.e., the fraction of particles that, whilst not truly localized, have R.M.S. displacements that diverge only logarithmically, as the system size $\mathcal{L}$ goes to infinity. This fraction should be contrasted with the delocalised fraction, i.e., the fraction that have R.M.S. displacements that diverge linearly with $\mathcal{L}$. One way to extract the quasi-localized fraction is via the order parameter (3.47)—specifically the amplitude of its power-law decay with $\mathcal{L}$. A simpler route is via the two-field correlator (3.55):

$$\widetilde{Q}^2 = lim_{k_\perp\to 0} \lim_{r\to\infty} \left(\widetilde{\ell}_</r\right)^{-\eta(k_\perp^2)} \left\langle \mathcal{L}^2\,\Omega(\mathbf{x}, k_\perp)\,\mathcal{L}^2\,\Omega(\mathbf{x}', k_\perp)^*\right\rangle = \mathcal{W}(0)^2. \tag{3.57}$$

The option of analyzing the quasi-localized fraction would not be available to percolation-based approaches to vulcanized matter, as such approaches do not account for the thermal motion of the constituents (e.g. macromolecules), but only the architecture of the structures they constitute. In fact, for the same reason, the entire circle of ideas described in the present chapter lie beyond the reach of percolation-based approaches. This shows up especially vividly in the context of the

vulcanization transition in low (and especially two) dimensions. Whereas percolation theory would indicate a lower critical dimension of unity, with nothing fundamentally new happening as one reduces the dimensionality through two, the present approach correctly finds a lower critical dimension at two dimensions for the amorphous solidification transition. This is because, in addition to incorporating the physics of percolation [34, 35], this approach contains the logically-independent physics of localization and the attendant issue of the spontaneous breaking of translational symmetry. Thus, there are qualitative, and not merely quantitative, distinctions between the vulcanization transition and resulting quasi-amorphous solid state in two- and in higher-dimensional settings, owing to the strong role played by Goldstone-type fluctuations in reduced dimensions.

The results discussed in the present section echo those found for a variety of two-dimensional statistical-mechanical systems (for a survey see, e.g., Ref. [33]), in the following sense. A sufficient density of random constraints triggers a phase transition from a liquid state to a quasi-amorphous solid state. In the liquid state there are no clusters of constituents that span the system (i.e. the system does not percolate), there are no quasi-localized particles, order-parameter correlations decay exponentially with distance, and the static shear modulus is zero. In the solid state a cluster does span the system (i.e. percolates), there are quasi-localized particles, the static shear modulus is non-zero, and order-parameter correlations decay algebraically, with a continuously-varying exponent η that depends, inter alia, on the scale set by the *probe wave-vector* $k_{\perp}$. However, the true long-range order found in higher dimensions, fails to set in, albeit only just, due to thermal fluctuations.

The situation is reminiscent of that found in the setting of the melting of two-dimensional crystals, triggered not by the density of constraints, but rather by thermal fluctuations. In this setting, at high temperatures one has a non-rigid phase with exponentially decaying positional correlations associated with unbound dislocations. This is the analog of the non-percolating state of quasi-amorphous solids. At lower temperatures one has a rigid phase, associated with bound dislocations and algebraically decaying positional correlations, but no true long-range positional order. This is the analog of the percolating regime of amorphous solids. The permanence of the architecture of the amorphous solid forming systems discussed in the present chapter prohibits the destruction by thermal fluctuations of a percolating raft of constituents. However, percolation does

not enforce true localization.

In two-dimensional crystallization one also has the opportunity for correlations in the *orientations* of the bonds connecting neighboring particles. Thus, at low temperatures one has, in addition to quasi-long range positional correlations, true long-range orientational correlations. This brings the opportunity for an intermediate regime of temperatures, in which dislocations are unbound but disclinations, which would disrupt the orientational order, remain bound: the hexatic phase of two-dimensional crystals.

This opportunity does not seem to be present in the model of vulcanized matter discussed here, which focuses exclusively on positional order and does not support topological excitations. Richer settings, such as those involving macromolecules with liquid crystalline degrees of freedom, seem likely to raise interesting opportunities for order in low-dimensional random systems.

3.8 Physical content of correlators

3.8.1 Identifying the statistical information in the two-field correlator

What is the meaning of the correlators in the amorphous solid state of the vulcanization field theory? Let us begin with the two-field correlator $\langle \Omega(k_1)\, \Omega(k_2)^* \rangle$. Specializing to the case in which the zero-replica entries $\mathbf{k}_1^0$ and $\mathbf{k}_2^0$ are zero, the interpretation of this replica quantity is given by

$$\Big\langle \Omega(k_1)\, \Omega(k_2)^* \Big\rangle\Big|_{\mathbf{k}_1^0=\mathbf{k}_2^0=\mathbf{0}} = \Big[\frac{1}{J^2} \sum_{j_1,j_2=1}^{J} \prod_{\alpha=1}^{n} \Big\langle e^{i\mathbf{k}_1^\alpha \cdot \mathbf{R}_{j_1} - i\mathbf{k}_2^\alpha \cdot \mathbf{R}_{j_2}} \Big\rangle \Big], \tag{3.58}$$

which expresses the connection with the (semi-microscopic) correlators of all pairs of particles that constitute the system. Consider a simple illustrative example, in which the positions of pairs of localized particles fluctuate about their mean positions according to a general Gaussian correlated distribution. For such particles we would then have

$$\begin{aligned} \Big\langle e^{i\mathbf{k}_1 \cdot \mathbf{R}_{j_1} - i\mathbf{k}_2 \cdot \mathbf{R}_{j_2}} \Big\rangle \;\; &= \;\; e^{ik_{1d} r_{j_1 d} - ik_{2d} r_{j_2 d}} e^{-\frac{1}{2}\Delta r_{j_1 j_1 d_1 d_2} k_{1d_1} k_{1d_2}} \\ &\quad \times e^{-\frac{1}{2}\Delta r_{j_2 j_2 d_1 d_2} k_{2d_1} k_{2d_2}} e^{\Delta r_{j_1 j_2 d_1 d_2} k_{1d_1} k_{2d_2}} \end{aligned} \tag{3.59}$$

where the mean, variances ($j_1 = j_2$) and co-variances ($j_1 \neq j_2$) of the positions are given by

$$\mathbf{r}_j = \langle \mathbf{R}_j \rangle, \tag{3.60a}$$

$$\Delta r_{j_1 j_2 d_1 d_2} = \langle (R_{j_1 d_1} - \langle R_{j_1 d_1} \rangle)\,(R_{j_2 d_2} - \langle R_{j_2 d_2} \rangle) \rangle, \tag{3.60b}$$

and summations over repeated cartesian indices d_1 and d_2 are implied.

Putting such contributions together from all pairs of *localized*, particles we have

$$\begin{aligned} \left\langle \Omega(k_1)\,\Omega(k_2)^* \right\rangle \Big|_{\mathbf{k}_1^0 = \mathbf{k}_2^0 = \mathbf{0}} &= Q^2 \int d\hat{\mathbf{r}}_1\, d\hat{\mathbf{r}}_2\, d\widehat{\Delta r}_{11}\, d\widehat{\Delta r}_{22}\, d\widehat{\Delta r}_{12}\, \mathcal{M}(\hat{\mathbf{r}}_1, \hat{\mathbf{r}}_2, \widehat{\Delta r}_{11}, \widehat{\Delta r}_{22}, \widehat{\Delta r}_{12}) \\ &\quad \times e^{i\hat{r}_{1d} \sum_{\alpha=1}^{n} k_{1d}^{\alpha} - i\hat{r}_{2d} \sum_{\alpha=1}^{n} k_{1d}^{\alpha}} e^{-\frac{1}{2} \widehat{\Delta r}_{11 d_1 d_2} \sum_{\alpha=1}^{n} k_{1d_1}^{\alpha} k_{1d_2}^{\alpha}} \\ &\quad \times e^{-\frac{1}{2} \widehat{\Delta r}_{22 d_1 d_2} \sum_{\alpha=1}^{n} k_{2d_1}^{\alpha} k_{2d_2}^{\alpha}} e^{\widehat{\Delta r}_{12 d_1 d_2} \sum_{\alpha=1}^{n} k_{1d_1}^{\alpha} k_{2d_2}^{\alpha}}, \end{aligned} \tag{3.61}$$

where we have introduced $\mathcal{M}$, the disorder-averaged joint distribution, over the pairs of localized particles, of the means, variances and co-variances of the particle positions. It is given by

$$\begin{aligned} &\mathcal{M}(\hat{\mathbf{r}}_1, \hat{\mathbf{r}}_2, \widehat{\Delta r}_{11}, \widehat{\Delta r}_{22}, \widehat{\Delta r}_{12}) \\ &\equiv \left[\frac{1}{(QJ)^2} \sum_{j_1, j_2 \,\mathrm{loc.}} \delta(\hat{\mathbf{r}}_1 - \mathbf{r}_{j_1}) \delta(\hat{\mathbf{r}}_2 - \mathbf{r}_{j_2}) \delta(\widehat{\Delta r}_{11} - \Delta r_{j_1 j_1}) \delta(\widehat{\Delta r}_{22} - \Delta r_{j_2 j_2}) \delta(\widehat{\Delta r}_{12} - \Delta r_{j_1 j_2}) \right]. \end{aligned}$$

The macroscopic translational invariance of the amorphous solid state ensures that $\mathcal{M}$ depends on $\hat{\mathbf{r}}_1$ and $\hat{\mathbf{r}}_2$ only through their difference, and thus we replace $\mathcal{M}$ by $V^{-1}\mathcal{M}(\hat{\mathbf{r}}_1 - \hat{\mathbf{r}}_2, \widehat{\Delta r}_{11}, \widehat{\Delta r}_{22}, \widehat{\Delta r}_{12})$. By appealing to permutation symmetry, including the zeroth replica, we can reinstate the dependence on the zeroth-replica wave vectors, and hence arrive at a hypothesized form for the two-point correlator:

$$\begin{aligned} \left\langle \Omega(k_1)\,\Omega(k_2)^* \right\rangle &= Q^2 \int d\hat{\mathbf{r}}_1\, d\hat{\mathbf{r}}_2\, d\widehat{\Delta r}_{11}\, d\widehat{\Delta r}_{22}\, d\widehat{\Delta r}_{12}\, V^{-1}\, \mathcal{M}(\hat{\mathbf{r}}_1 - \hat{\mathbf{r}}_2, \widehat{\Delta r}_{11}, \widehat{\Delta r}_{22}, \widehat{\Delta r}_{12}) \\ &\quad \times e^{i\hat{r}_{1d} \sum_{\alpha=0}^{n} k_{1d}^{\alpha} - i\hat{r}_{2d} \sum_{\alpha=0}^{n} k_{1d}^{\alpha}} e^{-\frac{1}{2} \widehat{\Delta r}_{11 d_1 d_2} \sum_{\alpha=0}^{n} k_{1d_1}^{\alpha} k_{1d_2}^{\alpha}} \\ &\quad \times e^{-\frac{1}{2} \widehat{\Delta r}_{22 d_1 d_2} \sum_{\alpha=0}^{n} k_{2d_1}^{\alpha} k_{2d_2}^{\alpha}} e^{\widehat{\Delta r}_{12 d_1 d_2} \sum_{\alpha=0}^{n} k_{1d_1}^{\alpha} k_{2d_2}^{\alpha}}. \end{aligned} \tag{3.62}$$

What about contributions to the double sum over particles in Eq. (3.58) associated with one or

two *unlocalized* particles? Such contributions certainly exist, except in the limit of large crosslink densities (where all constituents are bound to the infinite cluster and are, therefore, localized); in the liquid state they would, of course, be the only contributions. There, they would give rise to *diagonal* contributions, i.e., the correlator $\langle \Omega(k_1)\, \Omega(k_2)^* \rangle$ would vanish unless $k_1 = k_2$, owing to the intact symmetry of independent translations of the replicas. In the solid state, contributions associated with unlocalized particles are expected to gives rise to short-ranged correlations. As such correlations are not the main focus of the present chapter, we neglect contributions to the two-field correlator associated with unlocalized particles.

3.8.2 Evaluating the statistical information in the two-field correlator

In Section 3.8.1 we have connected the two-field correlator $\langle V\Omega(\hat{k})\, V\Omega(k')^* \rangle$ to the distribution $\mathcal{M}$ that characterizes pairs of localized particles [see Eq. (3.62)], and in Section 3.6.2 have evaluated the Fourier transform of this correlator, $\langle V\Omega(\mathbf{x}, k_\perp)\, V\Omega(\mathbf{x}', k'_\perp)^* \rangle$, within the Goldstone-type fluctuation approach [see Eq. (3.41)]. We now discuss the implications of resulting correlator for the properties of the distribution.

To do this, it is convenient to exchange the correlator in Eq. (3.41) for the Fourier transform:

$$\begin{aligned}
\langle \Omega(\hat{k})\, \Omega(k')^* \rangle &= \int \frac{d\mathbf{x}}{V}\, \frac{d\mathbf{x}'}{V}\, e^{i\mathbf{k}_{\rm tot}\cdot\mathbf{x}}\, e^{-i\mathbf{k}'_{\rm tot}\cdot\mathbf{x}'}\, \langle V\Omega(\mathbf{x}, k_\perp)\, V\Omega(\mathbf{x}', k'_\perp)^* \rangle \\
&\approx \widetilde{\mathcal{W}}(k_\perp)\, \widetilde{\mathcal{W}}(k'_\perp) \int \frac{d\mathbf{x}}{V}\, \frac{d\mathbf{x}'}{V}\, e^{i\mathbf{k}_{\rm tot}\cdot\mathbf{x}}\, e^{-i\mathbf{k}'_{\rm tot}\cdot\mathbf{x}'}\, \exp\left(\frac{T}{\mu_0}\, \mathcal{G}_{dd'}(\mathbf{x}-\mathbf{x}')\, k_{\perp d}\cdot k'_{\perp d'} \right) \\
&= \widetilde{\mathcal{W}}(k_\perp)\, \widetilde{\mathcal{W}}(k'_\perp)\, \delta_{\mathbf{k}_{\rm tot},\mathbf{k}'_{\rm tot}} \int \frac{d\mathbf{x}}{V}\, e^{i\mathbf{k}_{\rm tot}\cdot\mathbf{x}}\, \exp\left(\frac{T}{\mu_0}\, \mathcal{G}_{dd'}(\mathbf{x})\, k_{\perp d}\cdot k'_{\perp d'} \right), \qquad (3.63)
\end{aligned}$$

where $\widetilde{\mathcal{W}}(k_\perp)$ is the fluctuation-renormalized order parameter given in Eqs. (3.30b) and (3.31b). Next, in Eq. (3.62) we perform the integration over the center of mass of $\mathbf{r}_1$ and $\mathbf{r}_2$, and equate the resulting form of the correlator to the form given in Eq. (3.63), having dropped the hats on the dummy variables, thus arriving at a formula obeyed by the distribution $\mathcal{M}$:

$$\begin{aligned}
Q^2\, \delta_{\mathbf{k}_{1\rm tot},\mathbf{k}_{2\rm tot}} \int d\mathbf{x}\, d\Delta r_{11}\, d\Delta r_{22}\, d\Delta r_{12}\, \mathcal{M}(\mathbf{x}, \Delta r_{11}, \Delta r_{22}, \Delta r_{12})\, e^{i\mathbf{k}_{1\rm tot}\cdot\mathbf{x}} \\
\times e^{-\frac{1}{2}\Delta r_{11 d_1 d_2} \sum_{\alpha=0}^{n} k^\alpha_{1d_1} k^\alpha_{1d_2}}\, e^{-\frac{1}{2}\Delta r_{22 d_1 d_2} \sum_{\alpha=0}^{n} k^\alpha_{2d_1} k^\alpha_{2d_2}}\, e^{\Delta r_{12 d_1 d_2} \sum_{\alpha=0}^{n} k^\alpha_{1d_1} k^\alpha_{2d_2}} \\
= \widetilde{\mathcal{W}}(k_{1\perp})\, \widetilde{\mathcal{W}}(k_{2\perp})\, \delta_{\mathbf{k}_{1\rm tot},\mathbf{k}_{2\rm tot}} \int \frac{d\mathbf{x}}{V}\, e^{i\mathbf{k}_{1\rm tot}\cdot\mathbf{x}}\, \exp\left(\frac{T}{\mu_0}\, \mathcal{G}_{d_1 d_2}(\mathbf{x})\, k_{1\perp d_1}\cdot k_{2\perp d_2} \right). \qquad (3.64)
\end{aligned}$$

By solving this equation for $\mathcal{M}(\mathbf{x}, \Delta r_{11}, \Delta r_{22}, \Delta r_{12})$ one learns that it has weight only at values of $\big(\Delta r_{11}, \Delta r_{22}, \Delta r_{12}\big)$ of the form $\big(\xi_1^2\mathrm{I}, \xi_1^2\mathrm{I}, (T/\mu_0)\mathcal{G}_{d_1 d_2}(\mathbf{y})\big)$ for some values of the parameters $\big(\xi_1, \xi_1, \mathbf{y}\big)$, where I is the identity in D-dimensional cartesian space. Anticipating this, it is convenient to introduce the following parameterization in terms of a reduced distribution $\mathcal{M}(\mathbf{x}, \xi_1^2, \xi_2^2, \mathbf{y})$:

$$\begin{aligned}\mathcal{M}(\mathbf{x}, \Delta r_{11}, \Delta r_{22}, \Delta r_{12}) \;\; &= \;\; \int d\xi_1^2\, \widetilde{\mathcal{N}}\left(\xi_1^2\right)\, d\xi_2^2\, \widetilde{\mathcal{N}}\left(\xi_2^2\right)\, \delta\big(\Delta r_{11} - \xi_1^2\mathrm{I}\big)\, \delta\big(\Delta r_{22} - \xi_2^2\mathrm{I}\big) \\ &\qquad \times \int \frac{d\mathbf{y}}{V}\, \delta\big(\Delta r_{12} - (T/\mu_0)\, \mathcal{G}(\mathbf{y})\big)\, \mathcal{M}(\mathbf{x}, \xi_1^2, \xi_2^2, \mathbf{y}). \qquad (3.65)\end{aligned}$$

Note that $\mathcal{M}(\mathbf{x}, \xi_1^2, \xi_2^2, \mathbf{y})$ only becomes a true distribution when an appropriate Jacobian factor associated with the $\mathbf{y}$ dependence is introduced; nevertheless we shall continue to refer to it as a distribution. As shown in Appendix C, Eq. (3.64) can be solved for the reduced probability distribution; the solution is given in Eq. (C.9). Thus one finds for the full distribution:

$$\begin{aligned}\mathcal{M}(\mathbf{x}, \Delta r_{11}, \Delta r_{22}, \Delta r_{12}) \;&= \int d\xi_1^2\, \widetilde{\mathcal{N}}\left(\xi_1^2\right)\, d\xi_2^2\, \widetilde{\mathcal{N}}\left(\xi_2^2\right)\, \delta\big(\Delta r_{11} - \xi_1^2\mathrm{I}\big)\, \delta\big(\Delta r_{22} - \xi_2^2\mathrm{I}\big) \\ &\times \int \frac{d\mathbf{y}}{V} \left\{ \int đ\mathbf{q}\, e^{-i\mathbf{q}\cdot(\mathbf{x}-\mathbf{y})}\, \exp\left(\frac{1}{2}\big(\xi_1^2 + \xi_2^2\big)\, q^2 - \Delta r_{12 d_1 d_2}\, q_{d_1}\, q_{d_2} \right) \right\} \delta\big(\Delta r_{12} - (T/\mu_0)\mathcal{G}(\mathbf{y})\big). \qquad (3.66)\end{aligned}$$

This has the structure of a source term, associated with the range of values of $\mathcal{G}$, convoluted with an appropriate "propagator."

It should be borne in mind that, in this solution for the full distribution, Eq. (3.66), the integration over wave vectors $\mathbf{q}$ is subject to the usual cut-offs, i.e., those featuring in Eq. (3.26b). Thus, even though the exponent in the factor $\exp\big(\frac{1}{2}\big(\xi_1^2 + \xi_2^2\big)\, q^2 - \Delta r_{12 d_1 d_2}\, q_{d_1}\, q_{d_2}\big)$ *grows* at large $\mathbf{q}$ (i.e. the factor is *not* a decaying Gaussian factor), the large-wave-vector cut-off protects against divergence. In fact, if we focus on the distribution $\mathcal{M}$ at separations $\mathbf{x}$ that are large compared with the cut-off $\ell_<$ then for values of ξ_1 and ξ_2 with appreciable weight the aforementioned exponent is

small, and we may expand to obtain

$$\begin{aligned}
\mathcal{M}(\mathbf{x},\Delta r_{11},\Delta r_{22},\Delta r_{12}) &= \int d\xi_1^2\,\widetilde{\mathcal{N}}\left(\xi_1^2\right)\,d\xi_2^2\,\widetilde{\mathcal{N}}\left(\xi_2^2\right)\,\delta\big(\Delta r_{11}-\xi_1^2\mathrm{I}\big)\,\delta\big(\Delta r_{22}-\xi_2^2\mathrm{I}\big) \\
&\qquad\times\exp\left(-\frac{1}{2}\big(\xi_1^2+\xi_2^2\big)\,\nabla_{\mathbf{x}}^2+\Delta r_{12d_1d_2}\,\partial_{d_1}\partial_{d_2}\right) \\
&\qquad\times\int\frac{d\mathbf{y}}{V}\,\tilde{\delta}(\mathbf{x}-\mathbf{y})\,\delta\big(\Delta r_{12}-(T/\mu_0)\mathcal{G}(\mathbf{y})\big) \qquad (3.67a)\\
&\approx \int d\xi_1^2\,\widetilde{\mathcal{N}}\left(\xi_1^2\right)\,d\xi_2^2\,\widetilde{\mathcal{N}}\left(\xi_2^2\right)\,\delta\big(\Delta r_{11}-\xi_1^2\mathrm{I}\big)\,\delta\big(\Delta r_{22}-\xi_2^2\mathrm{I}\big) \\
&\qquad\times\frac{1}{V}\exp\left(-\frac{1}{2}\big(\xi_1^2+\xi_2^2\big)\,\nabla_{\mathbf{x}}^2+\Delta r_{12d_1d_2}\,\partial_{d_1}\partial_{d_2}\right) \\
&\qquad\times\delta\big(\Delta r_{12}-(T/\mu_0)\mathcal{G}(\mathbf{x})\big) \qquad (3.67b)\\
&\approx \int d\xi_1^2\,\widetilde{\mathcal{N}}\left(\xi_1^2\right)\,d\xi_2^2\,\widetilde{\mathcal{N}}\left(\xi_2^2\right)\,\delta\big(\Delta r_{11}-\xi_1^2\mathrm{I}\big)\,\delta\big(\Delta r_{22}-\xi_2^2\mathrm{I}\big) \\
&\qquad\times\frac{1}{V}\left\{1-\frac{1}{2}\big(\xi_1^2+\xi_2^2\big)\,\nabla_{\mathbf{x}}^2+\Delta r_{12d_1d_2}\,\partial_{d_1}\partial_{d_2}\right\} \\
&\qquad\times\delta\big(\Delta r_{12}-(T/\mu_0)\mathcal{G}(\mathbf{x})\big). \qquad (3.67c)
\end{aligned}$$

Here, $\partial_d \equiv \partial/\partial x_d$, and $\tilde{\delta}$ indicates the smoothed delta function resulting from the application of the wave-vector cut-off to the Fourier integration that yields it. We have, however, proceeded to the second and third lines without explicitly indicating the effect of this smoothing, viz., the replacement of the factor $\delta\big(\Delta r_{12}-(T/\mu_0)\mathcal{G}(\mathbf{x})\big)$ the same quantity *smeared* over a region around the point $\mathbf{x}$ having linear dimension of order the short-distance cut-off.

3.8.3 Two- (and higher-) field correlators as distributions of particle correlations

Let us pause to revisit the interpretation of the two-field correlator. To do this, we introduce the disorder-averaged distribution $\mathcal{M}_2$ of two-particle correlators $\mathcal{C}$, viz.,

$$\mathcal{M}_2[\mathcal{C}]\equiv\Big[J^{-2}\sum_{j_1,j_2=1}^{J}\prod_{\mathbf{k}_1,\mathbf{k}_2\neq\mathbf{0}}\delta_{\mathrm{c}}\big(\mathcal{C}_{\mathbf{k}_1\mathbf{k}_2}-\langle e^{i\mathbf{k}_1\cdot\mathbf{R}_{j_1}+i\mathbf{k}_2\cdot\mathbf{R}_{j_2}}\rangle\big)\Big], \qquad (3.68)$$

in which $\delta_{\rm c}(x+iy) \equiv \delta(x)\,\delta(y)$. We can then observe that the two-field correlator, Eq. (3.58), can be expressed as a suitable moment of $\mathcal{M}_2$:

$$\big\langle \Omega(k_1)\,\Omega(k_2)\big\rangle = \int \mathcal{D}\mathcal{C}\,\mathcal{M}_2[\mathcal{C}]\,\prod_{\alpha=0}^{n} \mathcal{C}_{\mathbf{k}_1^\alpha \mathbf{k}_2^\alpha}\,. \tag{3.69}$$

Note that we have appealed to replica permutation symmetry in order to reinstate the dependence on the zeroth-replica wave vectors.

It is straightforward to extend this discussion to the general case of r-particle correlators $\langle e^{i\mathbf{k}_1\cdot\mathbf{R}_{j_1}+i\mathbf{k}_1\cdot\mathbf{R}_{j_1}+\cdots+i\mathbf{k}_r\cdot\mathbf{R}_{j_r}}\rangle$, for which the distribution $\mathcal{M}_r$ is given by

$$\mathcal{M}_r[\mathcal{C}] \equiv \Big[\frac{1}{J^r}\sum_{j_1,\ldots,j_r=1}^{J}\prod_{\mathbf{k}_1,\mathbf{k}_2,\ldots,\mathbf{k}_r\neq\mathbf{0}} \delta_{\rm c}\big(\mathcal{C}_{\mathbf{k}_1\mathbf{k}_2\cdots\mathbf{k}_r} - \langle e^{i\mathbf{k}_1\cdot\mathbf{R}_{j_1}+i\mathbf{k}_1\cdot\mathbf{R}_{j_1}+\cdots+i\mathbf{k}_r\cdot\mathbf{R}_{j_r}}\rangle\big)\Big], \tag{3.70}$$

Observe that the r-field correlator can also be expressed as a suitable moment:

$$\big\langle \Omega(k_1)\,\Omega(k_2)\cdots\Omega(k_r)\big\rangle = \int \mathcal{D}\mathcal{C}\,\mathcal{M}_r[\mathcal{C}]\,\prod_{\alpha=0}^{n} \mathcal{C}_{\mathbf{k}_1^\alpha \mathbf{k}_2^\alpha\cdots\mathbf{k}_r^\alpha}\,. \tag{3.71}$$

Again we have appealed to replica permutation symmetry in order to reinstate the dependence on the zeroth-replica wave vectors. The distributions $\mathcal{M}_r$ are natural generalizations of the distribution of local density fluctuations, explored, e.g. in Ref. [34].

3.9 Concluding remarks

In this chapter we have identified the long wave-length, low energy Goldstone-type fluctuations of the amorphous solid state, and investigated their physical consequences. By constructing an effective free energy governing these fluctuations, we have determined the elastic properties of the amorphous solid, including its static shear modulus which, we have re-confirmed, vanishes as the third power of the amount by which the constraint density exceeds its critical value (at the classical level). We have also analyzed the effect of these fluctuations on the amorphous solid order parameter, finding that, in spatial dimensions greater than two, they induce a simple, rigid shift of the distribution of (squared) localization lengths. In addition, we have explored the properties of the order-parameter correlations in the amorphous solid state, establishing their physical content

in terms of a joint probability distribution characterizing pairs of localized particles. Moreover, we have computed the corresponding correlator induced by Goldstone-type fluctuations and, hence, obtained a specific formula for this joint probability distribution.

We have paid particular attention to systems of spatial dimension two. In this setting we have shown that fluctuations restore the symmetries broken spontaneously at the classical level, particle localization is destroyed, the order parameter is driven to zero, and order-parameter correlations decay as a power-law in the separation between points in the sample. The state is a *quasi-amorphous-solid* state, inasmuch as it possesses algebraically-decaying correlations and rigidity.

Chapter 4

Renormalized order parameter and its implications

With mute astonishment, it stands sustained
Through every part in symmetry, to endure,
Unhurt, the assault of Time with all his hours,
As the supreme Artificer ordained.

— William Wordsworth.

4.1 Introduction

In this chapter our aim is to calculate, beyond mean-field theory and within a renormalization group (RG) treatment, the gel fraction and the distribution of localization lengths characterizing the random solid state. The distribution of localization lengths can be regarded as one of the key signatures of the random solid state emerging from the V/G transition; it is measurable experimentally and in computer simulations. In Section 2.3, we sketched the mean-field calculation of the gel fraction and the distribution of localization lengths from the order parameter expectation value. Above the upper critical dimension, which is six in this setting, mean-field theory correctly captures the universal aspects of these quantities. However, below the upper critical dimension, critical fluctuations within the critical region of the solid state lead to qualitative corrections to the mean-field results. In this chapter, we develop a RG approach capable of incorporating fluctuation corrections to the expectation value of the order parameter and, thereby, yielding the gel fraction and distribution of localization lengths beyond mean-field theory. We implement the RG approach to first order in ϵ, i.e., the deviation of the spatial dimension D from the upper critical dimension (which is equal to six in our theory).

Our strategy here is to derive the order parameter (OP) expectation value from a calculation of the Equation of State (EOS) for the V/G field theory [up to one-loop order in an expansion in $\epsilon\,(=6-D)$]. The reader is aware by now that a translational symmetry in replicated space is spontaneously broken in the emergent random solid state; the nature of spontaneous symmetry breaking has been elucidated in Chapter 3. The breaking of an *external* symmetry makes the calculation of the EOS rather challenging in the V/G field theory. Moreover, the EOS plays an unconventional role in this theory by yielding an *integro-differential equation* whose solution is the distribution of localization lengths corrected by critical fluctuations. In this chapter, we present the scaling of physical quantities in the random solid state and discuss the general features of the fluctuation-corrected distribution. The work presented here extends the development of the RG approach to vulcanized matter [34, 35], by focusing on the critical properties of the emergent random solid state itself, rather than the critical point. To summarize, our specific aim is to determine the effects of critical fluctuation on the expectation value of the order parameter characterizing the random solid state.

Prior work aiming to characterize the random solid state beyond mean-field theory has been undertaken by Weigt et al. [37]. There, the focus was on the dependence of the distribution of localization lengths on the geometrical connectivity of the cluster, deep inside the solid state. It accomplished this by developing a Meyer cluster expansion for a suitable theory of replicated particles.

We remind the reader that in the vulcanization/gelation problem the fluctuations are induced both thermally and by the quenched disorder but the transition is driven by the quenched disorder alone. The universality class of the transition is expected to encompass all systems with a fraction of classical localized elements (i.e. gel) coexisting with a delocalized fraction (i.e. sol), where localization of the gel fraction is due to a sufficient density of random permanent constraints. Universality ensures that the distribution of localization lengths should be a generic feature of the emergent solid state in all such random system. Recent work using cavity method reinforces the mean-field university of the distribution of localization lengths in random solids, see Ref. [41].

Motivation for the present work also comes from the wish to establish a better understanding of how to implement, in general, RG ideas in settings of spatial (or, more generally, *external*) spon-

taneous symmetry breaking. This issue arises in the present context because in the random solid state the order parameter is spatially inhomogeneous—a manifestation of translational symmetry breaking, see Chapters 3 and Chapter 5. It is worth remembering how difficult it is to make analytical progress beyond mean-field theory with models for systems with comparable order, such as spin glasses. This difficulty originates from the complexity of their classical states, which is reflected in the replica symmetry breaking at mean-field level for models of such systems. These complications do not arise in our model, making it amenable to further analysis.

The work presented in this Chapter was done in collaboration with P. M. Goldbart, and partly with K. Esler.

4.2 Sketch of strategy

The challenging aspect of going beyond mean-field theory in the present context is as follows: the nature of the spontaneous translational symmetry breaking dictates that the exact expectation value of the order parameter (henceforth called the *ground state*) is spatially inhomogeneous, in contrast to a spatially homogeneous solution, e.g., as with the standard ϕ^4 field-theoretic description of the paramagnet-to-ferromagnet phase transition. Hence, when incorporating the effects of fluctuations on the random solid state, one needs to take into account the effects of the spatially-inhomogeneous saddle-point solution. At the mean-field level, the distribution of localization lengths was obtained from the integro-differential equation that emerges upon minimization of the tree-level effective free energy. Once fluctuations are incorporated, the *ground state* (and, from it, the fluctuation-corrected distribution) will be determined by minimizing the fluctuation-corrected effective free energy.

A well-developed scheme allowing a unified description of the unbroken- and the broken-symmetry phases in the entire critical region of a continuous phase transition has been established some time ago; for expositions, see Refs. [38]. This scheme involves the introduction of a symmetry-breaking field in order to render the free energy analytic in the critical region; the corresponding loop-expansion then has a non-zero radius of convergence about the critical point. To study the *spontaneously* symmetry-broken state, the symmetry-breaking field is taken to zero after all necessary renormalizations have been performed.

To apply this scheme to the V/G transition, we calculate the effective free energy, to one-

loop order. We then use dimensional regularization and minimal subtraction to renormalize the coupling constants in the effective free energy. We obtain the EOS from the effective free energy by variation with respect to the ground state in the presence of the symmetry-breaking field. The EOS is a universal functional relation between the symmetry-breaking field and the order parameter expectation value, and its scaling form is dictated by the solution of the appropriate RG equation.

4.3 Equation of State

We now come to the main section of the Chapter, in which we implement the strategy outlined above. By starting with the Landau-Wilson Hamiltonian (2.11), we calculate the effective free energy and use it to arrive at the scaling form of the EOS. For the sake of clarity of presentation, I reproduce Eq. (2.11) here,

$$\begin{aligned}
\mathcal{H}_{\rm VG} &= \sum_{\hat{k}\in{\rm HRS}} \frac{1}{2}(\hat{k}^2+\tau_0)|\Omega(\hat{k})|^2 - \frac{g_0}{3!}\sum_{\hat{k}_1,\hat{k}_2,\hat{k}_3\in{\rm HRS}} \Omega(\hat{k}_1)\Omega(\hat{k}_2)\Omega(\hat{k}_3)\delta(\hat{k}_1+\hat{k}_2+\hat{k}_3) \quad (4.1a)\\
&= \int_{\rm HRS} d^{(n+1)D}\hat{x}\left\{\frac{1}{2}|\widehat{\nabla}\Omega(\hat{x})|^2+\frac{1}{2}\tau_0\Omega(\hat{x})^2-\frac{g_0}{3!}\Omega(\hat{x})^3\right\}. \quad (4.1b)
\end{aligned}$$

4.3.1 Effective free energy

Let us begin with the effective free energy $\Gamma[M;\tau]$ associated with the Landau-Wilson theory (2.11). As usual, this entity is the generating functional of the vertex functions $\Gamma^N(\hat{x}_1,\ldots,\hat{x}_N;\tau)$, i.e.,

$$\Gamma[M;\tau]=\sum_{N=1}^{\infty}\frac{1}{N!}\int d\hat{x}_1\cdots d\hat{x}_N\,\Gamma^N(\hat{x}_1,\ldots,\hat{x}_N;\tau)\,M(\hat{x}_1)\cdots M(\hat{x}_N). \quad (4.2)$$

These vertex functions are related to the corresponding vertex functions $\Gamma^{N,L}(\hat{x}_1,\ldots,\hat{x}_N;\hat{y}_1,\ldots,\hat{y}_L)$ evaluated and renormalized *at the critical point* (i.e., $\tau=0$) via an expansion in powers of τ [38]:

$$\Gamma^N(\hat{x}_1,\ldots,\hat{x}_N;\tau)=\sum_{L=0}^{\infty}\frac{\tau^L}{L!}\int d\hat{y}_1\ldots d\hat{y}_L\,\Gamma^{N,L}(\hat{x}_1,\ldots,\hat{x}_N;\hat{y}_1,\ldots,\hat{y}_L) \quad (4.3)$$

The $\Gamma^{N,L}(\hat{x}_1,\ldots,\hat{x}_N;\hat{y}_1\ldots\hat{y}_L)$ are vertex functions in the field theory represented by the effective Hamiltonian (2.11) with both the quadratic 'mass' term and the cubic term are treated as

interactions. The symmetry is said to be spontaneously broken if the equation

$$\frac{\delta}{\delta M}\Gamma[M] = 0 \tag{4.4}$$

has a solution obeying $M \neq 0$. The relation between the vertex functions $\Gamma^{N,L}(\hat{x}_1, \ldots, \hat{x}_N; \hat{y}_1, \ldots, \hat{y}_L)$ of the critical theory and the vertex functions $\Gamma^N(\hat{x}_1, \ldots, \hat{x}_N; \tau)$ of the non-critical theory has been used to formulate a unified treatment of the effective free energy in the entire critical region [38]. As mentioned in the previous section, a symmetry breaking field is introduced and vertex functions are calculated and renormalized in the presence of this field. In the ϕ^4-theory of the magnetic transition, this symmetry-breaking field has the physical interpretation of a magnetic field; in our case it is only a convenient theoretical tool, devoid of direct physical interpretation.

We employ the dimensional regularization/mininal subtraction scheme to compute the renormalized effective free energy. This scheme has technical advantages compared to, for example, the momentum-shell renormalization scheme. In particular, in this scheme the renormalization factor Z_{Ω^2} for the quadratic interaction computed in the critical theory is identical to the renormalization factor Z_τ for the control parameter τ calculated in the non-critical theory; for details see Refs. [38]. This identity is reflected in the renormalization of the vertex functions $\Gamma^N(\hat{x}_1, \ldots, \hat{x}_N; \tau)$ of the non-critical theory and the vertex functions $\Gamma^{N,L}(\hat{x}_1, \ldots, \hat{x}_N; \hat{y}_1, \ldots, \hat{y}_L)$ of the critical theory; the divergences in the two theories are identical. Taking advantage of this identity, we are henceforth going to perform all the renormalization calculations in the non-critical theory, remembering that this step is only a technical simplification in our strategy involving renormalization of the critical theory. Calculating the renormalization factors for the non-critical theory is usually simpler than calculating the renormalization factors for a critical theory, justifying the implementation of the scheme delineated above.

The choice of the symmetry-breaking field in the present problem is

$$H(\hat{k}) \equiv \delta_{k_\parallel, \mathbf{0}} f(|k_\perp|), \tag{4.5}$$

where $f(|k_\perp|)$ is a function supported on all values of its argument except those near the origin. We need this 'limited support' condition to ensure that the symmetry-breaking field is approximately

constant over space so that it breaks the symmetry without affecting the spatial inhomogeneity of the ground state. If the function $f(|k_\perp|)$ did not fulfil the limited support condition introduced above, then it would be spatially inhomogeneous at length-scale shorter than the largest length-scale in the problem, viz., the system size. Such spatial inhomogeneity would adversely affect the spatial structure of the order-parameter expectation value, because, we are ultimately interested in its spontaneously generated value. In addition, the symmetry-breaking field has to obey the HRS constraint as do all other critical degrees of freedom in the field theory. Therefore, $H \to 0$ implies a limiting process within the family of such HRS fields, as provided for by the factor $\delta_{k_\parallel,\mathbf{0}}$.

4.3.2 Bare effective free energy to one-loop order

The one-loop correction to the effective free-energy, denoted by $\Delta\Gamma_{1-\text{loop}}[M]$, is the sum over all diagrams of the form shown in Fig. (4.1). Each of these diagrams is to be evaluated maintaining

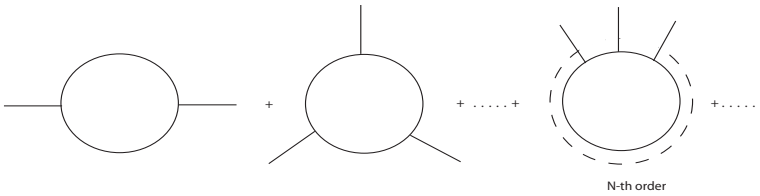

Figure 4.1: Feynman diagrams to one-loop order for the free-energy

the HRS constraint. The details of the evaluation of such HRS-constrained diagrams are discussed in Ref. [35]. In particular, it was shown there that imposing the HRS constraint on an N-point diagram in $(n+1)D$-space, where N is the number of replicated external momenta, is equivalent, in the replica limit (i.e. $n \to 0$), to multiplying by $N-1$ an *unconstrained* diagram in D-dimensional space. We use this result here, for a proof see the Ref. [35].

For a concrete comparison, recall that the one-loop correction to the free energy of a conventional theory like ϕ^4-theory, in which no such special multiplicative correction is required for each loop, is given by [38]

$$\Delta\Gamma_{1-\text{loop}}[M] = \int d\hat{x}d\hat{y}\,\frac{1}{2}\left\{\ln\frac{\delta^2\mathcal{H}}{\delta\Omega(\hat{x})\delta\Omega(\hat{y})}\bigg|_{\Omega=M} - \ln\frac{\delta^2\mathcal{H}}{\delta\Omega(\hat{x})\delta\Omega(\hat{y})}\bigg|_{\Omega=0}\right\}. \tag{4.6}$$

The logarithm in the above equation originates from summing the infinite series of one-loop dia-

grams contributing to the free-energy correction. In the present context, the HRS constraint alters every term in the series expansion of this logarithm. Our goal is to re-sum this series after applying the HRS constraint. In order to make this calculation more transparent, let us first pretend that the external momentum associated with $M(\hat{k})$ can be set to zero in all the diagrams in question. Then the N-point amputated diagram is equal to the integral

$$\frac{(N-1)}{2N}(g_0)^N \int d^D\mathbf{q}\, \frac{1}{(q^2+\tau_0)^N}, \tag{4.7}$$

where by the word 'amputated' we mean that each of these N-point quantities has to be multiplied by $M(\hat{k}_1)\cdots M(\hat{k}_N)\delta(\hat{k}_1+\cdots+\hat{k}_N)$ [or simply $M(\hat{x})^N$ in position space] in order to recover the net one-loop contribution to the free-energy. Next, we introduce a parameter α in order to sum the series of these one-loop terms. This parameter is taken to unity at the end of the calculation. This manipulation leads to

$$\Delta\Gamma_{1-\mathrm{loop}}[M] = -\int d\hat{x}\,\frac{1}{2}\,\alpha^2\frac{d}{d\alpha}\frac{1}{\alpha}\int d^D\mathbf{q}\ln\left(1-\frac{\alpha g_0 M(\hat{x})}{q^2+\tau_0}\right)\Bigg|_{\alpha=1}. \tag{4.8}$$

The operation $\alpha^2\frac{d}{d\alpha}\frac{1}{\alpha}$ generates the desired numerical prefactor $(N-1)$ for the N^{th} order term (corresponding to the N-point diagram) in the expansion of the logarithm in Eq. (4.8). As we are seeking after the EOS, all terms in the one-loop correction to the free-energy that do not depend explicitly on M vanish on taking the functional derivative of the free-energy with respect to M, and hence can be ignored. Keeping this in mind, we now present the one-loop correction to the free-energy without the zero external-momentum approximation made above. It is

$$\Delta\Gamma_{1-\mathrm{loop}}[M] = -\frac{1}{2}\,\alpha^2\frac{d}{d\alpha}\frac{1}{\alpha}\mathrm{Tr}\ln\mathbf{\Delta}(\hat{k},\hat{k}'), \tag{4.9}$$

where the kernel $\mathbf{\Delta}(\hat{q},\hat{q}')$ is given by the kernel

$$\mathbf{\Delta}(\hat{k},\hat{k}') = (\hat{k}^2+\tau_0)\,\delta(\hat{k}-\hat{k}') - \alpha\, g_0 \sum_{\hat{p}\in HRS} M(\hat{p})\,\delta(\hat{p}+\hat{k}-\hat{k}'), \tag{4.10}$$

and where the trace (Tr) is defined as the sum over all internal momenta $\hat{k}$ and $\hat{k}'$ obeying the HRS

constraint. The contribution of the one-loop correction of the free energy to the EOS is obtained by taking the functional derivative of $\Delta\Gamma_{1-\text{loop}}$ with respect to $M(\hat{p})$, resulting in

$$\begin{aligned}\frac{\delta}{\delta M(\hat{p})}\Delta\Gamma_{1-\text{loop}}[M] &= -\frac{1}{2}\,\alpha^2\,\frac{d}{d\alpha}\frac{1}{\alpha}\text{Tr}\left[\frac{-\alpha g_0\,\delta(\hat{p}+\hat{k}-\hat{k}')}{\mathbf{\Delta}(\hat{k},\hat{k}')}\right]\Bigg|_{\alpha=1} \\ &= \frac{g_0^2}{2}\,\text{Tr}\left[\frac{\delta(\hat{p}+\hat{k}-\hat{k}')\sum_{\hat{p}'\in HRS}M(\hat{p}')\delta(\hat{p}'+\hat{k}-\hat{k}')}{\mathbf{\Delta}^2(\hat{k},\hat{k}')}\right] \\ &= \frac{g_0^2}{2}\,\text{Tr}\left[\frac{\delta(\hat{p}+\hat{k}-\hat{k}')M(\hat{p})}{\mathbf{\Delta}^2(\hat{k},\hat{k}')}\right].\end{aligned} \tag{4.11}$$

Our goal is to identify the divergences in this one-loop contribution to the EOS, perform the renormalization and determine the scaling form of the EOS. However, it is unclear how to execute the standard renormalization procedure with the above form of the one-loop contribution. As translational symmetry is broken, momentum space fails to provide the basis space that diagonalizes the kernel $\mathbf{\Delta}$, so its diagonal form has to be determined. It is not clear how to implement the standard renormalization prescription in such a setting. This point merits further enquiry, the central question being: What is the renormalization prescription when translational symmetry is broken and the Gaussian propagator is not diagonal in momentum space? In such a setting, the field theory should be rephrased in the eigenfunction basis of the Gaussian propagator in order to perform perturbative expansions and implement the RG analysis. Integration over momentum indices would then be replaced by summation over eigenvalues of the Gaussian propagator. The momentum cutoffs are replaced by corresponding eigenvalue cutoffs. In the standard prescription of renormalization, the field, the control parameter and the coupling constant are renormalized in the process of integrating out the high-momentum degrees of freedom in the field theory. In the current setting, the degrees of freedom corresponding to the large eigenvalues is to be integrated out, but it is unclear to us how the renormalization prescription is to be modified. Neither is the issue of renormalizability of such a field theory is straightforward. We overcome these difficulties in this chapter as follows. We first take the external momentum of all the one-loop diagrams discussed above to be zero. This serves the purpose of allowing us to determine the renormalized form of the EOS and the critical exponents in a conventional manner, as will be clear from the presentation in the following subsections. We then incorporate corrections to this *renormalized* EOS so that it

is indeed the one-loop EOS for our system. This line of attack will become clearer as the reader proceeds through the presentation of the rest of the Chapter.

4.3.3 Zero external-momentum approximation

We have evaluated the one-loop contribution to the free energy in the zero external-momentum limit in the previous subsection; see Eq. (4.8). However, we cannot ignore the external momentum dependence of the two-point diagram, i.e., the first diagram in Fig. (4.1). As is conventionally the case, the two-point diagram has added divergence for non-zero external-momentum; for details see Refs. [38, 39]. This external-momentum-dependent divergence renormalizes the gradient term in the effective Hamiltonian (2.11). As usual, the external-momentum-independent divergence renormalizes the 'mass' term in the effective Hamiltonian. For details on the RG analysis in the critical region within the liquid state of the field theory described by the effective Hamiltonian (2.11), we encourage the reader to study Refs. [34, 35]. For the sake of brevity, in this Chapter we are going to borrow results from these references, thereby assuming familiarity on the part of the reader with earlier work on V/G field theory. The two-point, one-loop vertex function $\Gamma^{(2)}_{1-\text{loop}}$ in our theory is given by

$$\begin{aligned}\Gamma^{(2)}_{1-\text{loop}}(k) &= \frac{g_0^2}{2}\int d\mathbf{q}\frac{1}{(q^2+\tau_0)\left((\mathbf{q}-\mathbf{k})^2+\tau_0\right)} \\ &= \frac{g_0^2}{2^{(D+1)}\pi^{D/2}}\,\mathbb{G}(2-D/2)\int_0^1 dx\left[\tau_0+k^2x(1-x)\right]^{D/2-2} \qquad (4.12)\end{aligned}$$

where $\mathbb{G}$ is the Gamma function. The divergences show up in the Gamma function which has simple poles at $D = 4, 6, 8, \ldots$. The zero external-momentum ($\mathbf{k} = \mathbf{0}$) part of the vertex function has clearly been included in Eq. (4.8). The external-momentum-dependent part of the vertex function, to the lowest order in external-momentum, is equal to

$$\frac{g_0^2\,\tau_0^{-\epsilon/2}}{2^{(D+1)}\,\pi^{D/2}}\,(D/2-2)\mathbb{G}(2-D/2)\,\frac{k^2}{6}. \qquad (4.13)$$

By eliminating D in favor of $\epsilon = 6 - D$, and using basic properties of the Gamma functions, this expression can be simplified to

$$-\frac{g_0^2 \tau_0^{-\epsilon/2}}{2^{(D+1)}\pi^{D/2}} \mathbb{G}(\epsilon/2)\ \frac{k^2}{6}. \tag{4.14}$$

Next, we identify k^2 to be $\hat{k}^2$ in the expression above in order to determine the form of one-loop effective free energy. This identification is justified in the $n \to 0$ limit and has been used in earlier work, see Appendix A of Ref. [35]. The central point is that divergences in the field theory in the $(n+1)D$-replicated space is the same as that of the field theory in D-dimensional space, as long the HRS constraint is imposed on all diagrams before taking the $n \to 0$ limit. This mapping has been discussed in detail in the Ref. [35]. As a result, one finally obtains the one-loop effective free energy

$$\begin{aligned}\Gamma_{1-\text{loop}}[M] = \int_{\text{HRS}} d\hat{x} \Bigg[\frac{1}{2} \left(1 - \frac{g_0^2 \tau_0^{-\epsilon/2}}{2^{D+1}\pi^{D/2}} \frac{\mathbb{G}(\epsilon/2)}{6} \right) \left[\widehat{\nabla} M(\hat{x}) \right]^2 + \frac{1}{2}\tau_0 M(\hat{x})^2 - \frac{g_0}{3!} M(\hat{x})^3 \\ - \frac{1}{2}\alpha^2 \frac{d}{d\alpha} \frac{1}{\alpha} \int d\mathbf{q} \ln \left(1 - \frac{\alpha g_0 M(\hat{x})}{q^2 + \tau_0} \right) \Bigg|_{\alpha=1} \Bigg],\end{aligned} \tag{4.15}$$

where $M(x)$ is understood to be an HRS function. In the next section, we shall derive the EOS from this effective free-energy and renormalize it.

4.3.4 Unrenormalized Equation of State in the zero-external momentum approximation

The unrenormalized EOS is derived from the effective free energy by taking the functional derivative of Eq. (4.15) with respect to $M(x)$. We use the identity

$$\int \frac{d\mathbf{q}}{q^2 + c^2} = \frac{c^{D-2}\, \mathbb{G}(1 - D/2)}{2^D\, \pi^{D/2}} \tag{4.16}$$

to obtain to the following form of the unrenormalized EOS [23]:

$$\begin{aligned}H(x) = \left\{ 1 - \frac{g_0^2 \tau_0^{-\epsilon/2}}{2^{D+1}\pi^{D/2}} \frac{\mathbb{G}(\epsilon/2)}{6} \right\} (-\widehat{\nabla}^2) M(\hat{x}) + \tau_0 M(\hat{x}) \\ - \frac{g_0}{2} M(\hat{x})^2 - \frac{g_0^2}{2} \left\{ \frac{\mathbb{G}(\epsilon/2 - 2)}{2^D \pi^{D/2}} \right\} \Big(\tau_0 - g_0 M(\hat{x}) \Big)^{1-\epsilon/2} M(\hat{x}).\end{aligned} \tag{4.17}$$

The terms in the curly brackets are the divergent quantities. We use the relation

$$\mathbb{G}\left(\frac{\epsilon}{2}-2\right) \approx \frac{1}{\epsilon} - \frac{1}{2}\left(\gamma_E + \frac{3}{2}\right) + O(\epsilon), \tag{4.18}$$

where γ_E is Euler's constant, to derive the EOS to lowest order in ϵ:

$$\begin{aligned} H(x) = &\left\{1 - \frac{g_0^2 \tau_0^{-\epsilon/2}}{2^D \pi^{D/2}}\left(\frac{1}{6\epsilon} - \frac{\gamma_E}{12}\right)\right\}(-\widehat{\nabla}^2)M(\hat{x}) + \tau_0 M(\hat{x}) - \frac{g_0}{2}M(\hat{x})^2 \\ &+ \frac{1}{2}\left(\frac{g_0^2}{2^D\pi^{D/2}}\right)M(\hat{x})\Big(\tau_0 - g_0 M(\hat{x})\Big)\ln\left[\tau_0 - g_0 M(\hat{x})\right] \\ &- \left(\frac{g_0^2}{2^D\pi^{D/2}}\right)M(\hat{x})\Big(\tau_0 - g_0 M(\hat{x})\Big)\left\{\frac{1}{\epsilon} - \frac{1}{2}\left(\gamma_E + 2\right)\right\}. \end{aligned} \tag{4.19}$$

Note that in order to calculate the O(ϵ) correction to the EOS, it suffices to retain terms that are of zeroth order in epsilon within expressions that are proportional to g_0^2. This observation anticipates the result that the fixed-point value of the squared coupling constant g^2 is proportional to ϵ. All divergences appear as poles in $1/\epsilon$ in the EOS; these are the terms within curly brackets in Eq. (4.19). In the next subsection we use renormalizations of the field, the control parameter and the coupling constant to cure these divergences in the standard manner.

4.3.5 Renormalization

Before we execute the standard renormalization prescription, a few remarks may be useful. A cubic theory is strictly renormalizable only on the inclusion of a linear term $H(\hat{x})M(\hat{x})$ in the effective Hamiltonian. This is because the a cubic coupling generates tadpole diagrams that are linear in the order parameter, and the external field $H(\hat{x})$ has to be chosen such that the contribution of all such divergent tadpole-diagrams are cancel [39]. This additional renormalization of the field is implicitly assumed in the present context without further elaboration.

We renormalize Eq. (4.19) in the conventional manner [35]. First, we multiply both sides of the equation by $M(\hat{x})$. The combination $H(\hat{x})\,M(\hat{x})$ is mapped to the combination $H_R(\hat{x})\,M_R(\hat{x})$ in the renormalized theory, where subscript R denotes renormalized quantities. We use the following renormalization scheme:

$$\begin{aligned}
\text{Field renormalization}: &\quad M \to M_R = Z^{1/2}\, M \\
\text{Mass renormalization}: &\quad \tau_0 \to \tau_R = Z^{-1}\, Z_\tau\, \tau_0 \\
\text{Coupling const. renormalization}: &\quad g_0^2 \to g_R^2 = (4\pi)^{D/2}\, Z^{-3}\, Z_u\, \mu^\epsilon\, u
\end{aligned}$$

On rearranging the terms in Eq. (4.19), we obtain[1]

$$\begin{aligned}
H_R(\hat{x})\, M_R(\hat{x}) = &\left\{1 - \left(\frac{\mu^2}{\tau_R}\right)^{\epsilon/2}\left(\frac{u}{6\epsilon}\right)\right\} Z^{-1} M_R(\hat{x})(-\widehat{\nabla}^2) M_R(\hat{x}) + \left\{1 - \frac{\mu^\epsilon u}{\epsilon}\right\} Z_\tau^{-1} \tau_R M_R(\hat{x})^2 \\
&- \frac{g_R}{2}\left\{1 - \frac{2\mu^\epsilon u}{\epsilon}\right\} Z_u^{-1/2} M_R(\hat{x})^3 + \frac{\mu^\epsilon u}{2} M_R(\hat{x})^2 \Big(\tau_R - g_R M_R(\hat{x})\Big) \ln\left[\tau_R - g_R M_R(\hat{x})\right] \\
&+ \frac{u\gamma_E}{12}\left(\frac{\mu^2}{\tau_R}\right)^{\epsilon/2} M_R(\hat{x})(-\widehat{\nabla}^2) M_R(\hat{x}) + \frac{1}{2}\mu^\epsilon u(\gamma_E + 2) M_R(\hat{x})^2 \Big(\tau_R - g_R M_R(\hat{x})\Big).
\end{aligned} \tag{4.20}$$

From the first three terms on the right hand side of Eq.(4.20) we determine the renormalization factors, correct up to a one-loop order, for the V/G field theory. The same factors are known to renormalize the Potts model in the one-state limit [42] and has been obtained for the V/G field theory in earlier work [35]. They are

$$Z = 1 + \frac{1}{6}\frac{u}{\epsilon}, \tag{4.21a}$$

$$Z_\tau = 1 + \frac{u}{\epsilon}, \tag{4.21b}$$

$$Z_u = 1 + 4\,\frac{u}{\epsilon}. \tag{4.21c}$$

The calculation of the β-function from the renormalization factors has been presented in earlier work [35] and we just quote the relevant results here. The Wilson-Fisher fixed-point value for g is given by $u^* = 2\epsilon/7$. which, as anticipated in the previous section, is of order epsilon. As we are interested in studying the EOS at the Wilson-Fisher fixed point, we replace u by u^* in Eq. (4.20).

[1] In the calculation, we have taken the renormalization factors to be unity wherever this is consistent to order ϵ; as done before, we anticipate that any term proportional to g_0^2 will eventually be proportional to ϵ because the fixed-point value of the squared coupling constant is $\mathrm{O}(\epsilon)$.

The form of our renormalized EOS is then

$$\begin{aligned} H_R(\hat{x}) &= (-\widehat{\nabla}^2)M_R(\hat{x}) + \tau_R M_R(\hat{x}) - \frac{g_R^*}{2}M_R(\hat{x})^2 + \frac{\epsilon}{7}M_R(\hat{x})\Big(\tau_R - g_R^* M_R(\hat{x})\Big)\ln\left[\tau_R - g_R^* M_R(\hat{x})\right] \\ &\quad + \frac{\epsilon\gamma_E}{42}\widehat{\nabla}^2 M_R(\hat{x}) + \frac{\epsilon}{7}(\gamma_E + 2)M_R(\hat{x})\Big(\tau_R - g_R^* M_R(\hat{x})\Big). \end{aligned} \tag{4.22}$$

Note that by a trivial rescaling of the renormalized quantities M_R, τ_R and g_R, viz.,

$$M_R \rightarrow \left(1 + \frac{\gamma_e}{42}\,\epsilon\right) M_R \tag{4.23a}$$

$$\tau_R \rightarrow \left(1 + \frac{\gamma_E + 2}{7}\,\epsilon\right) \tau_R \tag{4.23b}$$

$$g_R^* \rightarrow \left(1 + \frac{\gamma_E + 2}{7}\,2\epsilon\right) g_R^* \tag{4.23c}$$

we can recast the Eq. (4.22) into the form,

$$H_R(\hat{x}) = (-\widehat{\nabla}^2)M_R(\hat{x}) + \tau_R M_R(\hat{x}) - \frac{g_R^*}{2}M_R(\hat{x})^2 + \frac{\epsilon}{7}M_R(\hat{x})\Big(\tau_R - g_R^* M_R(\hat{x})\Big)\ln\left[\tau_R - g_R^* M_R(\hat{x})\right], \tag{4.24}$$

correct to $O(\epsilon)$. This is the final form of the renormalized EOS at the fixed point. In the Subsection 4.3.7 we shall derive the scaling form of the EOS after identifying the RG-guided scaling variables and the functional form of $M_R(\hat{x})$. Note that from now on we shall drop the subscript R in order to streamline the notation; all quantities are renormalized unless stated otherwise.

4.3.6 Short inventory of exponents

In order to prepare the unsuspecting reader of the fusillade of standard critical exponents that is imminent in the next few subsections, it seems wise to catalogue all of them here for ready reference. The list is:

ν : Correlation length exponent, $\xi \sim |\tau|^{-\nu}$

β : Gel fraction exponent, $Q \sim |\tau|^{\beta}$

δ : External field exponent, $Q \sim H^{1/\delta}$

η : Anomalous dimension, Correlator $\sim k^{-2+\eta}$

f : Shear modulus exponent, Shear modulus $\sim |\tau|^f$

The hyperscaling relations that are repeatedly invoked are

$$\beta = \frac{(D-2+\eta)\nu}{2} \text{ and } \delta = \frac{D+2-\eta}{D-2+\eta}$$

There are, of course, a few other exponents [2] in the standard list of critical exponents. Thankfully, we shall not need the rest in this Thesis. The shear modulus exponent will be examined in Chapter 6.

4.3.7 Scaling form of the Equation of State in the zero external-momentum approximation

In this subsection we remind the reader of the scaling form of various central quantities in the theory and establish the scaling form of the EOS. The functional form of the N-point vertex function in the critical region is determined from the solution of the RG equation, see e.g., Ref. [38]. We use the hyperscaling relation $\beta = (D-2+\eta)\nu/2$ to rewrite the familiar scaling form of N-point vertex functions as

$$\Gamma^{(N)}(\{\hat{k}_i\}, \tau, g) \sim \mu^{\frac{N}{2}\eta} |\tau|^{(\nu D - N\beta)} F(\{\hat{k}_i\}/|\tau|^\nu), \tag{4.25}$$

where D is the dimension of space (as we have said before), F is a generic (N-dependent) scaling function, μ is the renormalization momentum scale, typically replaced by the high-momentum cutoff of the problem, and the other Greek symbols represent the standard scaling exponents. Here, we shall concentrate on the one-point vertex function, as it is related to the expectation value of the order parameter, whose scaling form we are after. First note that (the integral of) the one-point vertex function multiplied by the order-parameter expectation-value is scale independent, because the combination is an 'energy' term similar to the effective Hamiltonian, and is scale-independent by construction, i.e.,

$$\left[\int d^{D(n+1)}\hat{k} \;\; \Gamma^{(1)} \left(\{\hat{k}_i\}, \tau, g \right) M(\hat{k}) \right] \equiv [1], \tag{4.26}$$

[2] The word 'exponent' bearing the mathematical meaning of an 'index' was used as early as 1706. In 1734 G. B. Berkley in *The Analyst* wrote this intriguing sentence, *We may often observe that the Exponents of Fluxions... are confounded with the Fluxions themselves.* I couldn't figure out what it means, but it's an etymological curiosity I discovered in the Oxford English Dictionary.

where, in this Chapter, $[\cdots]$ denotes the engineering dimension of the enclosed quantity. which implies that

$$M(\hat{k}) \sim |\tau|^{\beta} F(\{\hat{k}_i\}/|\tau|^{\nu}) =: Q\, m(\{\hat{k}_i\}/|\tau|^{\nu}), \tag{4.27}$$

where m is a scaling function and Q is the gel-fraction. The gel fraction scales as τ^{β}. The scaling form of H can also be determined from the one-point vertex function. Note that $H(\hat{k})$ scales as $\Gamma^{(1)}(\{\hat{k}_i\}, \tau, g)$ because the combination $H(\hat{k})\, M(\hat{k})$ has the dimensions of energy density. In keeping with the conventional practice, we hide the explicit dependence on μ, and thus obtain

$$\begin{aligned} H(\hat{k}) &\sim |\tau|^{(\nu D - \beta)} F(\{\hat{k}_i\}/|\tau|^{\nu}) \\ &= |\tau|^{\nu(D+2-\eta)/2} F(\{\hat{k}_i\}/|\tau|^{\nu}) \\ &= |\tau|^{\beta\delta} F(\{\hat{k}_i\}/|\tau|^{\nu}) \\ &= Q^{\delta} f(\{\hat{k}_i\}/|\tau|^{\nu}; \tau Q^{-1/\beta}), \end{aligned} \tag{4.28}$$

where we have used the relation $\delta = (D+2-\eta)/(D-2+\eta)$ to obtain the final form; see Ref. [38]. In the last line of Eq. (4.28) we have included the scale-independent combination $\tau Q^{-1/\beta}$ as an argument of the new scaling function f. The EOS, Eq. (4.24), is to be recast in the scaling form dictated by Eq. (4.28). We have defined the scaling function in the scaling form of $M(\hat{x})$ to be $m(\hat{x})$, i.e.,

$$M(\hat{x}) \equiv Q^{\beta}\, m(|\tau|^{\nu} \hat{x}). \tag{4.29}$$

Note that the scaling function $m(\hat{x})$ has information about the distribution of localization lengths, which is a quantity of central interest in the present work.

The scaling variables for the EOS are $m(\hat{x})$ and $\theta \equiv \tau (g^* Q)^{-1/\beta}$, where we have included g^* in the scaling variable for simplification. The requirement that Eq. (4.24) be rewritable in the scaling form dictated by Eq. (4.28) is sufficient to determine the $O(\epsilon)$ correction to β and δ, i.e., $\beta = 1 - \epsilon/7$ and $\delta = 2 + 2\epsilon/7$; see Appendix G. From Eq. (4.24) and Eq. (4.28) and Appendix G we obtain

$$H = y^{\delta} \left[\frac{1}{y^{\delta-1}} (-\widehat{\nabla}^2) m + \theta m - \frac{1}{2} m^2 + \frac{\epsilon}{7} m(\theta - m) \ln\left[\theta - m\right] \right], \tag{4.30}$$

where $y \equiv g^* Q$ and we have rescaled H appropriately to absorb trivial constants. However, the

above equation cannot be fully correct, because the right-hand-side is not a function of the scaling variables θ and m alone, but also depends on y, which is not a scaling variable. Let us see what the remedy for this problem is.

RG analysis dictates that in the scaling regime the renormalized two-point Green function $G(\hat{k})$ is proportional to $1/\left(k^{2-\eta}+1/\xi\right)$, in contrast to its bare form, $1/(k^2+\tau_0)$, where ξ is the correlation length-scale. The anomalous exponent η originates in renormalizing the field, and is physically related to the existence of a short-distance cutoff, which in this problem is the typical size of the constituent particles ξ_0, e.g., the typical size of each uncrosslinked polymers. The functional form of $G(\hat{k})$ gives us an indication that the operator $(-\widehat{\nabla})^2$ [i.e., the Fourier conjugate of $\hat{k}^2$] also should be replaced by $(-\widehat{\nabla}^2)^{\frac{2-\eta}{2}}$ [i.e. the Fourier conjugate of $k^{2-\eta}$]. Not surprisingly, if we use this conjecture in Eq. (4.30) we discover that a universal form of the EOS is indeed obtained, and all dependence on the non-scaling variable y is absent. In the derivation of the scaling form of the EOS, it is to be remembered that the argument of m is the rescaled variable $|\tau|^{\nu}\hat{x}$. Thus the operator $(\widehat{\nabla})^{\frac{2-\eta}{2}}$ defined in $\hat{x}$ space is accompanied by a multiplicative factor $|\tau|^{\nu(2-\eta)}$ when defined in $\hat{r}$ space, where $\hat{r}\equiv|\tau|^{\nu}\hat{x}$. Using the hyperscaling relations (4.25), the factor $|\tau|^{\nu(2-\eta)}/y^{\delta-1}$ can be recast as $|\theta|^{\nu(2-\eta)}$. Finally, we arrive at the EOS:

$$H(\hat{x})=Q^{\delta}\left[|\theta|^{\nu(2-\eta)}(-\widehat{\nabla}^2)^{\frac{2-\eta}{2}}m(\hat{r})+\theta m(\hat{r})-\frac{1}{2}m(\hat{r})^2+\frac{\epsilon}{7}m(\hat{r})\big(\theta-m(\hat{r})\big)\ln\left[\theta-m(\hat{r})\right]\right], \quad (4.31)$$

where we have rescaled H to absorb trivial factors.

Let us now discuss the conjecture we made in the previous paragraph in more detail. In the V/G field theory the anomalous exponent η is $O(\epsilon)$, in contrast to the ϕ^4 theory, where it is $O(\epsilon^2)$. Therefore, in principle one should be able to derive the correct scaling form of the gradient term in the EOS, conjectured above, entirely from an honest calculation of one-loop diagrams. To this purpose, one would need to keep track of the diverging coefficient of the term $\hat{k}^2\ln\hat{k}$. This is much harder to achieve, especially because of the complications of calculating all N-point (one-loop) diagrams with non-zero external momenta in the calculation of the free energy Γ. We instead settle for the non-rigorous arguments given above, which nevertheless leads us to the correct scaling form of the EOS. We remind the reader that because translational symmetry is spontaneously broken in the V/G theory, the order parameter expectation value is momentum-dependent, requiring the

calculation external-momentum dependent diagrams in the free energy, as has been discussed in Subsection 4.3.2.

Now assume that the desired symmetry-breaking field H is taken to zero through the HRS sector, thereby breaking the symmetry spontaneously. Then the differential equation, whose solution produces the the one-loop corrected distribution of localization lengths, becomes

$$|\theta|^{\nu(2-\eta)}(-\widehat{\nabla}^2)^{\frac{2-\eta}{2}}m(\hat{r}) + \theta m(\hat{r}) - \frac{1}{2}m(\hat{r})^2 + \frac{\epsilon}{7}m(\hat{r})\Big(\theta - m(\hat{r})\Big)\ln\left[\theta - m(\hat{r})\right] = 0. \tag{4.32}$$

Recall, however, that we arrived at this form of the differential equation within the zero external-momenta approximation for the one-loop correction, which is given by the last term on the left-hand-side. As we have mentioned earlier, this is obviously not a justifiable approximation, because we are seeking a spatially-dependent order-parameter expectation value. Notwithstanding this short-coming, the exercise carried out till now in—proceeding with an approximated form of the one-loop correction—has its merit in guiding us to the scaling form of the exact differential equation, as we shall see in the next subsection.

4.3.8 The exact differential equation

In the latter part of Subsection 4.3.2 we presented the form of the bare one-loop correction to the free-energy without making the zero-external momentum approximation. In this subsection, we combine that form with results obtained in the preceding subsection to arrive at the exact differential equation for the scaling function $m(\hat{r})$. We denote the eigenvectors of the operator $\mathbf{\Delta}$ by $|\psi_\lambda\rangle$, i.e., $\mathbf{\Delta}|\psi_\lambda\rangle = \lambda|\psi_\lambda\rangle$, where λ is the corresponding eigenvalue. Using Eq. (4.11), the one-loop correction to the EOS becomes

$$\begin{aligned}
\frac{\delta\Delta\Gamma_{1-\text{loop}}[M]}{\delta M(\hat{p})} &= \frac{g_0^2}{2}\text{Tr}\left[M(\hat{p})\delta(\hat{p}+\hat{k}-\hat{k}')\sum_\lambda \frac{1}{\lambda^2}\langle\hat{k}|\psi_\lambda\rangle\langle\psi_\lambda|\hat{k}'\rangle\right] \\
&= \frac{g_0^2}{2}\int d\hat{k}\left[M(\hat{p})\sum_\lambda \frac{1}{\lambda^2}\langle\hat{k}|\psi_\lambda\rangle\langle\psi_\lambda|\hat{p}+\hat{k}\rangle\right] \\
&= \frac{g_0^2}{2}\int d\hat{r}\left[M(\hat{p})\sum_\lambda \frac{1}{\lambda^2}\langle\hat{r}|\psi_\lambda\rangle\langle\psi_\lambda|\hat{r}\rangle e^{i\hat{p}\cdot\hat{r}}\right],
\end{aligned} \tag{4.33}$$

where we have used the definition $\langle \hat{r}|\hat{k}\rangle \equiv e^{i\hat{k}\cdot\hat{r}}$. In real space, we obtain

$$\frac{\delta\Delta\Gamma_{1-\text{loop}}[M]}{\delta M(\hat{r})} = \frac{g_0^2}{2}\left[M(\hat{r})\sum_{\lambda}\frac{1}{\lambda^2}|\psi_\lambda(\hat{r})|^2\right]. \tag{4.34}$$

The details of the calculation of the eigenspectrum of $\mathbf{\Delta}$ are presented in Appendix F. In particular, there it is shown that the eigenvalues λ are of the form $\lambda \equiv k_\parallel^2 + \lambda_{lr}$ where λ_{lr} is the eigenvalue corresponding to the eigenfunction denoted by $\psi_{lr}^\perp(r_\perp)$ in $r_\perp$-space. The indices l and r label the angular and radial part of the eigenfunctions $\psi_{lr}^\perp(r_\perp)$, respectively. The form of λ becomes obvious on remembering that the translational symmetry in the solid state is preserved in $r_\parallel$-space and broken in $r_\perp$-space; hence, the eigenfunctions of the operator $\mathbf{\Delta}$ separate into plane waves in $r_\parallel$-space and eigenfunctions $\psi_{lr}^\perp(r_\perp)$ in $r_\perp$-space. Hence, we obtain the exact one-loop correction to the EOS

$$\frac{\delta\Delta\Gamma_{1-\text{loop}}[M]}{\delta M(\hat{r})} = \frac{g_0^2}{2}\int dk_\parallel\left[M(\hat{r})\sum_{\lambda_{lr}}\frac{1}{k_\parallel^2+\lambda_{lr}}\,|\psi_{lr}^\perp(r_\perp)|^2\right]. \tag{4.35}$$

Next, we use our understanding of the scaling form of the approximate differential equation (4.32) to recast the above contribution to the EOS into its scaling form. To this end, first note that the divergence found in Eq.(4.17) on integrating over the D-dimensional momentum $\mathbf{q}$ and the divergence encountered in Eq. (4.35) on integrating over the D-dimensional momentum $k_\parallel$ are analogous. We postulate that the renormalization process is identical, and the structure of the scaling form of the contribution (4.35) being considered presently is determined analogous to the approximate case considered in the preceding subsections; see Eq. (4.32). To the best of our understanding, deriving the scaling form of the EOS more rigorously would be quite intractable. We remind the reader, once again, that the conventional prescription of renormalization of field, control parameter and coupling constant in a conventional field theory (e.g., ϕ^4 theory) relies heavily on the translational invariance of the theory. Motivated be the above considerations, we argue that the scaling form of the exact one-loop contribution to the EOS is

$$\frac{\epsilon}{7}m(\hat{r})\Big(\theta - m(\hat{r})\Big)\ln\left[\theta - m(\hat{r})\right] \longrightarrow \frac{\epsilon}{7}\left[m(\hat{r})\sum_{\lambda_{lr}}|\psi_{lr}^\perp(r_\perp)|^2\,\lambda_{lr}\ln\lambda_{lr}\right]. \tag{4.36}$$

Using the above result, and the Eq. (4.32), we arrive at the differential equation whose solution provides us with the expectation value of the order parameter at the one-loop level;

$$|\theta|^{\nu(2-\eta)}(-\widehat{\nabla}^2)^{\frac{2-\eta}{2}}m(\hat{r}) + \theta m(\hat{r}) - \frac{1}{2}m(\hat{r})^2 + \frac{\epsilon}{7}m(\hat{r})\left[\sum_{\lambda_{lr}}|\psi_{lr}^{\perp}(r_{\perp})|^2\,\lambda_{lr}\ln\lambda_{lr}\right] = 0. \tag{4.37}$$

We remind the reader that the operator $(-\widehat{\nabla}^2)^{\frac{2-\eta}{2}}$ in the above equation is to be understood to be the Fourier transform of $\hat{k}^{2-\eta}$. One should also remember that the scaling function $m(\hat{r})$ in Eq. (4.37) is a HRS quantity, as the V/G field theory is defined on degrees of freedom restricted to the HRS. We will discuss the HRS constraint further in a Subsection 4.4.2.

4.4 Solution of the corrected differential equation

In this section we begin with the differential equation (4.37) derived in the previous section and end with the solution of the order-parameter expectation value in real space, which produces the correction to the distribution of localization lengths.

4.4.1 Simplified form of differential equation

In this subsection we present a simplified form of the differential equation, Eq. (4.37). Firstly, note that from earlier work [34] the values of the exponents ν, η and β are known to be given, to first order in ϵ, by

$$\begin{aligned}\nu^{-1} &= 2 - 5\epsilon/21\\ \eta &= -\epsilon/21\\ \beta &= 1 - \epsilon/7.\end{aligned} \tag{4.38}$$

As should be the case, on substituting the mean-field values of the exponents into Eq. (4.37) we recover the mean-field equation for the scaling function $m_0(\hat{r}_0)$ which, in terms of the scaled variables, is

$$|\theta_0|(-\widehat{\nabla}^2)m_0(\hat{r}_0) + \theta_0 m_0(\hat{r}_0) - \frac{1}{2}m_0(\hat{r}_0)^2 = 0, \tag{4.39}$$

where $\theta_0 \equiv \tau(gQ)^{-1}$ and $\hat{r}_0 \equiv \tau^{1/2}\hat{x}$ are the mean-field scaling variables, and $m_0(\hat{r}_0)$ is the mean-field solution. As we know the functional form of the mean-field solution $m_0(r_0)$, we also know the solution to the equation

$$|\theta|(-\widehat{\nabla}^2)m_0(\hat{r}) + \theta m_0(\hat{r}) - \frac{1}{2}m_0(\hat{r})^2 = 0, \tag{4.40}$$

where we have replaced the mean-field scaling variables θ_0 and $\hat{r}_0$ by the scaling variables θ and $\hat{r}$. This rather simple step is made explicit here to emphasize that we are not expanding the scaling functions around their mean-field scaling arguments but, rather, retaining their dependence on the appropriate RG-dictated scaling variables that differ at $O(\epsilon)$ from their mean-field counterparts. We expect the correction to the mean-field solution $m_0(\hat{r})$ to be of $O(\epsilon)$ at the one-loop level. Let us define this correction $m_1(\hat{r})$ via the equation

$$m(\hat{r}) = m_0(\hat{r}) + \epsilon\, m_1(\hat{r}). \tag{4.41}$$

On substituting this expansion of $m(\hat{r})$ into Eq. (4.37) and using Eq. (4.40), we obtain the following linear homogeneous differential equation for the correction function $m_1(\hat{r})$, correct to $O(\epsilon)$:

$$\left[|\theta|(-\widehat{\nabla}^2) + \theta - m_0(\hat{r})\right] m_1(\hat{r}) = \mathcal{S}(\hat{r}). \tag{4.42}$$

$\mathcal{S}(\hat{r})$ is a 'source term', and is given by

$$\mathcal{S}(\hat{r}) \equiv \frac{1}{\epsilon}\left(|\theta|(-\widehat{\nabla}^2) - |\theta|^{\nu(2-\eta)}(-\widehat{\nabla}^2)^{\frac{2-\eta}{2}}\right) m_0(\hat{r}) - \frac{1}{7}m_0(\hat{r})\left[\sum_{\lambda_{lr}} |\psi^{\perp}_{lr}(r_\perp)|^2\, \lambda_{lr} \ln \lambda_{lr}\right]. \tag{4.43}$$

Let us take a moment to appreciate the source term, which has two contributions: The first is from the correction to the 'gradient' term in the EOS, and its functional form is dictated by scaling arguments, and is thus exact to all orders in epsilon expansion. This term is more transparent in Fourier space and we will later discuss its calculation. The second contribution originates from the loop contribution to the free energy itself, and hence its functional form is specific to the one-loop order correction presented in this work.

In contrast to the mean-field equation (2.18), which produced an integro-differential equation for the distribution of localization lengths on using the Ansatz form (2.15) for the solution, the one-

loop differential equation is not amenable to a similar simplification. This is because the 'source' term does not simplify on using such an Ansatz form. However, as we shall soon demonstrate, one can obtain an *ordinary* differential equation for $m_1(\hat{r})$. We address a few issues related to the HRS constraint in in the next subsection, before proceeding to the subsections dealing with the solution of the differential equation (4.42).

4.4.2 Higher Replica Sector constraint revisited

In this subsection we analyze the implications of the HRS constraint on quantities defined in real space, in particular, on $m(\hat{r})$ because it features in the EOS[3]. It is obvious that the saddle-point solution

$$m_0(\hat{q}) = -\delta_{\hat{q},0} + \delta_{q_\parallel,0} \int d\zeta\, \mathcal{P}_0(\zeta)\, e^{-\hat{q}^2/2\zeta} \tag{4.44}$$

explicitly conforms to the HRS constraint, as it must. The Fourier transform of the saddle-point solution is given by

$$m_0(\hat{r}) = \int d\zeta\, \mathcal{P}_0(\zeta)\, e^{-\zeta r_\perp^2/2} - 1. \tag{4.45}$$

The nature of symmetry breaking dictates the form of the order-parameter expectation value $m(\hat{r})$, therefore

$$\begin{aligned} m(\hat{r}) &= \int d\zeta\, \mathcal{P}(\zeta)\, e^{-\zeta r_\perp^2/2} - 1 \\ &= \int d\zeta\, \left[\mathcal{P}_0(\zeta) + \epsilon \mathcal{P}_1(\zeta)\right]\, e^{-\zeta r_\perp^2/2} - 1 \\ &= m_0(|r_\perp|) + \epsilon m_1(|r_\perp|), \end{aligned} \tag{4.46}$$

where $\mathcal{P}(\zeta)$ is the corrected distribution of localization lengths and $\mathcal{P}_1(\zeta)$ is the $O(\epsilon)$ correction to the saddle-point distribution. Now note that as $\mathcal{P}(\zeta)$ and $\mathcal{P}_0(\zeta)$ are normalized probability distributions, integration of $\mathcal{P}_1(\zeta)$ must yield zero. In effect, this condition imposes the *boundary condition* $m_1(r_\perp = 0) = 0$, which, in return, is necessary and sufficient to ensure that $m(\hat{r})$ is a HRS function. In other words, if we are searching for solutions of our differential equation (4.42) in the class of functions that have the Ansatz form (4.46) and obey the above boundary condition,

[3]We remind the reader of the importance of the HRS constrint. This constraint modifies the evaluation of all the Feynman diagrams in the field theory, thereby altering the critical properties of the VG theory and classifying it in the percolation universality class, which is distinct from the scalar ϕ^3-theory universality class.

we are—in effect—scanning through the family of HRS functions.

The Ansatz (4.46) is a function of the magnitude of the $r_\perp$ vector alone, and this can be used to our advantage to obtain an ordinary differential equation. We define a new variable $\rho \equiv r_\perp^2/2$, and recast the differential equation (4.37) in terms of this new variable. The Laplacian operator in ρ space is

$$\widehat{\nabla}^2 = 2\rho \frac{\partial^2}{\partial \rho^2} + nD \frac{\partial}{\partial \rho}, \tag{4.47}$$

where we have used the fact that $r_\perp$ is an nD-dimensional vector. We shall only retain terms in the above operator identity that survive the $n \to 0$ limit. On substitution of $r_\perp$ in favor of ρ in Eq. (4.37), we obtain

$$\left[-2\rho|\theta| \frac{\partial^2}{\partial \rho^2} + \theta + 1 - \int d\zeta \mathcal{P}_0(\zeta) e^{-\zeta\rho} \right] m_1(\rho) = \mathcal{S}(\rho). \tag{4.48}$$

This is the form of the ordinary differential equation that we shall solve numerically, after substituting for an appropriate value of θ that we argue for in the following subsection.

4.4.3 Determining the value of the scaling variable θ

The differential equation (4.37) has a free scaling variable θ, whose value has to be determined in order to solve for $m_1(\hat{r})$. Recall that, at the mean-field level, the scaling variable θ_0 was determined by taking a zero-momentum limit through HRS; see Eq. (2.19). If we repeat the process for Eq.(4.37), it is obvious that at the zeroth order in ϵ we have $\theta = -1/2$, which is the same as its mean-field value. Next, we make the claim that to determine the $\mathrm{O}(\epsilon)$ correction $m_1(\hat{r})$ it is consistent to assign to θ its zeroth order value in ϵ. In order to verify this claim, note that in Eq. (4.48) the function $m_1(\hat{r})$ is an $O(\epsilon)$ correction, so every term in that equation can be consistently replaced by its $O(1)$ value. However, as the first part of the source term (4.43) has a factor of $1/\epsilon$, it is not immediately clear that replacing θ by its zeroth order value in ϵ is consistent. To make this evident, note that in $\hat{q}$-space the first part of the source term is proportional to

$$-|\theta| q_\perp^2 \left[\frac{1}{7} \ln|\theta| + \frac{1}{21} \ln|q_\perp| \right], \tag{4.49}$$

where we have used the relation $\nu(2-\eta) = 1 + \epsilon/7$, established by using the $O(\epsilon)$ values of the exponents. As the above expression does not depend on ϵ, it is consistent to assign θ its mean field value, as claimed.

To the careful reader, it may appear mysterious that the scaling variable $\theta \equiv \tau(g^*Q)^{-1/\beta}$ is being assigned a specific numerical value. In general, scaling variables in a renormalized theory are dimensionless quantities that are dependent on physical variables, which conspire to appear in a particular combination, predicted by the RG theory, and signify the universal relationship between these physical quantities in the critical region. Moreover, these scaling variables are typically dependent on the high-momentum cutoff μ, though such dependence is usually hidden, because requiring the scaling variables to be dimensionless is sufficient to reproduce the dependence on μ. Assigning a scaling variable a specific numerical value is a choice of the proportionality constant for power-law behavior, e.g., $Q \propto \tau^\beta$ and $\theta \sim \tau/Q^{1/\beta}$. In reality, this proportionality constant depends on the non-universal properties of the system. In the current setting, our objective is to evaluate a universal function, viz., the distribution of localization lengths. Therefore, it is harmless to fix the value of θ in Eq. (4.48) in such a way that the choice is consistent with the proper mean-field limit of the equation, which is what we have done here.

4.4.4 Evaluation of the source term

In this subsection[4] we present the calculation of source term in Eq. (4.48); see also Eq. (4.37). The source term, given by Eq. (4.43), has two parts. The first part, in momentum space, is of the form

$$\frac{1}{\epsilon}\left[|\theta| q_\perp^2 - |\theta|^{\nu(2-\eta)} (q_\perp^2)^{1-\eta/2}\right] \int d\zeta\, e^{-q_\perp^2/2\zeta} \mathcal{P}_0(\zeta). \tag{4.50}$$

On using the value of the exponents given in Eq.(4.38), we obtain the following expression for this first part:

$$-\frac{|\theta|}{7}\left[\ln|\theta|\, q_\perp^2 + \frac{1}{3} q_\perp^2 \ln|q_\perp|\right] \int d\zeta\, e^{-q_\perp^2/2\zeta} \mathcal{P}_0(\zeta), \tag{4.51}$$

correct to zeroth order in ϵ. As $q_\perp$, and its Fourier conjugate $r_\perp$, are zero-dimensional vectors in the replica limit, it is not obvious how to perform the Fourier transform of the above expression

[4] I thank Ken Esler for performing the numerical calculations for some of the results presented in this and the next subsection.

and arrive at its form in the real space. In Appendix E we present the mathematical details of Fourier transform in almost-zero dimensional space and calculate the Fourier transform of the expression (4.51). Expressed as a function of the variable $r \equiv |r_\perp|$, the result of the computation is

$$\frac{|\theta|}{7}\int d\zeta \left[\ln|\theta|\, r^2\zeta^2 + \frac{1}{3}\left\{\frac{1}{2}r^2\zeta^2 \mathrm{Ei}\left(\frac{\zeta r^2}{2}\right) - r^2\zeta^2\ln(r^2\zeta^2) + \zeta - \zeta e^{\zeta r^2/2}\right\}\right]\mathcal{P}_0(\zeta)\, e^{-\zeta r^2/2}, \quad (4.52)$$

where $\mathrm{E}i(\cdot)$ is the Exponential Integral function [43].

The evaluation of the second part of the source term (4.43) relies upon the calculation of the eigenspectrum of the kernel $\mathbf{\Delta}$, which is also the solid-state propagator for the V/G field-theory. The calculation of the eigenspectrum of the solid-state propagator is also relegated to Appendix F; for physical interpretation and further discussion see Ref. [64]. Here, we summarize the main features of the eigenspectrum of $\mathbf{\Delta}$. The eigenspectrum has only two *bound states*, corresponding to angular momentum indices $l = 0$ and $l = 1$. By the term bound state we mean normalized eigenfunctions of the correlator that have a finite support in the $r_\perp$-space and asymptotically vanishes for large values of $r_\perp$. The $l = 1$ sector bound state is the massless Goldstone branch and is determined analytically. The $l = 0$ sector bound state is denoted by $\psi_0(r)$, and corresponds to the eigenvalue $\lambda_{lr} \equiv \lambda_0 = 1 - 0.2667$ determined numerically; see Appendix F. As a reasonable approximation to the source term, we only include the contribution from these bound states in our calculation and ignore the contribution from all other eigenfunctions, which are *extended* in $r_\perp$-space. We expect the bound-state contribution to dominate in the source term, because these states carry higher weight in the region of $r_\perp$-space where the order-parameter expectation value $m_0(r_\perp)$ is non-zero, i.e., for length-scales from zero up to the the typical localization length (recall that $r_\perp$ is a variable scaled by the correlation length). To appreciate this point better, note that the functions $m_0(\rho)$ in Eq. (4.48), which is the Laplace transform of the scaled mean-field distribution $\mathcal{P}_0(\zeta)$, vanishes for large ρ. From the expression for the source term (4.43) it is clear that the source term, too, vanishes asymptotically at large ρ. Hence it suffices to retain contributions in the source term that

dominate at small ρ, justifying our approximation. We finally obtain

$$\mathcal{S}(r) = \frac{|\theta|}{7}\int d\zeta \left[\ln|\theta|\, r^2\zeta^2 + \frac{1}{3}\left\{\frac{1}{2}r^2\zeta^2 \mathrm{Ei}\left(\frac{\zeta r^2}{2}\right) - r^2\zeta^2\ln(r^2\zeta^2) + \zeta - \zeta e^{\zeta r^2/2}\right\}\right]\mathcal{P}_0(\zeta)\, e^{-\zeta r^2/2} - \frac{1}{7}\lambda_0 \ln\lambda_0 |\psi_0(r)|^2 \left[\int d\zeta \mathcal{P}_0(\zeta)\, e^{-\zeta r^2/2} - 1\right] \tag{4.53}$$

A plot of the source term $\mathcal{S}$ as a function of $\rho \equiv r^2/2$, is displayed in Fig. 4.2. This plot was obtained by numerically solving for the integro-differential equation (2.20) for the scaled mean-field distribution $\mathcal{P}(\zeta)$, and using the result to calculate $\mathcal{S}(\rho)$.

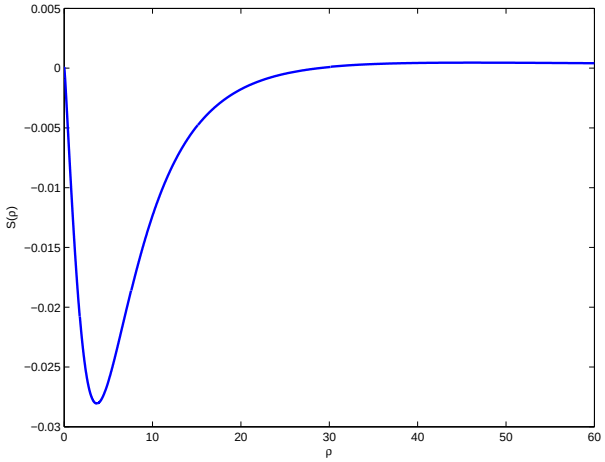

Figure 4.2: The source term $\mathcal{S}(\rho)$.

4.4.5 Solution of the equation

We solve for the differential equation (4.48) numerically. The solution $m_1(\rho)$ is plotted in Fig. 4.3. We use the boundary condition $m_1(\rho = 0) = 0$; see Eq. (4.46) and the discussion that follows it. Recall that the normalization condition on the distribution function $\mathcal{P}(\zeta)$ requires that the solution $m(\rho)$ is zero at the origin. Therefore, it is convenient to exponentiate the solution

$$m(\rho) = m_0(\rho) + \epsilon m_1(\rho) \approx m_0(\rho) e^{-\epsilon|m_1(\rho)|/m_0(\rho)}, \tag{4.54}$$

where, in the last step we have used the fact that the solution $m_1(\rho)$ is non-positive for all values of ρ. We remind the reader that the inverse Laplace transform of $m(\rho)+1$ is the corrected (scaled)

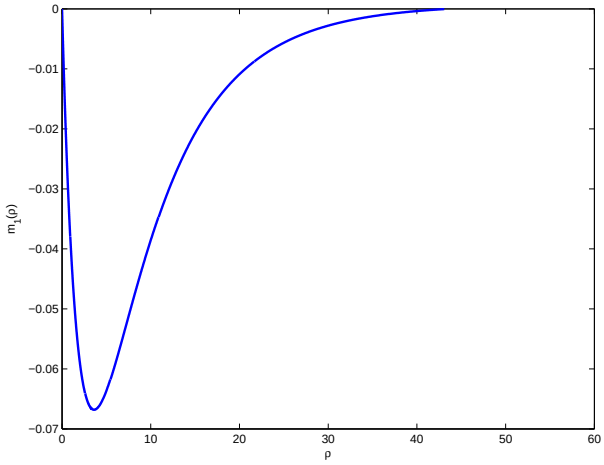

Figure 4.3: The correction to the scaling function, $m_1(\rho)$

distribution of localization lengths $\mathcal{P}(\zeta)$; see Eq. (4.46):

$$m(\rho) + 1 = \int d\zeta \, \mathcal{P}(\zeta) e^{-\zeta\rho}. \tag{4.55}$$

In order to exaggerate the general characteristics of the correction, we have plotted in Fig. 4.4 the scaling function $m(\rho) + 1$ [i.e., Laplace transform of $\mathcal{P}(\zeta)$] versus $m_0(\rho) + 1$ [i.e., Laplace transform of $\mathcal{P}_0(\zeta)$] for $\epsilon = 1$. Owing to difficulties with the numerical evaluation of the inverse Laplace transform, we settle for a comparison of the Laplace transform of the distributions instead. We discuss the general features of the correction to the distribution of localization lengths in the next subsection.

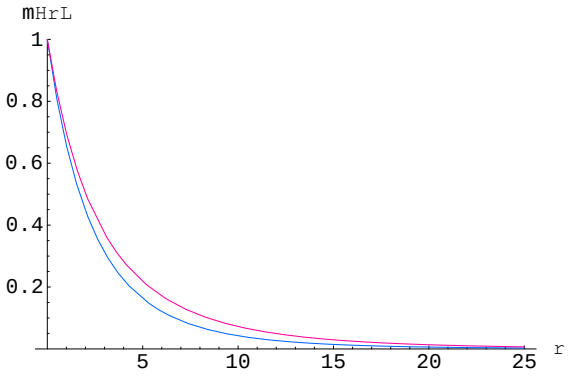

Figure 4.4: The corrected scaling function $m(\rho)$ (blue curve, lower curve) versus the mean-field function $m_0(\rho)$ (red curve, upper curve)

4.5 Discussion of results

We begin with a discussion of the qualitative features of the correction to the distribution of localization lengths. Firstly, I remind the reader of the connection between the scaled distribution of (inverse squared) localization lengths $\mathcal{P}_0(\zeta)$ and the distribution of (squared) localization lengths $\mathcal{N}(\xi^2_{\rm loc})$, because it is the latter that is easier to picture physically. This connection was made explicit in Eq. (2.16b). In real space, the saddle-point solution $m_0(\hat{r})$, given by Eq. (4.45), expressed as a function of $\mathcal{N}(\xi^2_{\rm loc})$, is

$$m_0(\hat{r}) = \int_0^\infty d\xi^2_{loc}\mathcal{N}(\xi^2_{loc})e^{-r_\perp^2/2\xi^2_{loc}} - 1. \tag{4.56}$$

Comparing the above equation defining $\mathcal{N}(\xi^2_{\rm loc})$ with Eq. (4.45), its easy to see that $\mathcal{N}(\xi^2) = \zeta^2\mathcal{P}_0(\zeta)$[5]. One can deduce from the correction to the scaling function $m(\rho)$ plotted in Fig. 4.4 that the peak of the distribution $\mathcal{P}_0(\zeta)$, and hence of $\mathcal{N}(\xi^2)$, has shifted in a manner that the typical localization length is *higher* than the corresponding mean-field estimate. This is expected intuitively; fluctuations should make the particles less localized. Moreover, as the contribution of fluctuations is dominant at length-scales lower than the correlation length-scale, the distribution function is strongly influenced by the inclusion of fluctuation corrections. This is because the typical localization length given by the distribution is of the same order of magnitude as the correlation length in the problem.

A discussion on the effect of Goldstone fluctuations in our calculation of the EOS is pertinent here. We contrast the EOS calculation in the V/G theory with that in the $O(N)$ model. We have mentioned in the introduction to Chapter 3 that in the $O(N)$ model, the broken symmetry is *internal* in nature, and the Goldstone modes associated with the direction transverse to the direction of magnetization go critical on the coexistence curve[6]. The effect of infrared divergences originating from the Goldstone modes on the the longitudinal susceptibility at coexistence and the EOS has been explored in detail in the literature [49]. For the present discussion, it suffices to quote

[5]There is a inconsequential difference in our notation here when compared to that of Eq. (2.16b). In this chapter, the localization length $\xi_{\rm loc}$ is measured in units of the correlation length ξ; recall that $r_\perp$ is a variable scaled by ξ. So the factors of $\tau = 1/\xi^2$ are hidden.

[6]Recall that the coexistence curve is defined to be a line of critical points given by the zero of the function f in the magnetic scaling relation $h/M^\delta = f(\tau/M^{1/\beta})$. In the h vs. T parameter space, this curve terminates on an ordinary critical point (also known as the critical isotherm) where *both* the correlation lengths for both the longitudinal and transverse fluctuations diverge.

the key observation that coexistence is described by a crossover between critical phenomena characterized by one divergent length-scale and critical phenomena characterized by two independent divergent length-scales. These length scales are associated with the transverse and the longitudinal fluctuations.

In the V/G theory we have external symmetry breaking in an abstract replicated space. *A priori*, it is not clear whether the physical system indeed has two independently diverging length-scales as in the $O(N)$ model. Here we argue that there is only one diverging length-scale in our problem. Before doing so, let us point out the part of our EOS calculation that would be invalidated if the situation were similar to the $O(N)$ model. In evaluating the source term, Eq. 4.43 in Subsection 4.4.4, we have argued that the contribution of the Goldstone modes is zero, because the eigenvalue of the kernel $\mathbf{\Delta}$ for these modes are zero, see Appendix F. However, this was done *after* renormalizing the divergences in the free energy. This implicitly assumes that the diverging correlation length-scale at the critical point, giving rise to critical infrared divergences, scales as the length-scale associated with the vanishing mass of the Goldstone fluctuations, giving rise to infrared Goldstone divergences. This assumption is evidently incorrect for the $O(N)$ model, in which the length-scale associated with the Goldstone fluctuations are divergent at all temperatures from zero to the critical temperature (for zero external magnetic field). In the V/G field theory, the Goldstone modes are defined as the zero eigenmodes of the Gaussian propagator of the replicated field theory. As shown in Appendix F, these zero modes are 'bound states' in the replicated space. These bound states are spatially localized, and have a characteristic length-scale proportional to the localization length-scale. As the localization length and the correlation length do not scale independently in the V/G field theory, it is reasonable to claim that the length-scale associated with the Goldstone fluctuations is not a new length-scale in the problem, unlike the case of the $O(N)$ model. Moreover, the external field H in our problem is not a physical field and cannot provide a new length-scale, as it does in the $O(N)$ model. Physically, as the Goldstone modes are identified with local displacements for shear deformations, the above argument transpires to the assertion that correlation length for random fluctuations in (replicated) shear deformations is not an independent length scale but, rather, scales as the correlation length scale. With these considerations, we argue that in the V/G theory, the zero modes do not play a special role in the

EOS calculation.

In Chapter 3, we identified a part of the Goldstone fluctuations to be local shear deformations and showed that inclusion of these fluctuation to *all orders in the Goldstone fields* led to a rigid shift of the distribution of localization lengths. In comparison, the work presented in this chapter includes all critical fluctuations near the upper critical dimension, up to *one-loop order,* and deduces the qualitative features of the correction to the distribution of localization lengths. In this chapter, the fluctuations considered are *additive* perturbations around the ground state. In Chapter 3 the fluctuations considered are Goldstone fluctuations that are *multiplicative*. Thus, there is no obvious contradiction in the results presented in the two chapters. Note that the prediction of a divergent shift in the distribution of localization lengths in two dimensions predicted in Chapter 3, is inaccessible using the tools discussed in the present chapter, because these tools are valid near the upper critical dimension and not the lower critical dimension.[7]

4.6 Conclusions

To the best of our knowledge, this work is the first calculation of an Equation of State for a field theory with broken translational symmetry. We have raised questions about the generalization of the Renormalization Group technique for systems with broken external symmetry, and we hope that this work stimulates future research in this direction. We have calculated the one-loop EOS for the vulcanization/gelation problem. The method used is applicable to the percolation field theory derived from the Random Resistor Model. The distribution of localization lengths in the critical region— a central quantity in the description of random solids—has been obtained from the Equation of State.

[7]Near the lower critical dimension usually a *non-linear sigma-model* is constructed for Goldstone fluctuations. The inclusion of both Goldstone and massive fluctuations in a field theory near the upper critical dimension in an epsilon expansion is less common and more difficult to execute, owing to difficulties with infrared divergences coming from Goldstone modes. See the discussion in Chapter 6 of D. J. Amit's book [38], and a wonderful discussion in a more general context in ref. [40].

Chapter 5

Goldstone fluctuations and their implications for the random solid—Part 2

Its symmetry is perfect and severe
Because the barbarous force of agonies
Broke it, and mended it, and made it clear.
— Elinor Wylie

5.1 Introduction

In this chapter we present a critical analysis of the construction of Goldstone fluctuations and the effective theory presented in the Chapter 3. We reveal certain shortcomings of the Goldstone construction and discuss their remedy. Some of the material presented in this chapter, in particular, the connection between Goldstone fluctuations and the shear deformations, originated in our quest to derive the phenomenological theory of rubber elasticity from the microscopic theory of vulcanization/gelation. Therefore, it is appropriate to review the classical theory of rubber elasticity in this chapter. As we shall see, the revised construction of the Goldstone fluctuations not only resolves certain deficiencies of the former construction, but also empowers us with tools for a new direction of enquiry.

The work presented in Chapter was done in collaboration with Xiaoming Mao, Xiangjun Xing, A. Zippelius and P. M. Goldbart.

5.2 Critique of 'Goldstone fluctuations and their implications for the random solid— Part 1'

In this section I criticize the results presented in the Chapter 3, and draw attention to the physical implications of some of the results and why they fall short of our expectations. The central questions are as follows:

1. Our first concern is the implication of the expression for the shear modulus, Eqs. (3.22b) and (3.23), derived in Chapter 3. These expressions indicate that the shear modulus for random solids is a functional of the distribution of localization lengths. We know that the distribution of localization lengths decays rapidly, beyond the typical localization length of the solid; see fig. (2.1) and the discussion thereafter. Recall that the typical localization length of the solid is of the same order of magnitude as the correlation length-scale. Moreover, deep inside the solid state, where it is justified to construct an effective theory retaining only the Goldstone fluctuations and ignoring all other fluctuations, the correlation length-scale is much smaller than the system size. Now, imagine performing uniform shear deformations on the system deep inside the solid state; in other words, shear deformations whose wavelength is of the same order of magnitude as the system size, and therefore much larger than the correlation length scale. For uniform shear deformations, the phenomena of localization of constituent particles of the solid occurs at a much smaller length-scale, and hence the functional form of the distribution of localization length—a detailed description of the phenomena of localization—should not play any role in determining the shear modulus. Stated in a different way, imagine the hypothetical situation of random solids with distinct distribution functions for their localization lengths, but all of these distributions decay very fast beyond a finite typical localization length scale. All of these solids should nevertheless have the same shear modulus [1]. Equation (3.23) contradicts this intuitive expectation.

2. The identification of the Goldstone fluctuations with (replicated) shear deformations presented in the previous chapter, though very convincing, is not completely rigorous. This identification, along with the mean-field results from the Landau theory, should have led to

[1] We are, of course, considering only *affine* deformations, i.e., the local deformation of the end-to-end vector of a constituent polymer of the solid is in geometric proportion to the deformation of the solid.

a derivation of the classical theory of rubber elasticity. To elaborate on this point, observe that in the previous chapter that the effective free energy for the Goldstone fluctuations, i.e., Eq. (3.22a), is quadratic in the Goldstone fields. For the sake of clarity I reproduce that equation here:

$$\mathcal{S}_u = \frac{\mu_n}{2T} \int_{\mathcal{V}} d\mathbf{x} \, (\partial_{\mathbf{x}} u_\perp \cdot \partial_{\mathbf{x}} u_\perp) \, . \tag{3.22a}$$

On using the connection between the Goldstone fields and the shear deformations, the above expression is also the (replicated) free energy for shear deformations. However, the classical theory of rubber elasticity is not quadratic in the shear deformations but in the full nonlinear *strain tensor* [2]. Therefore, the terms in the strain tensor that are non-linear in the shear deformation are missing from the free energy given by Eq. (3.22a). This is surprising, because we have not made any approximation of the Goldstone fields being small in magnitude in our derivation of Eq. (3.22a), and therefore non-linear terms in question shouldn't be missing. One can perhaps argue that the Landau-Wilson free energy, being a long-wavelength approximation to the actual free-energy of the system, is inadequate in producing the non-linear terms. For example, if one includes terms like $\hat{k}^4 \Omega(\hat{k})^4$ in the Landau-Wilson free energy, then terms that are quartic in the Goldstone field will be recovered. Inclusion of these 'irrelevant' [3] terms in the effective theory can generate terms cubic and quartic in the Goldstone field, and invoking full rotational symmetry one can perhaps organize these terms in a manner whereby the full nonlinear elasticity is recovered. This organization involves determining the relationship between the coefficients of terms (in the free energy) using invariances under symmetry operations (in our case, full rotational symmetry in replicated space). Such relationships between coefficients follow from Ward identities corresponding to the symmetries [38]. A similar algorithm has been carried through for the theory of nonlinear elasticity of liquid crystals; see Refs. [50]. However, we do not undertake this strategy here for reasons that will be clear once we present the revised Goldstone construction; see discussion at the end of Subsection 5.4.2.

[2] We review the classical theory of rubber elasticity in the next section for the reader who might be unfamiliar with it.

[3] It might be tempting to argue that terms like $\hat{k}^4 \Omega(\hat{k})^4$ are irrelevant in the renormalization group sense, but recall that the effective theory for the Goldstone fluctuations is strictly valid deep inside the solid phase, where the argument based on RG irrelevance are invalid because the system is not in the critical region.

3. The Goldstone construction presented in Chapter 3 treats the solution 'hill' to be a line whose thickness $\xi_{\rm typ}$ is much smaller than the wavelength of the Goldstone fluctuations; see Fig. 3.1 and the discussion surrounding it. What is the regime of validity of this approximation? Note that the thickness of the 'hill' is proportional to the typical localization length, which in turn is proportional to the correlation length for fluctuations. Beyond the correlation length-scale fluctuations are unimportant and a mean-field analysis is valid. Hence, if we are interested in the *critical* fluctuations of the solid, the thickness of the 'hill' is comparable to the wavelength of such fluctuations, and the critical region is therefore outside the regime of validity of the Goldstone construction presented in the Chapter 3. This scenario can be compared and contrasted with the Goldstone fluctuations of a liquid-gas interface at coexistence; see Ref. [26] for a review. There, the thickness of the interface is much smaller than the typical wavelength of the surface fluctuations of the interface between coexisting liquid and gas far from the liquid-gas transition.

Before presenting the resolution of the above problems, we first review the classical theory of the rubber elasticity. The classical theory is invoked in our discussion later, but the reader who needs no refresher on the topic may skip the next section.

5.3 A short review of the classical theory of rubber elasticity

Rubber (and other elastomers) can withstand very large strains—up to many hundreds of percents. On the other hand, the reversible strain is typically small for crystalline solids, and a theory of linear elasticity is sufficient to describe such materials. In this section we review the nonlinear theory of elasticity appropriate for rubbery materials [51].

The theory of elasticity involves two spaces, the *reference space* and the *target space*. The reference space is the position space of material points for the relaxed solid before deformation. The target space is the position space of material points of the relaxed solid after deformation. A material point $\mathbf{R}_I$ in the reference space has the position $\mathbf{R}_F = \mathbf{R}_I + \mathbf{u}(\mathbf{R}_I)$ in the target space, where $\mathbf{u}(\mathbf{R}_I)$ is the deformation vector that records how the relative separation of neighboring

points in the solid is altered under elastic deformations. The gradient of deformation is defined as

$$\Lambda_{ij} = \frac{\partial R_{Fi}}{\partial R_{Ij}}. \tag{5.1}$$

As a uniform displacement field $\mathbf{u}$ corresponds to translating the solid as a whole, it is only the gradient of displacements that contribute to the physical effects of elasticity. When $\underline{\underline{\Lambda}}$ is independent of the position $\mathbf{R}_I$ then the deformation is said to be *uniform*. We use double underscore to denote matrices in this Chapter. The deformation tensor $\underline{\underline{\Lambda}}$ is in turn used to define the right Cauchy-Green strain deformation tensor $\underline{\underline{C}}$ where

$$\underline{\underline{C}} = \underline{\underline{\Lambda}}^{\mathrm{T}} \cdot \underline{\underline{\Lambda}}, \tag{5.2}$$

where the superscript T implies the matrix transpose operation. One can also define the left Cauchy-Green tensor $\underline{\underline{B}}$ as follows:

$$\underline{\underline{B}} = \underline{\underline{\Lambda}} \cdot \underline{\underline{\Lambda}}^{\mathrm{T}}. \tag{5.3}$$

These two tensors behave differently under rotations of the reference and target space. We denote rotations in the target space by $\underline{\underline{O}}_T$ and rotations in the reference space by $\underline{\underline{O}}_R$. Then the deformation tensor transforms as

$$\underline{\underline{\Lambda}}' = \underline{\underline{O}}_T \cdot \underline{\underline{\Lambda}} \cdot \underline{\underline{O}}_R^{\mathrm{T}} \tag{5.4}$$

Owing to the relevant contractions, the right Cauchy-Green tensor is invariant under rotations of the target space and the left Cauchy-Green tensor in invariant under rotations of the reference space. Therefore, under rotations of both the reference and target space, the transformation on the Cauchy-Green tensors are as follows;

$$\underline{\underline{C}} = \underline{\underline{O}}_R^{\mathrm{T}} \cdot \underline{\underline{C}}' \cdot \underline{\underline{O}}_R \quad \text{and} \quad \underline{\underline{B}} = \underline{\underline{O}}_T^{\mathrm{T}} \cdot \underline{\underline{B}}' \cdot \underline{\underline{O}}_T \tag{5.5}$$

where $\underline{\underline{C}}'$ and $\underline{\underline{B}}'$ are the tensors in the rotated coordinates. Whether one chooses to write the free energy for the elastic solid in terms of the left or right Cauchy Green tensor, the free energy itself has to be invariant under rotations of both reference and target space. One can construct suitable invariants by taking the trace (Tr) and determinant (Det) of the tensor. Here we choose to use the

right Cauchy-Green tensor $\underline{\underline{C}}$. The lowest order (in $\underline{\underline{\Lambda}}$) invariants are

$$\mathrm{Tr}(\underline{\underline{\Lambda}}^{\mathrm{T}} \cdot \underline{\underline{\Lambda}}) \; ; \; \frac{1}{2}\left\{ \left(\mathrm{Tr}(\underline{\underline{\Lambda}}^{\mathrm{T}} \cdot \underline{\underline{\Lambda}})\right)^2 - \mathrm{Tr}(\underline{\underline{\Lambda}}^{\mathrm{T}} \cdot \underline{\underline{\Lambda}}) \right\} \; ; \; \mathrm{Det}(\underline{\underline{\Lambda}}^{\mathrm{T}} \cdot \underline{\underline{\Lambda}}) \tag{5.6}$$

In order to connect the coefficients in the free energy built from the above invariants to the various elastic moduli of classical elastic theory, we break up the deformation tensor $\underline{\underline{\Lambda}}$ into a unit tensor and the gradient tensor $\underline{\underline{u}}$,

$$\Lambda_{ij} \equiv \delta_{ij} + u_{ij}. \tag{5.7}$$

By using the above expression, the change of the square of the separation between two neighboring points is obtained as

$$d\mathbf{R}_F^2 - d\mathbf{R}_I^2 = 2\epsilon_{ij} dR_{Ii} dR_{Ij}, \tag{5.8}$$

where ϵ_{ij} is the symmetric strain tensor, defined as

$$\epsilon_{ij} = \frac{1}{2}\left(\frac{\partial u_i}{\partial x_j} + \frac{\partial u_j}{\partial x_i} + \frac{\partial u_i}{\partial x_j}\,\frac{\partial u_j}{\partial x_i} \right). \tag{5.9}$$

In *linear* elastic theory, the term quadratic in the displacement field $\mathbf{u}$ in the strain tensor is ignored. Recall that the free energy is a function of the the invariants constructed from the Cauchy-Green deformation tensor. Written in terms of the strain tensor, we obtain the well-known Lamé expression for the free energy f_{el} at second order in the strain,

$$f_{\mathrm{el}} = \frac{1}{2}\lambda \left[\mathrm{Tr}\,\underline{\underline{\epsilon}}\right]^2 + \mu\,\mathrm{Tr}\,\left(\underline{\underline{\epsilon}}^{\mathrm{T}} \cdot \underline{\underline{\epsilon}}\right). \tag{5.10}$$

The parameters λ and μ are the Lamé coefficients. The second Lamé coefficient μ turns out to be the shear modulus. This can be seen by deducting the term corresponding to the change of volume, $(1/3)\,\mathrm{Tr}\,\underline{\underline{\epsilon}}$, from the second term in the above equation, to obtain

$$f_{\mathrm{el}} = \frac{1}{2}B\,(\epsilon_{ii})^2 + \mu\left(\epsilon_{ij} - \frac{1}{3}\,\delta_{ij}\epsilon_{ll}\right)^2, \tag{5.11}$$

where we have used Einstein summation convention, and $B = \lambda + \frac{2}{3}\mu$ is the compression modulus. This is the familiar starting point of linear elastic theory, where only the linear terms in the

strain tensor are retained. Rubber is essentially incompressible, i.e., $B \gg \mu$. For incompressible systems, the divergence of the displacement vector $\mathbf{u}$ is zero and hence the strain tensor is traceless. Therefore, the elastic free energy for incompressible system can be taken to be

$$f_{el} = \mu \mathrm{Tr}\, \left(\underline{\underline{\epsilon}}^{\mathrm{T}} \cdot \underline{\underline{\epsilon}} \right). \tag{5.12}$$

Written in terms of the deformation tensor $\underline{\underline{\Lambda}}$ this free energy becomes

$$f_{el} = \frac{1}{2}\, \mu\, \mathrm{Tr}\, \left(\underline{\underline{\Lambda}}^{\mathrm{T}} \cdot \underline{\underline{\Lambda}} \right), \tag{5.13}$$

which, together with the incompressibility constraint, $\mathrm{Det}\, \underline{\underline{\Lambda}} = 1$ governs $\underline{\underline{\Lambda}}$. The expression in terms of $\underline{\underline{\Lambda}}$ is usually used when one is considering large deformations and hence is explicitly considering the regime of non-linear elasticity. When the system is not strictly incompressible, but has a very high bulk modulus B, then it can be shown that the free energy has the form [13],

$$f_{\mathrm{el}} = \frac{1}{2}\mu \left(1 - \frac{\mu}{3B}\right)^2 \mathrm{Tr}\, \left(\underline{\underline{\Lambda}}^{\mathrm{T}} \cdot \underline{\underline{\Lambda}} \right) + \frac{1}{2}\, B \left\{ \left(1 - \frac{\mu}{3B}\right)^3 \mathrm{Det}\, \underline{\underline{\Lambda}} - 1 \right\}^2, \tag{5.14}$$

where there are no condition on the determinant of $\underline{\underline{\Lambda}}$. This mysterious form is a result of making sure that the minimum of the free energy occurs for zero deformation, i.e., there are no volume changes in the equilibrated network unless an external deformation is imposed. Note that $\mu/B \sim 10^{-4}$ for rubber; therefore, to a very good approximation, rubber is incompressible.

5.4 Revised Goldstone construction and effective theory

5.4.1 Goldstone construction revisited

In this subsection we revisit the Goldstone construction presented in the previous chapter.[4] First we scrutinize the deformed order parameter, see Eq. (3.9a), which, for clarity of presentation, we

[4] I am indebted to Xiaoming Mao for kindly sharing her detailed notes on the derivations outlined in this section and in the relevant appendices. Various aspects of the revised effective theory for Goldstone fluctuations are the subject of ongoing research, and the discussion presented in this section is not meant to be either comprehensive or exhaustive.

reproduce here

$$V\Omega(k)=\int_{\mathcal{V}} d\mathbf{z}\, e^{i\mathbf{k}_{\rm tot}\cdot\mathbf{z}+ik_\perp\cdot u_\perp(\mathbf{z})}\,\mathcal{W}(k_\perp). \tag{3.9a}$$

The saddle-point solution, i.e., the undeformed state is given by Eq. (2.15), see also Eq. (2.9). We reproduce the former equation here,

$$\langle\Omega(\hat{k})\rangle_{\rm MF} = Q\,\delta_{k_\parallel,\mathbf{0}}\int_0^\infty d\zeta\;\;\mathcal{P}_0(\zeta)\,e^{-\hat{k}^2/2\tau_0\zeta} =: \delta_{k_\parallel,\mathbf{0}}\,\mathcal{W}(\hat{k}), \tag{2.15}$$

where we have purposefully hidden the LRS subtraction because it is not important for the following discussion. Here $\langle\cdots\rangle_{\rm MF}$ implies the mean-field expectation value. Note that in the above expression, the dependence of the function $\mathcal{W}$ on the full replicated wave-vector $\hat{k}$ is retained, in contrast to its dependence on $k_\perp$ alone, which would be the case on 'applying' the delta function; see Eq. (3.3) for the comparison. Recall that we have split up the $(n+1)D$-dimensional replicated vector $\hat{k}$ into the D-dimensional longitudinal and nD-dimensional transverse coordinates, $\hat{k}\equiv(k_\parallel,k_\perp)$, see Eq. (3.7) and the discussion surrounding it. Expressing the saddle-point solution as $\delta_{k_\parallel,\mathbf{0}}\,\mathcal{W}(\hat{k})$ or as $\delta_{k_\parallel,\mathbf{0}}\,\mathcal{W}(k_\perp)$ is completely equivalent, and it may seem unnecessary that we are making a distinction between the two. However, are the two expressions for the saddle-point equivalent when we are deforming it using the Goldstone construction? In other words, do we get the same deformed state on using either one of them? The answer to this question is 'No'.

Loosely stated, the Goldstone construction amounts to 'deforming' the delta function in the expression of the saddle-point; see Eq. (3.9a). Therefore, it is mathematically rigorous to deform the saddle-point solution $\delta_{k_\parallel,\mathbf{0}}\,\mathcal{W}(\hat{k})$ where the delta function, which is to be 'deformed', has not been 'applied' on the function $\mathcal{W}(\hat{k})$ to convert it into $\mathcal{W}(k_\perp)$. We now reconstruct the Goldstone fluctuations in the same manner explained in Chapter 3, but with the above correction, and try to convince the reader that the correction indeed makes a difference. The deformed order parameter is

$$V\Omega(\hat{k}) = Q\int_{\mathcal{V}} d\mathbf{z}\, e^{i\mathbf{k}_{\rm tot}\cdot\mathbf{z}+ik_\perp\cdot u_\perp(\mathbf{z})}\;\int_0^\infty d\zeta\;\;\mathcal{P}_0(\zeta)\,e^{-\hat{k}^2/2\tau_0\zeta}. \tag{5.15}$$

To simplify the notation, we drop the subscript from the distribution function and absorb the control parameter τ_0 into an appropriate redefinition of ζ and $\mathcal{P}_0(\zeta)$. We are not going to bother with the LRS (constant) subtraction in what follows. With this change of notation the deformed

order parameter is

$$V\Omega(\hat{k}) = Q \int_{\mathcal{V}} d\mathbf{z}\, e^{i\mathbf{k}_{\rm tot}\cdot\mathbf{z} + ik_\perp \cdot u_\perp(\mathbf{z})} \int_0^\infty d\zeta \;\; \mathcal{P}(\zeta)\, e^{-\hat{k}^2/2\zeta}. \tag{5.16}$$

What is the form of the deformed order parameter is real space? It is easy to check that the Fourier transform of the above expression is (see Appendix H)

$$\Omega(\hat{x}) = Q \int d\zeta\, \mathcal{P}(\zeta) \int d\mathbf{z} \left(\frac{\zeta}{2\pi}\right)^{D/2} \exp\left[-\frac{\zeta}{2}\left(x_\parallel - \mathbf{z}\right)^2 - \frac{\zeta}{2}\left(x_\perp - u_\perp(\mathbf{z})\right)^2\right] \tag{5.17}$$

Observe that in real space the revised Goldstone construction is glaringly different from the real space form of the old Goldstone construction, i.e., $\mathcal{W}(x_\perp - u_\perp(x_\parallel))$. It should be noted that the Goldstone field in the new construction is obviously the same as in the old construction; it is a transverse nD-dimensional vector that has a D-dimensional (longitudinal) vector as its argument. It is the deformation of the saddle point which is different; if the Gaussian 'smearing function' $e^{-\zeta/2\,(x_\parallel - \mathbf{z})^2}$ is replaced by the delta function $\delta(x_\parallel - \mathbf{z})$ then we recover the old Goldstone construction. However, from Eq. (5.17) it is not obvious under what physical approximation the old Goldstone construction is recovered. One would imagine that when the wavelength of the Goldstone fluctuations are much larger than the typical localization lengths, the old form of deformed saddle-point should be valid. However, certain aspects on the long-wavelength behavior of the fluctuations described by the old construction seems to be incorrect, for example, the dependence of the shear modulus on the details of the distribution of localization length, as we have discussed earlier. It is not clear to us why this is the case. However, the revised form of fluctuations eliminates all the problems we encountered with old Goldstone theory. We discuss these resolutions in the next few subsection.

5.4.2 Effective theory for the Goldstone fluctuations

In this subsection we derive the effective theory for the revised Goldstone fluctuations. We derive a revised expression for the shear modulus by expanding in the effective free energy up to second order in the Goldstone fields. We relegate the mathematical details to Appendix H.

Recall that the effective Hamiltonian for the V/G transition, given by Eq. (2.11), has a quadratic

and a cubic term in the order parameter. We substitute the Goldstone-fluctuated form of the order parameter, given by Eq. (5.16), into the effective Hamiltonian in order to derive the effective theory for the Goldstone fluctuations. The contribution from one of the two quadratic term is

$$\begin{aligned}\sum_{\hat{k}\in HRS} |\Omega(\hat{k})|^2 &= -Q^2 + \frac{Q^2}{V}\int d\mathbf{z}_1 d\mathbf{z}_2\, d\zeta d\zeta_1 d\zeta_2\, \mathcal{P}(\zeta_1)\,\mathcal{P}(\zeta_2)\,\delta\left(\zeta - \frac{1}{\zeta_1^{-1}+\zeta_2^{-1}}\right)\times \\ &\left(\frac{\zeta}{2\pi}\right)^{D/2} \exp\left[-\frac{\zeta}{2}|u_\perp(\mathbf{z}_1)-u_\perp(\mathbf{z}_2)|^2 - \frac{\zeta}{2}|\mathbf{z}_1-\mathbf{z}_2|^2\right].\end{aligned} \tag{5.18}$$

The contribution form the second quadratic term, which we refer to the 'gradient term', is

$$\begin{aligned}\sum_{\hat{k}\in HRS} \hat{k}^2|\Omega(\hat{k})|^2 &= \frac{Q^2}{V}\int d\mathbf{z}_1 d\mathbf{z}_2\, d\zeta d\zeta_1 d\zeta_2\, \mathcal{P}(\zeta_1)\,\mathcal{P}(\zeta_2)\,\delta\left(\zeta - \frac{1}{\zeta_1^{-1}+\zeta_2^{-1}}\right) \\ &\times\zeta^2\frac{\partial}{\partial\zeta}\left\{\left(\frac{\zeta}{2\pi}\right)^{D/2} \exp\left[-\frac{\zeta}{2}|u_\perp(\mathbf{z}_1)-u_\perp(\mathbf{z}_2)|^2 - \frac{\zeta}{2}|\mathbf{z}_1-\mathbf{z}_2|^2\right]\right\}.\end{aligned} \tag{5.19}$$

The contribution form the cubic term is

$$\begin{aligned}&\sum_{\hat{k}_1,\hat{k}_2,\hat{k}_3\in HRS} \delta_{\hat{k}_1+\hat{k}_2+\hat{k}_3,\hat{0}}\,\Omega(\hat{k}_1)\,\Omega(\hat{k}_2)\,\Omega(\hat{k}_3) \\ &= \int d\zeta_1 d\zeta_2 d\zeta_3 \mathcal{P}(\zeta_1)\mathcal{P}(\zeta_2)\mathcal{P}(\zeta_3)\left(2\pi\frac{\zeta_1\,\zeta_2\,\zeta_3}{\zeta_1+\zeta_2+\zeta_3}\right)^{D/2}\int d\mathbf{z}_1 d\mathbf{z}_2 d\mathbf{z}_3 \\ &\times\exp\left[-\frac{1}{2}\frac{\zeta_1\,\zeta_2}{\zeta_1+\zeta_2+\zeta_3}\left\{|\mathbf{z}_1-\mathbf{z}_2|^2+|u_\perp(\mathbf{z}_1)-u_\perp(\mathbf{z}_2)|^2\right\}\right] \\ &\times\exp\left[-\frac{1}{2}\frac{\zeta_2\,\zeta_3}{\zeta_1+\zeta_2+\zeta_3}\left\{|\mathbf{z}_2-\mathbf{z}_3|^2+|u_\perp(\mathbf{z}_2)-u_\perp(\mathbf{z}_3)|^2\right\}\right] \\ &\times\exp\left[-\frac{1}{2}\frac{\zeta_3\,\zeta_1}{\zeta_1+\zeta_2+\zeta_3}\left\{|\mathbf{z}_3-\mathbf{z}_1|^2+|u_\perp(\mathbf{z}_3)-u_\perp(\mathbf{z}_1)|^2\right\}\right]\end{aligned} \tag{5.20}$$

In the above expressions, wherever possible, we have made simplifications by invoking the $n \to 0$ limit. Note that the effective theory in the Goldstone fields is nonlocal. This nonlocal theory is the subject of ongoing research. Expanded in the Goldstone fields, it is the starting point for investigating *random stress* and *random elastic moduli* fluctuations in the solid. To give a glimpse

of this interesting direction of investigation, we first remind the reader of the identification of Goldstone fields as displacement fields for elastic deformations in a replicated theory. Therefore, the effective theory of Goldstone fluctuations is also the replicated elastic free energy for gels. Generically, a replicated elastic free energy arises on averaging over quenched disorder, using the replica trick, for a phenomenological model of a system with random elastic constants and random stresses. Therefore, the effective theory of Goldstone fluctuations can be used to extract information about random stress and elastic moduli fluctuations in gels.

What is the *local* effective theory for Goldstone fluctuations up to quadratic order in the fields? To derive such an effective theory, we need to expand the expressions given by eqs. (5.18, 5.19, 5.20) up to quadratic order in the Goldstone fields, perform a gradient expansion in the fields, and retain terms that are a function of the fields. The details of the derivation are presented in Appendix H. It turns out that the contribution of the 'gradient term', Eq. (5.19), is zero. The contribution from the expression in Eq. 5.18) is (see Appendix H for derivation)

$$\sum_{\hat{k}\in HRS} |\Omega(\hat{k})|^2 \Big|_{u_\perp=0}^{u_\perp} \approx -\frac{Q^2}{2V} \int d\mathbf{z}\, \partial_{\mathbf{z}} u_\perp(\mathbf{z}) \cdot \partial_{\mathbf{z}} u_\perp(\mathbf{z}), \tag{5.21}$$

where the scalar product is on both the nD components of $u_\perp$ and D components of space; see Eq. (3.22a). The contribution from the cubic term is

$$\sum_{\hat{k}_1,\hat{k}_2,\hat{k}_3\in HRS} \delta_{\hat{k}_1+\hat{k}_2+\hat{k}_3,\hat{0}}\, \Omega(\hat{k}_1)\, \Omega(\hat{k}_2)\, \Omega(\hat{k}_3) \Big|_{u_\perp=0}^{u_\perp} \approx \left(-\frac{Q^3}{3^D V} + \frac{3Q^3}{2V}\right) \int d\mathbf{z}\, \partial_{\mathbf{z}} u_\perp(\mathbf{z}) \cdot \partial_{\mathbf{z}} u_\perp(\mathbf{z}). \tag{5.22}$$

Using the effective free energy, Eq. (2.11), and comparing with Eq. (3.22a), we find that the shear modulus is given by

$$\mu_n = C\, g Q^3 \propto |\tau|^3, \tag{5.23}$$

where C is an unimportant numerical factor, and we have used the relation $Q = 2|\tau|/g$ between the gel fraction Q and the control parameter τ. Note that in the above expression, in contrast to the expression for the shear modulus given by Eq. (3.22b), the distribution of localization lengths does not feature at all. Hence, the shear modulus given by the revised theory of Goldstone fluctuations does not depend on the on the distribution of localization lengths, thereby resolving the criticism

we raised in Section 5.2. However, because we have expanded to quadratic order in the Goldstone field, the nonlinear theory of elasticity is still absent from our present discussion. Technically, there is no difficulty in retaining higher-order terms in the Goldstone fields, and deriving the nonlinear elasticity theory. However, in the next section we take a different route and explore the connection between Goldstone fluctuations and shear deformations using an equivalent, but physically more transparent, parametrization of the Goldstone fields. The theoretical reasoning presented in the next section forms the basis of the investigation discussed in Chapter 4, and is useful in understanding the replicated field theory of the V/G transition in a new light.

In passing, note that the (nonlocal) effective free energy for the revised Goldstone fluctuations [contributions (5.18), (5.19) and (5.20) added together] is *fully rotational invariant* in replicated space, i.e. invariant under both common and independent rotations of replicas. This deduction follows from observing how the Goldstone fields appear in the expressions referred above, viz., the rotational invariant combination $|u_\perp(\mathbf{z}_1) - u_\perp(\mathbf{z}_2)|^2$. The effective free energy for Goldstone fields must be rotationally invariant. Recall that in Section 5.2 we briefly mentioned how nonlinear elasticity for rubber could perhaps be recovered using our old Goldstone construction by including higher order (in Goldstone fields) terms in the effective theory, and using Ward identities [38] to ascertain the coefficients of these terms so that they combine to produce the theory nonlinear in strain. This strategy would follow the prescription of Refs. [50] where the nonlinear elastic theory of comparable translational symmetry broken phases was derived. However, this was achieved perturbatively in the Goldstone fields. In contrast, our (nonlocal) effective free energy for the revised Goldstone construction exhibits full rotational invariance *to all orders* in the Goldstone fields, making the above strategy to correct the old theory unmotivated.

5.5 Derivation of the classical theory of rubber elasticity

In this section we shall revisit the connection between Goldstone fluctuations and local displacements for shear deformations of the random solid, and thereby *derive* the classical theory or rubber elasticity, which until now has been a *phenomenological* theory. One can ask, why take the trou-

ble?[5] After all, the classical theory of rubber elasticity has been remarkably successful. A blend of phenomenology and molecular-level reasoning, it is based on a few simple assumptions, and bears great predictive and descriptive power. The shear modulus μ is given by $n_c T$, where the constant n_c is usually referred as "the density of effective chains in the network." The classical theory, i.e. Eq. (5.13), explain many essential features of rubbery materials, such as their stress-strain curves (at least for deformations that are not too large), the striking temperature dependence of their shear moduli, etc.

However, there are several important issues unresolved by the classical theory. Firstly, for a given crosslink density, the shear modulus is not calculated within the theory.[6] Second, in the intermediate-strain range there is universal and significant downward deviation of the experimental stress-strain curve, compared with the theoretical prediction. Finally, the issue of polymer entanglement is not addressed by the classical theory.

Subsequent efforts to improve the classical theory of rubber elasticity have focused on various directions (for one overview see Ref. [11]). The non-Gaussian nature of the chain statistics, due to the finite extensibility of the polymers, has been taken into account, and explains the large-deformation behavior of the stress-strain curve. Purely mathematical modeling, as in the theories due to Mooney, Rivlin and others (see, e.g., Ref. [51]), also provided useful insight. At the microscopic level, the effects of chain entanglement have long been emphasized and modeled via various approximation schemes, most notably the Edwards tube model [66] and its derivatives, although results from these models are often either inconclusive or contradictory. It seems fair to say that none of these efforts is as successful as the classical theory, either in terms of simplicity of assumptions, or in terms of broad descriptive power. The main virtue of V/G theory described in this Thesis is that it follows the Landau paradigm of modern condensed matter physics, inasmuch as it concentrates on order parameters, symmetries and length-scales. In particular, because of its independence on microscopic details, the Landau theory of the V/G transition can be regarded as

[5] Those who are blessed with an exalted faith in *ordinary* things are prone to raise such questions. It is *obvious* to them that rubber is elastic, and there is no need to *prove* it. For the less blessed, skepticism into the very nature of things is inseparably coupled to a pathological curiosity, making the obvious questionable—seeking the *extraordinary* secrets in ordinary things!

[6] We remind the reader that the classical theory was developed *before* percolation theory was. Therefore, how an infinite network emerges during the random crosslinking process was not understood. In fact, near the vulcanization point, the "effective chains" of the classical theory bear little resemblance to the original polymer chains before crosslinking.

the right theory to address the universal, long length-scale properties of rubbery materials, and therefore the phenomenological theory of classical rubber elasticity should be derivable from it. Thereby, not only is the statistical-mechanical root of elasticity theory revealed, but also its applicability to a wide class of random solids is demonstrated. It also constitutes a starting-point for the investigation of sample-to-sample fluctuations in various forms of vulcanized matter.

In order to carry out our agenda, we revisit the Landau theory and order parameter for the V/G transition that we introduced in Chapter 2. The reason for doing so is will become clear as we progress with our discussion in the next subsection.

5.5.1 Re-examining the order parameter and Landau theory for V/G transition

In the brief introductory chapter, chapter 2, the order parameter and the Landau theory for the V/G transition was discussed. In this section we are going to generalize the Landau theory, relaxing the $(n+1)$-replica permutation symmetry to n-replica permutation symmetry, and thereby making the distinction between the *preparation ensemble* and the *measurement ensemble* alluded to in the paragraph following Eq. (2.6) in see Section 2.1.2. To elaborate on this idea, recall that in the replica theory, n replicas are introduced in order to perform the disorder average; therefore, physical observables map on to corresponding replicated quantities in the replica formalism. The zeroth replica (the preparation ensemble) in the replicated theory encodes the probability distribution of quenched random disorder, i.e., the distribution of random crosslinks between constituent particles. The n other replicas (measurement ensembles) are introduced to perform the disorder average over the quenched variables. For a specific choice of disorder distribution, namely the Deam-Edwards distribution, the effective theory turns out to be symmetric under permutations of both the preparation and measurement ensembles, but this not generally the case for an arbitrary choice of disorder distribution, and hence the $(n+1)$-permutation symmetry is not an universal feature of the theory. Therefore, the Landau theory presented in Chapter 2 [see Eq. (2.11)] was a simpler version of the more general theory that we introduce here. The extra permutation symmetry, although not founded on general physical grounds, was a useful mathematical simplification. However, it is expected that the critical behavior of the V/G transition should remain unaffected by

this generalization of the Landau theory to one having reduced replica permutation symmetry. This expectation is indeed correct, see Chapter 6 for further details. If the generalized Landau theory [Eq. (5.26) below] had a different critical behavior compared to its simpler incarnation [Eq. (2.11] it would not make any sense to work with the latter, because the universal aspects of gels/vulcanized matter would not be captured. Historically, the simpler Landau theory (2.11) has been used to establish the cumulative knowledge of V/G transition that the work in this Thesis is founded upon, and this was successful because the universality class of the theory in not affected by whether one has n- or $(n+1)$-replica permutation symmetry. One may ask, then why this need for generalization? The reader will appreciate this need by proceeding through the rest of this chapter and Chapter 6. Succinctly stated, the generalized Landau theory gives us independent control over the preparation and measurement ensembles, helping us capture some physical aspects of the problem to be discussed here, that one is unable to capture otherwise.

In Section 2.2 we introduced the order parameter for the vulcanization gelation transition. In order to streamline the presentation in this section, we present the real-space version of the order parameter as a function of $(1+n)D$-vectors $\hat{x} = (\mathbf{x}^0, \ldots, \mathbf{x}^n)$:

$$\Omega(\hat{x}) = \Omega(\mathbf{x}^0, \ldots, \mathbf{x}^n) = \frac{1}{J} \sum_{j=1}^{J} \Big\langle \prod_{\alpha=0}^{n} \delta(\mathbf{x}^\alpha - \mathbf{R}_j^\alpha) \Big\rangle_{1+n} - \frac{1}{V_0 V^n}. \tag{5.24}$$

Recall that $\mathbf{R}_j^\alpha$ (with $\alpha = 0, 1, \ldots, n$) are the replicated position D-vectors of the N monomers (with $j = 1, \ldots, N$) that comprise the system. We distinguish between V_0, the volume of the system in the preparation ensemble, and V, the volume of the system in the measurement ensembles. In Eq. (5.24), the angular brackets $\langle \cdots \rangle_{1+n}$ denotes an average over the replica field theory. We remind the reader, that the order parameter of the V/G transition gives the conditional probability that a monomer found at $\mathbf{x}^0$ at the time of cross-linking is later found at $\{\mathbf{x}^1, \ldots, \mathbf{x}^n\}$ in n independent measurements after cross-linking, averaged over all monomers. The one-replica parts of Ω (for $\alpha = 0, \ldots, n$) are defined via

$$\Omega_\alpha(\mathbf{x}^\alpha) \equiv \int \prod_{\beta(\neq\alpha)} d\mathbf{x}^\beta \, \Omega(\hat{x}) = \frac{1}{J} \sum_{j=1}^{J} \Big\langle \delta(\mathbf{x}^\alpha - \mathbf{R}_j^\alpha) \Big\rangle_{1+n} - \frac{1}{\mathcal{V}_\alpha}. \tag{5.25}$$

where $\mathcal{V}_\alpha \equiv (V_0, V, \ldots, V)$. Of these, $\Omega_0(\mathbf{x}^0)$ describes the density fluctuations in the preparation ensemble, and $\Omega_\alpha(\mathbf{x}^\alpha)$ (for $\alpha = 1, \ldots, n$) describe density fluctuations in the measurement ensemble.

We now present the generalized Landau effective Hamiltonian for the V/G transition, generalized via making the distinction between preparation and measurement ensembles, as already discussed. In what follows, we impose the HRS constraint in the field theory in a slightly different way, for reasons that should be clear later. The effective Hamiltonian in real space is [cite for Eq. 2.11)]

$$\begin{aligned} \mathcal{H}_{VG}[\Omega] &= \int d\hat{x} \left\{ \frac{K_0}{2}(\nabla_0\Omega)^2 + \frac{K}{2}\sum_{\alpha=1}^{n}(\nabla_\alpha\Omega)^2 + \frac{\tau}{2}\Omega^2 - \frac{g}{3!}\Omega^3 \right\} \\ &\quad + \frac{B_0}{2}\int d\mathbf{x}^0(\Omega_0)^2 + \frac{B}{2}\sum_{\alpha=1}^{n}\int d\mathbf{x}^\alpha(\Omega_\alpha)^2, \end{aligned} \tag{5.26}$$

where ∇^0 and ∇^α are, respectively, derivatives with respect to $\mathbf{x}^0$ and $\mathbf{x}^\alpha$. (B_0, K_0) and (B, K) are, respectively, inverse susceptibility for density fluctuations and chain stretchability in the preparation and measurement ensembles. The chain stretchability is proportional to the squared radius of gyration of each constituent polymer chain in the isotropic state (the larger the K's, the softer the chains). It is customary to absorb constants such as K_0 and K, appearing in front of the gradient term, into a rescaling of the order-parameter field in a generic field theory. However, in order to emphasize the physical meaning of these parameters in the elastic theory we are aiming at, we retain the constants explicitly in the field theory. If we were to impose the HRS constraint in the manner we have done so far (we call it the *hard HRS constraint*), we need to take B_0 and B to be infinite. As B_0 and B correspond to compressibility of the system in the preparation and measurement ensemble, taking them to infinity is equivalent to disallowing density inhomogeneity, i.e., studying an incompressible system. The hard HRS constraint, expressed as a constraint on the allowed wave-vectors of which the the order parameter is a function of (see Section 2.3), can be recovered by expressing Eq. (5.26) in momentum space and recognizing that having B_0 and B be infinite penalizes the LRS sector by assigning it an infinite energy cost. When B_0 and B are very large but not infinite, we call the HRS constraint a *soft HRS constraint*. In this case, the system is not incompressible but has a very large bulk modulus. We will use the soft HRS constraint in this section because we are aiming at deriving the classical theory of rubber elasticity

[see Eq. (5.14)]. The free energy of the classical theory has a term proportional to the bulk modulus—rubber is not strictly incompressible, although its bulk modulus is much larger than its shear modulus, as discussed in Section 5.3. For simplicity, we consider the case of equal bulk moduli in the preparation and measurement ensembles (i.e. $B_0 = B$) in this section. We also assume that $K_0 = K$, i.e., the chain stretchability is the same in the preparation and measurement ensembles (before and after crosslinking). The reader may wonder: if these parameters are equal why make the distinction between the preparation ensemble and measurement ensembles at this point? Imagine applying an elastic deformation on the random solid. In the replicated theory of the random solid, the measurement ensembles would be deformed and the preparation ensemble would not. This is because the crosslink distribution, encoded in the preparation ensemble, is the same in the deformed and undeformed solid[7]. Hence, the distinction between the preparation and measurement ensembles is physical in origin; the preparation ensemble is not deformed under elastic forces, whereas the measurement ensembles do. In Chapter 6 we shall explore the consequences of controlling the parameters B_0 and B independently.

In the absence of any externally imposed deformation, the saddle-point equation, obtained from Eq. (5.26)by varying with respect to the order parameter in the standard manner, is solved by the following generalized Ansatz [cite for Eq. 2.17)]:

$$M_0(\hat{x}) = Q \int d\mathbf{z} \int d\zeta_0 d\zeta \, \mathcal{P}(\zeta_0, \zeta) \left(\frac{\zeta_0}{2\pi}\right)^{D/2} \left(\frac{\zeta}{2\pi}\right)^{nD/2} \exp\left[-\frac{\zeta_0}{2}\left(\mathbf{x}^0 - \mathbf{z}\right)^2 - \frac{\zeta}{2}\sum_{\alpha=1}^{n}\left(\mathbf{x}^\alpha - \mathbf{z}\right)^2\right] - \frac{Q}{V^0 V^n}, \quad (5.27)$$

where the parameters ζ_0 and ζ serve to distinguish between the preparation and measurement ensembles. This form of the Ansatz was used for a somewhat different, but not completely unrelated, direction of investigation in Ref. [37]. In that work, it was proved that a physical distribution of localization lengths can be defined by integrating the function $\mathcal{P}(\zeta_0, \zeta)$ over ζ_0. I choose to digress briefly and allude to this point because the careful reader may find it confusing to interpret the physical content of the generalized Ansatz form in the same spirit as was done for the old form, Eq. (2.17). Localization of particles is a concept relevant in the measurement ensembles alone; the

[7] We are assuming that other parameters, such as temperature, chain stretchability etc., are equal in the preparation and measurement ensemble and that these parameters are not altered by deforming the solid.

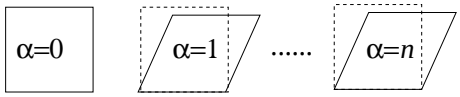

Figure 5.1: An externally imposed deformation changes affinely the boundary of the system in the n replicas of the measurement ensemble, but not that of the preparation ensemble, i.e. the 0^{th} replica.

preparation ensemble specifies the disorder distribution. Therefore, the function $\mathcal{P}(\zeta_0, \zeta)$ does not have a direct interpretation as the distribution of localization lengths, but once integrated over ζ_0 one can indeed define such a distribution function; for details see Ref. [37].

5.5.2 Elastic deformations and rubber elasticity

We now come to the main point of this section: obtaining the elastic free energy for isotropic random solids. To do this, we shall impose an arbitrary homogeneous deformation of the boundary of the system, which we encode in the matrix $\underline{\underline{\Lambda}}$ and illustrate in Fig. 5.1. We shall not make any assumptions about how the interior of the system changes in response to this deformation. Our aim is to determine the new saddle point $M_{\underline{\underline{\Lambda}}}(\hat{x})$ that minimizes the free energy and is consistent with the deformation of the system—the consistency condition is explained below. We proceed by hypothesizing a modification of the original saddle-point solution (i.e. $M_0(\hat{x})$ given by Eq. (2.17), reproduced below for easy comparison)

$$M_0(\hat{x}) = Q \int d\mathbf{z} \int d\zeta\, \mathcal{P}_0(\zeta) \left(\frac{\zeta}{2\pi}\right)^{(n+1)D/2} \exp\left[-\frac{\zeta}{2}\sum_{\alpha=0}^{n}(\mathbf{x}^\alpha - \mathbf{z})^2\right] - \frac{Q}{V^{1+n}} \tag{5.28a}$$

$$M_{\underline{\underline{\Lambda}}}(\hat{x}) = Q \int d\mathbf{z} \int d\zeta\, \mathcal{P}_0(\zeta) \left(\frac{\zeta}{2\pi}\right)^{(n+1)D/2} \exp\left[-\frac{\zeta}{2}\left(\mathbf{x}^0 - \mathbf{z}\right)^2 - \frac{\zeta}{2}\sum_{\alpha=1}^{n}\left(\mathbf{x}^\alpha - \underline{\underline{\Lambda}}\cdot\mathbf{z}\right)^2\right] - \frac{Q}{V_0 V^n} \tag{5.28b}$$

In general, the determinant, $\mathrm{Det}\underline{\underline{\Lambda}}$ $(= V/V_0)$, may differ from unity, corresponding to a change in system volume. By substituting this modified Ansatz into the saddle-point equation obtained in the usual way from the effective Hamiltonian, Eq. (5.26), we find that the Ansatz is indeed a solution, provided $\mathcal{P}(\zeta)$ is the *same* distribution as defined by Eq. (2.20) (in the limit $n \to 0$). The interpretation of the deformed saddle point, given by Eq. (5.28b), is as follows. After

the deformation, the same fraction of the monomers (i.e. Q) are localized. In the preparation ensemble, a localized monomer continues to exhibit Gaussian fluctuations around the point $\mathbf{z}$ with an unchanged variance $\zeta^{-1/2}$. However, in the measurement ensemble it fluctuates around the new point $\underline{\underline{\Lambda}}\cdot\mathbf{z}$ with the original variance $\zeta^{-1/2}$. This implies that *the average position of each monomer, parameterized by* $\mathbf{z}$*, is deformed affinely, whereas the fluctuations around* $\mathbf{z}$ *remain intact.* Previous work had arrived at the same conclusion through a slightly different route [31]. Note that $\mathbf{z}$, as well as $\mathbf{x}^0$, are confined to the volume (i.e. the range over which $\mathbf{z}$ is integrated) of the preparation ensemble. Observe, furthermore, that $M_{\underline{\underline{\Lambda}}}(\hat{x})$ is vanishingly small whenever $\mathbf{x}^\alpha$ and $\underline{\underline{\Lambda}}\cdot\mathbf{x}^0$ are widely separated, for any $\alpha = 1,\ldots,n$. It therefore follows that the $\mathbf{x}^\alpha$, i.e. the measurement ensemble coordinates, are confined to the preparation ensemble transformed by the distortion $\underline{\underline{\Lambda}}$. Keeping this in mind, and studying Fig. 5.1, it is clear that $\underline{\underline{\Lambda}}$ is the homogeneous deformation imposed on the boundary of the system. We now calculate the elastic free energy density of rubber $f_{\rm el}(\underline{\underline{\Lambda}})$ at the mean-field level. To do this, we insert the deformed saddle point given by Eq. (5.28b) into the effective Hamiltonian (5.26) and subtract its expression for the undeformed ($\underline{\underline{\Lambda}} = \mathbf{I}$) saddle point. Then, dividing appropriately by n to implement the replica trick and taking the replica limit $n \to 0$, we find

$$\begin{aligned} f_{\rm el}(\underline{\underline{\Lambda}}) &= \lim_{n\to 0}\frac{1}{n}\Big(\mathcal{H}[M_{\underline{\underline{\Lambda}}}] - \mathcal{H}[M_0]\Big) \\ &= \frac{1}{2}\,\mu\,\mathrm{Tr}\,\underline{\underline{\Lambda}}^{\mathrm{T}}\,\underline{\underline{\Lambda}} + \frac{1}{2\,\det\underline{\underline{\Lambda}}}\,\tilde{B}(\det\underline{\underline{\Lambda}} - 1)^2, \qquad (5.29a) \\ \mu &\propto |\tau|^3\,, \qquad \tilde{B} \propto B_0\ . \qquad (5.29b) \end{aligned}$$

It is clear that the first term in Eq. (5.29a) coincides with the free energy density of classical theory of rubber elasticity, Eq. (5.13); the second term describes the energy cost for *volume changes*, with the bulk modulus $\tilde{B}$ related to the parameter B_0. Consequently, what we have derived, Eqs. (5.29), is the classical elasticity model of rubber elasticity, generalized to finite bulk moduli systems. In the limit $\tilde{B} \to \infty$, the incompressibility constraint $\det\underline{\underline{\Lambda}} \equiv 1$ is restored. As expected, the shear modulus given by Eq. (5.29b) scales as $|\tau|^3$ is a mean-field result.

We emphasize that Eq. (5.29a) is derived from the Landau theory of VT, which includes the the most relevant contributions. Therefore, it is *independent* of short-distance details and thus

provides a *universal* mean-field description for the elasticity of *all forms of vulcanized matter near the vulcanization point*, provided that the corresponding transition is described by the Landau theory. This observation may explain, in part, the huge success of the classical theory of rubber elasticity, Eq. (5.14). Though I only presented the derivation of isotropic rubber elasticity from the Landau theory in this Thesis, an analogous derivation of the neo-classical theory for nematic elastomers from an appropriately modified Landau theory has been performed, guided by the same physical principles as described here; for details see Ref. [15].

The present work also constitutes a starting point for studying spatial fluctuations, both thermal and quenched, in vulcanized matter of various forms. Sufficiently close to the vulcanization point, critical fluctuations of the V/G order-parameter field Ω become important, and they change qualitatively the scaling of μ; this issue will be addressed in Chapter 6. Nevertheless, the *form* of the elasticity theory, Eq. (5.29a), continues to hold even after the incorporation of critical fluctuations.

5.6 Goldstone fluctuations and local displacements

Let us now revisit the connection between Goldstone fluctuations and local displacements in the light of the discussion presented in this chapter. A few remarks are in order. In this chapter we have introduced the concepts of a preparation and measurement ensembles. This is a fresh element in our understanding of the physical system and elastic deformations—and hence the corresponding Landau theory and Goldstone fluctuations—that was absent from the simpler discussion presented in Section 3.3.2. The focus of this subsection is to reconcile the Goldstone fluctuations (and their identification as local displacements) within the Landau theory used in the previous chapter with the construction of elastic deformations within the generalized Landau theory used in the present chapter.

If we consider elastic deformations that are non-uniform, the the deformation tensor $\underline{\underline{\Lambda}}$ can be written as $\underline{\underline{\Lambda}} = \underline{\underline{\mathrm{I}}} + \underline{\underline{u}}$; see Eq. (5.7). Any elastic deformation can be decomposed into a antisymmetric and symmetric tensor; the antisymmetric tensor corresponds to rotations and the symmetric tensor corresponds to extensions and compressions along a set of orthogonal principal axes, i.e., purely elastic deformations (without any rotations). Recall that symmetric tensors can always be diagonalized; therefore it suffices to consider a diagonal gradient tensor (in a properly chosen

principal basis). With this knowledge, one can rewrite Eq. (5.28b) as follows:

$$M_{\underline{\underline{\Lambda}}}(\hat{x}) \;=\; Q\int d\mathbf{z}\int d\zeta\,\mathcal{P}_0(\zeta)\,\left(\frac{\zeta}{2\pi}\right)^{(n+1)D/2}\exp\left[-\frac{\zeta}{2}\left(\mathbf{x}^0-\mathbf{z}\right)^2-\frac{\zeta}{2}\sum_{\alpha=1}^{n}\left(\mathbf{x}^\alpha-\mathbf{z}-\mathbf{u}(\mathbf{z})\right)^2\right] - \frac{Q}{V_0V^n} \tag{5.30}$$

Note that the displacement vector $\mathbf{u}(\mathbf{z})$ is the same in all the replicas 1 to n. We have considered deformations in the measurement ensembles that are replica independent; however, there is no particular reason to be confined to such replica independent deformations. Therefore, let us generalize the above expression and make the field $\mathbf{u}(\mathbf{z})$ replica dependent. We obtain

$$M_{\underline{\underline{\Lambda}}}(\hat{x}) \;=\; Q\int d\mathbf{z}\int d\zeta\,\mathcal{P}_0(\zeta)\,\left(\frac{\zeta}{2\pi}\right)^{(n+1)D/2}\exp\left[-\frac{\zeta}{2}\left(\mathbf{x}^0-\mathbf{z}\right)^2-\frac{\zeta}{2}\sum_{\alpha=1}^{n}\left(\mathbf{x}^\alpha-\mathbf{z}-\mathbf{u}^\alpha(\mathbf{z})\right)^2\right] - \frac{Q}{V_0V^n} \tag{5.31}$$

Now note the following property of the deformed saddle-point expression, above. If $\mathbf{u}^\alpha(\mathbf{z})=\mathbf{a}^\alpha$, where $\mathbf{a}^\alpha$ are constant vectors, then the expression is another saddle-point of the Landau theory, related to the old saddle point by the symmetry of independent translations in all the replicas (see Section 3.3.1 for a discussion). For the impatient reader, here is a quick and dirty way of recognizing the fact that *independent* uniform translations on the saddle-point $M_0(\hat{x})$ lead to a new symmetry-related saddle point $M_0(\hat{x}+\hat{a})$. The saddle-point $M_0(\hat{x})$ is only invariant under *common* translations; hence it will change under *independent* translations. However, recall that the effective theory for V/G transition is invariant under independent translations. Therefore, the effective energy for both $M_0(\hat{x})$ and $M_0(\hat{x}+\hat{a})$ is identical. One can only conclude that $M_0(\hat{x}+\hat{a})$ is another saddle-point, related to $M_0(\hat{x})$ by translations[8].

The independent, uniform translations, given by $\mathbf{u}^\alpha(\mathbf{z})=\mathbf{a}^\alpha$ ($\alpha=1$ to n) in Eq. (5.31) seem to be of the *restricted* form $\hat{a}=(\mathbf{a}^0=\mathbf{0},\mathbf{a}^1,\ldots,\mathbf{a}^\alpha,\ldots,\mathbf{a}^n)$. However, note that an arbitrary independent translation of the form $\hat{a}=(\mathbf{a}^0,\mathbf{a}^1,\ldots,\mathbf{a}^\alpha,\ldots,\mathbf{a}^n)$, can be written as $\hat{a}=(\mathbf{a}^0=\mathbf{0},\mathbf{a}^1-\mathbf{a}^0,\ldots,\mathbf{a}^\alpha-\mathbf{a}^0,\ldots,\mathbf{a}^n-\mathbf{a}^0)+(\mathbf{a}^0,\ldots,\mathbf{a}^0)$; i.e., a replicated vector of the restricted form

[8]The situation is analogous to $O(N)$ vector model. The ground state is invariant under uniform rotations about the direction of magnetization. However, arbitrary uniform rotations lead to a new ground state, related to the old one by rotation of the direction of magnetization.

plus a common translation. But recall that the saddle-point is invariant under common translations, hence the choice $\mathbf{a}^0 = 0$ is a choice in eliminating the common translations, and is not really a restriction on the independent translations being considered here. The key point is this: any independent uniform translation $\hat{a}$ can be either decomposed into $\hat{a} \equiv (\mathbf{0}, \mathbf{b}^1, \ldots, \mathbf{b}^\alpha, \ldots, \mathbf{b}^n) + (\mathbf{a}^0, \ldots, \mathbf{a}^0)$; i.e., a nD dimensional vector $\{\mathbf{b}^\alpha\}$ (with α running form 1 to n), and a D dimensional vector $\mathbf{a}^0$. Recall that in Chapter 3 we made a decomposition in the same spirit of $(n+1)D$ dimensional vectors into longitudinal and transverse vectors; $\hat{a} \equiv (a_\perp, a_\parallel)$. The motivation for doing so was also to identify the common translations and relative translations corresponding to an arbitrary translational vector. However, in that chapter we made a symmetric choice for identifying the common translations; we had a $(n+1)$-replica permutation symmetric theory and the need to distinguish between the zeroth replica and the other replicas had not arisen. In the light of the distinction between preparation and measurement ensembles, it seems more convenient to decompose an arbitrary vector in the manner discussed above. Recall that Goldstone fluctuations are non-uniform deformations of the saddle-point such that in the extremely long-wavelength limit, such deformations are uniform *relative* translations (see Section 3.3). Therefore, $\mathbf{u}^\alpha(\mathbf{z})$ in Eq. (5.31) are Goldstone fluctuations for the same reason that $u_\perp(\mathbf{z})$ in Eq. (5.17) are. *This rigorously established the identification of Goldstone fields as replicated local displacements.*

What, if any, are the differences between the physical implications of the two parametrization of Goldstone fluctuations discussed so far? A conclusive answer still eludes us. However, to explore the connection between them, let us write Eq. (5.17) in the following equivalent form,

$$\Omega(\hat{x}) = Q \int d\zeta\, \mathcal{P}(\zeta) \int d\mathbf{z} \left(\frac{\zeta}{2\pi}\right)^{D/2} \exp\left[-\frac{\zeta}{2}\left(\hat{x} - \hat{u}(\mathbf{z}) - \hat{z}\right)^2\right], \tag{5.32}$$

where, $\hat{z} \equiv (\mathbf{z}, \ldots, \mathbf{z})$, and $\hat{u} = (u_\parallel, u_\perp)$ with the constraint that $u_\parallel = 0$. A general choice of parametrization of all replicated vectors $\hat{u}$ for which $u_\parallel = 0$ is the following: $\hat{u} \equiv (\mathbf{u}^0 = -\sum_{\alpha=1}^n \mathbf{u}^\alpha, \mathbf{u}^1, \ldots, \mathbf{u}^\alpha, \ldots, \mathbf{u}^n)$[9]. Note that Eq. (5.31) can also be written in the same form as Eq. (5.32) with the displacement vector $\hat{u}$ defined to be $\hat{u} \equiv \{\mathbf{u}^0 = \mathbf{0}, \ldots, \mathbf{u}^\alpha, \ldots, \mathbf{u}^n\}$. Hence, the difference between the two parametrizations is in the Goldstone field belonging to the zeroth replica. For replica-independent Goldstone fields, i.e., when the displacements are the same in all the repli-

[9]This follows immediately from the definition $u_\parallel \equiv \frac{1}{\sqrt{1+n}} \sum_{\alpha=0}^n \mathbf{u}^\alpha$.

cas, the difference between the two parametrizations is of order n. The two parametrization of the Goldstone fields are connected by a common *non-uniform* translation. We remind the reader that although *common uniform* translations do not change the effective energy of the system, *common nonuniform* translations (i.e. common deformations) do change the effective energy, hence, the two parameterizations are not equivalent. This does not necessarily mean that they lead to different physical results, and we are yet to discover a setting where they do. Current research is focussed on developing a general theory of rubber elasticity that is capable of incorporating the effects of local quenched randomness in elastic properties in the random solid. In derivation of the classical theory, given in this chapter, we have only considered *uniform replica-independent* deformations, i.e., the deformation matrix $\underline{\underline{\Lambda}}$ is a constant in all the replicas. Ongoing research is focused on understanding the implications of general replica-dependent deformations $\mathbf{u}^{\alpha}(\mathbf{z})$; and, hopefully, a connection between effective theory for the generalized Goldstone fluctuations and the phenomenological theory of random elastic fluctuations will emerge. In this setting, the parametrization that respects the physical distinction between preparation and measurement ensembles seems to be favorable.

5.7 Conclusions

In this chapter we have discussed the shortcomings of the Goldstone construction presented in the previous chapter, together with the resolution of these shortcomings. Along the way, we have made rigorous the identification of Goldstone fields with replicated local displacements for elastic deformations rigorous, and derived the phenomenological theory of classical rubber elasticity. The effective theory of the revised Goldstone fluctuations is the starting point for current research on quenched random stress and elastic moduli fluctuations that are unique to random solids.

Chapter 6

Scaling of the Shear Modulus

> What is it indeed that gives us the feeling of elegance in a solution, in a demonstration? It is the harmony of the diverse parts, their symmetry, their happy balance; in a word it is all that introduces order, all that gives unity, that permits us to see clearly and to comprehend at once both the ensemble and the details.
> —J. H. Poincaré, in *Mathematical Maxims and Minims*, by N. Rose (Rome Press Inc., 1988).

6.1 Introduction

The main focus of this chapter is determining the scaling of the static shear[1] modulus as a function of the density of crosslinks in the critical region of the vulcanization/gelation transition. The scaling behavior of the shear modulus in gels and vulcanized matter is a very controversial issue, and I enunciate the nature of controversy right away to motivate the rather terse presentation in the rest of this chapter. Recall that in Section 5.3 I introduced the basic concepts of classical elasticity theory, in particular the shear deformation tensor $\underline{\underline{\Lambda}}$, which we shall invoke here. Consider a spatially homogeneous[2], volume-preserving shear deformation $\underline{\underline{\Lambda}}$, with $\det \underline{\underline{\Lambda}} = 1$. Under such a deformation, the increase in the free energy of a gel, to leading order in $\underline{\underline{\Lambda}}$, is given by [see eqs.(5.12, 5.13)]

$$\delta f_{\rm el} = V\mu \left({\rm Tr}\, \mathbf{g} - D \right), \qquad \mathbf{g} \equiv \underline{\underline{\Lambda}}^{\rm T} \cdot \underline{\underline{\Lambda}}, \tag{6.1}$$

where $\mathbf{g}$ is the metric tensor (in the parlance of Section 5.3, the right Cauchy-Green deformation tensor) and D is the spatial dimensionality. The shear modulus is expected, on general grounds,

[1] The word 'shear' was first used in scientific literature in 1850. E. Clark, in Britannia and Conway Bridges I, p. 389, wrote: *Examples of this kind of strain occur in the rivet which unites the two blades of a pair of scissors, or the rivet on which the blade rotates in an ordinary pocket-knife.* How apt!

[2] Recall that a homogeneous deformation is described by a constant matrix $\underline{\underline{\Lambda}}$, such that $\mathbf{R}_F = \underline{\underline{\Lambda}} \cdot \mathbf{R}_I$, where $\mathbf{R}_I$ and $\mathbf{R}_F$ are the positions of mass points before and after deformation.

to obey a universal scaling law near the critical point,

$$\mu = \mu_0 \, \Theta(-\tau) \, |\tau|^f, \tag{6.2}$$

where f is called the shear modulus exponent, and we remind the reader that the control parameter τ, first introduced in Eq. 2.11, measures deviation of the crosslink density from its critical value. Recall that $\tau < 0$ in the solid phase, see Section 2.3. Here Θ denoted the Heaviside step function. To summarize, shear modulus is zero in the liquid state and scales with the control parameter as a power law with exponent f in the critical region of the solid state. The controversy surrounds the value of f.

Values reported for the exponent f, either from experiments or computer simulations, are rather scattered, and seem to suggest four different universality classes [52]. For systems with *entropic* elasticity which is the focus of this chapter, values of f usually fall into one of two classes.[3] Firstly, most numerical simulations [53] involving phantom networks, as well as many gelation experiments, suggest that f has the same value as the conductivity exponent t (≈ 1.9 in three dimensions) of random resistor networks (RRN), supporting a conjecture of de Gennes' [9]. A second class of experiments, as well as some simulations, support the scaling result $f = D\nu$ (≈ 2.6 for three dimensions), where ν is the percolation correlation-length exponent, as proposed in Ref. [54]. The purpose of this chapter is to use heuristic and analytical methods to outline a resolution of the long-standing apparent contradiction between the two plausible arguments, mentioned above, as well as the inconsistency across experimental and simulational data. In the next section we present the arguments supporting the two conjectures; the *de Gennes conjecture* and the *Daoud-Coniglio conjecture*.

The work presented in this Chapter was done in collaboration with Xiangjun Xing and P. M. Goldbart.

[3] We are not considering systems undergoing *rigidity percolation*. Rigidity percolation is a percolation transition in a system of mechanical units (for example, springs introduces with some probability between neighboring points on a lattice) in which the system becomes rigid at a critical probability, p_R, which is greater than the percolation threshold p_c. Therefore, the presence of an infinite cluster does not ensure rigidity: the system is not rigid between p_c and p_R. The *rigidity percolation universality class* is distinct from the *connectivity percolation universality class*, see Refs. [55] for further details. In rigidity percolation systems the elasticity is not entropic but *energetic* in origin. Thermal fluctuations are not included—the elasticity of such systems is a zero temperature phenomena.

6.2 The two conjectures for the value of shear modulus exponent

6.2.1 The de Gennes conjecture: overview and comments

The de Gennes conjecture relies upon the mapping between the conductivity of the infinite cluster in the Random Resistor Networks (RRN) model, and the shear modulus for the gel in the gelation transition [9]. The Random Resistor model is a lattice model of bond percolation where each bond (a resistor of finite resistance) is introduced between regular lattice points (which are otherwise disconnected, i.e., absent bonds has infinite resistance). When resistors are introduced with high enough probability, a typical realization of the infinite lattice has an infinite spanning cluster of connected resistors. Therefore, the electric conductance of the system (measured between any two boundaries that are infinitely apart) is zero below the percolation transition and non-zero above it. de Gennes modeled the infinite cluster in the gel to be a random network of Gaussian springs connecting the 'nodes' of the cluster. These Gaussian springs are roughly the *effective entropic springs* that the 'links' between two neighboring 'nodes' can be thought to be, in the 'node-link-blob' picture of the infinite cluster. Let me briefly explain the 'node-link-blob' picture of the percolative infinite cluster. Though this is a cartoon picture of a generic infinite cluster at the percolation transition, for concreteness, consider the infinite cluster formed by the process of crosslinking polymers and focus on its geometrical properties alone. Near the percolation (gelation) transition this cluster is a fractal object. The bulk of the infinite cluster is made of polymers that are attached to it by a single crosslinks; they are the 'dangling ends'. The polymers that are attached to cluster by at least two crosslinks are essential to form the 'mesh' of the infinite cluster, with typical mesh size $\xi_{\rm perc}$, i.e., the percolation correlation length. The 'nodes' refer to the nodes in this mesh, i.e., monomers whose removal from the infinite cluster will reduce the number of loops. The 'links' are units that connect the mesh; cutting a link will disconnect two nodes. The links are however decorated with 'blobs'; these 'blobs' are the redundant polymers that are either dangling or multiply connect two monomers. The Gaussian spring in de Gennes model are the *effective chains* composed of the links and blobs.

The elastic energy in de Gennes model of the infinite cluster is given by

$$f_{\rm el} = \frac{1}{2} \sum_{ij} \Gamma_{ij} \left(\mathbf{u}_i - \mathbf{u}_j \right)^2 \tag{6.3}$$

where Γ_{ij} is the spring constant for the spring connecting the nodes i, j, with local displacement of which are $\{\mathbf{u}_i$ and $\mathbf{u}_j\}$ respectively. The matrix Γ_{ij} encodes information about both the connectivity of the nodes and the strengths of the effective springs. The requirement of mechanical equilibrium of the nodes of the network leads to the condition

$$\sum_{j} \Gamma_{ij} \left(\mathbf{u}_i - \mathbf{u}_j \right) = 0 \ \text{ for all } \ i. \tag{6.4}$$

The above equation can analogously be interpreted as Kirchhoff's equation of electrical current balance for an electrical network, if Γ_{ij} represents the local conductance for a conductor connecting (i, j) [4]. If the elastic system is macroscopically isotropic, the local displacement are, *on the average*, identical in all spatial directions and the vectorial problem expressed in terms of $\{\mathbf{u}_i\}$ is reduced to a scalar problem expressed in terms of the magnitudes $\{u_i\}$. In this case the scalar quantity u_i can be interpreted as the voltage at node i. Using this mapping, $2f_{\rm el}$ is the Joule dissipation of the electrical network of random resistors. The relationship between the current density J and the electric field ∇u, i.e., $J = \Sigma \nabla u$, can be mapped to the relationship between mechanical stress $F = -\mu \nabla u$, where Σ is the conductivity of the network. Therefore, the mapping indicates that *the electric conductivity of an isotropic random resistor network scales in the same way as the elastic modulus of the equivalent isotropic network of Gaussian springs.*

There are number of assumptions in the de Gennes mapping, and I would like to emphasize them here. These considerations were not made when de Gennes first proposed the mapping, but grew out of studies by many authors [55] over the last two decades. First, the mapping is from a vectorial problem to a scalar problem, the isotropy of space being invoked as justification. Let us

[4] If nodes i and j are not connected then the conductor has zero conductance, therefore, Γ_{ij} encodes both the connectivity and the local conductivity of the network.

revisit the Hamiltonian given by Eq. (6.3) and introduce a general form of the elastic energy,

$$f_{\rm el} = \frac{1}{2}\sum_{ij}\Gamma_{ij}\left[\alpha\left(\mathbf{u}_i-\mathbf{u}_j\right)_{\parallel}^2+\beta\left(\mathbf{u}_i-\mathbf{u}_j\right)_{\perp}^2\right], \tag{6.5}$$

where $(\mathbf{u}_i-\mathbf{u}_j)_{\parallel}$ is the relative displacement in the direction parallel to the bond $\{i,j\}$, and $(\mathbf{u}_i-\mathbf{u}_j)_{\perp}$ is the relative displacement perpendicular to it. The new parameters α and β allow us to control these terms separately. For $\alpha=\beta$, we recover the elastic Hamiltonian (6.3), and the problem is indeed a scalar one. Note however, that when $\alpha=\beta$, the network is not quite the network of physical springs as suggested by de Gennes, but when $\beta=0$ it is. This is because when $\alpha=\beta$, two particles are pulled to each other even when their relative displacement is *perpendicular* to the bond (spring) connecting them. The model with $\beta=0$ is known as the *central-force network*. The Hamiltonian for the central force networks is usually expressed in the form,

$$f_{\rm el} = \frac{1}{2}\sum_{ij}\Gamma_{ij}\left[\alpha\left(\mathbf{u}_i-\mathbf{u}_j\right)\cdot\hat{\mathbf{R}}_{ij}\right]^2, \tag{6.6}$$

where $\hat{\mathbf{R}}_{ij}$ is the unit vector pointing at node j from node i. The above form of the Hamiltonian makes the vectorial nature of Random Spring Network (or central-force network) explicit, and shows that the de Gennes mapping refers to a somewhat unphysical isotropic spring network[5]. However, the de Gennes mapping can be made exact for a very special Random Spring Network [63]. Let me mention this in passing.

In the elastic Hamiltonian 6.3 it is assumed that the nodes have a mean equilibrium position about which local displacements $\mathbf{u}_i$ are considered. Therefore, the springs are of nonzero natural length. Now, consider a Random Spring Network made of springs that have *zero* natural length. The Hamiltonian for such a system need not be written in terms of local displacements, but can be written in terms of the *positions* of the nodes. Of course, this network is somewhat strange; the minimum energy configuration of the system is when it has collapsed to a point, but imagine

[5]The reader may find this presentation too naïve, because I have avoided the discussion of rigidity percolation in central-force-networks. The connectivity percolation threshold coincides with the rigidity threshold only when both central-force and bond-bending forces are present. For purely central force networks, the thresholds are different, and so is the scaling of elastic modulus, thereby classifying the system in the *rigidity percolation universality class*. However, these considerations are for systems at zero temperature, exhibiting *energetic* elasticity. My naïvety of presentation will perhaps be excusable on remembering that the Thesis deals with *entropic* elasticity alone; see Refs. [55], [56]

imposing boundary condition so that this cannot happen [63]. The Hamiltonian of this *central-force network* is

$$f_{\rm el} = \frac{1}{2}\sum_{ij}\Gamma_{ij}\left(\mathbf{R}_i - \mathbf{R}_j\right)^2. \tag{6.7}$$

With appropriate boundary condition it is now clear that the de Gennes mapping is exact for this network, because of the scalar nature of the problem. For further details, see Ref. [63]. We shall be making use of this exact mapping later in this chapter.

6.2.2 The Daoud-Coniglio conjecture: overview and comments

The Daoud-Coniglio conjecture [54] follows a different route by focussing on the expected singularity of the free energy for a strong gel at the critical point. To appreciate their scaling argument, let us reconsider the elastic Hamiltonian (6.3) as a model for the infinite cluster. As mentioned in the previous section, the infinite cluster can be modeled as a mesh of nodes and macrolinks. The spring constants for these macrolinks are given by the elements of the matrix Γ_{ij}. Let us define K to be the average spring constant of the macrolinks. The typical linear dimension of these macrolinks is the percolation correlation length ξ. How does the free energy of the system scale? For a system of size $L_{\rm sys}$, there are $L_{\rm sys}/\xi$ elements in series, and each element is made of $(L_{\rm sys}/\xi)^{D-1}$ springs in parallel. Therefore the elastic modulus μ is given by $\mu = K(L_{\rm sys}/\xi)^{D-1}(L_{\rm sys}/\xi)^{-1}$. We expect that the spring-constant of the macrolink should scale as $|\tau|^{\phi}$, where τ is the control parameter for the percolation transition and ϕ is an appropriate exponent. The logic behind this expectation will be explained later. Therefore, the scaling for μ would

$$\mu \sim L^{D-2}|\tau|^{\phi+(D-2)\nu}, \tag{6.8}$$

where we have used the scaling relation $\xi \sim |\tau|^{-\nu}$. Hence, the shear modulus should scale as $f = \phi + (D-2)\nu$. The question is, what is the value of ϕ, i.e., the exponent for the spring constant of the macrolinks?

Daoud and Coniglio argued that the $\phi = 2\nu$, leading to $f = D\nu$. The gist of their argument is as follows. The mean fluctuation in the energy of a macrolink-spring is $K\langle(x - \langle x\rangle)^2\rangle/2$, where x is the spring elongation. But this is equal to k_BT, by invoking energy equipartition theorem.

Therefore, $K \propto 1/\langle (x - \langle x \rangle)^2 \rangle$. What is the fluctuation in the elongation of the macrolink-spring? As there are macrolinks of all sizes up to the correlation length scale, a generous estimate of this fluctuation is the correlation length. Therefore, $K \sim 1/\xi^2_{\rm perc} \sim |\tau|^{2\nu}$. As there is no other relevant length scale in the problem, this is a plausible scaling argument.

In order to compare the Daoud-Coniglio conjecture with the de Gennes conjecture, let us start from the the scaling relationship $f = \phi + (D-2)\nu$ and find out what value of ϕ is consistent with the de Gennes conjecture. If one assumes that the spring-constant exponent ϕ is equal to the resistance exponent for the equivalent Random Resistor Network (RRN) then the relationship $f = \phi + (D-2)\nu$ implies $f = t$, i.e., the conductivity exponent[6]. Arguments supporting the equality of the spring constant exponent and the resistance exponent provide the essence of the mapping of springs to resistances described in the previous section.

In the next section we make a short digression to establish the scaling of shear modulus using the conventional V/G theory [see Eq. (2.11)]. In later sections, we use the generalized V/G Hamiltonian (5.26) to present a resolution of the controversy surrounding the scaling of shear modulus. The reader may wish to skip the next section, and return to it later to appreciate why the generalization of the V/G theory was necessary.

6.3 Scaling of shear modulus in V/G field theory

In this section we outline the method of encoding elastic deformations in a field theory via a change of the Euclidean metric of space.[7] Along the way, we determine the shear-modulus scaling of the V/G field theory (2.11). Any elastic deformation can be decomposed into a set of pure compressions and dilations in the principal basis, along with rotations. Hence it suffices to consider a diagonal deformation tensor $\underline{\underline{\Lambda}}$. Consider pure shear deformations, i.e., those for which $\mathrm{Det}\,\underline{\underline{\Lambda}} = 1$. Consider *small* (and, in general, non-uniform) deformations. We define an *infinitesimal* gradient tensor $\underline{\underline{u}}$ [see Eq. (5.7)] via

$$\underline{\underline{\Lambda}} = \underline{\underline{I}} + \underline{\underline{u}} \ \text{ where } \ \mathrm{Tr}\,\underline{\underline{u}} = 0. \tag{6.9}$$

[6]The resistance exponent for the RRN model of percolation is defined as the exponent governing the scaling of the average resistance $R(x - x')$ between two points x and x' (where x and x' belong to the same cluster), i.e., the exponent in the relationship, $R(x - x') \sim |x - x'|^{\phi/\nu}$; see ref. [58]

[7]I thank Prof. E. Fradkin for informative and stimulating discussion on the work presented in this section.

As we are considering $\underline{\underline{\Lambda}}$ to be diagonal, the gradient tensor $\underline{\underline{u}}$ is diagonal, too. Under deformations, the mass point at position $\mathbf{x}_I$ in reference space is displaced to the $\mathbf{x}_F \equiv \mathbf{x}_I + \mathbf{u}(\mathbf{x}_I)$ in target space, where $\mathbf{u}(\mathbf{x}_I)$ is an infinitesimal displacement vector[8]. This transformation from reference space to the target space can be encoded as a change in the flat-space metric $\underline{\underline{\delta}}$ of the reference space, thereby assigning a nontrivial metric $\underline{\underline{\eta}}$ in the target space[9]. Using the covariance relation for the metric tensors, i.e., $\delta_{ij}\, dx^i_I dx^j_I = \eta_{ij}\, dx^i_R dx^j_R$, the metric η_{ij} is determined to be

$$\eta^{ij} \approx \delta^{ij} \left(1 - 2\, u^i\right), \tag{6.10}$$

to first order in the displacements u_i, where no summation is implied in the above equation. The explicit form of the metric is not important for our discussion; the key point is that *infinitesimal elastic displacements can be encoded into a change of metric*. With this change of metric, the field theory of the deformed system is given by [cite for Eq. (2.11)]

$$\mathcal{H}_{\underline{\underline{\eta}}} = \int_{\text{HRS}} d^{(n+1)D}\hat{x}\, \sqrt{\text{Det}\, \underline{\underline{\eta}}} \left\{ \frac{1}{2} \sum_{\alpha=1}^{n} \eta^{ij}\, \nabla_i^\alpha \Omega\, \nabla_j^\alpha \Omega + \frac{1}{2}\tau_0 \Omega^2 - \frac{v}{3!}\Omega^3 \right\}, \tag{6.11}$$

where Einstein summation convention is implied over the spatial indices i, j. In comparison to Eq. (2.11), we have changed the notation slightly; the cubic coupling constant is now denoted by v instead of g, so as to avoid confusion with the metric tensor. The careful reader will notice that this form of the deformed Hamiltonian is not strictly correct. As discussed in Section 5.6, elastic deformations affect only the measurement ensembles 1 to n, and leave the preparation ensemble unaffected, and one could introduce replica dependent metric $\underline{\underline{\eta}}^\alpha$ to make this distinction. The arguments that follow do not depend on this detail however, so we choose to ignore this subtlety for the time being. Note that volume-preserving (i.e. pure shear) deformations imply $\text{Det}\, \underline{\underline{\eta}} = 1$.

[8] In order to avoid confusion, note that in Section 5.3 we used $\mathbf{R}_I$ to denote the mass points in the reference space and $\mathbf{R}_F$ to denote the mass points in the target space. In this section we change the notations to $\mathbf{x}_I$ and $\mathbf{x}_F$ respectively because the field theory is defined on the replicated space denoted by $(\mathbf{x}^0, \cdots, \mathbf{x}^1)$, and although this abstract replicated space do not strictly denote the mass points of the solid, the effect of deformations is the same on this space; see Section 5.6.

[9] Caveat: The definition of the metric tensor $\underline{\underline{\eta}}$ in this section is different from the definition of the metric tensor $\underline{\underline{g}}$ in the rest of the chapter: $\underline{\underline{\eta}} = \underline{\underline{g}}^{-1}$. At the risk of offending the reader, we compromise on this non-uniformity of notation because it is popular in the field theory literature, referred to in this section, to define the tensor as is done here. In the rest of the chapter we use $\underline{\underline{g}}$.

The stress-energy tensors for the field theory is defined via [59]

$$\text{Bare stress-energy tensor: } T^{ij} = -\frac{2}{\sqrt{\text{Det}\,\underline{\underline{\eta}}}}\frac{\delta\,\mathcal{H}_{\underline{\underline{\eta}}}}{\delta\,\eta_{ij}}, \tag{6.12a}$$

$$\text{Renormalized stress-energy tensor: } T_R^{ij} = -\frac{2}{\sqrt{\text{Det}\,\underline{\underline{\eta}}}}\frac{\delta\,\Gamma_{\underline{\underline{\eta}}}}{\delta\,\eta_{ij}}, \tag{6.12b}$$

where Γ is the effective free energy introduced in Chapter 4. Why do we care about the stress-energy tensor? To appreciate why, note that from Eq. (6.10) the change of the (diagonal) metric $\delta\,\eta_{ij} = -2\delta_{ij}\,u_i$. Therefore, the change of effective free energy $\delta\,\Gamma_{\underline{\underline{\Lambda}}}$ under shear deformation is $\delta\,\Gamma_{\underline{\underline{\eta}}} \sim T_R^{ii}\,u_i$. But the change in effective free energy under for infinitesimal shear deformation is equal to the shear modulus times the displacements. Therefore, the (diagonal) stress-energy tensor is proportional to the shear modulus μ. In the rest of this section we establish, from general field theory arguments, that the stress-energy tensor cannot acquire an anomalous dimension under renormalization. This establishes that the shear modulus cannot acquire an anomalous dimension either, and the scaling of the shear modulus must be correctly by naïve scaling arguments.

The liquid state is invariant under shear deformations but the random solid state is not. However, the reader is aware that the random solid state breaks the symmetry associated with shear deformations *spontaneously*. This implies that the current associated with this symmetry is conserved, an assertion well known in the field theory literature; see for example ref. [25]. This assertion is sufficient to prove that the stress-energy tensor cannot acquire an anomalous dimension. Let me sketch the proof here.

The partition function $\mathcal{Z}$ for the undeformed system is

$$\mathcal{Z} \sim \int \mathcal{D}\Omega \exp\left[-\mathcal{H}[\Omega(\hat{x})] + \int d\hat{x}\, H(\hat{x})\Omega(\hat{x})\right], \tag{6.13}$$

where $H(\hat{x})$ is a conjugate field that we have introduced in the usual way. The partition function for the deformed system is

$$\mathcal{Z}_{\underline{\underline{\eta}}} \sim \int \mathcal{D}\Omega \exp\left[-\mathcal{H}_{\underline{\underline{\eta}}}[\Omega(\hat{x})] + \int d\hat{x}\sqrt{\text{Det}\,\underline{\underline{\eta}}}\, H(\hat{x})\Omega(\hat{x})\right]. \tag{6.14}$$

The partition function, being an integration over all fields and spacial variables, cannot be affected by a change in metric. Therefore, $\mathcal{Z} = \mathcal{Z}_{\underline{\underline{\eta}}}$. Note that the change in the square root of the determinant of a metric is given by the relation [59]

$$\delta\sqrt{\mathrm{Det}\,\underline{\underline{\eta}}} = \frac{1}{2}\delta^{ij}\,\delta\eta_{ij}. \tag{6.15}$$

Recall that δ^{ij} is the flat Euclidean metric. The above equation implies that the change in the source term is $\frac{1}{2}\sqrt{\mathrm{Det}\,\underline{\underline{\eta}}}\;\delta^{ij}\,\delta\eta_{ij}\,H(\hat{x})\,\Omega(\hat{x})$. Also note that Eq. (6.12a) gives the the change in the effective Hamiltonian to be $\delta\mathcal{H}_{\underline{\underline{\eta}}} = -\frac{1}{2}\sqrt{\mathrm{Det}\,\underline{\underline{\eta}}}\,T^{ij}\,\delta\eta_{ij}$. Therefore, we can re-express the identity $\mathcal{Z}_{\underline{\underline{\eta}}} - \mathcal{Z} = 0$ by expanding the exponential in the small parameter $\delta\eta_{ij}$ thus obtaining

$$\int \mathcal{D}\Omega\left[T^{ij} + \delta^{ij}\,H(\hat{x})\Omega(\hat{x})\right]\,\delta\eta_{ij}\,\exp\left\{-\mathcal{H}[\Omega(\hat{x})] + \int d\hat{x}\,H(\hat{x})\Omega(\hat{x})\right\} = 0 \tag{6.16}$$

This is invariant under renormalization. By using the definition of the partition function, and the fact that $\delta\eta_{ij}$ is diagonal, the Eq. (6.16) can be written as [38]

$$\mathcal{Z}_{T^{ii}(\hat{x})} + H(\hat{x})\,\frac{\delta\mathcal{Z}}{\delta H(x)} = 0, \tag{6.17}$$

where $\mathcal{Z}_{T^{ii}(\hat{x})}$ denotes the generating functional of correlation functions with a $T^{ii}(\hat{x})$ operator insertions, i.e., generating functional of $\langle T^{ii}(\hat{x})\,\Omega(\hat{y})\,\Omega(\hat{z})\cdots\rangle$ etc. In comparison, recall that $\mathcal{Z}$ is the generating function of correlations $\langle\Omega(\hat{y})\,\Omega(\hat{z})\cdots\rangle$ etc. On performing a Legendre transformation between the conjugate field $H(\hat{x})$ and the order parameter expectation value $M(\hat{x})$, we can express the above equation in terms of the effective free energy (i.e., the generating functional of *connected* correlations) Γ, which was introduced in Chapter 4,

$$\Gamma_{T^{ii}(\hat{x})} + \frac{\delta\,\Gamma}{\delta M(\hat{x})}\,M(\hat{x}) = 0, \tag{6.18}$$

where $\Gamma_{T^{ii}}(\hat{x})$ is the generating functional of connected correlations with $T^{ii}(\hat{x})$ operator insertion, and $M(\hat{x}) \equiv \langle\Omega(\hat{x})\rangle_H$, i.e., the expectation value of the order parameter in the presence of the field $H(\hat{x})$; see chapter 4. Note that Eq. (6.18) is meaningful in both the solid and the liquid state; in the liquid state the field $H(\hat{x})$ is responsible for a non-vanishing $M(\hat{x})$, whereas in the solid state

$M(\hat{x})$ is the spontaneously-generated order parameter expectation value in the $H(\hat{x}) \to 0$ limit.

The Eq. (6.18) implies that the insertion of the stress-energy operator in any vertex function is finite; the renormalized stress-energy tensor does not acquire an anomalous dimension. This can also be deduced from the Eq. (6.18) by applying the expansion of the effective free energy Γ in terms of the vertex functions Γ^N given by Eq. (4.2), and the scaling of the vertex functions given by Eq. (4.25). For example, the lowest order term in the expansion of $\Gamma_{T^{ii}(\hat{x})}$ is $\Gamma^1_{T^{ii}(\hat{x})}\, M(\hat{x})$, and of $\frac{\delta \Gamma}{\delta M(\hat{x})}\, M(\hat{x})$ is $\Gamma^1(\hat{x})\, M(\hat{x})$; implying $\Gamma^1_{T^{ii}(\hat{x})} = \Gamma^1(\hat{x})$. Therefore, our conclusion is that the *stress-energy tensor, and hence the shear-modulus in V/G theory, do not acquire an anomalous dimension under renormalization.* Therefore, naïve scaling argument will suffice to determine the scaling of shear modulus. To this effect, recall that the elastic free energy density for shear deformations, at lowest order in the displacements $\mathbf{u}(\mathbf{x})$, can be written as

$$f_{el} \approx \mu \int d\mathbf{x}\, (\nabla \mathbf{u}(\mathbf{x}))^2 \tag{6.19}$$

The gradient of the displacements is obviously scale invariant. The free energy density should be scale invariant. Therefore, the shear modulus should scale as the inverse of the volume of integration in the expression above. The question arises, *what is this volume*? As we are interested in the critical behavior, the system is being probed at all length-scales up to the correlation length-scale, beyond which critical fluctuations can be ignored and mean-field theory gives the correct scaling. Therefore, the volume of integration should be $\xi^D_{\rm perc}$, the only diverging length scale in the problem. Therefore, $\mu \sim \xi^{-D}_{\rm perc} = |\tau|^{D\nu}$, implying that $f = D\nu$ which is consistent with the Daoud-Coniglio conjecture.

We conclude from this section that the shear modulus scaling determined from the old V/G theory is in accord with with Daoud-Coniglio conjecture, and that if the controversy over the value of the exponent f is to be resolved, the theory would have to be generalized. In the next section, we resume our mission of resolving the controversy over the value of shear modulus exponent by utilizing the generalized Landau theory introduced in Chapter 5.

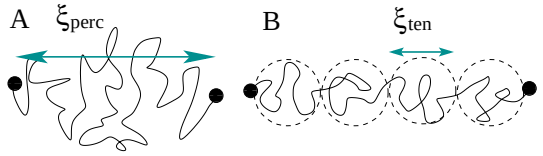

Figure 6.1: The infinite cluster is a network of effective chains: (A) In a dense melt each effective chain is one single thermal blob with typical size $\xi_{\rm perc}$, and contributes $k_{\rm B}T$ to the shear rigidity. (B) In a phantom network each chain is sequence of "tension blobs" (dashed circles), each of size $\xi_{\rm ten}$. Each tension blob contributes $k_{\rm B}T$ to the shear rigidity.

6.4 Resolution of controversy over shear modulus exponent

This section is divided into two parts. In the first part I present heuristic reasoning to outline the physical arguments that emerge from a RG calculation discussed in the second part.

6.4.1 Heuristic reasoning

Let us first consider gelation in a dense system with strong inter-particle repulsions, and let the system be near the critical point. Then the characteristic length-scale for density fluctuations $\xi_{\rm den}$ is much smaller than the percolation correlation length $\xi_{\rm perc}$ (beyond which the infinite cluster is effectively homogeneous). Now let again invoke the "nodes-links-blobs" picture [57, 60], in which the incipient infinite cluster is a network of effective chains, connected to one another at effective vertices, called nodes. For our purposes, it is adequate to treat the effective chains as quasi-one-dimensional objects having some average thickness. The end-to-end displacement of these effective chains has a certain distribution with a characteristic length-scale, which is presumably identical to the percolation correlation length $\xi_{\rm perc}$. In the absence of external stress, we expect these chains to exhibit a type of random walk [61], owing to thermal fluctuations. Therefore, the end-to-end displacements should scale *sub-linearly* with the contour length. In the language of polymer physics, *every effective chain constitutes a single "thermal blob"*; see Fig. 6.1 and Ref. [8]. Under a small shear deformation, each chain will be slightly stretched or compressed, thus contributing $k_{\rm B}T$ to the shear modulus. As there are roughly $\xi_{\rm perc}^{-d}$ effective chains per unit volume, the shear modulus should scale as $k_{\rm B}T\xi_{\rm perc}^{-d} \sim |\tau|^{d\nu}$, near the critical point. We note that the shear modulus has dimensions of energy per unit volume; hence, this scaling is also mandated by dimensional analysis, provided that $\xi_{\rm perc}$ is the only important length-scale near the transition.

Let us now consider typical numerical simulations of phantom networks, i.e., systems without inter-particle repulsions. The crucial observation, made above, that the equilibrium conformations of the effective chains are unstretched random walks (i.e. "thermal blobs") with typical size $\xi_{\rm perc}$ now breaks down, for the following reason. In such simulations, the sol fraction (i.e. the finite clusters) are usually removed completely, as they do not interact with the gel fraction. The resulting gel is very sparse, and would tend to collapse so as to maximize the entropy. To prevent this, the system size is usually fixed during shear deformation. Consequently, long effective chains are *strongly stretched*. The conformation of the infinite cluster is such that the net *entropic* force at each node vanishes, i.e., the cluster is *statistically* in mechanical equilibrium. Therefore, the mean tension S carried by each chain has the same order of magnitude. As shown Fig. 6.1B, S defines a length-scale, $\xi_{\rm ten} \equiv k_{\rm B}T/S$, beyond which chain conformations are dominated by tension, and are thus effectively straight. By contrast, within $\xi_{\rm ten}$ thermal fluctuations dominate, so that chain conformations are random walks. $\xi_{\rm ten}$ is, by definition, the typical size of a "tension blob" [62] for a polymer under tension S. Near the critical point, $\xi_{\rm ten}$ is much smaller than $\xi_{\rm perc}$, which diverges as $|r|^{-\nu}$. It follows that the number of tension blobs on each chain, as well as the chain's end-to-end displacement, scales *linearly* with its contour length in a phantom network. Under a shear deformation, every tension blob contributes $k_{\rm B}T$ to the overall shear rigidity [62]. Therefore, a typical chain, comprising many tension blobs, contributes a term to the total shear rigidity that is *proportional to its contour length*. This should be contrasted with the case of melt, in which every chain contributes k_BT, *independent of its contour length*. In a coarse-grained description, we may replace every tension blob by a *mechanical* spring of natural length zero and force constant $k_{\rm B}T/\xi_{\rm ten}^2$, without changing the elasticity. The resulting model is a randomly diluted network of *mechanical* springs of zero natural length *at zero temperature*, which can be mapped into the randomly diluted resistance network model [63]. As we have discussed earlier, in this mapping the coordinates of nodes are mapped into voltages, and the shear modulus into the conductivity. Therefore the shear modulus of a randomly diluted entropic phantom network is equivalent to the conductivity of a random resistor network, as de Gennes conjectured and many numerical simulations have supported.

6.4.2 Analytical reasoning

In Subsection 5.5.1 we have extended the Landau theory for V/G transition to the case of tunable repulsive interactions. At this point the reader is encouraged to revisit that section. For the sake of clarity of presentation, I reproduce here the generalized Landau effective Hamiltonian [given by Eq. (5.26)]:

$$\begin{aligned}
\mathcal{H}_{VG}[\Omega] &= \mathcal{H}_X + \mathcal{H}_D \\
\mathcal{H}_X &= \int d\hat{x} \left\{ \frac{K_0}{2} (\nabla^0 \Omega)^2 + \frac{K}{2} \sum_{\alpha=1}^{n} (\nabla^\alpha \Omega)^2 + \frac{\tau}{2} \Omega^2 - \frac{v}{3!} \Omega^3 \right\}, \qquad (6.20a) \\
\mathcal{H}_D &= \frac{B_0}{2} \int d\mathbf{x}^0 \, \Omega_0(\mathbf{x}^0)^2 + \frac{B}{2} \sum_{\alpha=1}^{n} \int d\mathbf{x}^\alpha \, \Omega_\alpha(\mathbf{x}^\alpha)^2, \qquad (6.20b)
\end{aligned}$$

where we have used v, instead of g, to denote the coupling constant for the cubic term. Recall that ∇^0 and ∇^α are, respectively, derivatives with respect to $\mathbf{x}^0$ and $\mathbf{x}^\alpha$ and that the non-negative parameters B_0 and B are, respectively, the compressibility of the system in the preparation and the measurement states. Therefore, Eq. (6.20b) defines the free-energy cost for density fluctuations. The fields $\Omega_\alpha(\mathbf{x}^\alpha)$ are the LRS part of the order parameter, defined in Eq. (5.25), and they describe density fluctuations in the system. We remind the reader that a large value of B_0 would ensure that the system is cross-linked in a state with almost uniform density profile, i.e., vanishingly small fluctuations in Ω_0. On the other hand, B characterizes the repulsive interactions between particles in the measurement state. In a typical vulcanization experiment on a concentrated solution or melt, both B_0 and B are large, so that the density remains essentially uniform across the transition. It is important, however, to realize that B_0 and B are separately adjustable (as are K_0 and K), e.g., via tuning the solvent quality before and after crosslinking. For gelation, the network formation process commonly lasts for an extended period. As a result, B may differ from B_0, even by a large factor (e.g. due to correlations built up during the course of the chemical reaction), even if all external physical conditions remain unchanged.

In strong contrast, in typical numerical simulations of phantom systems, all polymers (or particles) are ascribed to lattice sites, and then crosslinks are randomly introduced, connecting some neighboring particles. After removing the sol part, the system is allowed to relax at nonzero temperature, with intra-cluster repulsion completely ignored. This corresponds to a large positive value

for B_0 but a *vanishing* value of B. As we shall soon see, it is this *qualitative* difference between B_0 and B that is responsible for conductivity-like scaling of the shear modulus in phantom networks.

To study the elastic properties, we consider deforming the system *after* cross-links have been introduced (revisit the discussion in Subsection 5.5.2). As shown in Fig. 5.1, this amounts to making an affine change $\underline{\underline{\Lambda}}$ of the boundaries for measurement replicas (1 through n), leaving the preparation replica intact. Reiterating discussion presented in Section 5.5.2, this change of boundaries is equivalent to making the linear coordinate transformation

$$\mathbf{R}^\alpha \to \underline{\underline{\Lambda}} \cdot \mathbf{R}^\alpha, \quad \mathbf{x}^\alpha \to \underline{\underline{\Lambda}} \cdot \mathbf{x}^\alpha, \quad \text{for } 1 \leq \alpha \leq n, \tag{6.21}$$

which restores the original boundary conditions for the n measurement replicas. Under this transformation, $\mathcal{H}_D$ of Eq. (6.20b) is unchanged, provided we redefine B appropriately. As for $\mathcal{H}_X$, Eq. (6.20a), we find that all terms are invariant under the transformation (in the $n \to 0$ limit), except for the gradient term with coefficient K, which becomes

$$\frac{K}{2} \sum_{\alpha=1}^{n} (\nabla^\alpha \Omega)^2 \longrightarrow \frac{K}{2} \sum_{d,d'=1}^{D} g^{-1}_{dd'} \sum_{\alpha=1}^{n} \nabla^\alpha_d \Omega \, \nabla^\alpha_{d'} \Omega \,, \tag{6.22}$$

where $\mathbf{g}$ is the metric tensor defined in Eq. (6.1).

An RG analysis of the full model, described by $\mathcal{H}_{VG}[\Omega]$, is not presented here. We shall only present results for two limiting cases: (a) $B_0 = B = +\infty$, i.e., vulcanization in an incompressible polymer melt; and (b) $B_0 = +\infty$ but $B = 0$, i.e., phantom networks. We apply a momentum-shell RG transformation (see ref. [34] for earlier work), thus integrating out short length-scale fluctuations recursively, whilst rescaling the order-parameter field Ω and spatial coordinates such that K_0 and K remain unity. The renormalizations of r and v turn out to be independent of B and $\mathbf{g}$, i.e., the parameters describing the measurement ensemble. To one-loop order we find:

$$\frac{d\tau}{dl} = \tau \left(2 + \frac{1}{6} v^2\right) + \frac{v^2}{2}, \qquad \frac{dv}{dl} = \frac{1}{2} \epsilon \, v - \frac{7}{4} v^3, \tag{6.23}$$

where $\epsilon \equiv 6 - d$. For $d < 6$ there is a nontrivial fixed point at $(\tau^*, v^{*2}) = (\epsilon/14, 2\epsilon/7)$. Correspondingly, the critical exponents (η, ν) are given by $(-\frac{1}{21}\epsilon, \frac{1}{2} + \frac{5}{84}\epsilon)$, which agree with results from the

the ϵ expansion for the percolation transition [65], [58].

The flow of $\mathbf{g}$ determines the elastic properties. Expressing $\mathbf{g}$ as $g\tilde{\mathbf{g}}$, where $\tilde{\mathbf{g}}$ has unit determinant [so that $g^d = \det(\mathbf{g})$] we find that, regardless of the value of B, $\tilde{\mathbf{g}}$ does not flow. Therefore, renormalization of the metric $\mathbf{g}$ is completely controlled by its determinant. For $B = B_0 = +\infty$, we find the flow equation

$$\frac{dg}{dl} = \frac{2}{3}v^2\left(1 - g^3\right)g. \tag{6.24}$$

For $d < 6$, $v^2 \to v^{*2} = 2\epsilon/7 > 0$, and hence g flows to unity. Qualitatively, this implies a symmetry between the preparation and and measurement ensembles. It also suggests that the correlation length $\xi_{\rm perc}$ is the only relevant length-scale, in agreement with the preceding heuristic argument that, in a dense melt, each effective chain constitutes a single thermal blob of typical size $\xi_{\rm perc}$. Near the fixed point, the singular part of the free energy (i.e. the elastic free energy) has the scaling form

$$f_{\rm s} = |\tau|^{d\nu}\,\psi_1(\mathbf{g}^*) = |\tau|^{d\nu}\psi_1(\tilde{\mathbf{g}}). \tag{6.25}$$

As the shear modulus is given by an appropriate derivative of $f_{\rm s}$ with respect to $\mathbf{g}$ [cf. Eq. (6.1)], we immediately see that it scales as $|\tau|^{d\nu}$.

Now consider the second case, viz., $(B_0, B) = (+\infty, 0)$, for which we find

$$\frac{dg}{dl} = \frac{2}{3}v^2 g \longrightarrow \frac{4}{21}\epsilon\, g. \tag{6.26}$$

Now g, and also the metric tensor $\mathbf{g}$, are *relevant* near the percolation fixed point, with a positive crossover exponent ϕ_g of $4\epsilon/21$, echoing our heuristic argument that effective chains are strongly stretched in a phantom network. In general, the singular part of free energy should then have the scaling form

$$f_{\rm s} = |\tau|^{d\nu}\,\psi_2(\mathbf{g}/|\tau|^{\phi_g}). \tag{6.27}$$

For a pure shear with $\det(\mathbf{g}) \equiv 1$, this f_s must agree with Eq. (6.1), up to a constant independent of $\mathbf{g}$. Therefore the shear-modulus exponent is given by $d\nu - \phi_g = 3 - \frac{5}{21}\epsilon$, which, to the same order in ϵ, is identical to the conductivity exponent of a random resistor network [65].

This equivalence between critical exponents of phantom elastic networks and random resistor

networks should in fact hold to all orders in ϵ. To see this analytically, we note that setting $(B_0, B) = (\infty, 0)$ in H_D is equivalent to setting $B_0 = B = 0$, *together with the hard constraint* $\Omega^0(\mathbf{x}) \equiv 0$, which explicitly excludes configurations having nonzero density fluctuations in the preparation ensemble. The resulting model then becomes formally identical to the Harris-Lubensky formulation of the random resistor network problem [65], with the nd ($\to 0$) coordinates associated with the measurement ensembles $(\mathbf{x}^1, \ldots, \mathbf{x}^n)$ mapped onto the D ($\to 0$) replicated voltages ϑ, provided the stated limits are taken. Thus, the pair of systems are governed by identical RG equations and, hence, critical exponents.

Having established the two limiting cases, $B = \infty$ and $B = 0$, it is natural to ask which one is the more stable. As B, like τ, has naïve dimension 2, it is always relevant near 6 dimensions. Therefore, if we keep B_0 large and tune B to be small, the shear modulus exponent should cross over—from the conductivity one, t, to the incompressible system one, $d\nu$—when $|\tau|$ becomes smaller than B. This should be readily realizable in a numerical simulation, if one were to retain the sol part of the system and turn on a small repulsion. In principle, this cross-over might also be observed in gelation experiments on non-dense solutions, provided $|\tau|$ is sufficiently small.

6.5 Conclusions

In this chapter we have introduced the reader to the controversy over the value of shear modulus exponent in random solids based on two different conjectures. We have presented a short overview on the physical motivation behind the two conjectures and the arguments supporting them. We have used a generalized version of the Landau theory for V/G transition to tune the strength of repulsive interaction in the system, and have argued, based on a renormalization group calculation, that in two different limiting cases the two distinct conjectured values of shear modulus are obtained. Our analysis is valid above the lower critical dimension of two, and below the upper critical dimension of six, for the V/G transition. Future work is focussed on understanding the crossover regime by implementing the RG scheme for all values of the parameters controlling the repulsive interaction in the preparation and the measurement ensemble.

Appendix A

From Landau-Wilson Hamiltonian to elastic free energy

In this appendix we show how to get from the Landau-Wilson effective Hamiltonian $\mathcal{H}_\Omega$, Eq. (3.21), to the elastic free energy (3.22b). Specifically, we compute the increase $\mathcal{H}_u$ in $\mathcal{H}_\Omega$ when the classical value $\Omega_{\rm cl}$, Eqs. (3.3) and (3.4), is replaced by Goldstone-distorted classical state (3.9a), parametrized by $u_\perp(\mathbf{x})$. There are three terms in (3.21) to be computed. Two are "potential" terms, which we shall see to have no dependence on $u_\perp(\mathbf{x})$; the third is a "gradient" term, and this is the origin of the dependence of $\mathcal{H}_u$ on $u_\perp(\mathbf{x})$.

Before focusing on any individual terms, we note that we can express summations over higher-replica sector wave vectors as unrestricted summations, less lower-replica sector contributions; e.g.,

$$\sum_{k\in\mathrm{HRS}} = \sum_{k} - \sum_{k\in\mathrm{1RS}} - \sum_{k\in\mathrm{0RS}} . \tag{A.1}$$

Here, the two components of the lower-replica sector, viz., the one- and zero-replica sectors, are respectively denoted 1RS and 0RS.

Applying this sector decomposition to the first term in Eq. (3.21), and recognizing that there is no contribution from the one-replica sector and that the zero-replica sector contribution is simple, we have

$$\sum_{k\in\mathrm{HRS}} |\Omega(k)|^2 = \left(\sum_{k} - \sum_{k\in\mathrm{1RS}} - \sum_{k\in\mathrm{0RS}}\right) |\Omega(k)|^2 = \sum_{k} |\Omega(k)|^2 - 0 - Q^2. \tag{A.2}$$

Recall that we are concerned with the increase in $\mathcal{H}_\Omega$ due to the Goldstone distortion. Evidently, of the contributions considered so far only the unrestricted sum has the possibility of being sensitive

to the distortion. However, as we shall now see, not even this contribution has such sensitivity:

$$\begin{aligned}
\frac{1}{V^n}\sum_k |\Omega(k)|^2 &= V\int đk_\parallel đk_\perp \int \frac{d\mathbf{x}_1}{V}\frac{d\mathbf{x}_2}{V}\, e^{-i\mathbf{k}_{\rm tot}\cdot\mathbf{x}_1 + i\mathbf{k}_{\rm tot}\cdot\mathbf{x}_2} e^{-ik_\perp\cdot u_\perp(\mathbf{x}_1)+ik_\perp\cdot u_\perp(\mathbf{x}_2)}\,\mathcal{W}(k_\perp)^2 \\
&= V\int \frac{d\mathbf{x}_1}{V}\frac{d\mathbf{x}_2}{V}\int đk_\perp\,\mathcal{W}(k_\perp)^2\, e^{-ik_\perp\cdot(u_\perp(\mathbf{x}_1)-u_\perp(\mathbf{x}_2))}\int đk_\parallel\, e^{-i\mathbf{k}_{\rm tot}\cdot(\mathbf{x}_1-\mathbf{x}_2)} \\
&= V\int \frac{d\mathbf{x}_1}{V}\frac{d\mathbf{x}_2}{V}\int đk_\perp\,\mathcal{W}(k_\perp)^2\, e^{-ik_\perp\cdot(u_\perp(\mathbf{x}_1)-u_\perp(\mathbf{x}_2))}(1+n)^{-\frac{D}{2}}\,\delta(\mathbf{x}_1-\mathbf{x}_2) \\
&= (1+n)^{-\frac{D}{2}}\int đk_\perp\,\mathcal{W}(k_\perp)^2, \qquad \text{(A.3)}
\end{aligned}$$

independent of $u_\perp(\mathbf{x})$. Note that here and elsewhere in the present Appendix we shall anticipate the taking of the replica limit by omitting factors of V^n.

Turning to the third term in (3.21), the nonlinearity, and handling the constraints on the summation with care, we are faced with the term

$$\begin{aligned}
V\sum_{k_1,k_2,k_3}\delta_{k_1+k_2+k_3,0}\;\Omega(k_1)\,\Omega(k_2)\,\Omega(k_3) &= \int đk_1 đk_2 đk_3\int dy\, e^{-iy\cdot(k_1+k_2+k_3)} \\
&\quad\times\int d\mathbf{x}_1\,d\mathbf{x}_2\,d\mathbf{x}_3\, e^{i\mathbf{k}_{1\rm tot}\cdot\mathbf{x}_1+i\mathbf{k}_{2\rm tot}\cdot\mathbf{x}_2+i\mathbf{k}_{3\rm tot}\cdot\mathbf{x}_3} e^{ik_{1\perp}\cdot u_\perp(\mathbf{x}_1)+ik_{2\perp}\cdot u_\perp(\mathbf{x}_2)+ik_{3\perp}\cdot u_\perp(\mathbf{x}_3)} \\
&\quad\times\mathcal{W}(k_{1\perp})\,\mathcal{W}(k_{2\perp})\,\mathcal{W}(k_{3\perp}) \\
&= \int đk_{1\parallel} đk_{2\parallel} đk_{3\parallel}\int \frac{dy_\parallel}{V} e^{-iy_\parallel\cdot(k_{1\parallel}+k_{2\parallel}+k_{3\parallel})}\int đk_{1\perp} đk_{2\perp} đk_{3\perp}\int dy_\perp e^{-iy_\perp\cdot(k_{1\perp}+k_{2\perp}+k_{3\perp})} \\
&\quad\times\int d\mathbf{x}_1\,d\mathbf{x}_2\,d\mathbf{x}_3\, e^{i\mathbf{k}_{1\rm tot}\cdot\mathbf{x}_1+i\mathbf{k}_{2\rm tot}\cdot\mathbf{x}_2+i\mathbf{k}_{3\rm tot}\cdot\mathbf{x}_3} e^{ik_{1\perp}\cdot u_\perp(\mathbf{x}_1)+ik_{2\perp}\cdot u_\perp(\mathbf{x}_2)+ik_{3\perp}\cdot u_\perp(\mathbf{x}_3)} \\
&\quad\times\mathcal{W}(k_{1\perp})\,\mathcal{W}(k_{2\perp})\,\mathcal{W}(k_{3\perp}) \\
&= (1+n)^D\int đ\mathbf{k}_1 đ\mathbf{k}_2 đ\mathbf{k}_3\int \frac{d\mathbf{y}}{V}\, e^{-i\mathbf{y}\cdot(\mathbf{k}_1+\mathbf{k}_2+\mathbf{k}_3)}\int đk_{1\perp} đk_{2\perp} đk_{3\perp}\int dy_\perp\, e^{-iy_\perp\cdot(k_{1\perp}+k_{2\perp}+k_{3\perp})} \\
&\quad\times\int d\mathbf{x}_1\,d\mathbf{x}_2\,d\mathbf{x}_3\, e^{i\mathbf{k}_1\cdot\mathbf{x}_1+i\mathbf{k}_2\cdot\mathbf{x}_2+i\mathbf{k}_3\cdot\mathbf{x}_3} e^{ik_{1\perp}\cdot u_\perp(\mathbf{x}_1)+ik_{2\perp}\cdot u_\perp(\mathbf{x}_2)+ik_{3\perp}\cdot u_\perp(\mathbf{x}_3)} \\
&\quad\times\mathcal{W}(k_{1\perp})\,\mathcal{W}(k_{2\perp})\,\mathcal{W}(k_{3\perp}) \\
&= (1+n)^D\int đk_{1\perp} đk_{2\perp} đk_{3\perp}\;\delta_{k_{1\perp}+k_{2\perp}+k_{3\perp},0}\int\frac{d\mathbf{y}}{V}\int d\mathbf{x}_1\,d\mathbf{x}_2\,d\mathbf{x}_3\;\delta(\mathbf{x}_1-\mathbf{y})\,\delta(\mathbf{x}_2-\mathbf{y})\,\delta(\mathbf{x}_3-\mathbf{y}) \\
&\quad\times e^{ik_{1\perp}\cdot u_\perp(\mathbf{x}_1)+ik_{2\perp}\cdot u_\perp(\mathbf{x}_2)+ik_{3\perp}\cdot u_\perp(\mathbf{x}_3)}\,\mathcal{W}(k_{1\perp})\,\mathcal{W}(k_{2\perp})\,\mathcal{W}(k_{3\perp}) \\
&= (1+n)^D\int đk_{1\perp} đk_{2\perp} đk_{3\perp}\;\delta_{k_{1\perp}+k_{2\perp}+k_{3\perp},0}\int\frac{d\mathbf{y}}{V}\, e^{i(k_{1\perp}+k_{2\perp}+k_{3\perp})\cdot u_\perp(\mathbf{y})}\,\mathcal{W}(k_{1\perp})\,\mathcal{W}(k_{2\perp})\,\mathcal{W}(k_{3\perp}) \\
&= (1+n)^D\int đk_{1\perp} đk_{2\perp} đk_{3\perp}\;\delta_{k_{1\perp}+k_{2\perp}+k_{3\perp},0}\,\mathcal{W}(k_{1\perp})\,\mathcal{W}(k_{2\perp})\,\mathcal{W}(k_{3\perp}). \qquad \text{(A.4)}
\end{aligned}$$

This is independent of $u_\perp(\mathbf{x})$.

Turning to the second term in (3.21), the gradient term, we have

$$\begin{aligned}\frac{1}{V^n}\sum_k k\cdot k\,|\,\Omega(k)|^2 &= V\int đk_\parallel\, đk_\perp\,\left(k_\parallel\cdot k_\parallel + k_\perp\cdot k_\perp\right)\\ &\times\int \frac{d\mathbf{x}_1}{V}\frac{d\mathbf{x}_2}{V}\, e^{-i\mathbf{k}_{\rm tot}\cdot\mathbf{x}_1+i\mathbf{k}_{\rm tot}\cdot\mathbf{x}_2}\\ &\times e^{-ik_\perp\cdot u_\perp(\mathbf{x}_1)+ik_\perp\cdot u_\perp(\mathbf{x}_2)}\,\mathcal{W}(k_\perp)^2. \end{aligned}\tag{A.5}$$

Of the two contributions arising from this term, from $k_\parallel^2$ and from $k_\perp^2$, the latter has no $u_\perp(\mathbf{x})$ dependence. This follows via the mechanism that we saw for the first term, viz., the development of a factor of $\delta(\mathbf{x}_1-\mathbf{x}_2)$. As for the former contribution, to evaluate it we replace $k_\parallel\cdot k_\parallel$ by $(1+n)^{-1}\mathbf{k}_{\rm tot}\cdot\mathbf{k}_{\rm tot}$ and generate this factor via suitable derivatives:

$$\begin{aligned}\frac{1}{V^n}\sum_k k\cdot k\,|\Omega(k)|^2 &= V\int đk_\parallel\, đk_\perp\, k_\parallel\cdot k_\parallel\\ &\times\int \frac{d\mathbf{x}_1}{V}\frac{d\mathbf{x}_2}{V}\, e^{-i\mathbf{k}_{\rm tot}\cdot\mathbf{x}_1+i\mathbf{k}_{\rm tot}\cdot\mathbf{x}_2}\\ &\times e^{-ik_\perp\cdot u_\perp(\mathbf{x}_1)+ik_\perp\cdot u_\perp(\mathbf{x}_2)}\,\mathcal{W}(k_\perp)^2\\ &= (1+n)^{-D/2}(1+n)^{-1}V\int đk_\perp\, đ\mathbf{k}_{\rm tot}\\ &\times\int \frac{d\mathbf{x}_1}{V}\frac{d\mathbf{x}_2}{V}\,\left(\partial_{-i\mathbf{x}_1}e^{-i\mathbf{k}_{\rm tot}\cdot\mathbf{x}_1}\right)\cdot\left(\partial_{i\mathbf{x}_2}e^{i\mathbf{k}_{\rm tot}\cdot\mathbf{x}_2}\right)\\ &\times e^{-ik_\perp\cdot u_\perp(\mathbf{x}_1)}\,e^{ik_\perp\cdot u_\perp(\mathbf{x}_2)}\,\mathcal{W}(k_\perp)^2. \end{aligned}\tag{A.6}$$

Next, we integrate by parts, once with respect to $\mathbf{x}_1$ and once with respect to $\mathbf{x}_2$, to transfer the derivatives to the exponential factors containing $u_\perp$, arriving at

$$\begin{aligned}&(1+n)^{-1-D/2}V\int \frac{d\mathbf{x}_1}{V}\frac{d\mathbf{x}_2}{V}\\ &\times\int đ\mathbf{k}_{\rm tot}\; e^{-i\mathbf{k}_{\rm tot}\cdot(\mathbf{x}_1-\mathbf{x}_2)}\int đk_\perp\,\mathcal{W}(k_\perp)^2\\ &\times\left(\partial_{-i\mathbf{x}_1}e^{-ik_\perp\cdot u_\perp(\mathbf{x}_1)}\right)\cdot\left(\partial_{i\mathbf{x}_2}e^{ik_\perp\cdot u_\perp(\mathbf{x}_2)}\right). \end{aligned}\tag{A.7}$$

Powers of $k_\parallel$ higher than two would, via the corresponding derivatives, produce higher gradients of $u_\perp$, as well as nonlinearities involving lower-order derivatives. By performing the derivatives that

we have here, as well as the $\mathbf{k}_{\rm tot}$ integration, which generates a factor $\delta(\mathbf{x}_1 - \mathbf{x}_2)$ and allows us to integrate over, say, $\mathbf{x}_2$, we obtain

$$(1+n)^{-1-D/2} V^{-1} \int đk_\perp \, \mathcal{W}(k_\perp)^2 \\ \times \int d\mathbf{x} \, (k_\perp \cdot \partial_{\mathbf{x}} u_\perp(\mathbf{x})) \cdot (k_\perp \cdot \partial_{\mathbf{x}} u_\perp(\mathbf{x})) \,, \tag{A.8}$$

where the scalar products inside the parentheses are over nD-component replica-transverse vectors whilst the outside scalar product is over D-component position vectors. The next step is to observe that, owing to the rotationally invariant form of $\mathcal{W}(k_\perp)$, Eq. (3.4a), the $k_\perp$ integration includes an isotropic average of two components of $k_\perp$, and is therefore proportional to the identity in nD-dimensional replica-transverse space. Thus, we arrive at the form

$$\frac{(1+n)^{-1-D/2}}{nD} \int đk_\perp \, \mathcal{W}(k_\perp)^2 \; k_\perp \cdot k_\perp \\ \times \int \frac{d\mathbf{x}}{V} \, (\partial_{\mathbf{x}} u_\perp(\mathbf{x}) \partial_{\mathbf{x}} u_\perp(\mathbf{x})) \,, \tag{A.9}$$

which involves the two types of scalar product mentioned beneath Eq. (A.8). Reinstating the factor of Vc from Eq. (3.21), we identify the stiffness divided by the temperature) μ_n/T and, hence, arrive at Eqs. (3.22).

Appendix B

Evaluating the shear modulus

In this appendix we display the main steps for obtaining the stiffness μ_0, Eqs. (3.23), by evaluating the formula for μ_n, given in Eq. (3.22b) and derived in App. A, in terms of the elements of the classical state, Eqs. (3.4). This involves the evaluation of the RHS of Eq. (3.22b), which proceeds as follows:

$$
\begin{aligned}
&\int đk_\perp\, k_\perp^2\, \mathcal{W}(k_\perp)^2 \\
&\quad = Q^2 \int đk_\perp\, k_\perp^2 \int_0^\infty d\xi^2\, \mathcal{N}\big(\xi^2\big)\, d\xi'^2\, \mathcal{N}\big(\xi'^2\big)\, e^{-\left(\xi^2+\xi'^2\right)k_\perp^2/2} \\
&\quad = Q^2 \int_0^\infty d\xi^2\, \mathcal{N}\big(\xi^2\big)\, d\xi'^2\, \mathcal{N}\big(\xi'^2\big) \int đk_\perp\, k_\perp^2 e^{-\left(\xi^2+\xi'^2\right)k_\perp^2/2} \\
&\quad = Q^2 \int_0^\infty d\xi^2\, \mathcal{N}\big(\xi^2\big)\, d\xi'^2\, \mathcal{N}\big(\xi'^2\big) \\
&\qquad\qquad \times \partial_{-A/2}\big|_{A=\xi^2+\xi'^2} \int đk_\perp\, e^{-Ak_\perp^2/2} \\
&\quad = Q^2 \int_0^\infty d\xi^2\, \mathcal{N}\big(\xi^2\big)\, d\xi'^2\, \mathcal{N}\big(\xi'^2\big) \\
&\qquad\qquad \times \partial_{-A/2}\big|_{A=\xi^2+\xi'^2} (2\pi A)^{-nD/2} \\
&\quad = Q^2 \int_0^\infty d\xi^2\, \mathcal{N}\big(\xi^2\big)\, d\xi'^2\, \mathcal{N}\big(\xi'^2\big) \\
&\qquad\qquad \times nD(2\pi A)^{-nD/2} A^{-1}\big|_{A=\xi^2+\xi'^2} \\
&\quad \overset{n\to 0}{\approx} nDQ^2 \int_0^\infty d\xi^2\, \mathcal{N}\big(\xi^2\big)\, d\xi'^2\, \mathcal{N}\big(\xi'^2\big)\, \big(\xi^2+\xi'^2\big)^{-1}
\end{aligned}
\tag{B.1}
$$

Appendix C

From the correlator to the distribution

In this appendix we give the technical steps involved in going from the two-field correlator to the distribution $\mathcal{M}$, as discussed in Sec. 3.8.2. Beginning with Eq. (3.64), setting $\mathbf{k}_{2\mathrm{tot}}$ to be $\mathbf{k}_{1\mathrm{tot}}$, and reorganizing, we obtain

$$\begin{aligned} Q^2 \int d\Delta r_{11}\, d\Delta r_{22}\, d\Delta r_{12}\, e^{-\frac{1}{2}\Delta r_{11 d_1 d_2} \sum_{\alpha=0}^{n} k^{\alpha}_{1 d_1} k^{\alpha}_{1 d_2}}\, e^{-\frac{1}{2}\Delta r_{22 d_1 d_2} \sum_{\alpha=0}^{n} k^{\alpha}_{2 d_1} k^{\alpha}_{2 d_2}}\, e^{\Delta r_{12 d_1 d_2} \sum_{\alpha=0}^{n} k^{\alpha}_{1 d_1} k^{\alpha}_{2 d_2}} \\ \times \int d\mathbf{x}\, e^{i\mathbf{k}_{\mathrm{tot}}\cdot\mathbf{x}}\, \mathcal{M}(\mathbf{x}, \Delta r_{11}, \Delta r_{22}, \Delta r_{12}) \;= \widetilde{\mathcal{W}}(k_{1\perp})\, \widetilde{\mathcal{W}}(k_{2\perp}) \\ \times \int \frac{d\mathbf{x}}{V}\, e^{i\mathbf{k}_{1\mathrm{tot}}\cdot\mathbf{x}}\, e^{\frac{T}{\mu_0}\, \mathcal{G}_{d_1 d_2}(\mathbf{x})\, k_{1\perp d_1}\cdot k_{2\perp d_2}} \end{aligned}$$

. (C.1)

Inserting the parameterization (3.65) for $\mathcal{M}$, performing the resulting integrations over Δr_{11}, Δr_{22} and Δr_{12} on the LHS, exchanging factors of $\widetilde{\mathcal{W}}$ for $\widetilde{\mathcal{N}}$ via Eq. (3.31b), canceling factors of Q, and identifying the Fourier transform

$$\mathcal{M}(\mathbf{q}, \xi_1^2, \xi_2^2, \mathbf{y}) \equiv \int d\mathbf{x}\, e^{i\mathbf{q}\cdot\mathbf{x}}\, \mathcal{M}(\mathbf{x}, \xi_1^2, \xi_2^2, \mathbf{y}), \tag{C.2}$$

we arrive at the following equation:

$$\begin{aligned} \int d\xi_1^2\, \widetilde{\mathcal{N}}\left(\xi_1^2\right)\, d\xi_2^2\, \widetilde{\mathcal{N}}\left(\xi_2^2\right)\, d\mathbf{y}\, \mathcal{M}(\mathbf{k}_{1\mathrm{tot}}, \xi_1^2, \xi_2^2, \mathbf{y})\, e^{-\frac{1}{2}\xi_1^2 k_1^2 - \frac{1}{2}\xi_2^2 k_2^2 + \frac{T}{\mu_0}\, \mathcal{G}_{d_1 d_2}(\mathbf{y})\, k_{1 d_1}\cdot k_{2 d_2}} \\ = \int d\xi_1^2\, \widetilde{\mathcal{N}}\left(\xi_1^2\right)\, d\xi_2^2\, \widetilde{\mathcal{N}}\left(\xi_2^2\right)\, e^{-\frac{1}{2}\xi_1^2 k_{1\perp}^2 - \frac{1}{2}\xi_2^2 k_{2\perp}^2} \int d\mathbf{y}\, e^{i\mathbf{k}_{1\mathrm{tot}}\cdot\mathbf{x}}\, e^{\frac{T}{\mu_0}\, \mathcal{G}_{d_1 d_2}(\mathbf{y})\, k_{1\perp d_1}\cdot k_{2\perp d_2}}. \end{aligned} \tag{C.3}$$

In order to clarify the content of this equation, we re-write the wave-vector dependence on the LHS in terms of replica-longitudinal (more precisely, $k_\perp$) and replica-transverse (in fact $\mathbf{k}_{\rm tot}$) components [see Eqs. (3.7,3.8b)], noting that $\mathbf{k}_{1\rm tot} = \mathbf{k}_{2\rm tot}$ and writing $\mathbf{q}$ for each, to obtain

$$\begin{aligned}\int d\xi_1^2\,\widetilde{\mathcal{N}}\left(\xi_1^2\right)\,d\xi_2^2\,\widetilde{\mathcal{N}}\left(\xi_2^2\right)\int d\mathbf{y}\,\mathcal{M}(\mathbf{q},\xi_1^2,\xi_2^2,\mathbf{y})\,e^{-\frac{1}{2}\xi_1^2k_{1\perp}^2-\frac{1}{2}\xi_2^2k_{2\perp}^2+\frac{T}{\mu_0}\,\mathcal{G}_{d_1d_2}(\mathbf{y})\,k_{1\perp d_1}\cdot k_{2\perp d_2}}\\ \times e^{-\frac{\mathbf{q}\cdot\mathbf{q}}{2(1+n)}(\xi_1^2+\xi_2^2)+\frac{T}{\mu_0}\,\mathcal{G}_{d_1d_2}(\mathbf{y})\,q_{d_1}q_{d_2}}\\ =\int d\xi_1^2\,\widetilde{\mathcal{N}}\left(\xi_1^2\right)\,d\xi_2^2\,\widetilde{\mathcal{N}}\left(\xi_2^2\right)\,e^{-\frac{1}{2}\xi_1^2k_{1\perp}^2-\frac{1}{2}\xi_2^2k_{2\perp}^2}\int d\mathbf{y}\,e^{i\mathbf{q}\cdot\mathbf{y}}\,e^{\frac{T}{\mu_0}\,\mathcal{G}_{d_1d_2}(\mathbf{y})\,k_{1\perp d_1}\cdot k_{2\perp d_2}}.\end{aligned}\tag{C.4}$$

Next, we identify Laplace transformations with respect to ξ_1^2 and ξ_2^2, equate the entities being transformed on the LHS and RHS, and take the replica limit, thus arriving at

$$\begin{aligned}e^{-\frac{1}{2}\left(\xi_1^2+\xi_2^2\right)q^2}\int d\mathbf{y}\,\mathcal{M}(\mathbf{q},\xi_1^2,\xi_2^2,\mathbf{y})\,e^{\frac{T}{\mu_0}\,\mathcal{G}_{d_1d_2}(\mathbf{y})\,k_{1\perp d_1}\cdot k_{2\perp d_2}}\,e^{\frac{T}{\mu_0}\,\mathcal{G}_{d_1d_2}(\mathbf{y})\,q_{d_1}q_{d_2}}\\ =\int d\mathbf{y}\,e^{i\mathbf{q}\cdot\mathbf{y}}\,e^{\frac{T}{\mu_0}\,\mathcal{G}_{d_1d_2}(\mathbf{y})\,k_{1\perp d_1}\cdot k_{2\perp d_2}}.\end{aligned}\tag{C.5}$$

The next steps are to move the Gaussian prefactor to the RHS, and to introduce the dummy variable $\mathbf{g}$, which takes on the values held by the second-rank tensor $\mathcal{G}(\mathbf{y})$:

$$\begin{aligned}\int d\mathbf{g}\,e^{\frac{T}{\mu_0}\,\mathbf{g}_{d_1d_2}\,k_{1\perp d_1}\cdot k_{2\perp d_2}}\int d\mathbf{y}\,\delta\big(\mathbf{g}-\mathcal{G}(\mathbf{y})\big)\,\mathcal{M}(\mathbf{q},\xi_1^2,\xi_2^2,\mathbf{y})\,e^{\frac{T}{\mu_0}\,\mathcal{G}_{d_1d_2}(\mathbf{y})\,q_{d_1}q_{d_2}}\\ =\int d\mathbf{g}\,e^{\frac{T}{\mu_0}\,\mathbf{g}_{d_1d_2}\,k_{1\perp d_1}\cdot k_{2\perp d_2}}e^{\frac{1}{2}\left(\xi_1^2+\xi_2^2\right)q^2}\int d\mathbf{y}\,e^{i\mathbf{q}\cdot\mathbf{y}}\,\delta\big(\mathbf{g}-\mathcal{G}(\mathbf{y})\big).\end{aligned}\tag{C.6}$$

Again equating entities being transformed, this time being transformed with respect to $\mathbf{g}$, we find

$$\int d\mathbf{y}\,\delta\big(\mathbf{g}-\mathcal{G}(\mathbf{y})\big)\,\mathcal{M}(\mathbf{q},\xi_1^2,\xi_2^2,\mathbf{y})\;=e^{\frac{1}{2}\left(\xi_1^2+\xi_2^2\right)q^2}\int d\mathbf{y}\,e^{i\mathbf{q}\cdot\mathbf{y}}\,\delta\big(\mathbf{g}-\mathcal{G}(\mathbf{y})\big)\,e^{-\frac{T}{\mu_0}\,\mathcal{G}_{d_1d_2}(\mathbf{y})\,q_{d_1}q_{d_2}}.\tag{C.7}$$

Next, we equate entities being transformed as $\int d\mathbf{y}\,\delta\left(\mathbf{g}-\mathcal{G}(\mathbf{y})\right)\cdots$, thus arriving at the Fourier transform of the reduced distribution:

$$\mathcal{M}(\mathbf{q},\xi_1^2,\xi_2^2,\mathbf{y})=e^{\frac{1}{2}\left(\xi_1^2+\xi_2^2\right)q^2}\,e^{i\mathbf{q}\cdot\mathbf{y}}\,e^{-\frac{T}{\mu_0}\,\mathcal{G}_{d_1d_2}(\mathbf{y})\,q_{d_1}q_{d_2}}.\tag{C.8}$$

Finally, we invert the Fourier transform to arrive at the reduced distribution:

$$\mathcal{M}(\mathbf{x},\xi_1^2,\xi_2^2,\mathbf{y}) = \int đ\mathbf{q}\, e^{-i\mathbf{q}\cdot\mathbf{x}}\, \mathcal{M}(\mathbf{q},\xi_1^2,\xi_2^2,\mathbf{y}) = \int đ\mathbf{q}\, e^{-i\mathbf{q}\cdot(\mathbf{x}-\mathbf{y})}\, e^{\frac{1}{2}(\xi_1^2+\xi_2^2)\mathbf{q}\cdot\mathbf{q}}\, e^{-\frac{T}{\mu_0}\, \mathcal{G}_{d_1 d_2}(\mathbf{y})\, q_{d_1} q_{d_2}}. \tag{C.9}$$

Convergence of this inversion is furnished by the cut-off nature of the $\mathbf{q}$ integration. Inserting this formula into the parameterization (3.65) we arrive at a formula for the full distribution:

$$\begin{aligned}\mathcal{M}(\mathbf{x},\Delta r_{11},\Delta r_{22},\Delta r_{12}) = &\int d\xi_1^2\, \widetilde{\mathcal{N}}\left(\xi_1^2\right)\, d\xi_2^2\, \widetilde{\mathcal{N}}\left(\xi_2^2\right)\, \delta\big(\Delta r_{11} - \xi_1^2 \mathrm{I}\big)\, \delta\big(\Delta r_{22} - \xi_2^2 \mathrm{I}\big) \\ &\times \int \frac{d\mathbf{y}}{V}\, \left\{ \int đ\mathbf{q}\, e^{-i\mathbf{q}\cdot(\mathbf{x}-\mathbf{y})}\, e^{\frac{1}{2}(\xi_1^2+\xi_2^2)q^2}\, e^{-\frac{T}{\mu_0}\, \mathcal{G}_{d_1 d_2}(\mathbf{y})\, q_{d_1} q_{d_2}} \right\} \delta\big(\Delta r_{12} - (T/\mu_0)\, \mathcal{G}(\mathbf{y})\big).\end{aligned} \tag{C.10}$$

Appendix D

Elastic Green function

The elastic Green function $\mathcal{G}_{dd'}(\mathbf{x}-\mathbf{x}')$ featuring in Eq. (3.26a) arises via functional integration over the displacement field $\mathbf{u}(\mathbf{x})$. This integration comprises fields configurations that are (i) volume-preserving (at least to leading order in the gradient of the displacement field), and (ii) have Fourier content only from wave-lengths lying between the short- and long-distance cut-offs $\ell_<$ and $\ell_>$. As the weight in Eq. (3.26a) is Gaussian with respect to $\mathbf{u}(\mathbf{x})$, we have that $(T/\mu_0)\,\mathcal{G}_{dd'}(\mathbf{x}-\mathbf{x}')$ is proportional to the inverse of the operator appearing sandwiched between two displacement fields in the exponent of the Gaussian,

$$\frac{\mu_0}{T}\int_{\mathcal{V}} d\mathbf{x}\,\big(\partial_{\mathbf{x}}\mathbf{u}\cdot\partial_{\mathbf{x}}\mathbf{u}\big), \tag{D.1}$$

provided this inverse is the one associated with the Hilbert space of vector-field configurations contributing to the functional integral. An application of the divergence theorem shows that, in addition to conditions (i) and (ii), the Green function obeys the equation

$$-\nabla_x^2\,\mathcal{G}_{dd'}(\mathbf{x}) = \delta_{dd'}\,\delta(\mathbf{x}), \tag{D.2}$$

in which the delta function is to be interpreted as the identity in the appropriate Hilbert space, mentioned above. To determine $\mathcal{G}_{dd'}(\mathbf{x})$ we express it in its Fourier representation:

$$\mathcal{G}_{dd'}(\mathbf{x}) = \int \bar{d}\mathbf{k}\, e^{-i\mathbf{k}\cdot\mathbf{x}}\,\mathcal{G}_{dd'}(\mathbf{k}). \tag{D.3}$$

Next, we insert this representation into Eq. (D.2) to obtain

$$-\nabla_x^2 \int đ\mathbf{k}\, e^{-i\mathbf{k}\cdot\mathbf{x}}\, \mathcal{G}_{dd'}(\mathbf{k}) = \int đ\mathbf{k}\, k^2 e^{-i\mathbf{k}\cdot\mathbf{x}}\, \mathcal{G}_{dd'}(\mathbf{k})$$
$$= \int_{2\pi/\ell_>}^{2\pi/\ell_<} đ\mathbf{k}\, e^{-i\mathbf{k}\cdot\mathbf{x}} \big(\delta_{dd'} - k^{-2}\, k_d\, k_{d'}\big). \tag{D.4}$$

where $\ell\!\!\!^{-}_< \equiv \ell_</2\pi$ and $\ell\!\!\!^{-}_> \equiv \ell_>/2\pi$. The final term, the integral representation of the appropriate delta function, accommodates restrictions (i) and (ii). Then, from the linear independence of the plane waves, we see that the Fourier integral representation of the Green function is given by Eq. (D.3), with the amplitude given by

$$\mathcal{G}_{dd'}(\mathbf{k}) = \begin{cases} \big(k^2\, \delta_{dd'} - k_d\, k_{d'}\big)/k^4, & \text{for } \ell\!\!\!^{-1}_> < k < \ell\!\!\!^{-1}_<; \\ 0, & \text{otherwise;} \end{cases} \tag{D.5}$$

as given in Eq. (3.26b).

Before computing the real-space form of this D-dimensional Green function, we evaluate it at argument $\mathbf{x} = \mathbf{0}$, as well as at small argument ($|\mathbf{x}| \ll \ell_<$). At $\mathbf{x} = \mathbf{0}$ we have

$$\mathcal{G}_{dd'}(\mathbf{x})|_{\mathbf{x}=\mathbf{0}} = \int_{\text{h.c.o.}} đ\mathbf{k}\, \big(k^2\, \delta_{dd'} - k_d\, k_{d'}\big)\, k^{-4} \tag{D.6a}$$
$$= \delta_{dd'} \frac{D-1}{D} \int_{\text{h.c.o.}} đ\mathbf{k}\, k^{-2} \tag{D.6b}$$
$$= \delta_{dd'}\, \Gamma_D\,, \tag{D.6c}$$
$$\Gamma_D \equiv \frac{D-1}{D} \frac{\Sigma_D}{(2\pi)^D} \int_{\ell\!\!\!^{-1}_>}^{\ell\!\!\!^{-1}_<} dk\, k^{D-3}. \tag{D.6d}$$

Here and elsewhere, the subscript h.c.o. indicates that the integration is subject to the hard cut-off shown explicitly in Eq. (D.6d). Evaluating the last integral for $D \geq 2$, and for $D > 2$ retaining only the dominant contribution, gives Γ_D, as given in Eq. (3.32).

Now generalizing to $|\mathbf{x}|$ small but nonzero, i.e., $|\mathbf{x}| \ll \ell_<$, we have, by expanding the exponential

in Eq. (D.3),

$$\begin{aligned}
\mathcal{G}_{dd'}(\mathbf{x}) &\approx \delta_{dd'}\,\Gamma_D - \frac{1}{2}[(D+1)\delta_{dd'} - 2\hat{x}_d\,\hat{x}_{d'}]\,|\mathbf{x}|^2 \\
&\quad \times \frac{\Sigma_D}{(2\pi)^D}\frac{1}{D(D+2)}\int_{\ell_>^{-1}}^{\ell_<^{-1}} dk\,k^{D-1} \qquad \text{(D.7)} \\
&\approx \delta_{dd'}\,\Gamma_D - \frac{1}{2}[(D+1)\delta_{dd'} - 2\hat{x}_d\,\hat{x}_{d'}]\,|\mathbf{x}|^2 \\
&\quad \times \frac{\Sigma_D}{\ell_<^D}\frac{1}{D^2(D+2)}, \qquad \text{(D.8)}
\end{aligned}$$

where, again, we have retained only the dominant contribution. Specializing to $D = 2$ and $D = 3$ we find

$$\mathcal{G}^{(2)}_{dd'}(\mathbf{x}) \approx \delta_{dd'}\,\Gamma_2 - \frac{1}{64\pi}\frac{|\mathbf{x}|^2}{\ell_<^2}[3\,\delta_{dd'} - 2\hat{x}_d\,\hat{x}_{d'}], \qquad \text{(D.9)}$$

$$\mathcal{G}^{(3)}_{dd'}(\mathbf{x}) \approx \delta_{dd'}\,\Gamma_3 - \frac{1}{45\pi\ell_<}\frac{|\mathbf{x}|^2}{\ell_<^2}[2\,\delta_{dd'} - \hat{x}_d\,\hat{x}_{d'}]. \qquad \text{(D.10)}$$

We now compute the real-space form of this D-dimensional Green function, valid for arbitrary $|\mathbf{x}|$:

$$\begin{aligned}
\mathcal{G}_{dd'}(\mathbf{x}) &= \int đ\mathbf{k}\,e^{-i\mathbf{k}\cdot\mathbf{x}}\,\mathcal{G}_{dd'}(\mathbf{k}) \qquad \text{(D.11)} \\
&= \int_{\text{h.c.o.}} đ\mathbf{k}\,e^{-i\mathbf{k}\cdot\mathbf{x}}\,\left(k^2\,\delta_{dd'} - k_d\,k_{d'}\right)k^{-4} \qquad \text{(D.12)} \\
&= -\left(\delta_{dd'}\nabla^2 - \partial_d\,\partial_{d'}\right)\mathcal{H}(\mathbf{x}), \qquad \text{(D.13)} \\
\mathcal{H}(\mathbf{x}) &\equiv \int_{\text{h.c.o.}} đ\mathbf{k}\,e^{-i\mathbf{k}\cdot\mathbf{x}}\,k^{-4} \qquad \text{(D.14)} \\
&= \int_{\ell_>^{-1}}^{\ell_<^{-1}} đk\,k^{D-1}\int đ^{D-1}\hat{\mathbf{k}}\;\frac{e^{-i\mathbf{k}\cdot\mathbf{x}}}{k^4}. \qquad \text{(D.15)}
\end{aligned}$$

Specializing to the case of $D = 3$, and using spherical polar co-ordinates (k, θ, φ), we have

$$\begin{aligned}
\mathcal{H}^{(3)}(\mathbf{x}) &= (2\pi)^{-3}\int_{\ell_>}^{\ell_<}\frac{dk}{k^2}\int_0^{2\pi}d\varphi\int_0^{\pi}d\theta\,\sin\theta\,e^{-ik|\mathbf{x}|\cos\theta} \\
&= \frac{|\mathbf{x}|}{2\pi^2}\int_{|\mathbf{x}|/\ell_>}^{|\mathbf{x}|/\ell_<}dz\,\frac{\sin z}{z^3}. \qquad \text{(D.16)}
\end{aligned}$$

To control the potential divergence at small z we add and subtract the small-z behavior of $\sin z$,

thus obtaining

$$\mathcal{H}^{(3)}(\mathbf{x}) = \frac{|\mathbf{x}|}{2\pi^2}\int_{|\mathbf{x}|/\ell_>}^{|\mathbf{x}|/\ell_<} dz\,\left(\frac{\sin z - z}{z^3} + \frac{1}{z^2}\right) \tag{D.17}$$

$$= \frac{|\mathbf{x}|}{2\pi^2}\Big(\mathrm{Si}_3(|\mathbf{x}|/\ell_<) - \mathrm{Si}_3(|\mathbf{x}|/\ell_>)\Big) + \frac{\ell_> - \ell_<}{2\pi^2}, \tag{D.18}$$

$$\mathrm{Si}_3(t) \equiv \int_0^t dz\,\frac{\sin z - z}{z^3}, \tag{D.19}$$

where $\mathrm{Si}_3(z)$ is a generalized sine integral, which has asymptotic behavior

$$\mathrm{Si}_3(t) \approx \begin{cases} -t/3!, & \text{for } t \ll 1, \\ -(\pi/4) - t^{-1}, & \text{for } t \gg 1. \end{cases} \tag{D.20}$$

Using this behavior to approximate $\mathcal{H}^{(3)}(\mathbf{x})$ in Eq. (D.18), and inserting the result into Eq. (D.13), noting that the final term vanishes under differentiation, we obtain for $\ell_< \ll |\mathbf{x}| \ll \ell_>$

$$\mathcal{G}^{(3)}_{dd'}(\mathbf{x}) \approx \left(\delta_{dd'}\nabla^2 - \partial_d\,\partial_{d'}\right)\frac{|\mathbf{x}|}{8\pi} \tag{D.21}$$

$$= \frac{1}{8\pi\,|\mathbf{x}|}\left(\delta_{dd'} + \hat{x}_d\,\hat{x}_{d'}\right) \tag{D.22}$$

Now specializing to the case of $D = 2$, and using plane polar co-ordinates (k, φ), we have

$$\mathcal{H}^{(2)}(\mathbf{x}) = (2\pi)^{-2}\int_{\ell_>^{-1}}^{\ell_<^{-1}}\frac{dk}{k}\int_0^{2\pi} d\varphi\, e^{-ik|\mathbf{x}|\cos\varphi}$$

$$= \frac{|\mathbf{x}|^2}{2\pi}\int_{|\mathbf{x}|/\ell_>}^{|\mathbf{x}|/\ell_<}\frac{dz}{z^3}\int_0^{2\pi} đ\varphi\, e^{-iz\cos\varphi}. \tag{D.23}$$

To control the potential divergence at small z we add and subtract the small-z behavior of the

integrand, thus obtaining

$$\begin{aligned}
\mathcal{H}^{(2)}(\mathbf{x}) &= \frac{|\mathbf{x}|^2}{2\pi}\int_{|\mathbf{x}|/\ell_>}^{|\mathbf{x}|/\ell_<}\frac{dz}{z^3}\int_0^{2\pi}đ\varphi\left(e^{-iz\cos\varphi}-\left[1-\tfrac{1}{4}z^2\right]\right) \\
&\qquad +\frac{|\mathbf{x}|^2}{2\pi}\int_{|\mathbf{x}|/\ell_>}^{|\mathbf{x}|/\ell_<}\frac{dz}{z^3}\left(1-\tfrac{1}{4}z^2\right) \qquad \text{(D.24)} \\
&= \frac{|\mathbf{x}|^2}{2\pi}\Big(\mathcal{S}(|\mathbf{x}|/\ell_<)-\mathcal{S}(|\mathbf{x}|/\ell_>)\Big)+\frac{\ell_>^2-\ell_<^2}{4\pi} \\
&\qquad -\frac{|\mathbf{x}|^2}{8\pi}\ln\left(\ell_>/\ell_<\right), \qquad \text{(D.25)} \\
\mathcal{S}(t) &\equiv \int_0^t\frac{dz}{z^3}\int_0^{2\pi}đ\varphi\,\left(e^{-iz\cos\varphi}-\left[1-\tfrac{1}{4}z^2\right]\right). \qquad \text{(D.26)}
\end{aligned}$$

Noting that $\mathcal{S}(t)$ has asymptotic behavior [36]

$$\mathcal{S}(t)\approx\begin{cases}\frac{1}{128}t^2, & \text{for } t\ll 1,\\ \frac{1}{4}\ln\left(t/2e^{1-\gamma}\right), & \text{for } t\gg 1,\end{cases} \qquad \text{(D.27)}$$

where γ $(=0.5772\ldots)$ is the Euler-Mascheroni constant and using this to approximate $\mathcal{H}^{(2)}(\mathbf{x})$ in Eq. (D.25), and inserting the result into Eq. (D.13), noting that the constant term vanishes under differentiation, we obtain for $\ell_< \ll |\mathbf{x}| \ll \ell_>$ the result

$$\mathcal{G}^{(2)}_{dd'}(\mathbf{x})\approx-\frac{1}{4\pi}\Big(\delta_{dd'}\ln\left(e^{\gamma+\frac{1}{2}}\,|\mathbf{x}|/2\ell_>\right)-\hat{x}_d\,\hat{x}_{d'}\Big). \qquad \text{(D.28)}$$

Appendix E

Transforms and manipulations in almost-zero dimensions

In this appendix we briefly overview the mathematics of zero dimensional functions, in particular zero-dimensional Fourier transforms, in order to facilitate the presentation of manipulations in $r_\perp$ space. The $r_\perp$-space is nD dimensional; in the replica limit $n \to 0$ it is almost zero-dimensional. By almost zero dimension space, we imply a limiting process whereby the dimension of a space (large enough to accommodate radial and angular momentum) is taken to zero, analytically continuing functions in that space, and the orthogonal basis for the expansion of these functions. An arbitrary function $f(\mathbf{r})$ in D dimensions can be separated into hyperspherical coordinates; $f(\mathbf{r}) = \sum_{l\{m\}} R_{l\{m\}}(r) Y_{l\{m\}}(\Theta)$ where $R_{l\{m\}}(x)$ are the radial functions and $Y_{l\{m\}}(\Theta)$ are the hyperspherical harmonics, whose argument is the set of angles denoted by the shorthand Θ. The set of angular indices are denoted by the shorthand $l\{m\}$. An useful properties of the hyperspherical harmonics is

$$\mathbb{C}_l(\hat{n} \cdot \hat{n}') = N_l \sum_{l\{m\}} Y_{l\{m\}}(\Theta) Y^*_{l\{m\}}(\Theta') \tag{E.1}$$

where $\mathbb{C}_l^\alpha$ is the l-th Gegenbauer polynomial for D dimensions, $\alpha \equiv D/2 - 1$ and N_l is a normalization constant given by

$$N_l = \alpha\,(\alpha+1)\cdots(\alpha+l-1)\,\frac{2\pi^{D/2}}{\Gamma\,(D/2+l)}, \tag{E.2}$$

The first few Gegenbauer polynomials are given by

$$\begin{aligned}
\mathbb{C}_0^\alpha(z) &= 1 \\
\mathbb{C}_1^\alpha(z) &= 2\alpha z \\
\mathbb{C}_2^\alpha(z) &= 2\alpha(\alpha+1)z^2 - \alpha \\
\mathbb{C}_3^\alpha(z) &= \frac{1}{3}\left[4\alpha(\alpha+1)(\alpha+2)z^3 - 6\alpha(\alpha+1)z\right],
\end{aligned} \tag{E.3}$$

from which it is clear that in the $D \to 0$ limit, all the Gegenbauer polynomials with $l \geq 3$ vanish, and the $l = 0$ and $l = 2$ polynomials become identical. The following identities are going to be useful, the first one is the orthogonality condition for the Gegenbauer polynomials and the second one is the expansion of a plane wave,

$$\begin{aligned}
\frac{1}{N_l}\int d\Omega_\Theta \mathbb{C}_l^\alpha(\hat{n}\cdot\hat{n}')\mathbb{C}_{l'}^\alpha(\hat{n}\cdot\hat{n}'') &= \delta_{ll'}\mathbb{C}_l^\alpha(\hat{n}'\cdot\hat{n}'') \\
e^{i\mathbf{k}\cdot\mathbf{r}} &= \sum_l^\infty i^l A(l,D)\,\mathbb{J}_l^D(kr)\mathbb{C}_l^\alpha(\hat{k}\cdot\hat{r})
\end{aligned} \tag{E.4}$$

where $A(l, D)$ is a coefficient dependent on the angular momentum index l and the dimension of space D. The functions $\mathbb{J}_l^D$ are the D dimensional generalization of the ordinary Bessel functions and obeys the equation

$$\frac{d}{dr^2}\mathbb{J}_l^D(r) + \left(\frac{D-1}{r}\right)\frac{d}{dr}\mathbb{J}_l^D(r) - \frac{l(l+D-2)}{r^2}\mathbb{J}_l^D(r) = 0 \tag{E.5}$$

Moreover, it is easy to check that if one makes the transformation $\mathbb{J}_l^D(r) \to \mathrm{J}(r)/r^{D/2-1}$ then the equation satisfied by $J(r)$ is

$$r^2\frac{d}{dr^2}\mathrm{J}(r) + r\frac{d}{dr}\mathrm{J}(r) + \left[r^2 - (l+D/2-1)^2\right]\mathrm{J}(r) = 0 \tag{E.6}$$

which implies that $\mathrm{J}(r)$ is the ordinary Bessel function and $\mathbb{J}_l^D(r) = \mathrm{J}_{l+D/2-1}(r)/r^{D/2-1}$. In the $D \to 0$ limit we therefore have the identities $\mathbb{J}_2^D(r) = r\mathrm{J}_1(r)$ and $\mathbb{J}_1^D(r) = r\mathrm{J}_0(r)$. Recall that the volume of D-dimensional unit sphere is given by $\int d\Omega_\Theta = 2\pi^{D/2}/\Gamma(D/2)$. Using the above relations, and using the Refs. [48] we obtain the zero dimensional expansion of the plane wave to

be

$$e^{i\mathbf{k}\cdot\mathbf{r}} = 1 - A\,kr\,J_1(kr) - 2iA\,kr\,\mathrm{J}_0(kr)\left\{\frac{\mathbf{k}\cdot\mathbf{r}}{kr}\right\} \tag{E.7}$$

where $A = \Gamma(D/2)/2\pi^{D/2}$, i.e., inverse of the volume of a D dimensional sphere. In the above expression, $D \to 0$ limit is to be taken after performing all calculations which uses the plane-wave expansion. Next, let us use this expansion to perform the Fourier transform of the Gaussian form $e^{-\zeta\mathbf{r}^2/2}$, as a quick verification. The main steps in the calculation are as follows,

$$\begin{aligned}
\int d\mathbf{r} e^{-\zeta r^2/2} e^{i\mathbf{k}\cdot\mathbf{r}} &= \int r^{D-1} dr \int d\Omega_\Theta \left[1 - Akr\mathrm{J}_1(kr)\right] e^{-\zeta r^2/2} \\
&= \int r^{D-1} dr \int d\Omega_\Theta e^{-\zeta r^2/2} - A\,k \int d\Omega_\Theta \int dr \mathrm{J}_1(kr) e^{-\zeta r^2/2} \\
&= 1 - A\frac{2\pi^{D/2}}{\Gamma(D/2)}\left[1 - e^{-k^2/2\zeta}\right] \\
&= e^{-k^2/2\zeta},
\end{aligned} \tag{E.8}$$

which is indeed the expected result for the Fourier transform of a Gaussian. We use the same technology to determine the Fourier transform of $-k^2 e^{-k^2/2\zeta}$ used in the text. The result is $r^2\zeta^2 e^{-\zeta r^2/2}$. Note that this is consistent with the fact that this Fourier transform should be equal to $\widehat{\nabla}^2 e^{-\zeta r^2/2}$; one can easily verify it to be the case by using the radial representation $\nabla^2 = \frac{d^2}{dr^2} + \frac{D-1}{r}\frac{d}{dr} + ...$, and taking $D \to 0$.

Finally, we use the same technology to arrive at the Fourier transform of $-q^2(\ln q)\, e^{-q^2/2\zeta}$. We quote the final result here,

$$\left[\frac{1}{2}r^2\zeta^2 \mathrm{Ei}\left(\frac{\zeta r^2}{2}\right) - r^2\zeta^2 \ln(r^2\zeta^2) + \zeta\right] e^{-\zeta r^2/2} - \zeta \tag{E.9}$$

where $\mathrm{Ei}(\cdot)$ is the Exponential Integral function.

Appendix F

Solid state propagator

In this Appendix [1]we present the calculation of the solid-state propagator in brief. For a discussion of the physical content of the solid-state propagator, see [64].

In the ordered state of a field theory, one needs to expand the fluctuating fields $\Omega(\hat{x})$ around the stable saddle-point solution given by Eq. (2.15). It is easy to check that on performing this expansion for the VG field-theory, the inverse of the kernel $\mathbf{\Delta}_0(\hat{k}, \hat{k}')$ defined in Eq. (4.10) is the solid state propagator at the Gaussian level. One using the saddle-point solution, see Eq.(2.15), the kernel can be written as

$$\mathbf{\Delta}(\hat{k}, \hat{k}') = \left(\hat{k}^2 + |\tau_0|\right) \delta(\hat{k} - \hat{k}') - 2|\tau_0| \int d\zeta \, \mathcal{P}_0(\zeta) e^{-(k_\perp - k'_\perp)^2/2|\tau_0|\zeta}. \tag{F.1}$$

We can now rewrite the kernel in terms of the mean-field scaling variables $\theta \equiv \tau_0 (g_0 Q)^{-1}$ and $\hat{q} \equiv \hat{k}|\tau_0|^{-1/2}$ introduced in the text, and thereby obtain

$$\mathbf{\Delta}(\hat{q}, \hat{q}') = \left(|\theta_0|\hat{q}^2 + |\theta_0|\right) \delta(\hat{q} - \hat{q}') - \int d\zeta \, \mathcal{P}_0(\zeta) e^{-(q_\perp - q'_\perp)^2/2\zeta}, \tag{F.2}$$

where $q_\perp$ is the rescaled transverse momentum. We denote the eigenvectors of the operator $\mathbf{\Delta}$ by $|\psi_\lambda\rangle$ and the corresponding eigenvalue by λ. We can formally write

$$\mathbf{\Delta}^{-1}(\hat{q}, \hat{q}') = \sum_\lambda \frac{1}{\lambda} \langle \hat{q}|\psi_\lambda\rangle\langle\psi_\lambda|\hat{q}'\rangle \tag{F.3}$$

[1]I thank Ken Esler for performing the numerical calculations for some of the results presented in this Appendix.

The operator in Eq. F.2 can be rewritten as a differential operator in real space,

$$\mathbf{\Delta}(\hat{r}) = -|\theta|\nabla^2 + |\theta| - \int d\zeta\, \mathcal{P}_0(\zeta) e^{-\zeta r_\perp^2/2} \tag{F.4}$$

where $\hat{r}$ and $r_\perp$ are rescaled real-space replicated vector and the corresponding transverse vector respectively. We obtain the following eigenvalue equation for the eigenfunctions $\psi_\lambda(\hat{r})$,

$$\left[-|\theta|(\nabla_\parallel^2 + \nabla_\perp^2) + |\theta| - \int d\zeta\, \mathcal{P}_0(\zeta) e^{-\zeta r_\perp^2/2}\right] \psi_\lambda(\hat{r}) = \lambda \psi_\lambda(\hat{r}), \tag{F.5}$$

where we have separated the Laplacian operator in $(n+1)D$ replicated space into a the longitudinal (D-dimensional) and transverse (nD-dimensional) Laplacian operator represented by $\nabla_\parallel^2$ and $\nabla_\perp^2$ respectively. It is immediately obvious that $\psi_\lambda(\hat{r})$ can be written as a separable function of longitudinal and transverse coordinates, $\psi_\lambda(\hat{r}) \equiv \psi^\parallel(r_\parallel)\psi^\perp(r_\perp)$. The longitudinal part is simply plane wave $\psi^\parallel(r_\parallel) = (1/\sqrt{V})e^{iq_\parallel \cdot r_\parallel}$ and the eigenvalue equation reduces to

$$\left[-|\theta|\nabla_\perp^2 + \left\{(1+q_\parallel^2)|\theta| - \lambda\right\} - \int d\zeta\, \mathcal{P}_0(\zeta) e^{-\zeta r_\perp^2/2}\right] \psi^\perp(r_\perp) = 0. \tag{F.6}$$

We introduce new parameters s and t where $\lambda/|\theta| \equiv 1 + q_\parallel^2 + s$ and $t \equiv 1/|\theta|$. At the mean-field level, $\theta = -1/2$. Note that since λ is the eigenvalues of the inverse of a stable propagator it must non-negative, implying that $s \geq -1$, which will be verified in our calculation. With these definitions, we obtain from the above equation

$$\left[-\nabla_\perp^2 - s - t\int d\zeta \mathcal{P}_0(\zeta) e^{-\zeta r_\perp^2/2}\right] \psi_s^\perp(r_\perp) = 0. \tag{F.7}$$

We choose to call the third term on the left-hand side of the above equation the 'potential' term, drawing the analogy to a quantum mechanical problem. As this potential term is dependent only on the magnitude of $r_\perp$, we can separate the angular and radial dependence of the eigenfunction, i.e., $\psi_s^\perp(r_\perp) \equiv R_{sl}(r)Y_{l\{m\}}(\Theta)$ where $R_{sl}(r)$ is the radial function of the radial coordinate $r \equiv |r_\perp|$ and $Y_{l\{m\}}(\Theta)$ is the l-th hyperspherical harmonics. The latter is a function of the $nD-1$ angles represented by Θ, see, for example Ref. [44]. Here $\{m\}$ represents the set of indices, besides the angular momentum index l, that specify the hyperspherical harmonics. The Eq. (F.7) reduces to

the radial equation

$$\frac{d^2R_{sl}(r)}{dr^2}+\frac{nD-1}{r}\frac{dR_{sl}(r)}{dr}+\left(t\int d\zeta\,\mathcal{P}_0(\zeta)e^{-\zeta r^2/2}-\frac{l(l+nD-2)}{r^2}\right)R_{sl}(r)=-sR_{sl}(r). \quad \text{(F.8)}$$

On transforming to a new radial function defined as $R_{sl}(r)\equiv\chi_{sl}(r)/r^{(nD-1)/2}$ the Eq. (F.8) reduces to

$$-\frac{d^2\chi_{sl}(r)}{dr^2}+\left(-t\int d\zeta\,\mathcal{P}_0(\zeta)e^{-\zeta r^2/2}+\frac{l(l+nD-2)}{r^2}+\frac{(nD-1)(nD-3)}{4r^2}\right)\chi_{sl}(r)=s\chi_{sl}(r). \quad \text{(F.9)}$$

The definition of the normalization conditions of the radial 'wave-functions' $R_{sl}(r)$, $\chi_{sl}(r)$ and $Y_{l\{m\}}(\Theta)$ is clarified below:

$$\begin{aligned}&\int_0^\infty R_{sl}(r)r^{nD-1}dr=1\ \Rightarrow\int_0^\infty\chi_{sl}(r)dr=1\\ &\text{and}\int d\Omega_\Theta Y_{l\{m\}}Y^*_{l'\{m'\}}=\delta_{ll'}\delta_{\{m\}\{m'\}},\end{aligned} \quad \text{(F.10)}$$

where $d\Omega_\Theta$ represents the angular measure in polar coordinates for nD-dimensional space as a function of the set Θ of $nD-1$ angles.

In the light of the decomposition of the $(n+1)D$-dimensional replicated space into nD and D dimensional spaces, and the corresponding functions introduced above, let us present the formal structure of the propagator, i.e., the inverse of the kernel $\mathbf{\Delta}$. We define Θ and Θ' to be the set of angles subtended by $q_\perp$ and $q'_\perp$ respectively to an arbitrarily chosen direction in nD space, we have

$$\begin{aligned}\mathbf{\Delta}^{-1}(\hat{q},\hat{q}')&=\sum_\lambda\frac{1}{\lambda}\langle\hat{q}|\psi_\lambda\rangle\langle\psi_\lambda|\hat{q}'\rangle=\sum_\lambda\frac{1}{\lambda}\langle q_\parallel,q_\perp|\psi_\lambda\rangle\langle\psi_\lambda|q'_\parallel,q'_\perp\rangle\\ &=\sum_{sl\{m\}}\frac{\delta(q_\parallel-q'_\parallel)}{q_\parallel^2+1+s}\,\bar{R}_{sl}(|q_\perp|)Y_{l\{m\}}(\Theta)\bar{R}^*_{sl}(|q'_\perp|)Y^*_{l\{m\}}(\Theta')\\ &=\sum_{sl}\frac{1}{N_l}\frac{\delta(q_\parallel-q'_\parallel)}{q_\parallel^2+1+s}\,\mathbb{C}_l^{nD/2-1}\left(\frac{q_\perp}{|q_\perp|}\cdot\frac{q'_\perp}{|q'_\perp|}\right)\,\bar{R}_{sl}(|q_\perp|)\bar{R}^*_{sl}(|q'_\perp|),\end{aligned} \quad \text{(F.11)}$$

where bar on functions imply Fourier transforms of corresponding real space functions. In the last step of the derivation, we have used the sum rule for hyperspherical harmonics $\mathbb{C}_l^{nD/2-1}(\cdots)$ is the l-th Gegenbauer polynomial for nD dimensions. We encourage the reader to study Appendix E in

order to reproduce the derivation, and clarify the notation. N_l is a normalization constant defined there.

Recall from Appendix E that all the Gegenbauer polynomials except the $l = 0$ and $l = 1$ vanish in the zero-dimensional limit. Hence we only have to worry about the $l = 0$ and $l = 1$ sector in evaluating the radial wave-function numerically. Numerical solution of the radial equation (F.9) affirms that there is a single 'bound state' for $l = 0$ with 'energy' $s = -s_0$. The $l = 1$ sector corresponds to the Goldstone mode, which is a bound state with $s = -1$ and the wave-function is known analytically as discussed later on. There are no other bound states. We therefore obtain the formal expression,

$$\begin{aligned}\mathbf{\Delta}_0(\hat{q},\hat{q}') = \delta(q_\parallel - q'_\parallel)\Bigg[&\frac{1}{q_\parallel^2+1+s_0}\bar{R}_{s_0 0}(|q_\perp|)\bar{R}^*_{s_0 0}(|q'_\perp|)\\ &+\frac{1}{q_\parallel^2}\left\{\frac{q_\perp}{|q_\perp|}\cdot\frac{q'_\perp}{|q'_\perp|}\right\}\bar{R}_{-11}(|q_\perp|)\bar{R}^*_{-11}(|q'_\perp|)+\ldots\Bigg]\end{aligned} \tag{F.12}$$

The dots in the above equation represent contribution from 'extended states' to be discussed later.

As the Eq. [F.9] can be interpreted as the radial equation of a quantum problem, we will refer to the terms within brackets as the *effective potential*. The effective potential for $l = 0$ is plotted in Fig. [F.1]. For $l = 0$ we find numerically that the single bound state is for $s = s_0 = 0.267$ at zero

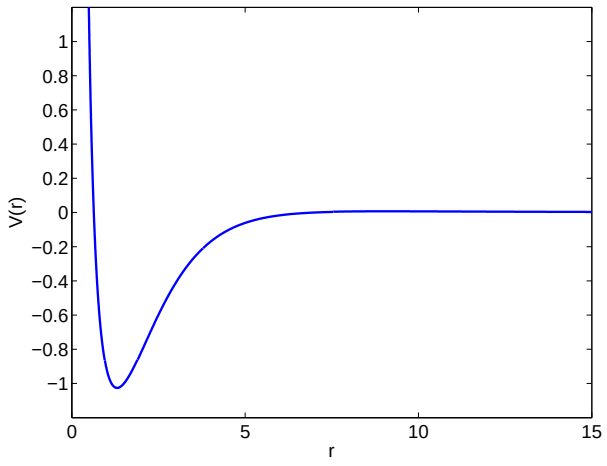

Figure F.1: The effective potential for l=0

dimensions. The wave-function is plotted in Fig.[F.2].

Now we focus on the the $l = 1$ sector of the eigenspectrum of the kernel $\mathbf{\Delta}$. It was known from

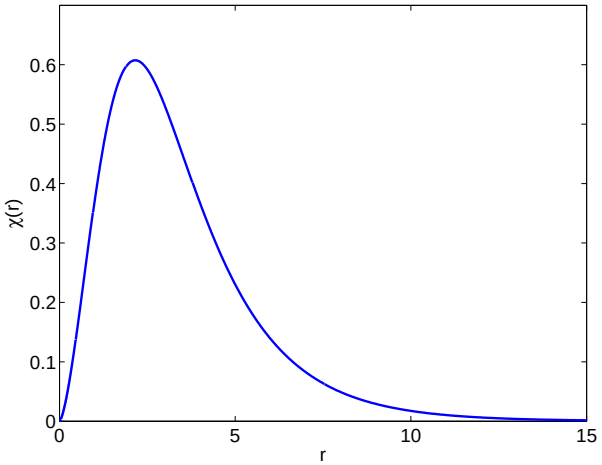

Figure F.2: The bound state for $l = 0$

earlier work [46] that the $l = 1$ sector corresponds to the zero mode (or the Goldstone branch). These zero modes are fluctuations associated with the broken translational symmetry [46], and can be determined analytically. Thereby, we determine the wave-function associated with the $l = 1$ sector analytically.

Recall that the saddle-point solution (2.15) is independent of $r_{\|}$-space. An uniform translation amounts to $\hat{r} \to \hat{r} + \hat{a}$, where $\hat{a}$ is the uniform translation vector. One can decompose $\hat{a}$ into $a_{\|}$ and $a_{\perp}$, the corresponding longitudinal and transverse vectors. Hence under a small uniform translation the change of the ground state is proportional to

$$\delta M_0(\hat{r}) \propto r_{\perp} \cdot a_{\perp} \int_0^{\infty} d\zeta\, \zeta\, \mathcal{P}_0(\zeta) e^{-\zeta r_{\perp}^2/2}. \tag{F.13}$$

We will now verify that this is indeed a solution of the Eq. [F.7] with $s = -1$. Using the following equalities,

$$\begin{aligned} -\nabla_{\perp}^2 \delta M_0(\hat{r}) &= \int_0^{\infty} d\zeta\, a_{\perp} \cdot r_{\perp} \left[2\zeta^2 - r_{\perp}^2 \zeta^3\right] \mathcal{P}_0(\zeta) e^{-\zeta r_{\perp}^2/2} \\ &= \int_0^{\infty} d\zeta\, a_{\perp} \cdot r_{\perp} \left[-4\zeta^2 \mathcal{P}_0(\zeta) - 2\zeta^3 \frac{d\mathcal{P}_0(\zeta)}{d\zeta}\right] e^{-\zeta r_{\perp}^2/2}; \\ \int_0^{\infty} d\zeta \mathcal{P}_0(\zeta) \int_0^{\infty} d\zeta' \zeta' \mathcal{P}_0(\zeta') e^{-(\zeta+\zeta')r_{\perp}^2/2} &= \int_0^{\infty} d\zeta \zeta\, e^{-\zeta r_{\perp}^2/2} \int_0^{\zeta} d\zeta' \mathcal{P}_0(\zeta) \mathcal{P}_0(\zeta'), \end{aligned} \tag{F.14}$$

and using the Eq. [2.20] for the distribution function, the reader can easily verify that $\delta M_0(\hat{r})$ is indeed an eigenfunction solution for eigenvalue $s = -1$. Hence the radial wave-function for the zero mode is

$$R_{-11}(r) = \sqrt{\frac{2}{\pi}} \frac{1}{\langle\sqrt{\zeta}\rangle}\, r \int_0^\infty d\zeta\, \zeta\, \mathcal{P}_0(\zeta) e^{-\zeta r^2/2}, \tag{F.15}$$

where we have used the identity $\int_0^\infty r e^{-\zeta r^2/2} r^{nD-1} dr = \sqrt{\pi/2\zeta}$ and the definition $\langle\sqrt{\zeta}\rangle \equiv \int_0^\infty d\zeta\, \sqrt{\zeta}\, \mathcal{P}_0(\zeta)$ to normalize the wave-function. Using the methods presented developed in Appendix E one can easily show that the Fourier transform of the wave-function agrees with the equivalent expression in momentum space in Ref. [46].

We discuss briefly the extended states, i.e., eigenfunctions of the kernel $\mathbf{\Delta}$ that have an infinite support in $r_\perp$ space. The states in an analogous quantum problem are the scattering states which are extended oscillatory waves. In our case, one can easily check from Eq. (F.8) and Eq. (E.5) that these extended states behave as the generalized Bessel functions far away from origin, with appropriate phase shift that we denote by $\delta(s, l)$ As discussed before, there are only two channels; $l = 0$ and $l = 1$. In the $l = 0$ channel the radial functions for the extended states are $\mathbb{J}_0^{nD}(\sqrt{s}\, r + \delta(s, 0)) = r\mathrm{J}_1(\sqrt{s}\, r + \delta(s, 0))$. In the $l = 1$ channel the radial functions are $\mathbb{J}_1^{nD}(\sqrt{s}\, r + \delta(s, 1)) = r\mathrm{J}_0(\sqrt{s}\, r + \delta(s, 1))$. These functions are normalizable using the relation,

$$\int dr r^{nD-1} r\mathrm{J}_l(r) = 1 \tag{F.16}$$

Owing to the fast decay of the effective potential in the $r_\perp$ space the Bessel functions are a very good approximation to the extended states. The phase shift $\delta(s, l)$ as a function of 'energy' s is to be determined numerically.

Appendix G

Calculation of β and δ from the Equation of State

The requirement that the renormalized Equation of State, Eq. (4.24) be cast into the scaling form determines the exponents β and δ, which can also be independently evaluated from the hyperscaling relations. On substituting $M_R(\hat{x})$ in Eq. (4.24) by the scaling form Eq. (4.29) with mean-field value of β and by trivially rescaling the field $H_R(\hat{x})$ by g^* we have

$$H = y^2 \left\{ ... + \frac{\tau}{y}\, m - \frac{1}{2}\, m^2 + \frac{\epsilon}{7}\, m \left(\frac{\tau}{y} - m \right) \ln \left[\frac{\tau}{y} - m \right] + \frac{\epsilon}{7}\, m \left(\frac{\tau}{y} - m \right) \ln y \right\}, \tag{G.1}$$

where $y \equiv g^* Q$ and we have chosen to hide the gradient term since it plays no role in the present calculation. We drop the subscript R denoting renormalized quantity. The exponents β and δ have $\mathrm{O}(\epsilon)$ correction; let us denote $\beta = 1 + b$ and $\delta = 2 + d$ where b and d are $\mathrm{O}(\epsilon)$ terms. We have

$$H = y^\delta \left\{ \cdots + \frac{x}{y^{b+d}}\, m - \frac{1}{2y^d} m^2 + \frac{\epsilon}{7y^d}\, m \left(\frac{x}{y^b} - m \right) \ln \left[\frac{x}{y^b} - m \right] + \frac{\epsilon}{7y^d}\, m \left(\frac{x}{y^b} - m \right) \ln y \right\} \tag{G.2}$$

Using the simplification $y^a \approx 1 + a \ln y$ for small a, we find that in order for the the coefficient of $\ln y$ to vanish, y not being a scaling variable, requires

$$d + b = \frac{\epsilon}{7} \text{ and } d = \frac{2\epsilon}{7}. \tag{G.3}$$

Therefore, up to $\mathrm{O}(\epsilon)$, $\delta = 2 + 2\epsilon/7$ and $\beta = 1 - \epsilon/7$. As a check on consistency, using the hyperscaling relations $\beta = (D - 2 + \eta)\nu/2$ and $\delta = (D + 2 - \eta)/(D - 2 + \eta)$ and the values of the exponents $\nu^{-1} = 2 - 5\epsilon/21$ and $\eta = -\epsilon/21$ and $D = 6 - \epsilon$ we get the same result.

Appendix H

Notes on the revised Goldstone fluctuations

In this Appendix we present the details of some of the calculations using the revised Goldstone fluctuation discussed in Chapter 5.

H.1 Fourier transform of the revised Goldstone-deformed order parameter

In this section we present the details of the Fourier transformation of the revised Goldstone-deformed order parameter given by Eq. (5.16). We freely use the decomposition of the $(n+1)D$ dimensional vector $\hat{k}$ into the D-dimensional vector $k_\parallel$ and the nD-dimensional vector $k_\perp$ in this derivation, for a refresher see Section 3.3. The main steps in performing the Fourier transformation are as follows:

$$
\begin{aligned}
V\Omega(\hat{x}) &= Q\int đ\hat{k}\int d\mathbf{z}\, e^{i\mathbf{k}_{\rm tot}\cdot\mathbf{z}+ik_\perp\cdot u_\perp(\mathbf{z})}\int_0^\infty d\zeta\ \ \mathcal{P}(\zeta)\, e^{-\hat{k}^2/2\zeta}e^{-i\hat{k}\cdot\hat{x}} && \text{(H.1)}\\
&= Q\int_0^\infty d\zeta\ \ \mathcal{P}(\zeta)\int d\mathbf{z}\int đk_\parallel e^{-k_\parallel^2/2\zeta}e^{ik_\parallel\cdot x_\parallel}e^{i\mathbf{k}_{\rm tot}\cdot\mathbf{z}}\times\\
&\qquad\qquad \int đk_\perp\, e^{-k_\perp^2/2\zeta}e^{ik_\perp\cdot x_\perp}e^{ik_\perp\cdot u_\perp(\mathbf{z})} && \text{(H.2)}\\
&= Q\int_0^\infty d\zeta\ \ \mathcal{P}(\zeta)\int d\mathbf{z}\left(\frac{\zeta}{2\pi}\right)^{(n+1)D/2} e^{-\frac{\zeta}{2}(1+n)(\mathbf{x}_{\rm cm}-\mathbf{z})^2}\, e^{-\frac{\zeta}{2}(x_\perp-u_\perp(\mathbf{z}))^2} && \text{(H.3)}\\
&\xrightarrow{n\to 0} Q\int_0^\infty d\zeta\ \ \mathcal{P}(\zeta)\int d\mathbf{z}\left(\frac{\zeta}{2\pi}\right)^{D/2} e^{-\frac{\zeta}{2}\left(x_\parallel-\mathbf{z}\right)^2}\, e^{-\frac{\zeta}{2}(x_\perp-u_\perp(\mathbf{z}))^2}. && \text{(H.4)}
\end{aligned}
$$

The last expression is the same as Eq. (5.17).

H.2 Derivation of the effective theory for revised Goldstone fluctuations

In this section we present the mathematical details of the derivation of the effective theory for the revised Goldstone fluctuations, i.e., eqs. (5.18, 5.19, 5.20).

We use Eq. (5.17) to derive the contribution of the quadratic term in the effective Hamiltonian to the effective theory for Goldstone fluctuations. The main steps are as follows:

$$
\begin{aligned}
& V \int đ\hat{k} |\Omega(\hat{k})|^2 \\
= \;& Q^2 \int đk_{\parallel} đk_{\perp} \int d\mathbf{z}_1 \, d\mathbf{z}_2 \exp\left[i\mathbf{k}_{\rm tot} \cdot (\mathbf{z}_1 - \mathbf{z}_2)\right] \exp\left[ik_{\perp} \cdot (u_{\perp}(\mathbf{z}_1) - u_{\perp}(\mathbf{z}_2))\right] \times \\
& \int d\zeta_1 \mathcal{P}(\zeta_1) \, d\zeta_2 \mathcal{P}(\zeta_2) \exp\left[-\frac{\hat{k}^2}{2\zeta_1} - \frac{\hat{k}^2}{2\zeta_2}\right] \qquad \text{(H.5a)} \\
= \;& \frac{Q^2}{V} \int d\mathbf{z}_1 d\mathbf{z}_2 \int d\zeta \; d\zeta_1 \, d\zeta_2 \, \mathcal{P}(\zeta_1) \, \mathcal{P}(\zeta_2) \, \delta\left(\zeta - \frac{1}{\zeta_1^{-1} + \zeta_2^{-1}}\right) \times \\
& \left(\frac{\zeta}{2\pi}\right)^{(n+1)D/2} \exp\left[-\frac{\zeta}{2}|u_{\perp}(\mathbf{z}_1) - u_{\perp}(\mathbf{z}_2)|^2\right] \exp\left[-(1+n)\,\frac{\zeta}{2}\,|\mathbf{z}_1 - \mathbf{z}_2|^2\right] \qquad \text{(H.5b)}
\end{aligned}
$$

The contributions of the final expression in the LRS is easily determined; in the ORS it is Q^2/V^n, and in the 1RS it is zero. On making simplifications valid in the $n \to 0$ limit we obtain,

$$
\begin{aligned}
\sum_{\hat{k} \in HRS} |\Omega(\hat{k})|^2 \;=\; & -Q^2 + \frac{Q^2}{V} \int d\mathbf{z}_1 \, d\mathbf{z}_2 \, d\zeta \, d\zeta_1 \, d\zeta_2 \, \mathcal{P}(\zeta_1) \, \mathcal{P}(\zeta_2) \, \delta\left(\zeta - \frac{1}{\zeta_1^{-1} + \zeta_2^{-1}}\right) \times \\
& \left(\frac{\zeta}{2\pi}\right)^{D/2} \exp\left[-\frac{\zeta}{2}|u_{\perp}(\mathbf{z}_1) - u_{\perp}(\mathbf{z}_2)|^2 - \frac{\zeta}{2}|\mathbf{z}_1 - \mathbf{z}_2|^2\right]. \qquad \text{(H.6)}
\end{aligned}
$$

This is identical to the Eq. (5.18), which we set out to derive here. Next, we do a expansion for

small $u_\perp$ and in the gradient of $u_\perp$.

$$\begin{aligned}
&\sum_{\hat{k}\in HRS} |\Omega(\hat{k})|^2\Big|_{u_\perp=0}^{u_\perp} \\
&\quad\approx \frac{Q^2}{V}\int d\mathbf{z}_1\, d\mathbf{z}_2\, d\zeta\, d\zeta_1\, d\zeta_2\, \mathcal{P}(\zeta_1)\,\mathcal{P}(\zeta_2)\,\delta\left(\zeta-\frac{1}{\zeta_1^{-1}+\zeta_2^{-1}}\right)\times \\
&\qquad\left(\frac{\zeta}{2\pi}\right)^{D/2}\exp\left[-\frac{\zeta}{2}|\mathbf{z}_1-\mathbf{z}_2|^2\right]\left\{-\frac{\zeta}{2}|u_\perp(\mathbf{z}_1)-u_\perp(\mathbf{z}_2)|^2\right\} \qquad \text{(H.7a)}\\
&\quad= \frac{Q^2}{V}\int d\mathbf{r}\, d\mathbf{R}\, d\zeta\, d\zeta_1\, d\zeta_2\, \mathcal{P}(\zeta_1)\,\mathcal{P}(\zeta_2)\,\delta\left(\zeta-\frac{1}{\zeta_1^{-1}+\zeta_2^{-1}}\right)\times \\
&\qquad\left(\frac{\zeta}{2\pi}\right)^{D/2}\exp\left[-\frac{\zeta}{2}\mathbf{r}^2\right]\left\{-\frac{\zeta}{2}\Big|\mathbf{r}\cdot\nabla u_\perp(\mathbf{R})\Big|^2\right\}, \qquad \text{(H.7b)}
\end{aligned}$$

where in the last expression we have made the change of variables to $\mathbf{r}=\mathbf{z}_1-\mathbf{z}_2$ and $\mathbf{R}=\frac{\mathbf{z}_1+\mathbf{z}_2}{2}$. On performing the Gaussian integral over $\mathbf{r}$ we obtain

$$\sum_{\hat{k}\in HRS} |\Omega(\hat{k})|^2\Big|_{u_\perp=0}^{u_\perp} \approx -\frac{Q^2}{2V}\int d\mathbf{z}\,\partial_{\mathbf{z}}u_\perp(\mathbf{z})\cdot\partial_{\mathbf{z}}u_\perp(\mathbf{z}), \qquad \text{(H.8)}$$

which is identical to Eq. (5.21).

Now let us pay attention to the contribution of the 'gradient term' of the effective Hamiltonian to the effective theory of Goldstone fluctuations. The main step are as follows:

$$\begin{aligned}
&V\int đ\hat{k}|\Omega(\hat{k})|^2\,\hat{k}^2 \\
&\quad= Q^2\int đk_\parallel đk_\perp\int d\mathbf{z}_1\, d\mathbf{z}_2\exp\left[i\mathbf{k}_{\rm tot}\cdot(\mathbf{z}_1-\mathbf{z}_2)\right]\exp\left[ik_\perp\cdot(u_\perp(\mathbf{z}_1)-u_\perp(\mathbf{z}_2))\right]\times \\
&\qquad\int d\zeta_1\mathcal{P}(\zeta_1)\, d\zeta_2\mathcal{P}(\zeta_2)\,\left(k_\parallel^2+k_\perp^2\right)\exp\left[-\frac{\hat{k}^2}{2\zeta_1}-\frac{\hat{k}^2}{2\zeta_2}\right] \qquad \text{(H.9a)}\\
&\quad= \frac{Q^2}{V}\int d\mathbf{z}_1 d\mathbf{z}_2\int d\zeta\; d\zeta_1\, d\zeta_2\,\mathcal{P}(\zeta_1)\,\mathcal{P}(\zeta_2)\,\delta\left(\zeta-\frac{1}{\zeta_1^{-1}+\zeta_2^{-1}}\right)\times \\
&\qquad\zeta^2\frac{\partial}{\partial\zeta}\left\{\left(\frac{\zeta}{2\pi}\right)^{(D/2}\exp\left[-\frac{\zeta}{2}|u_\perp(\mathbf{z}_1)-u_\perp(\mathbf{z}_2)|^2\right]\exp\left[-\frac{\zeta}{2}\,|\mathbf{z}_1-\mathbf{z}_2|^2\right]\right\}. \qquad \text{(H.9b)}
\end{aligned}$$

The last expression is identical to Eq. (5.19). Now, let us make a gradient expansion for small $u_\perp$, the first few steps are very similar to the ones that lead to Eq. (H.7b). The main steps for the rest

of the algebraic manipulation are,

$$\begin{aligned}
&\sum_{\hat{k}\in HRS} |\Omega(\hat{k})|^2\,\hat{k}^2\Big|_{u_\perp=0}^{u_\perp} \\
&\quad= \frac{Q^2}{V}\int d\mathbf{r}\,d\mathbf{R}\,d\zeta\,d\zeta_1\,d\zeta_2\,\mathcal{P}(\zeta_1)\,\mathcal{P}(\zeta_2)\,\delta\left(\zeta-\frac{1}{\zeta_1^{-1}+\zeta_2^{-1}}\right)\times \\
&\qquad \zeta^2\frac{\partial}{\partial\zeta}\left[\left(\frac{\zeta}{2\pi}\right)^{D/2}\exp\left[-\frac{\zeta}{2}\mathbf{r}^2\right]\left\{-\frac{\zeta}{2}\Big|\mathbf{r}\cdot\nabla u_\perp(\mathbf{R})\Big|^2\right\}\right] \qquad \text{(H.10a)} \\
&\quad= \frac{Q^2}{2}\,d\zeta\,d\zeta_1\,d\zeta_2\,\mathcal{P}(\zeta_1)\,\mathcal{P}(\zeta_2)\,\delta\left(\zeta-\frac{1}{\zeta_1^{-1}+\zeta_2^{-1}}\right)\times \\
&\qquad \zeta^2\frac{\partial}{\partial\zeta}\,[1]\int d\mathbf{R}\,\partial_{\mathbf{R}}u_\perp(\mathbf{R})\cdot\partial_{\mathbf{R}}u_\perp(\mathbf{R}) \\
&\quad= 0. \qquad \text{(H.10b)}
\end{aligned}$$

The simplification in the second last step follows on performing the Gaussian integration over $\mathbf{r}$. Hence, the contribution of the 'gradient term' is zero.

References

[1] See, for example, Ref. [11] for a review of seminal contribitions to the statistical mechanics of polymers by Sir Sam Edwards and some discussion of current work, Ref. [8] and Ref. [9] for introduction to polymer science, and Ref [10] for lattice models of polymers. For a more technical review of knot theory in polymers, see for example; S. Necheav, *Statistics of knots and entangled random walks* in lectures presented at Les Houches 1998 summer school on *Topological Aspects of Low Dimensional Systems*, July 7 - 31, 1998 (cond-mat/9812205).

[2] P.J. Flory, J. Amer. Chem. Soc. **63**, 3083 (1941); **63**, 3091 (1941), **63**, 3096 (1941); W. H. Stockmayer, J. Chem. Phys. **11**, 45 (1943), **12**, 125 (1944). See also P. J. Flory, *Principles of Polymer Chemistry* (Cornell University Press, 1971).

[3] P.-G. de Gennes, J. Phys. (Paris) **37**, L1 (1976); **36**, 1049 (1975); D. Stauffer, J. Chem Soc., Faraday Trans., II **72**, 1354 (1976). For a review, see D. Stauffer, A. Coniglio, and M. Adam, Adv. in Ploym. Sci. **44**, 103 (1982) and ref. therein. Also see ref. [9].

[4] See for example, O. Stenull, *Renormalized field theory of random resistor networks*, Ph.D. Thesis (2000) (unpublished) and referecnes therein. A partial list of important refs. are: A. B. Harris *et al.*, Phys. Rev. Lett. **35**, 327 (1975); M. J. Stephen, Phys. Rev B **33**, 4444 (1978); C. Dasgupta *et al.*, Phs. Rev B **17**, 1375 (1978); A. B. Harris *et al.*, Phys. Rev. Let. **53**, 743 (1984); Y. Park *et al.*, Phys. Rev. B **35**, 5048 (1987); A. B. Harris *et al.*, Phys. Rev. B **35**, 6964 and 6987 (1987).

[5] S. F. Edwards, Proc. Phys. Soc. (London) **85**, 613 (1965); r. t. Deam and S. F. Edwards, Phil. Trans. R. Soc. **280A**, 317 (1976); R. C. Ball and S.F. Edwards, Macromol. **13**, 748 (1980). See also, ref. [11] and [14].

[6] See S. Panyukov and Y. Rabin, Phys. Rep. **269**, 1 (1996) and references therein.

[7] P. M. Goldbart and N. Goldenfeld, Phys. Rev. Lett. **58**, 2676 (1987); Phys. Rev. A **39**, 1402 (1989).

[8] M. Rubenstein and R. H. Colby, *Polymer Physics* (Oxford University Press, 2003);

[9] P. G. de Gennes, *Scaling Concepts in Polymer Physics* (Cornell University Press, Ithaca, NY, 1979).

[10] C. Vanderzande, *Lattice models of Polymers* (Cambridge University Press, 1998).

[11] P. M. Goldbart, N. Goldenfeld and D. Sherrington, *Stealing the Gold – A Celebration of the Pioneering Physics of Sam Edwards* (Oxford University Press, 2005).

[12] M. Warner and E. M. Terentjev, Prog. Polym. Sci. **21**, 853 (1996).

[13] M. Warner and E. M. Terentjev, *Liquid Crystal Elastomers*, (Oxford University Press, 2003).

[14] M. Doi and S. F. Edwards, *The Theory of Polymer Dynamics* (Oxford University Press, 1986).

[15] X. Xing, S. Mukhopadhyay, P. M. Goldbart and A. Zippelius, *From vulcanization to isotropic and nematic rubber elasticity*, cond-mat/0411660 (submitted to EPL)

[16] See for example, J. Cardy, *Scaling and renormalization in statistical physics* (Cambridge University Press, 1996); M. Le Bellac, *Quantum and statistical field theory* (Oxford University Press, 1991); N. Goldenfeld, *Lectures on phase transitions and the renormalization group* (Addison-Wesley 1992). For a modern applications of RG, see Y. Oono, *Renormalization and Asymptotics*, Int. J. Mod. Phys. B, **14**, 1327 (2000). For recent reviews, see the series titled *Renormalization group theory in the new millenium*, Phys. Rep., **344**, 155, (2001); **348**, 1 (2001), **352** 215 (2001); **363**, 219 (2002). For non-perturbative aspects of RG, see for example, K. Aoki, Int. J. Mod. Phys., **14**, 1249 (2000).

[17] *Slow relaxations ans nonequilibrium dynamics in condensed matter* (Springer, 2003), edited by J.-L. Barrat, M. Feigelman, J. Kurchan and J. Dalibard.

[18] H. Löwe, P. Möller and A. Zippelius, *Dynamics od gelling liquids: a short survey*, cond-mat/0412101.

[19] P. M. Goldbart, H. E. Castillo and A. Zippelius, Adv. Phys. **45**, 393 (1996).

[20] H. E. Castillo, P. M. Goldbart and A. Zippelius, Europhys. Lett. **28**, 519 (1994).

[21] See, e.g., P. M. Goldbart, J. Phys. Cond. Matt. **12**, 6585 (2000).

[22] J. Kurchan, cond-mat/0209399.

[23] When performing the Fourier transform of any expression in replicated space where a restricted (HRS) sum over wave-vectors features, it is useful to first accertain the Fourier transform of the expression obtained on relaxing the HRS constraint, and then explicitly subtracting the LRS contributions from this transformed expression. As the LRS subtraction involves ORS and 1RS quantities that are function of either none, or just one, of the D-dimensional wave-vectors $(\mathbf{k}_0, \ldots, \mathbf{k}_\alpha, \ldots, \mathbf{k}_n)$, the above algorithm makes the determination of Fourier tranforms simple, and can be considered to be a practical definition of Fourier transforms in our replicated theory.

[24] S. J. Barsky and M. Plischke, Phys. Rev. E **53**, 871 (1996).

[25] See for example, S. Coleman, *Aspects of symmetry* (Cambridge Universirty Press, 1985).

[26] D. J. Wallace, in *Perturbative approach to surface fluctuations*, pp. 173-216 in: *Recent Advances in Field Theory and Statistical Mechanics*, edité par J.-B. Zuber and R. Stora (Les Houches Session XXXIX, 1982), (Amsterdam: North-Holland, 1984).

[27] I. Low and A. V. Manohar, Phys. Rev. Lett. **88**, 101602 (2002).

[28] H. E. Castillo, P. M. Goldbart and A. Zippelius, Phys. Rev. B **60**, 14702 (1999).

[29] L. D. Landau and E. M. Lifshitz, *Theory of Elasticity* (Pergammon Press, Oxford, 1986).

[30] H. Kleinert, *Gauge Fields in Solids*, Vol. 2, p. 746 et seq. (World Scientific, Singapore, 1989).

[31] H. E. Castillo and P. M. Goldbart, Phys. Rev. E 58, R24 (1998); and Phys. Rev. E 62, 8159 (2000)

[32] B. Jancovici, Phys. Rev. Lett. **19**, 20 (1967); H. J. Mikeska and H. Schmidt, J. Low Temp. Phys. **2**, 371 (1970).

[33] Nelson, D. R. (2001). *Defects and Geometry in Condensed Matter Physics*, Cambridge University Press, Cambridge, U.K.

[34] W. Peng, H. E. Castillo, P. M. Goldbart and A. Zippelius, Phys. Rev. B **57**, 839 (1998); W. Peng and P. M. Goldbart, Phys. Rev. E **61**, 3339 (2000).

[35] H.-K. Janssen and O. Stenull, Phys. Rev. E **64**, 026119 (2001); W. Peng, P. M. Goldbart and A. J. McKane, Phys. Rev. E **64**, 031105 (2001).

[36] We thank Michael Stone for guidance on this point.

[37] K. Broderix, M. Weight, and A. Zippelius, Eur. Phys. J. **B 29**, 441 (2002)

[38] See for example, Zinn-Justin, *Quantum field theory and critical phenomena* (Oxford University Press, 2002); D. J. Amit, *Field theory, the renormalization group and critical phenomena* (World Scientific, 1984).

[39] J. C. Collins, *Renormalization: An Introduction to Renormalization, the Renormalization Group and the Operator-Product Expansion* (Cambridge University Press, 1984).

[40] Uwe Tauber, online lecture notes, `www.phys.vt.edu/ tauber/utauber.html`, see chapter 5, in particular section 5.4. Also see ref. [49].

[41] X. Mao, P. M. Goldbart, M. Mezard and M. Weigt, cond-mat/0506194

[42] O. F. de A. Bonfirm, J. E. Kirkham and A. J. McKane, J. Phys A, **14**, 2391, (81)

[43] See, for example, *Mathworld*, `http://mathworld.wolfram.com/`

[44] Page 237, Bateman Manuscript Project, Vol. 2, by California Institute of Technology (McGraw Hill, 1982).

[45] C. M. Bender, S. Boettcher and L. Lipatov, *Almost zero-dimensional quatum field theories*, Phys. Rev. D, **46**, 5557 (1992)

[46] H. E. Castillo, *Statistical mechanics of the amorphous solid state of randomly crosslinked macromolecules*, Ph.D. thesis (1999).

[47] T. Nakayama, K. Yakubo and R. L. Orbach, *Dynamical properties of fractal neworks: sclaing, numerical simulations, and physical realizations*, Rev. Mod. Phys., **66**, 381 (1994)

[48] See for example, *Hyperspherical Harmonics* by John Avery, pages 27-31 (Klumer Academic Publishers, 1989) for Geigenbauer polynomials and pages 50-53 for generalized Bessel functions. Also see Z.Y. Wen and J. Avery, *Some properties of hyperspherical harmonics*, J. Math. Phys, **26**, 396 (1985)

[49] See for example, E. Brezin and D.J. Wallace, Phys. Rev. B, **7**, 1967 (1973); D. Nelson, Phys. Rev. B, **13**, 2222 (1976); I. D. Lawrie, J. Phys. A: Math Gen., **14**, 2489 (1981); Hans-Otto Heuer, J. Phys. A: Math Gen., **25**, 47 (1992) and references therein.

[50] G. Grinstein and R. A. Pelcovits, Phys. Rev. Lett. **47**, 856 (1981); Phys. Rev. A **26**, 915 (1982); C.S.O'Hern and T. C. Lubensky, Phys. rev. E, **58**, 5948 (1998).

[51] L. R. G. Treloar, *The Physics of Rubber Elasticity* (Clarendon Press, Oxford, 1975).

[52] For a brief overview, see E. Del Gado *et al.*, Phys. Rev. E **65**, 041803 (2002) and reference therein.

[53] Recent numerical studies include: M. Plischke *et al.*, Phys. Rev. Lett. **80**, 4907 (1998); Phys. Rev. E **60**, 3129 (1999); O. Farago and Y. Kantor, Phys. Rev. Lett. **85**, 2533 (2000), Phys. Rev. E **62**, 6094 (2000).

[54] M. Doaud, A. Coniglio, J. Phys. A **14**, L-30 (1981).

[55] S. Feng and P. N. Sen, Phys. Rev. Lett. **52**, 216 (1984);Y. Kantor and I. Webman, Phs. Rev. Let. **52**, 1891 (1984); S. Feng, M. F. Thorpe and E. Garboczi, Phys. Rev. B **31**, 276 (1985); A. R. Day, R. R. Tremblay and A.-M. S. Tremblay, Phys. rev. Lett. **56**, 2501 (1986); see also Ref. [63].

[56] See for example, C. F. Moukarzel and P. M. Duxbury, cond-mat/9807001 and references therein.

[57] See, e.g., T. Nakayama *et al.*, Rev. Mod. Phys. **66**, 381 (1994), and references therein.

[58] See for example, O. Stenull, *Renormalized field theory of random resistor networks*, Ph.D. thesis (2000).

[59] P. D. Francesco, P. Mathieu and D. Sénéchal, *Conformal Field Theory* (Springer, 1996).

[60] The arguments we present are not dependent on the details of the "nodes-links-blobs" picture. In particular, the internal structure of the effective chains will not feature.

[61] Owing to the complicated internal structure of these chains and repulsive interactions, this random walk is not expected to be ideal.

[62] For a discussion of thermal blobs, tension blobs and force-extension curves for polymers, see, e.g., Ref. [8].

[63] W. Tang, M. F. Thorpe, Phys. Rev. B, **36**, 3798 (1987).

[64] S. Mukhopadhyay, K. Esler, P. M. Goldbart, *Correlations in the random solid state* (in preparation).

[65] A. B. Harris, T. C. Lubensky, Phys. Rev. Lett. **35**, 327(1975); Phys. Rev. B **35**, 6964 (1987).

[66] S. F. Edwards and T. A. Vilgis, Rep. Prog. Phys. **51**, 243-297 (1988).

List of Publications

1. *Goldstone fluctuations in the amorphous solid state*, Swagatam Mukhopadhyay, Paul M. Goldbart and Annette Zippelius; Euro Phys. Lett. **67**, 49-55 (2004)

2. *Goldstone-type fluctuations and their implications for the amorphous solid state*, Paul M. Goldbart, Swagatam Mukhopadhyay and Annette Zippelius; Phys. Rev. B **70**, 184201 (2004)

3. *Scaling of entropic shear rigidity*, Xiangjun Xing, Swagatam Mukhopadhyay and Paul M. Goldbart; Phys. Rev. Lett. **93**, 225701 (2004)

4. *From vulcanization to isotropic and nematic rubber elasticity*, Xiangjun Xing, Swagatam Mukhopadhyay, Paul M. Goldbart and Annette Zippelius; cond-mat/0411660

5. *Double-exchange model for noninteracting electron spins coupled to a lattice of classical spins: Phase diagram at zero temperature*, David Pekker, Swagatam Mukhopadhyay, Nandini Trivedi and Paul M. Goldbart; Phys. Rev. B (in press, 2005)

6. *Global entanglement and quantum criticality in spin chains*, Tzu-Chieh Wei, Dyutiman Das, Swagatam Mukhopadhyay, Smitha Vishveshwara and Paul M. Goldbart; Physical Review A 71, 060305(R) (2005)

7. *Schemes for synthesizing arbitrary two-photon polarization mixed states*, Tzu-Chieh Wei, Joseph B. Altepeter, David Branning, Paul M. Goldbart, D. F. V. James, Evan Jeffrey, Paul G. Kwiat, Swagatam Mukhopadhyay and Nicholas A. Peters; Phys. Rev. A 71, 032329 (2005)

8. *Renormalized order parameter in the random solid state*, Swagatam Mukhopadhyay and Paul Goldbart; to be submitted in Phys. Rev. B.

9. *Correlations in the random solid state*, Swagatam Mukhopadhyay, Kenneth P. Esler and Paul Goldbart; in preparation.

Author's Biography

Swagatam Mukhopadhyay was born in Siliguri, a town at the foothills of the Himalayan range in Darjeeling district, West Bengal, India, on September 10, 1976. He received his Bachelor in Science (Honors) in Physics from Siliguri College, North Bengal University, India, in 1997. He received his Master of Science from Indian Institute of Technology, Kanpur, India, in 2000.